USC
UNIVERSIDADE DE SANTIAGO DE COMPOSTELA

DOCTORAL THESIS

# DEVELOPMENT AND EVOLUTION OF THE VERTEBRATE HYPOTHALAMUS: EVIDENCES IN CHONDRICHTHYANS

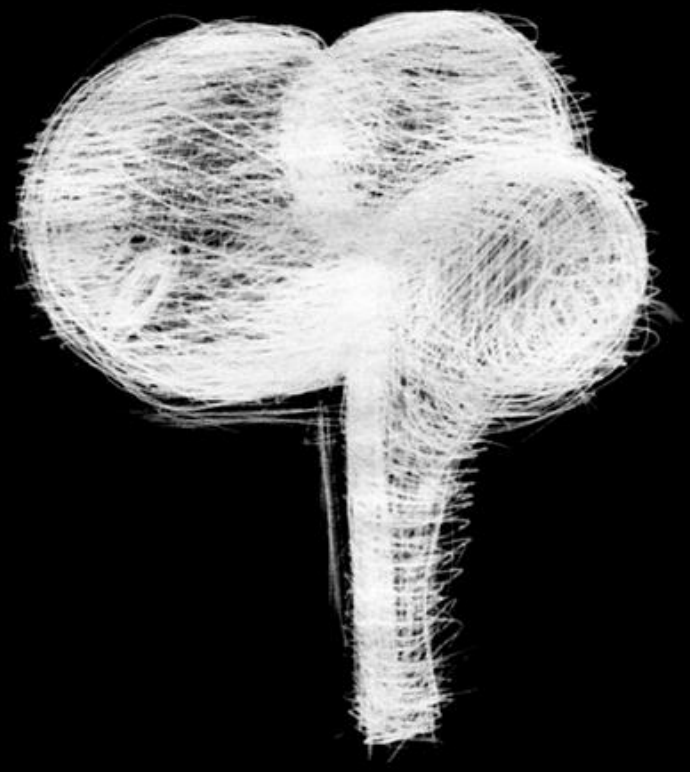


Gabriel Nicolás Santos Durán

DEPARTAMENTO DE BIOLOXÍA CELULAR E ECOLOXÍA
PROGRAMA DE DOUTORADO
INTERUNIVERSITARIO EN NEUROCIENCIA
FACULTADE DE BIOLOXÍA



SANTIAGO DE COMPOSTELA
2015

USC
UNIVERSIDADE
DE SANTIAGO
DE COMPOSTELA

DOCTORAL THESIS

# DEVELOPMENT AND EVOLUTION OF THE VERTEBRATE HYPOTHALAMUS: EVIDENCES IN CHONDRICHTHYANS

*Asdo*. Gabriel Nicolás Santos Durán

DEPARTAMENTO DE BIOLOXÍA CELULAR E ECOLOXÍA
PROGRAMA DE DOUTORAMENTO
INTERUNIVERSITARIO EN NEUROCIENCIA
FACULTADE DE BIOLOXÍA

SANTIAGO DE COMPOSTELA
2015

Santiago de Compostela, 2015

AUTORIZACIÓN DAS DIRECTORAS DA TESE DOUTORAL

DNA. ISABEL RODRÍGUEZ-MOLDES REY, CATEDRÁTICA DO ÁREA DE BIOLOXÍA CELULAR E DNA. EVA CANDAL SUÁREZ, PROFESORA CONTRATADA DOUTORA DO DEPARTAMENTO DE BIOLOXÍA CELULAR E ECOLOXÍA DA UNIVERSIDADE DE SANTIAGO DE COMPOSTELA, COMO DIRECTORAS DA TESE DE DOUTORAMENTO TITULADA "EVOLUTION AND DEVELOPMENT OF THE VERTEBRATE HYPOTHALAMUS: EVIDENCES IN CHONDRICHTHYANS" PRESENTADA POR D. GABRIEL N. SANTOS DURÁN ALUMNO DE PROGRAMA DE DOUTORAMENTO INTERUNIVERSITARIO EN NEUROCIENCIA (UNIVERSIDADE SANTIAGO DE COMPOSTELA, UNIVERSIDADE DE VIGO, UNIVERSIDADE DE A CORUÑA)

Autorizan a presentación da tese indicada, considerando que reúne os requisitos esixidos no artigo 34 do Regulamento de Estudos de Doutoramento, e que como Directoras da mesma non incurren nas causas de abstención establecidas na lei 30/1992.

Asimismo, avalan a solicitude de Mención Internacional por estimar que se axusta á normativa en vigor.

Santiago de Compostela, a 28 de Setembro de 2015.

As Directoras da Tese

Asdo.: Isabel Rodríguez-Moldes Rey

Asdo.: Eva Candal Suárez

USC
UNIVERSIDADE
DE SANTIAGO
DE COMPOSTELA

FINANCIACIÓN DE LA INVESTIGACIÓN

La realización de esta Tesis ha sido posible gracias a la financiación de los siguientes organismos:

- Ministerio de Educación y Ciencia- Dirección General de Investigación-FEDER (BFU2007-61154). Título del proyecto: Formación del patrón del encéfalo en condríctios (peces cartilaginosos).

- Ministerio de Ciencia e Innovación- Dirección General de Investigación-FEDER (BFU2010-15816). Título del proyecto: Buscando la condición ancestral de la organización cerebral de gnatóstomos: regionalización, migración, proyecciones y asimetrías en el cerebro en desarrollo de un tiburón.

- Dirección Xeral de I+D - Xunta de Galicia (10PXIB200051PR). Título del proyecto: Control de la expresión génica in ovo durante el desarrollo del sistema nervioso de peces. Identificación de los mecanismos conservados evolutivamente.

- Consellería de Economía e Industria – Programa xeral de Consolidación e estruturación das unidades de investigación do sistema galego de I+D+I. IN845B-2010/159 (Año 2010).

- Conselleria de Cultura, Educación e Ordenación Universitaria – Proxectos Plan Galego IDT-Consolidación e Estruturación de Unidades de Investigación competitivas (GPC). CN 2012/237 (Año 2012).

- Ministerio de Economía y Competitividad - Dirección General de Investigación Científica y Técnica-FEDER (BFU2014-58631-P). Título del proyecto: Estudio de la neurogénesis en cerebro embrionario y adulto desde una perspectiva evolutiva.

CONTRATOS Y BECAS

La realización de esta Tesis ha sido posible gracias a la concesión de contratos de investigación asociados a los siguientes proyectos de investigación: BFU2007-61154, BFU2010-15816 y CN 2012/237.

DISPONIBILIDAD DE EMBRIONES DE LA PINTARROJA

La disponibilidad de embriones ha sido posible gracias a la financiación de European Community – Research Infrastructure Action bajo el programa específico FP7 “Capacities” (ASSEMBLE grant agreement no. 227799) y a la colaboración de la Estación de Bioloxía Mariña da Graña de la Univesidad de Santiago de Compostela, el “Aquarium Finisterrae” de A Coruña, el Acuario de O Grove y el Acuario de Gijón.

DISPONIBILIDAD DE LAS SONDAS DE GENES DE PINTARROJA

La disponibilidad de las sondas de los genes ha sido posible gracias al proyecto de secuenciacion EST del genoma de pintarroja, coordinado por la Dra. Sylvie Mazan (CNRS, Roscoff, Francia), financiado por Génoscope, Evry (Francia).

USC
UNIVERSIDADE
DE SANTIAGO
DE COMPOSTELA


*A mis padres y mis hermanas*

*A Vero*

USC
UNIVERSIDADE
DE SANTIAGO
DE COMPOSTELA

*"Begin at the beginning and go on till you come to the end; then stop"*

(Lewis Carrol 1865, Alice in Wonderland)

*..."yo puedo tener (y de hecho he tenido) muchos nuevos proyectos en mi vida, pero vida personal y familiar sólo tendré una"...*

(Berto Pena)

*..."lo curioso de la teoría de la evolución es que todo el mundo cree que la entiende"...*

(Stuart Kaufman)

*..."los biólogos tenemos la fea costumbre de perdernos en los detalles...si los coches estuvieran formados por proteínas y ADN la gran mayoría de los artículos del Pubmed pondría que las tuercas y las ruedas son importantes para el funcionamiento del coche porque aparecieron pronto en la evolución de los medios de transporte y los biólogos nos pasaríamos la vida estudiando la variabilidad de tuercas y ruedas en vez de preguntarnos porqué realmente un coche se mueve -o no-"...*

(conversación en redes sociales)

USC
UNIVERSIDADE
DE SANTIAGO
DE COMPOSTELA

En primer lugar quiero dar gracias a las personas que han hecho posible esta tesis. Gracias a mis tutoras. A Isa por darme la oportunidad de conocer este mundo y por su entusiasmo sin límites ni barreras. A Eva por ser además de una jefa una AMIGA. También por compartir conmigo la forma de ver el desarrollo, la investigación, el trabajo y por los bocadillos de nocilla o la pizza los días que "hay que decidir cosas". Gracias a las dos por las cosas que me habéis enseñado consciente o inconscientemente y por vuestro duro trabajo robándole horas al sueño para sacar adelante lo que haga falta. Y sobre todo, GRACIAS, a las dos por vuestra ayuda en este final de tesis tan particular.

Una tesis marca una etapa importante en la vida, porque uno no es la misma persona antes de empezarla que al finalizarla. Esto es así, por las cosas que pasan "dentro de la tesis" como por las cosas que ocurren "fuera". Por esta razón, también quiero dedicárle este trabajo a mis abuelos Gabriel, Margot, Luz-Mary (Ua), Darío y a mis tíos Beatriz y Nicolás. También se lo quiero dedicar a mis padres, Gabriel y Luz, que a lo largo de estos años han (hemos!) tenido que hacer frente tanto a situaciones que veíamos muy lejanas, como a otras que nunca se nos habrían pasado por la cabeza. Gracias por enseñarme todo lo que no está escrito en esta tesis. Gracias a mi padre por su paciencia, su apoyo y su actitud. Gracias a mi madre, por ser un terremoto, y ayudarme a ver las cosas importantes de la vida (aunque probablemente no sean las que ella está pensando). Gracias a Natalia por ser la mejor hermana que se puede tener. Gracias por compartir conmigo tantos momentos buenos y otros no tan buenos. En serio. Gracias!! Por supuesto esta tesis también se la quiero dedicar a mi hermana Luz. Gracias también a mi familia tanto paterna como materna por hacer que los obstáculos de la vida sean más pequeños.

Y, sobre todo, gracias a Vero. Gracias por tener paciencia conmigo desde "el minuto uno". Gracias por ayudarme a re-descubrir la forma de ver muchas cosas en la vida, por ayudarme con TODO (hasta con los experimentos!), por hacerme sentir que nunca estoy solo y que puedo (podemos!) con todo y por otro montón de cosas que NO SE PUEDEN EXPLICAR CON PALABRAS. De todo corazón: GRACIASSSSSSSS!!!!!!!!!!!!!!

También quiero dar las gracias a mis compis de laboratorio, a los chicos de la "old school" Ivan, Antón, Idoia, Sol, David (aunque hayas abandonado el BC3), Blanca, Maru, Sylvia y Dani. Gracias por enseñarme a "hacer poyata" y/o compartir tantas tonterías/freakadas de esas que hacen los cafés divertidos, las comidas relajadas y las tardes amenas (especial mención a la época batamanta y la lista de frases de Sol). Gracias a Nuria por traer su "asentoh" al laboratorio y por su apoyo durante el tramo más duro de nuestras respectivas tesis. Gracias también a las nuevas incorporaciones Santi, Alberto, "Dani B" y Sheila por traer vidilla al laboratorio. Gracias a Ramón, Sole, Celina, Manolo y Suso por hacer del departamento el lugar que es. Especial mención a Fátimeeeee (QUÉ-PASA-Chavaaaaaaaaaal!) y Miguel por ayudarnos con todo tipo de cosas de la vida del "investigador Jr." y por compartir con nosotros bromas, chascarrillos y algo de humor negro.

Gracias a los que siempre "están ahí". A la gente que ha hecho que la Universidad y el Postgrado sea una etapa tan especial en Santiago: Antonio, Luis, Juan, María, DVD, Andrea, MónicaM, MónicaR., Xoa, More, Vane, Puala, Dieguín, Bea O., David, Diana, Bea B., Ana, Jesús, Juan y Ángela. También a los que han contribuido a crear todos los buenos momentos que tengo asociados a Vigo (aunque algunos sean algo borrosos por el trajín de las noches): Javi, Txudo, Cede, Jr., Buba, Tole y Pani. Y cómo no, darle las gracias a Nico, Jaco y Mato por haberme hecho participar de esa "*masa amorfa y verde que crece sin control*" (Mato et al., 2010) que fue Green Fandango. Gracias hacer que lo pasáramos genial, por descubrirme "la coru" sus gentes, sus garitos y un montón de buena música. Gracias por ayudarme a compaginar el grupo de música y el grupo de investigación. Y sobre todo gracias por enseñarme a soñar con cosas aparente imposibles y por el *"sí!!, vamos a hacerlo!!"*.

USC
UNIVERSIDADE
DE SANTIAGO
DE COMPOSTELA

**RESUMO**

O hipotálamo é un centro integrador conservado cunha organización complexa resultado dun proceso de formación do patrón complexo. No presente traballo, adoptamos un enfoque *evo-devo* e o marco teórico do modelo prosomérico para entender a organización do hipotálamo dos vertebrados. Aquí estudamos os patróns de expresión dos *ScFoxg1a*, *ScDlx2/5*, *ScOtp*, *ScShh*, *ScNkx2.1*, *ScTbr1*, *ScNeurog2*, *ScLhx5*, *ScLhx9*, *ScDlx2/5*, *ScNkx2.8*, *ScEmx2*, *ScLmx1b*, *ScPitx2*, *ScPitx3a*, *ScNeurog2*, *ScFoxa1* e *ScFoxa2* xunto coa immunoreactividade a Pax6, PCNA e outros immunomarcadores no hipotálamo embrionario e territorios adxacentes do cerebro anterior dun peixe cartilaxinoso, o melgacho, *Scyliorhinus canicula*. A nosa análise comparativa revela a existencia de trazos conservados pero tamén suxire unha organización alternativa á proposta polo modelo prosomérico para o hipotálamo e mesmo para o prosencefalo anterior de vertebrados.

**PALABRAS CHAVE**

Hipotálamo, condríctios, *evo-devo*, modelo prosomérico, prosencéfalo

**RESUMEN**

El hipotálamo es un centro integrador conservado con una organización compleja resultado de un proceso de formación del patrón complejo. En el presente trabajo, adoptamos un enfoque *evo-devo* y el marco teórico del modelo prosomérico para entender la organización del hipotálamo de los vertebrados. Aquí estudiamos los patrones de expresión de los genes *ScFoxg1a*, *ScDlx2/5*, *ScOtp*, *ScShh*, *ScNkx2.1*, *ScTbr1*, *ScNeurog2*, *ScLhx5*, *ScLhx9*, *ScDlx2/5*, *ScNkx2.8*, *ScEmx2*, *ScLmx1b*, *ScPitx2*, *ScPitx3a*, *ScNeurog2*, *ScFoxa1* y *ScFoxa2* junto con la immunoreactividad a Pax6, PCNA y otros immunomarcadores en el hipotálamo embrionario y territorios adyacentes del cerebro anterior de un pez cartilaginoso, la pintarroja, *Scyliorhinus canicula*. Nuestro análisis comparativo revela la existencia de rasgos conservados pero también sugiere una organización alternativa a la propuesta por el modelo prosomérico para el hipotálamo e incluso para el prosencéfalo anterior de vertebrados.

**PALABRAS CLAVE**

Hipotálamo, condríctios, *evo-devo*, modelo prosomérico, prosencéfalo

**SUMMARY**

The hypothalamus is a conserved integrative center with a complex organization result of a complex patterning processes. Here we make use of a *evo-devo* approach and the theoretical framework of the prosomeric model to understand the organization of the vertebrate hypothalamus. We studied the gene expression patterns of *ScFoxg1a*, *ScDlx2/5*, *ScOtp*, *ScShh*, *ScNkx2.1*, *ScTbr1*, *ScNeurog2*, *ScLhx5*, *ScLhx9*, *ScDlx2/5*, *ScNkx2.8*, *ScEmx2*, *ScLmx1b*, *ScPitx2*, *ScPitx3a*, *ScNeurog2*, *ScFoxa1* and *ScFoxa2* besides immunoreactivity to Pax6, PCNA and other immunomarkers in the embryonic hypothalamus and neighbour prosencephalic territories of a cartilaginous fish, the catshark, *Scyliorhinus canicula*. Our comparative analysis reveals the existence of conserved traits but also suggests an alternative organization to that proposed by the prosomeric model for the hypothalamus and even for the anterior prosencephalon of vertebrates.

**KEYWORDS**

hypothalamus, chondrichthyans, *evo-devo*, prosomeric model, prosencephalon

USC
UNIVERSIDADE
DE SANTIAGO
DE COMPOSTELA

# CONTENTS

USC
UNIVERSIDADE
DE SANTIAGO
DE COMPOSTELA

# GENERAL INTRODUCTION

Every scientific work should start with, at least, one question. To understand the work in the following pages we must translate the title of this thesis into some questions like: "*how did the development of the vertebrate hypothalamus change through evolution?* and *what can we learn from chondrichthyans?"* The next part of a scientific work must be to wholly understand those questions. So, through the course of this introduction we are going to deepen in the main concepts here referred.

USC
UNIVERSIDADE
DE SANTIAGO
DE COMPOSTELA

# GENERAL INTRODUCTION

## 1. CHANGE, EVOLUTION, HOMOLOGY AND DEVELOPMENT

### 1.1 Change and Evolution

Evolution is a process that involves change over time. The concept that all organisms on Earth have evolved from a common ancestral life-form by means of genomic and morphological transformations -evolution as such- is a documented fact (Kutschera and Niklas, 2004). Recognizing what has changed among organisms is the first step to reconstruct the evolutionary history. These reconstructions, in turn, help us to understand why these changes have occurred, how (by virtue of which mechanisms*)* and when did they occur (Northcutt, 2002; Butler and Hodos, 2005). Extensive research has been made on what is different among organisms. However, a more difficult question to address is why organisms are different, and the mechanisms that account for the origin of species (i.e. transformation and diversification) are still very much under investigation. Darwin (1859) would be the first to summarize a coherent body of observation that solidified the concept of organism evolution into a true scientific theory, proposing natural selection as the basic mechanism on the origin of new species (reviewed in Kutschera and Niklas, 2004). However, the fail to find a holistic satisfactory explanation concerning these mechanisms of evolution in all five kingdoms of life has been demanding a constant review and expansion of the initial theory of Darwin. In fact, the last version of the theory -"the expanded synthesis"- is an open system composed of many sub-theories dealing with various aspects of the evolutionary process (Kutschera and Niklas, 2004).

### 1.2 Homology

Comparing different organisms under different approaches turns fundamental to answer *what* is different among them. On which concerns to morphological sciences, this task involves comparing structures, their origin, and recognizing similar and dissimilar characters. However, the characters considered have to reflect a continuity of biological information from a common antecessor (van Valen, 1982)**.** This idea on continuity of information can be traced back to several Greek philosophers (reviewed in Kutschera and Niklas, 2004; Kleisner, 2007) and is the essence under the different interpretations of the concept of homology (van Valen, 1982). The

term *homologue* was first employed by Owen in 1843, before the appearance of Darwin´s evolution theory to define the same organ in different animals under every variety of forms and functions (reviewed in Puelles and Medina, 2002) and has become a central issue in biology (Gilbert et al., 1996; Puelles and Medina, 2002; Kleisner, 2007; Sommer, 2008). Under Owen´s view the sameness of characters are identified with reference to an archetype (understood as a "rational plan") (Kleisner, 2007). Darwin´s findings provided a new explanation to Owen´s homology (Butler and Saidel, 2000; Puelles and Medina, 2002) since under the Darwinian view, the homology is explained in terms of inheritance from a hypothetical common ancestor (Gilbert et al., 1996; Kleisner, 2007). Thus, similar and also dissimilar characters, when connected through intermediate -extant or fossil- forms, have homology relationships (Sommer, 2008). So, after 1859 the paradigm changed from the "ideal" concept of homology to the historical concept of homology. However, much of the practical knowledge continued to have meaning within new evolutionary interpretations and the determination of homologies did not improve (Kleisner, 2007).

### 1.3 Dawn and re-birth of homology: homology in development

By the 1930s and 1940s, the discovery of Mendel´s work and the rise of population genetics turned evolution into a mathematically proven fact also providing a mechanism for evolution. This made the construction of phylogenetic trees based on homologies to seem speculative, old fashioned and unscientific compared to the unambiguous mathematical elegance of population genetics. So, the rise of genetics was in detriment of sciences focused on the study of complex characters as most of the morphological sciences (paleontology, embryology, taxonomy...) (Gilbert et al., 1996; Hall, 2003a; Müller, 2007). The understanding of evolution split into two major fields that persist to the present day: genetics versus morphological sciences (Gilbert et al., 1996; Kutschera and Niklas, 2004). The rediscovery of homologies -and morphological sciences- came hand by hand with the rise of molecular biology, the discovery of the DNA structure, DNA homologies, homeotic mutations, homeobox genes and clusters, both in in drosophila and vertebrates. These genes encode DNA-binding proteins -transcription factors- that profoundly influence embryonic development since they are responsible of the specification of cells along the antero-posterior and dorso-ventral axis. These genes are homologous from arthropods to vertebrates, show similar chromosomic organization and similar expression patterns through the anterior-posterior axis, which stresses the similarities of embryonic development across phyla.

Now a new kind of homology seems to emerge: generative homology, homology of process or deep homology (Butler and Saidel, 2000; Gilbert and Bolker, 2001; Kleisner, 2007; Shubin et al., 2009). In the light of these concepts, "the processes, themselves, can be considered homologous, just as structures can be considered homologous" (Gilbert and Bolker, 2001). Moreover, these signaling genes were identified as intervening in the most important

evolutionary developmental mechanisms (Hall, 2003b) leading to the idea that if animals are different is because, at least in part, their developmental process also differ (reviewed in Medina et al., 2011). Now, a new discipline known as evolutionary-developmental biology or "evo-devo" (Hall, 2003b) tries to explore how developmental process evolved and how they ultimately achieved the various body plans of past and present-day organisms. Noteworthy, *evo-devo* reconciles genetics, development, evolution and evolutionary theories leading to inclusion of this discipline in the last evolutionary theory, the expanded synthesis theory (Kutschera and Niklas, 2004).

### 1.4 Limits of homologies establishment

Along the course of the human and scientific though, the problem of evolution has been always the same; however, approaches and paradigms evolved as knowledge advanced. As pointed above, to date there is no a consensus about the concept of homology. Principles are known but interpretations abound (Abouheif et al., 1997; Butler and Saidel, 2000; Hall, 2003a; Kleisner, 2007). However all the concepts pursue the same goal: to establish guidelines or principles that ensure a correct reconstruction of the evolutionary history. Developmental or evo-devo perspectives seem reliable approaches for establishing homologies since development is hierarchically over structure and, in turn, structure is hierarchically over function (Gilbert et al., 1996; Abouheif et al., 1997; Hall, 2003b). However, although development theoretically deals with assumptions and old problems linked to the historical concept of homology, they also meet with new and old limitations.

The developmental approach also presents bias since, when studying a particular structure, it assumes that processes involved in embryogenesis -previous to organogenesis- are equivalent among vertebrates, just as the historical approach neglected variations in the molecular embryology to be behind variable structures (Puelles and Medina, 2002; Butler and Hodos, 2005). In the same line, it is also assumed that the expression of homologous genes is triggered by homologous processes among different vertebrates.

Furthermore, through development, different levels of complexity are probably transversally connected through cascades, signaling pathways and/or genetic networks (Hall, 2003b). A genetic hierarchy and modularity have been recognized, however, it is not well understood on which genes they depend. The developmental approach also meets with old problems of homology establishment, like determining reliable levels of hierarchy and comparing features from its different levels (Striedter, 1998; Northcutt, 2002; Puelles and Medina, 2002;), either structural or genetic. Furthermore, alternative views argue that although genetic modules are plausible, a genetic hierarchy is unlikely to exist under an evolutionary reasoning and current experimental data (Salazar-Ciudad, 2009).

Moreover, there is controversy concerning the establishment of homologies comparing different levels of hierarchy. Some authors suggest that homologies stipulated at one level does not imply homology at the others (Striedter and Northcutt, 1991; Butler and Saidel, 2000). For example, the fact that during development certain neurons share the similar transcription factors among different vertebrates does not mean that they would have similar electrical properties or the same connections in the adults. Thus, comparing elements of different levels of hierarchy would lead to misleading interpretations (Striedter and Northcutt, 1991; Striedter, 1998). Other authors argued that only a partial relationship can be established among different levels of hierarchy (Striedter, 1998; Kleisner, 2007). However, other authors hold that analyzing homology phylogenetically at different levels of hierarchy at the same time, contrary to be misleading, leads to recognize different evolutionary scenarios of developmental integration, opportunity and constraint for a character (Abouheif, 1997; Puelles and Medina, 2002). For example, if certain neurons share similar transcription factors that determine similar neurochemical properties but distinct connections during the development of different vertebrates, this could be revealing a differential developmental integration that determines a certain behavior depending on different evolutionary scenario.

The developmental approach is linked to another problem: the existence of alternative programs of development that lead to the same structure (Butler and Hodos, 2005). In the same organism the same structure can arise from different sources under certain circumstances. This is the case of the regeneration of the lenses in amphibians (Hall, 2003c). Such exceptions are few but do occur, so we must be careful when the developmental approach is used to establish homologies.

Furthermore, when one tries to understand the evolution of a character, as evolution is also a dynamic process, different situations must be taken into consideration (i.e. reversals, rudiments, vestiges or atavisms) to ensure a correct evolutionary interpretation since developmental mechanisms may be conserved among these situations (Hall, 2003c).

## 2. COMPARATIVE NEUROANATOMY, NEURAL TUBE HISTOGENESIS, HYPOTHALAMUS AND BRAIN MODELS

### 2.1 Comparative neuroanatomy

For neuroanatomical studies, different features can be compared for two different taxa, including gene and/or protein expression patterns, cell morphology, neuronal clusters, neurochemical properties, electrophysiological properties, connectivity, topological similarity, topographical similarity, similarity in their relationships to some consistent feature of the two species and similarity of embryological derivation and behavioral outcomes, among others (Butler and Hodos, 2005). As exposed above, due to the fact that development is hierarchically over structure (Gilbert et al., 1996; Hall, 2003b), the study of "high on the hierarchy

processes/features" will probably tell us more about important changes among vertebrate brains and the mechanisms underlying such differences than "down on the hierarchy processes/features". To compare high on the hierarchy processes concerning brain development we need to understand key processes driving neural histogenesis susceptible of being compared among vertebrates. Furthermore, we have to understand particularities of the region considered, besides the theoretical frameworks used to understand vertebrate brain organization.

### 2.2 Neural tube histogenesis

In the early development of vertebrate embryos, at the end of gastrulation, the embryo harbors 3 different embryonic sheets known as ectoderm, mesoderm and endoderm from outside to inside. A portion of the ectoderm is specified to become neural ectoderm or neural plate, which can be differentiated from the remaining ectodermal epithelium by its columnar appearance. The neural plate forms the neural tube by a process called neurulation during which the embryo is referred as neurula. The edges of the neural plate fold upward forming the neural folds (and a U-shaped neural groove) that fuse in the midline to form a hollow tube (**Figure 1A**). Of note, the cells at the dorsal-most portion of the neural tube become the neural crest.

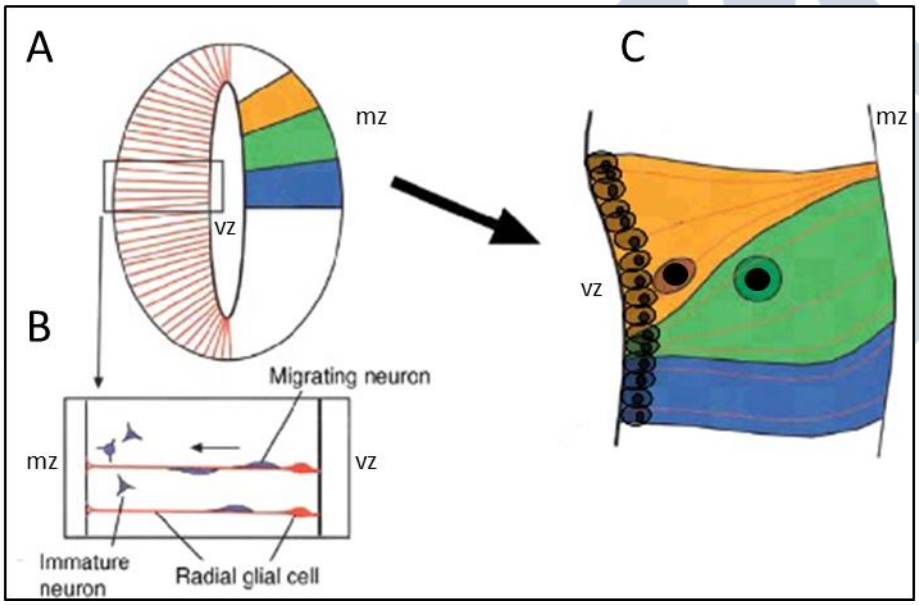


**Figure 1:** Histogenesis of the neural tube. A) Drawing of a transverse section of the neural tube representing radial glia and histogenetic domains. B) Detail of cell cycle across the neural wall. C) Detail of three dorso-ventral radial neuroepithelial domains. Each color represents a hypothetical specification code. Abbreviations: mz, marginal or mantle zone; vz, ventricular zone. Adapted from Medina, 2008.

The neural tube proliferates and gives rise to the brain, rostrally, and the spinal cord, caudally. This tube is a pseudostratified neuroepithelium of rapidly dividing stem cells. The nuclei move within the cells as they go through the cell cycle from the inter-most to the outer-most surface of the tube and back (**Figure 1B**). Once the cell cycle ends, daughter cells have two options: re-enter cell cycle to continue proliferating or migrate and differentiate into glia or neurons. Of note, these can be short-range (local) migrations, next to their birth place, or long-rage migrations, when they move away from the place of birth.

Neuroepithelial stem cells integrate information from diffusive signals along the developing neural tube through development. This integration lead to the expression of different groups of transcription factors which drive main morphogenetic process as cell proliferation, differentiation and migration. Moreover, the study of expression patterns of transcription factors reveals the existence of radial histogenetic units defined by genetically coded neuroepithelial domains with common morphogenetic properties (**Figure 1C**). Morphogenetic domains and properties vary across the neural tube as the epigenetic landscape varies in a certain organism. Among vertebrates, the bases of homologies establishment just relays in the existence of neuroepithelial domains expressing similar genetic codes due to a similar epigenetic landscape, but leading to different morphogenetic properties and thus to a different structure, i.e., although mechanisms are conserved, certain differences among them may create different but homologous structures. Thus, the study of transcription factor expression patterns is based on the compared analysis of histogenetic properties, defined by neuroepithelial gene specification codes in a region (as could be the hypothalamus), among different vertebrates (Puelles and Medina, 2002; Medina, 2008).

### 2.3 Brain morphogenesis

During the early development, two prominent external constrictions divide the early developing brain (neural tube) into three main vesicles related to the basic structure of the adult brain. These vesicles represent the fundamental antero-posterior (i.e., rostro-caudal) subdivisions of the vertebrate brain: forebrain (or prosencephalon), medbrain (or mesencephalon) and hindbrain (or rhombencephalon). Classically, it has been considered that they become subdivided into secondary vesicles as development proceeds. The prosencephalon would give rise to the telencephalon and the diencephalon (where the hypothalamus would form), the mesencephalon would remain as a single vesicle and the rombencephalon would become subdivided into the metencephalon and the myelencephalon. An alternative conception of the brain regionalization considers the diencephalon (primary prosencephalon) subdivided into synencephalon (pretectal area), dorsal thalamus and ventral thalamus, whereas the hypothalamus together with the preoptic region and telencephalic hemispheres would form the secondary prosencephalon (see below).

### 2.4 The hypothalamus

Phylogenetically, the hypothalamus is one of the oldest cerebral structures, and has remarkably similar nuclear differentiation and fiber connections in all vertebrates (Sarnat and Netsky, 1981; Kandel and Schwartz, 2001). Functionally, the hypothalamus has a central role in body homeostasis. It links the central nervous system to the endocrine system, the autonomic nervous system and peripheral tissues. It receives external (visual, olfactory and gustatory) and internal stimulus, integrates them, and produces behavioral and regulatory responses such as

feeding, escape, attack, aggression, sex, skin color, growth, salt and water balance and sexual development, among others (Sarnat and Netsky, 1981; Kandel and Schwartz, 2001; Butler and Hodos, 2005).

Concerning its organization, the hypothalamus presents an elusive structure that has been difficult to systematize due to the fact that cell groups of the hypothalamus do not clearly define clusters and that this region is crossed by diffuse fiber systems that are among the most complex fiber systems of the brain (Simerly, 2004). This situation improved with the appearance of molecular techniques which lead to the identification of genes involved in the development and function of hypothalamic cells (Swanson, 1999; Puelles and Rubenstein, 2003; Puelles, 2009). However, the debate around the structure and organization of the hypothalamus is still open even under the light of molecular biology tools (Shimamura et al., 1995; Puelles and Rubenstein, 2003; Medina, 2008; Szabó et al., 2009; Shimogori et al., 2010; Álvarez-Bolado et al., 2012; Puelles et al., 2012; Croizier et al., 2015). This has been so, since the hypothalamus develops under a complex patterning process that converges at the rostral and ventral-most point of the brain, yielding a complex organization susceptible of different interpretations (Shimamura et al., 1995; Puelles and Rubenstein, 2003; Medina, 2008; Szabó et al., 2009; Shimogori et al., 2010; Álvarez-Bolado et al., 2012; Puelles et al., 2012; Croizier et al., 2015).

### 2.5 Brain Models

When investigating about structural neurobiology or comparative neuroanatomy, different kinds of models can be elaborated: adult structure *vs* morphogenesis; segmental *vs* longitudinal; morphological *vs* genetic… Models can be based on different kinds of data (morphological, histological, neurochemical, hodological and genetic, among others). Of note, on a good model, different kinds of data should fit easily. The main advantage of a model is that it led us to understand a particular aspect of the brain function, structure, organization or morphogenesis of a particular taxon (Puelles, 2009).

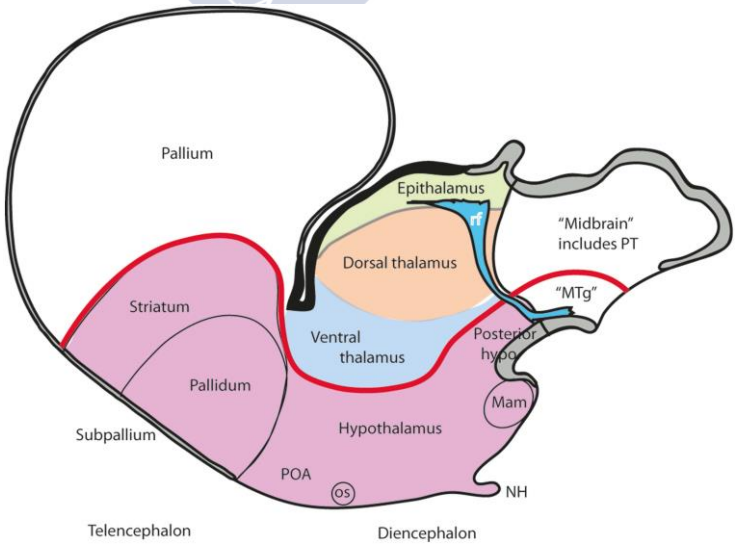


**Figure 2:** The secondary prosencephalon according to the columnar model. Red line represents the alar-basal boundary. From Puelles and Rubenstein, 2015. Abbreviations: hypo, hypothalamus; NH, neurohypophysis; Mam, mamillary bodies; MTg, mesencephalic tegmentum; os, optic stalk; POA, preoptic area; PT, pretectum; rf; retroflex fascicle.

Morphogenetic models help us understanding brain development and structure. It also helps making comparisons, setting

up homologies and, eventually, understanding vertebrate brain evolution. While some authors focus on functional principles to define brain structure, others understand morphological and ontogenic structural data as more relevant (Puelles, 2009). There are two main paradigms on morphogenesis and brain organization: columnar *vs* segmental models (Puelles, 2009; Puelles et al., 2012; Puelles and Rubenstein, 2015).

**Columnar models**

The first of these models (Columnar model of brain morphogenesis) was proposed by J. B. Johnston, C. J. Herrick and collaborators at the beginning of the twenty century influencing the comprehension of the brain structure since 1910 to the present days. This model is based on the organization of the functional components of the cranial and spinal nerves in functional columns. The model proposes that this columnar organization spreads into the entire brain including the prosencephalon, an assumption that –for some authors- seems to misfit with the organization of this region (Puelles, 2009). Under this point of view, the hypothalamus is part of the diencephalon and is literally "located under the thalamus" (Figure 2). For Le Gros Clark (1938), the preopto-hypothalamic continuum was divided into four main rostrocaudal regions: preoptic area, anterior hypothalamus (previously referred as supraoptic), tuberal or medial hypothalamus, and mamillar or posterior hypothalamus (reviewed in Simerly, 2004).

**Segmental models**

The segmental model was initially proposed by Orr (1887) who was the first to coin the term "neuromere" at the end of the nineteen century. Such paradigm is the origin of models as those proposed by von Kupffer (1906) and His (1895). This paradigm proposes that the brain and the set of spinal and cranial nerves consisted of a number of segmental units –"neuromeres"- that resemble the concept of metameres. It understands the brain as a tube divided on a set of successive transversal segments

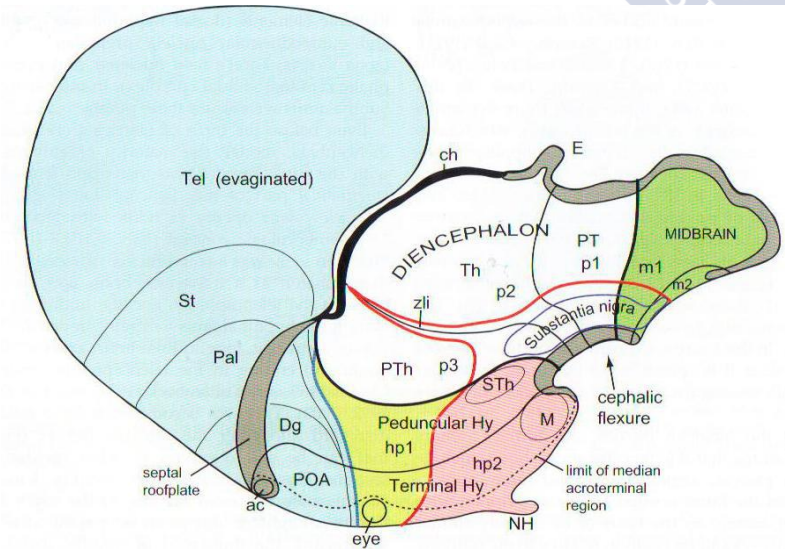


**Figure 3:** The secondary prosencephalon according to the prosomeric model. Red line represents the alar-basal boundary. From Puelles et al., 2012. Abbreviations: ac, anterior commissure; ch, choroid plexus; Dg, diagonal band; E, epiphysis; hp1, prosomere hp1 or peduncular; hp2, prosomere hp2 or terminal; Hy, hypothalamus; m1, mesomere 1; m2, mesomere 2; M, mamillary bodies; NH, neurohypophysis; p1, prosomere 1; p2, prosomere 2; p3, prosomere 3; Pal, pallidum; PT, pretectum; PTh, prethalamus; St, striatum; Sth, subthalamic nucleus; Tel, telencephalon (evaginated); zli, zona limitans inthrathalamica

Worth mentioning is the model of brain morphogenesis of His (1895). Although it is not explicitly neuromeric, it introduced important concepts that remain to our days such as the floor, basal, alar and roof plates, the alar-basal boundary (or sulcus limitans of His), the concept of isthmus and the idea of a morphogenetic deformation of the neural tube due to axial bending (for revision, see Puelles, 2009; Puelles and Rubenstein, 2015).

The prosomeric model and its different updates (Puelles and Rubenstein, 1993, 2003, 2015; Puelles et al., 2012), is a modern and explicit segmental model of brain morphogenesis based on gene expression patterns, morphological and ontogenic data. It establishes that segments in which the brain is subdivided are genetically specified and generically referred as neuromeres (or prosomeres, mesomeres and rhombomeres depending on the region considered: prosencephalon, mesencephalon or rhombencephalon, respectively). Of note, it suggests an alternative hypothalamic organization compared to that stated in columnar models. Firstly, it supports the preoptic area as part of the telencephalon, referred as non-evaginated telencephalon (reviewed in Medina et al., 2011; Moreno and González, 2011). Besides, it argues that the hypothalamus is located under the telencephalon rather than under the thalamus (**Figure 3**).

The prosomeric model is nowadays well accepted and has been proved to be useful as framework in comparative neuroanatomy being recently developed also for biomedical purposes (Puelles et al., 2012; Puelles and Rubenstein, 2015). In comparative terms, a great degree of conservation in the compartments proposed by the model has been proven in different groups of vertebrates. However, there are also differences on telencephalon and hypothalamus that raised controversy concerning the number of segments in these regions (Puelles and Rubenstein, 2003). In fact, lasts modifications of the model concern the hypothalamic region (Puelles and Rubenstein, 2003, 2015; Morales-Delgado et al., 2011, 2014; Puelles et al., 2012).

Other models propose a change in certain traits of the prosomeric model such as the position of the alar-basal boundary yielding a configuration that, in turn, has been suggested to fit with the organization of columnar paradigms (Diez-Roux et al., 2011). Moreover, alternative models of hypothalamic organization were proposed based on certain developmental genes (Shimogori et al., 2010) yielding an interpretation fairly different from that proposed by Puelles and collaborators (Puelles et al., 2012; Puelles and Rubenstein, 2015). Other models are based on fate maps and gliogenesis and neurogenesis (Álvarez-Bolado et al., 2012). Of note, these alternative models intend to be a sum of results for a certain taxon rather than a paradigm reflecting vertebrate hypothalamic organization.

### 3. CARTILAGINOUS FISHES IN EVO-DEVO STUDIES

To understand the origin of a certain group of animals, the study of the basal members of the group of interest, besides outer groups, results fundamental. This approach has led to recognize that all vertebrates are characterized by the presence of paired lateral eyes, a relatively

large brain/body ratio, and two ectodermal tissues that arise lateral to the developing neural tube: the neural crest and neurogenic placodes. These tissues were argued to be key for the origin of vertebrates due to its derivatives (special sense organs and other neural and non-neural structures) (Gans and Northcutt, 1983; Butler and Hodos, 2005). Noteworthy, the existence of paired eyes would not be possible without the presence of a prechordal plate mesoderm which seems to be present in *Haikouella* fossils, a transition form between cephalochordates and vertebrates (Butler and Hodos, 2005).

The study of the chondrichthyan class, an ancient lineage of jawed vertebrates (gnathostomes), turns essential in order to understand the rise of such a group and, besides, the origin of vertebrates. Indeed, extant gnathostomes can be divided into two groups: chondrichthyan -or cartilaginous fishes- and osteichthyan -or bony vertebrates-, the last comprising ray and lobe finned fishes and tetrapods (**Figure 4**).

Chondrichthyan-osteichthyan comparisons allow us to make important phylogenetically inferences about the nature of the last common ancestor of jawed vertebrates (Gillis and Shubin, 2009). Agnathan-gnathostome comparisons are also necessary to identify traits acquired by jawed vertebrates but also common traits of vertebrates (Kuratani et al., 2002). Despite the diversity of animal forms observed in the taxon, gnathostomes are characterized by a highly conserved body plan, including important morphological innovations such as the jaw, true teeth, gill arches lying internally to the gills and branchial blood vessels, paired appendages, a horizontal semicircular canal in the inner ear, and myelinated nerve fibers (Coolen et al., 2009).

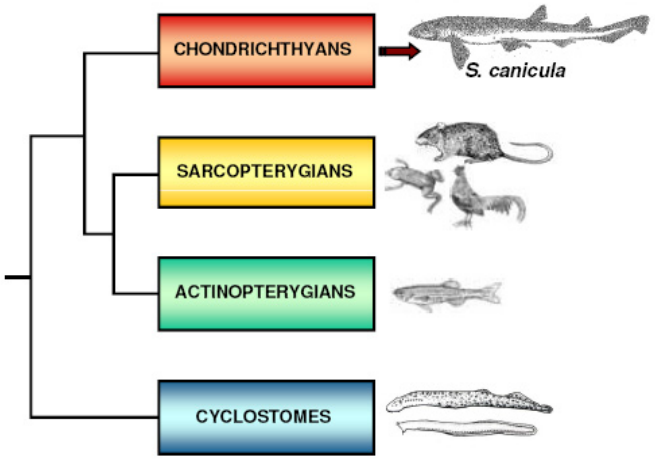


**Figure 4:** Phylogenetic position of chondrichthyans among gnathostomes. From Coolen et al. 2009.

Moreover, within chondrichthyans, the model used in this study, *Scyliorhinus canicula*, results an informative and interesting representative of the group for many different research purposes. The lesser-spotted dogfish (catshark) belongs to *Scyliorhinidae*, the largest family in the largest order of extant sharks, the *Carcharhiniformes*, which form a clade with the *Lamniformes*, *Orectologiformes*, and *Herodontiformes*. This group is often termed the *Galeomorph* superorder. Inside *Carcharhiniformes*, phylogenetic analysis based on molecular data suggests that *S. canicula* holds the important distinction of being one of the most evolutionarily basal members of the *Carcharhiniformes*, a group that has become the most

dominant group of sharks alive today (see Coolen et al., 2009). Besides, *Galeomorph* sharks possess brains as large as those of birds and mammals relative to their body size (Northcutt, 2002) with extensive neuronal proliferation and migration (Butler and Hodos, 2005) which makes them a relevant model for comparative studies of brain organization and development (Coolen et al., 2009).

This species also exhibits a slow growth rate and a long life cycle; its maximum reported lifespan is 12 years. The embryonic development of cartilaginous fishes varies considerably in length, as the rate of development is temperature dependent and also species specific. In *Scyliorhinus*, an incubation time of 6-8 month has been described (Ivory et al., 2004). Once outside of the egg, juveniles are totally able to explore and interact with its habitat. The period since the juvenile (posthatching) leaves the egg until it reaches sexual maturity it is about one year (Coolen et al., 2009).

Moreover, its relatively small size among sharks and easy maintenance (Ballard et al., 1993) makes *S. canicula* a good model organism to manage in laboratory conditions. This species also exhibits a slow growth rate and a long life cycle, an advantage to follow quick changes during development that could not be appreciated in other model organisms. The species lacks a sharply defined breeding season: at any time of the year many of the females can be found carrying a pair of recently fertilized eggs. However, different records of Atlantic Ocean show monthly variations in catches ranging from 10% of such "pregnant" females in August and September to more than 40% in June and July. Relatively little is known about the behavior of this species in the wild. Such basic knowledge, in particular, of reproductive and feeding behavior, will be important for improving maintenance conditions (Coolen et al., 2009).

### 3.1 General anatomy the shark hypothalamus. Insights from *S. canicula*

Characteristically, the hypothalamus of adult sharks contains large cavities that are recesses of the third ventricle: preoptic, infundibular and posterior recesses. Accordingly, the shark hypothalamus could be defined as the large forebrain region formed by the walls of the recesses of the third ventricle. Taking this into account and mainly influenced by a columnar vision of the brain organization (see above), the shark hypothalamus has been classically considered to be organized into three main subdivisions from rostral to caudal (see Smeets et al., 1983; Smeets, 1998): i) preoptic or anterior hypothalamus (**Figures 5, 6b-d**), which includes the preoptic and anterior (supraoptic) regions according to Le Gros Clark (1938) since in chondrichthyans such subdivision results misleading; ii) tuberal or medial hypothalamus (**Figures 5, 6e-i**) and iii) mamillar or posterior hypothalamus (**Figure 6g-i**).

i) Preoptic or anterior hypothalamus.

The preoptic region harbor two cell clusters organized around the preoptic recess: the magnocellular and parvocellular preoptic nuclei (**Figure 6b-d**). The **magnocellular preoptic nucleus** contains neurosecretory neurons whose axons mostly form the hypothalamus-hypophyseal tract that courses along the hypothalamic floor to end in the neurointermediate lobe (formed in the tuberal hypothalamus by the association of the hypothalamic neural lobe and the pars intermedia of the hypophysis), although extrahypophyseal projections have been also reported (Meurling et al., 1996). The magnocellular preoptic nucleus, the hypothalamus–hypophyseal tract, and the neurointermediate lobe of the hypophysis form the classic neurosecretory system. The **parvocellular preoptic nucleus** contains neurons of peptidergic and aminergic nature, most of them cerebrospinal fluid (CSF)-contacting cells that form a circumventricular organ known as preoptic recess organ (Rodríguez-Moldes and Anadón, 1987; Molist et al., 1993; Rodríguez-Moldes et al., 1993; Carrera et al., 2008, 2012). Cells of this organ may regulate the adenohypophyseal functions, as some of their axons terminate on portal capillaries that form a neurohemal structure (the median eminence), which drain toward the adenophypophysis (Rodríguez-Moldes et al., 1993; Meurling et al., 1996; Anadón et al., 2000). The **suprachiasmatic nucleus** (**Figure 6d**), a conserved nucleus rich in catecolaminergic cells located close to the optic chiasm, also contributes in part to innervate the neurointermediate lobe of the hypothalamus (Molist et al., 1993; Carrera et al., 2012)

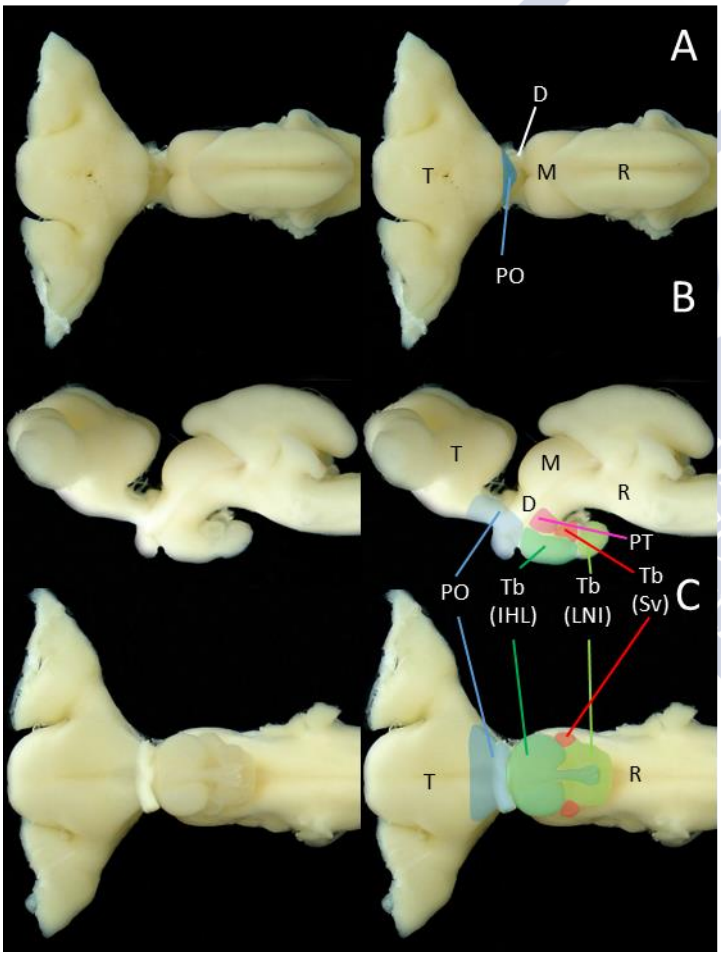


**Figure 5.** Principal regions of the hypothalamus of a juvenile *S. canicula*. A) Dorsal view. B) Lateral view. C) Ventral view. Abbreviations: D, diencephalon; IHL, inferior hypothalamic lobes; LNI, neurointermediate lobe; M, mesencephalon; PO, preoptic area; PT, posterior tuberculum; R, rhombencephalon; Sv, saccus vasculosus; T, telencephalon; Tb, tuberal region.

ii) Tuberal or medial hypothalamus

The tuberal region contains conserved structures related to the hypothalamo-hypophyseal system, as the **hypothalamic-hypophyseal tract,** that courses along the neurohypophyseal stalk

(**Figure 6f**); the **lateral tuberal nucleus**, that is located periventricularly in the paired ventromedial eminences of the infundibular walls and is formed in part by CSF-contacting neurons; the **median eminence** and the **neurointermediate lobe or neurophypophysis** proper (**Figure 5B, C**).

Other characteristic structures only present in the tuberal hypothalamus of gnathostome fishes are the inferior hypothalamic lobes (**Figures 5B, C; Figure 6f-h**) and the saccus vasculosus (**Figure 5B, C; Figure 6i**). The **inferior hypothalamic lobes** are lateral expansions of the infundibular walls which are related to the control of feeding behavior. The **saccus vasculosus** is a circumventricular organ of enigmatic function that develops adjacent to the neurohypophysis and to the posterior recess walls as a highly vascularized neuroepithelium that contains an specialized glial cell type, the coronet cells, and CSF-contacting type neurons (for more information see, Sueiro et al., 2007; Rodríguez-Moldes, 2011). The **saccus vasculosus** develops from the caudal portion of the infundibular walls in close developmental relationship with the evagination that originates the neurointermediate lobe of the hypophysis (van de Kamer and Shuurmans, 1953; Sueiro et al., 2007; see also **Figure 7**). Although it was previously thought to be involved in pressure perception, recent studies point the saccus vasculosus as involved in circadian functions (Nakane et al., 2013).

iii) Mamillar or caudal hypothalamus

In the caudal and classical mamillary region, mamillary derivatives are mostly occupied by functionally integrated structures that form two continuous circumventricular organs: the **paraventricular organ** (**Figure 6g-h**) and its caudo-medial continuation the **posterior recess organ** (**Figure 6i; Figure 7**). The walls of both organs are characteristically folded and formed by a high density of CSF-contacting neurons of catecholaminergic, serotoninergic, and peptidergic nature (Rodríguez-Moldes and Anadón, 1987; Meurling and Rodríguez, 1990; Molist et al., 1993; Sueiro et al., 2007; Carrera et al., 2008, 2012)

**Figure 6**. Overall anatomy of the *S. canicula* brain. **A**. Drawing showing a sagittal view of the adult *S. canicula* brain. **B (b-i)**. Micrographs of transverse sections at the levels indicated in **A**. Abbreviations (colored regions): ca, commissura anterior; chopt, chiasma opticum; Cpii, commissura postinfundibularis pars inferior; cpo, commissura postoptica; dec tapal, decussation tractus pallii; dienc, diencephalon; emth, eminentia thalami; fbt, fasciculus basalis telencephali; hypoph, hypophysis; inf, infundibulum; K, nucleus K; lih, lobus inferior hypothalami; M, mamillar region; Nlobl, nucleus lobi lateralis; Nlobld, nucleus lobi lateralis pars dorsalis; Nloblv, nucleus lobi lateralis pars ventralis; Nlt, lucleus lateralis tuberis; Nmh, nucleus medius hypothalami; Nph, nucleus periventricularis hypothalami; Nsc, nucleus suprachiasmaticus; Nsv, nucleus sacci vasculosi; plev, plica encephali ventrale; PO, preoptic region; Po, nucleus preopticus; rmam, recessus mamillaris; rpo, recessus preopticus; shyp, sulcus hypothalamicus; sth, sulcus thalamohypothalamicus; Sv, saccus vasculosus; Tb, tuberal region; thvm; thalamus ventralis pars medialis; topt, tractus opticus; tpal, tractus pallii; tpohyp, tractus preopticohypophyseus; PT; posterior tuberculum; tsv, tractus sacci vasculosi; Tubp, nucleus tuberculi posterioris. Scale bars: a) 10mm; B (b-i) 1mm. Adapted from Smeets et al. (1983).ventrale; PO, preoptic region; Po, nucleus preopticus; rmam, recessus mamillaris; rpo, recessus preopticus; shyp, sulcus hypothalamicus; sth, sulcus thalamohypothalamicus; Sv, saccus vasculosus; Tb, tuberal region; thvm; thalamus ventralis pars medialis; topt, tractus opticus; tpal, tractus

pallii; tpohyp, tractus preopticohypophyseus; PT; posterior tuberculum; tsv, tractus sacci vasculosi; Tubp, nucleus tuberculi posterioris. Scale bars: a) 10mm; B (b-i) 1mm. Adapted from Smeets et al. (1983).

.

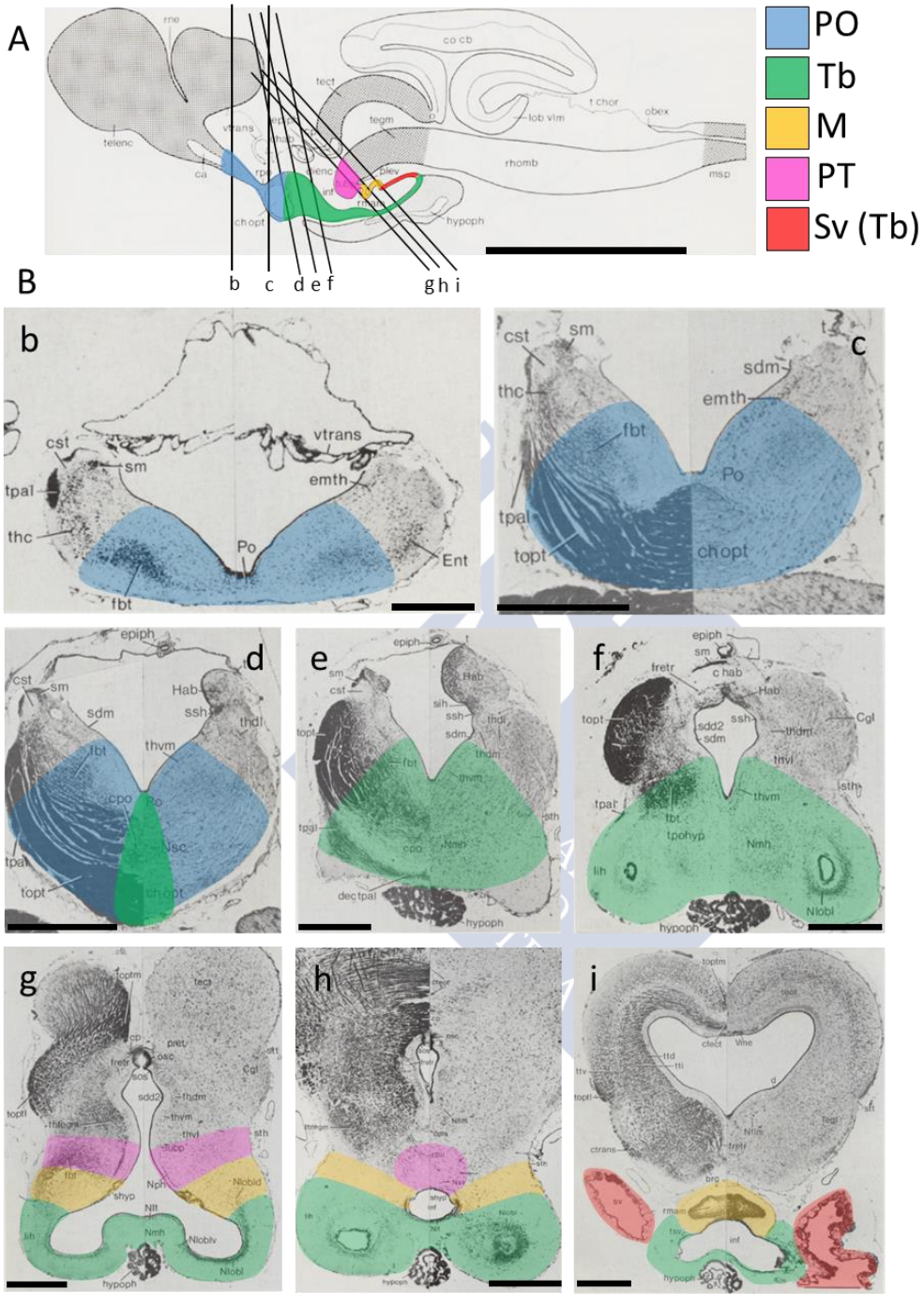


These three hypothalamic subdivisions were considered in the earliest studies performed by our group on the shark (adult) hypothalamus, which were mainly focused on the ultrastructure and

chemoarchitecture of circumventricular structures (Rodríguez-Moldes, 1986; Rodríguez-Moldes and Anadon, 1987; Rodríguez-Moldes et al., 1990, 1993; Molist et al., 1993, 1995). Once realizing the usefulness of the segmental perspective for stablishing brain homologies, studies on the organization of the adult shark brain started to be interpreted under the segmentary approach (Anadón et al., 2000; Teijido et al., 2002) and, accordingly, the preoptic area passed to be considered appart from the hypothalamus (and from the telencephalon).

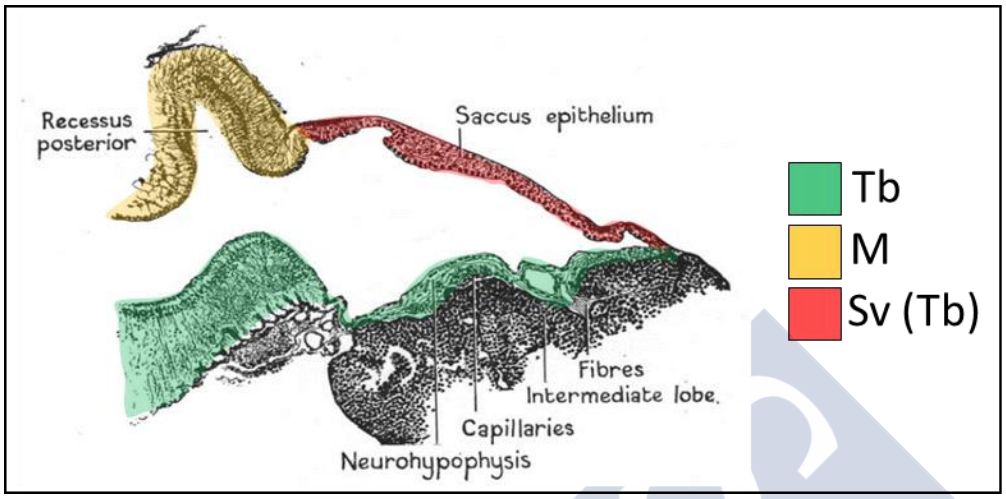


**Figure 7.** Sagittal section of an adult *S. canicula* showing saccus vasculosus, hypophysis, and part of the infundibular region. Abbreviations: Tb, tuberal region; M, mamillar region; Sv, saccus vasculosus. Adapted from van de Kamer and Shuurmans (1953).

The recognizing of the hypothalamus, preoptic area and telencephalon as subdivisions of the secondary prosencephalon, as initialy proposed in the prosomeric model articulation (Puelles and Rubenstein, 1993), was considered in the earliest developmental studies about the shark brain performed by our group (Carrera et al., 2008**;** Ferreiro-Galve et al., 2008). However, based on genetic evidences in the hypothalamus of other species interpreted under the prosomeric framework (reviewed in Medina et al., 2011; Moreno and Gonzalez, 2011), the preoptic region passed to be considered a subpallial derivative, i.e. part of the basal telencephalon, which has been recognized in our developmental studies about shark brain organization (Rodríguez-Moldes, 2009; Carrera et al., 2012; Quintana-Urzainqui et al., 2012, 2015).

Nevertheless, the scenario still remain misleading. To date, in amniotes, it seems clear a correlation between the preoptic area conceived by Le Gros Clarke, as concept of adult celular masses, and the preoptic area (POA or PO), as concept of progenitor or histogenetic domains expressing subpallial markers like *Dlx*, *Nkx2.1* or *Shh* (reviewed in Moreno et al, 2009; see also Flames et al., 2007; Bardet et al., 2010). It also seems clear, a correlation between the adult cell mases of the anterior hypothalamus (neurosecretory populations) and the histogenetic concept of anterior hypothalamus [referred as paraventricular domain (Pa), in the updated prosomeric model; see Puelles et al. 2012] characterized by the expression of markers like *Otp* or *Sim1* (reviewed in Moreno and González, 2011; see also Puelles et al., 2012). However, in chondrichthyans, since the preoptic area concept referres to celular masses of the preoptic and

anterior hypothalamus of Le Gros Clark (see above), it remains unclear whether it develops from POA/PO-like histogenetic domains, Pa-like histogenetic domains or both. This thesis will contribute to shed light on this question.

Also controversial in terms of ascription is the structure known as the posterior tuberculum, a well conserved structure characterized by rich distribution of catecholaminergic cells located caudally beyond the mamillary recess (**Figures 5B; 6g, h**). In studies performed in sharks it has been firstly ascribed to the hypothalamus following a columnar interpretation of the diencephalon (Smeets et al., 1983; Molist et al., 1992, 1993; Smeets, 1998; Anadón et al., 2000). Later on, in agreement with a segmental approach, it has been considered part of the diencephalon proper (caudal prosencephalon), basically a derivative of the basal part of the prosomere 3 (Carrera et al., 2008, 2012; Ferreiro-Galve et al., 2008; Rodríguez-Moldes, 2009). In bony fishes it has been defined by the expression of markers like *Otp*, *Neurog2* or *Foxa2* (Vernier and Wulliman, 2008). Moreover, although it is recognized as a typical structure of anamniotes, it seems also conserved in anmiotes (Vernier and Wulliman, 2008). Again, this work could help to clarify the situation of the posterior tubercle concerning the hypothalamus, its segmental correspondence and the existence of homologue structures in other vertebrates.

**References**


Abouheif, E. (1997). Developmental genetics and homology: a hierarchical approach. *Trends Ecol. Evol.* 12, 405-8.

Álvarez-Bolado, G., Paul, F. A., and Blaess, S. (2012). Sonic hedgehog lineage in the mouse hypothalamus: from progenitor domains to hypothalamic regions. *Neural Dev.* 7, 4.

Anadón, R., Molist, P., Rodríguez-Moldes, I., López, J.M., Quintela, I., Cerviño, M.C., Barja, P., and González, A. (2000). Distribution of choline acetyltransferase (ChAT) immunoreactivity in the brain of an elasmobranch, the lesser-spotted dogfish (*Scyliorhinus canicula*). *J. Comp. Neurol*. 420, 139-70.

Ballard, W. W., Mellinger, J., and Lechenault, H. (1993). A series of normal stages for development of *Scyliorhinus canicula*, the lesser spotted dogfish (*Chondrichthyes*: *Scyliorhinidae*). *J. Exp. Zool.* 267, 318-36.

Bardet, S. M., Ferran, J. L. E., Sanchez-Arrones, L., and Puelles, L. (2010). Ontogenetic expression of sonic hedgehog in the chicken subpallium. *Front. Neuroanat.* 4, 28.

Butler, A. B., and Hodos, W. (2005). "The Visceral Brain: theHypothalamus and the Autonomic Nervous System", in *Comparative Vertebrate Neuroanatomy: Evolution and Adaptation*, eds A. B. Butler and W. Hodos (Hoboken, NJ: John Wiley & Sons), 445-67.

Butler, A. B., and Saidel, W. M. (2000). Defining sameness: historical, biological, and generative homology. *Bioessays* 22, 846-53.

Carrera, I., Anadón, R., and Rodríguez-Moldes, I. (2012). Development of tyrosine hydroxylase-immunoreactive cell populations and fiber pathways in the brain of the dogfish Scyliorhinus canicula: new perspectives on the evolution of the vertebrate catecholaminergic system. *J. Comp. Neurol.* 520, 3574-603.

Carrera, I., Molist, P., Anadón, R., and Rodríguez-Moldes, I. (2008). Development of the serotoninergic system in the central nervous system of a shark, the lesser spotted dogfish Scyliorhinus canicula. *J. Comp. Neurol.* 511, 804-31.

Coolen, M., Menuet, A., Chassoux, D., Compagnucci, C., Henry, S., Lévèque, L., et al. (2009). "The Dogfish *Scyliorhinus canicula*, a Reference in Jawed Vertebrates," in *Emerging Model Organisms*. A Laboratory Manual, eds R. R. Behringer, A. D. Johnson, and R. E. Rrumlauf (Cold Spring Harbor, NY: Cold Spring Harbor Laboratory Press), 431-46.

Croizier, S., Chometton, S., Fellmann, D., and Risold, P. (2015). Characterization of a mammalian prosencephalic functional plan. *Front. Neuroanat.* 8, 161

Darwin, C. R. (1859). *On the origin of species by means of natural selection, or the preservation of favoured races in the struggle for life*. John Murray, (London).

Diez-Roux, G., Banfi, S., Sultan, M., Geffers, L., Anand, S., Rozado, D., Magen, A., Canidio, E., Pagani, M., Peluso, I., et al. (2011). A high-resolution anatomical atlas of the transcriptome in the mouse embryo. *PLoS Biol.* 9, e1000582.

Ferreiro-Galve, S., Carrera, I., Candal, E., Villar-Cheda, B., Anadón, R., Mazan, S., Rodríguez-Moldes, I. (2008). The segmental organization of the developing shark brain based on neurochemical markers, with special attention to the prosencephalon. *Brain Res. Bull*. 75, 236-40.

Flames, N., Pla, R., Gelman, D. M., Rubenstein, J. L. R., Puelles, L., and Marín, O. (2007). Delineation of multiple subpallial progenitor domains by the combinatorial expression of transcriptional codes. *J. Neurosci.* 27, 9682-95.

Gans, C., and Northcutt, R. G. (1983). Neural crest and the origin of vertebrates: a new head. *Science* 220, 268-73.

Gilbert, S. F., and Bolker, J. A. (2001). Homologies of process and modular elements of embryonic construction. *J. Exp. Zool.* 291, 1-12.

Gilbert, S. F., Opitz, J. M., and Raff, R. A. (1996). Resynthesizing evolutionary and developmental biology. *Dev. Biol.* 173, 357-72.

Gillis, J. A., and Shubin, N. H. (2009). The evolution of gnathostome development: Insight from chondrichthyan embryology. *Genesis* 47, 825-41.

Hall, B. K. (2003a). Unlocking the Black Box between genotype and phenotype: cell condensations as morphogenetic (modular) units. *Biol. Philos.* 18, 219-47.

Hall, B. K. (2003b). Evo-Devo: evolutionary developmental mechanisms. *Int. J. Dev. Biol.* 47, 491-5.

Hall, B. K. (2003c). Descent with modification: the unity underlying homology and homoplasy as seen through an analysis of development and evolution. *Biol. Rev. Camb. Philos. Soc.* 78, 409-33.

Herrick, C. J. (1910). The morphology of the forebrain in amphibia and reptilia. *J. Comp. Neurol. Psychol*. 20, 413-547.

His, W. (1895). Die Anatomische Nomenclatur. Nomina Anatomica. *Arch. Anat. Entwickelungsges* 1895 (Suppl.),1-180.

Ivory, P., Jeal, F. and Nolan, C. P. (2004). Age Determination, Growth and Reproduction in the Lesser-spotted Dogfish, *Scyliorhinus canicula*. *J. Northw. Atl. Fish. Sci*., 35, 89-106.

Kandel, E., and Schwartz, J. (2001). "Sistema Nervioso Autónomo e Hipotálamo," in *Principios de Neurociencia*, eds E. R. Kandel, J. H. Schwartz, and T. M. Jessell (Aravaca: McGraw-Hill Interamericana), 960-81.

Kleisner, K. (2007). The formation of the theory of homology in biological sciences. *Acta Biotheor*. 55, 317-40.

Kuratani, S., Kuraku, S., and Murakami, Y. (2002). Lamprey as an evo-devo model: lessons from comparative embryology and molecular phylogenetics. *Genesis* 34, 175-83.

Kutschera, U., and Niklas, K. J. (2004). The modern theory of biological evolution: an expanded synthesis. *Naturwissenschaften* 91, 255-76.

Le Gros Clark, W. E. (1938). "Morphological Aspects of the Hypothalamus", in *The Hypothalamus*, eds W. E. Le Gros Clark, J. Beattie, G. Riddoch and N. M. Dott (Edinburgh: Oliver and Boyd), 1-68.

Medina, L. (2008). "Evolution and Embryological Development of the Forebrain," in *Encyclopedia of Neuroscience*, eds M. D. Binder, N. Hirokawa, and U. Windhorst (Berlin: Springer-Verlag), 1172-92.

Medina, L., Bupesh, M., and Abellán, A. (2011). Contribution of genoarchitecture to understanding forebrain evolution and development, with particular emphasis on the amygdala. *Brain. Behav. Evol.* 78, 216-36.

Meurling, P., and Rodríguez, E.M. (1990). The paraventricular and posterior recess organs of elasmobranchs: a system of cerebrospinal fluid-contacting neurons containing immunoreactive serotonin and somatostatin. *Cell Tissue Res.* 259, 463-73.

Meurling, P., Rodríguez, E. M., Peña, P., Grondona, J. M., and Pérez, J. (1996). Hypophysial and extrahypophysial projections of the neurosecretory system of cartilaginous fishes: an immunocytochemical study using a polyclonal antibody against dogfish neurophysin. *J. Comp. Neurol.* 373, 400-21.

Molist, P., Rodríguez-Moldes, I., and Anadón, R. (1992). Immunocytochemical and electron-microscopic study of the elasmobranch nucleus sacci vasculosi. *Cell Tiss. Res*. 270, 395-404.

Molist, P., Rodríguez-Moldes, I., and Anadón, R. (1993). Organization of catecholaminergic systems in the hypothalamus of two elasmobranch species, *Raja undulata* and *Scyliorhinus*

*canicula*. A histofluorescence and immunohistochemical study. *Brain Behav. Evol*. 41, 290-302.

Molist, P., Rodríguez-Moldes, I., Batten, T. F. C., and Anadón, R. (1995). Distribution of calcitonin gene-related peptide-like immunoreactivity in the brain of the small-spotted dogfish, *Scyliorhinus canicula*. *J. Comp. Neurol*, 352, 335-50.

Morales-Delgado, N., Castro-Robles, B., Ferrán, J. L., Martínez-de-la-Torre, M., Puelles, L., and Díaz, C. (2014). Regionalized differentiation of CRH, TRH, and GHRH peptidergic neurons in the mouse hypothalamus. *Brain Struct. Funct.* 219, 1083-1111.

Morales-Delgado, N., Merchan, P., Bardet, S. M., Ferrán, J. L., Puelles, L., and Díaz, C. (2011). Topography of somatostatin gene expression relative to molecular progenitor domains during ontogeny of the mouse hypothalamus. *Front. Neuroanat.* 5, 10.

Moreno, N., and González, A. (2011). The non-evaginated secondary prosencephalon of vertebrates. *Front. Neuroanat.* 5, 12.

Moreno, N., González, A., and Rétaux, S. (2009). Development and evolution of the subpallium. *Semin. Cell Dev. Biol.* 20, 735-43.

Müller, G. B. (2007). Evo-devo: extending the evolutionary synthesis. *Nat. Rev. Genet.* 8, 943-9.

Nakane, Y., Ikegami, K., Iigo, M., Ono, H., Takeda, K., Takahashi, D., Uesaka, M., Kimijima, M., Hashimoto, R., Arai, N., et al. (2013). The saccus vasculosus of fish is a sensor of seasonal changes in day length. *Nat. Commun.* 4, 2108.

Northcutt, R. G. (2002). Understanding vertebrate brain evolution. *Integr. Comp. Biol.* 42, 743-56.

Orr, H. (1887). Contribution to the embryology of the lizard. *J. Morphol*. 1, 311-72.

Owen, R. (1843). *Lectures on the comparative anatomy and physiology of the invertebrate animals, delivered at the Royal College of Surgeons, in 1943*, eds Longman, Brown, Green and Longmans (London).

Puelles, L. (2009). "Forebrain development: prosomere model," in *Developmental Neurobiology*, ed. G. Lemke (London; Burlington, MA; San Diego, CA: Academic Press), 315-19.

Puelles, L., and Medina, L. (2002). Field homology as a way to reconcile genetic and developmental variability with adult homology. *Brain Res. Bull.* 57, 243-55.

Puelles, L., and Rubenstein, J.L.R. (1993) Expression patterns of homeobox and other putative regulatory genes in the embryonic mouse forebrain suggest a neuromeric organization. *Trends Neurosci*. 16, 472-79.

Puelles, L., and Rubenstein, J. L. R. (2003). Forebrain gene expression domains and the evolving prosomeric model. *Trends Neurosci.* 26, 469-76.

Puelles, L., and Rubenstein, J. L. R. (2015). A new scenario of hypothalamic organization: rationale of new hypotheses introduced in the updated prosomeric model. *Front. Neuroanat.* 9, 27.

Puelles, L., Martínez, S., Martínez-de-la-Torre, M. S., and Rubenstein, J. (2012). "Hypothalamus," in *The Mouse Nervous System*, eds C. Watson, G. Paxinos, and L. Puelles (San Diego, CA: Academic Press), 221-312.

Quintana-Urzainqui, I., Sueiro, C., Carrera, I., Ferreiro-Galve, S., Santos, G., Pose-Méndez, S., Mazan, S., Candal, E., and Rodríguez-Moldes, I. (2012). Contributions of developmental studies in the dogfish *Scyliorhinus canicula* to the brain anatomy of elasmobranchs: Insights on the basal ganglia. *Brain Behav. Evol*. 80, 127-41.

Quintana-Urzainqui, I., Rodríguez-Moldes, I., Mazan, S., and Candal, E. (2015). Tangential migratory pathways of subpallial origin in the embryonic telencephalon of sharks: evolutionary implications. *Brain Struct Funct*. 220, 2905-26

Rodríguez-Moldes, I. (1986). *Estudio ultraestructural e histofluorescente del hipotálamo de la pintarroja con especial referencia a los sistemas licor-contactantes y al saco vasculoso*. Ph. D. thesis, Universidad de Santiago de Compostela,

Rodríguez-Moldes, I. (2009). A developmental approach to forebrain organization in elasmobranchs: new perspectives on the regionalization of the telencephalon. *Brain Behav. Evol*. 74, 20-9.

Rodríguez-Moldes, I. (2011). "Functional Morphology of the Brains of Cartilaginous Fishes," in *Encyclopedia of Fish Physiology: From Genome to Environment*, Vol 1, ed. A. Farrell (San Diego: Academic Press) pp. 26-36.

Rodríguez-Moldes, I., and Anadón, R. (1987). Aminergic neurons in the hypothalamus of the dogfish, *Scyliorhinus canicula L.* (Elasmobranch). A histofluorescence study. *J. Hirnforsch.* 28, 685-93.

Rodríguez-Moldes, I., Manso, M.J., Becerra, M., Molist, P., and Anadón, R. (1993). Distribution of substance P-like immunoreactivity in the brain of the elasmobranch *Scyliorhinus canicula*. *J. Comp. Neurol*. 335, 228-44.

Rodríguez-Moldes, I., Timmermans, J.-P., Adriaensen, D., De Groodt-Lasseel, M.H.A., Scheuermann, D., and Anadón, R. (1990). Immunohistochemical localization of calbindin-D28k in the brain of a cartilaginous fish, the dogfish (*Scyliorhinus canicula* L.). *Acta Anat.* 137, 293-302.

Salazar-Ciudad, I. (2009). Looking at the origin of phenotypic variation from pattern formation gene networks. *J. Biosci.* 34, 573-87.

Sarnat, H. B., and Netsky, M. G. (1981). "Epithalamus and Hypothalamus," in *Evolution of the Nervous System*, eds H. B. Sarnat and M. G. Netsky (New York, NY; Oxford: Oxford University Press), 296-320.

Shimamura, K., Hartigan, D. J., Martinez, S., Puelles, L., and Rubenstein, J. L. (1995). Longitudinal organization of the anterior neural plate and neural tube. *Development* 121, 3923-33.

Shimogori, T., Lee, D. A., Miranda-Angulo, A., Yang, Y., Wang, H., Jiang, L., Yoshida, A. C., Kataoka, A., Mashiko, H., Avetisyan, M., et al. (2010). A genomic atlas of mouse hypothalamic development. *Nat. Neurosci.* 13, 767-75.

Shubin, N., Tabin, C., and Carroll, S. (2009). Deep homology and the origins of evolutionary novelty. *Nature* 457, 818-23.

Simerly, R. B. (2004). "Anatomical Substrates of Hypothalamic Integration," in *The Rat Nervous System*, ed. G. Paxinos, 3rd ed. (San Diego, CA: Academic Press), 336-351.

Smeets, W. (1998). "Cartilaginous Fishes," in *The Central Nervous System of Vertebrates*, eds R. Nieuwenhuys, H. J. Ten Donkelaar, and C. Nicholson (Berlin: Springer-Verlag), 521-654.

Smeets, W., Nieuwenhuys, R., and Roberts, B. (1983). *The Central Nervous System of Cartilaginous Fishes. Structure and Functional Correlations*, eds. W. Smeets, R. Nieuwenhuys, and B. Roberts (Berlin Heildelberg New York: Springer).

Sommer, R. J. (2008). Homology and the hierarchy of biological systems. *Bioessays* 30, 653–8.

Striedter, G. F. (1998). Stepping into the same river twice: homologues as recurring attractors in epigenetic landscapes. *Brain. Behav. Evol.* 52, 218-31.

Striedter, G. F., and Northcutt, R. G. (1991). Biological hierarchies and the concept of homology. *Brain. Behav. Evol.* 38, 177-89.

Sueiro, C., Carrera, I., Ferreiro, S., Molist, P., Adrio, F., Anadón, R., and Rodríguez-Moldes, I. (2007). New insights on Saccus vasculosus evolution: a developmental and immunohistochemical study in elasmobranchs. *Brain. Behav. Evol.* 70, 187-204.

Swanson, L. W. (1999). The neuroanatomy revolution of the 1970s and the hypothalamus. *Brain Res. Bull.* 50, 397.

Szabó, N.-E., Zhao, T., Cankaya, M., Theil, T., Zhou, X., and Álvarez-Bolado, G. (2009). Role of neuroepithelial Sonic hedgehog in hypothalamic patterning. *J. Neurosci.* 29, 6989-7002.

Teijido, O., Manso, M.J., Anadon, R. (2002). Distribution of thyrotropin-releasing hormone immunoreactivityin the brain of the dogfish *Scyliorhinus canicula*. *J. Comp. Neurol*. 454, 65-81.

Van de Kamer, J. C., and Shuurmans, A. J. (1953). Development and structure of the saccus vasculosus of *Scylliorhinus caniculus* (L.). *J. Embryol. Exp. Morphol*. 1, 85-96.

van Valen, L. M. (1982). Homology and causes. *J. Morphol.* 173, 305-12.

Vernier, P., and Wullimann, M. (2008). "Evolution of the posterior tuberculum and preglomerular nuclear complex," in *Encyclopedia of Neuroscience*, eds M. D. Binder, N. Hirokawa, and U. Windhorst (Berlin: Springer-Verlag), 1404-16.

von Kupffer K. (1906). "Die Morphogenie des Centralnervensystems", in: *Handbuch der Vergleichenden und Experimentellen Entwicklungslehre der Wirbeltiere*, ed. O. Hertwig vol 2, part III. (Fisher, Jena), p 1-2

USC
UNIVERSIDADE
DE SANTIAGO
DE COMPOSTELA

# RATIONALE AND AIMS

USC
UNIVERSIDADE
DE SANTIAGO
DE COMPOSTELA

## RATIONALE AND AIMS

To understand evolution, one has to understand change. On which concerns to morphological sciences, this task involves comparing structures recognizing similar and dissimilar characters under defined criteria. As the emergence of a certain structure relays on its developmental process, the differences observed between homologue structures during development can account for the variability of morphological structures. Such approach has been undertaken to understand the development and evolution (*evo-devo*) of the vertebrate brain, revealing important relationships in the prosencephalon, the most variable region of the neural tube. In this territory, an extensive work has been done during the last two decades, particularly focused on the telencephalon. However, in other prosencephalic regions, as the case of the hypothalamus, comparative relationships are not well understood, in spite that the hypothalamus has been a central concept in neuroanatomy and physiology because of its involvement in the coordination of autonomic, limbic and endocrine responses. Such organization has been difficult to systematize mainly because the hypothalamus develops at the ventral and rostral-most point of the brain where complex patterning process take place. As a result, the two main schools of brain organization, the columnar *vs* the segmental school, understand the hypothalamus in different ways relaying on different principles.

Noteworthy, during last years, a better understanding of non-telencephalic prosencephalon, and a growing body of developmental data on the hypothalamus, has favored a recent and novel segmental proposal on hypothalamic organization. Such organization is framed on the prosomeric framework developed by Puelles and Rubenstein and relays on different developmental data centered on the expression patterns of transcription factors and signaling molecules involved in the brain development of mammals. Noteworthy, the prosomeric framework has been a useful comparative tool for *evo-devo* studies.

In spite of the growing body of hypothalamic data from vertebrates of the osteichthyan lineage (bony fishes and tetrapods), a considerable lack of information exists about its out-group, chondrichthyans or cartilaginous fishes, which represent a fundamental group to understand the transition from jawless (agnathans) to jaw (gnatosthomes) vertebrates. Therefore, the scarcity of genoarchitectonic studies in basal vertebrates hampers the completion of the evolutionary scheme for hypothalamic development. In order to fill the gap of knowledge about the development of the hypothalamus in basal vertebrates and to shed light into the ancestral condition of this region along vertebrate phylogeny we have carried out a combination of anatomical and molecular experiments in *Scyliorhinus canicula*, the current model organism representative of cartilaginous fish.

The present thesis contains a corpus of results obtained by *in situ* hybridization and immunohistochemistry providing a comprehensive work on hypothalamic organization on sharks,

also addressing evolutionary trends under a prosomeric framework approach. In the last years, it has been highlighted the great potential of the shark *Scyliorhinus canicula* (known as catshark or lesser spotted dogfish) as model for identifying details of morphogenetic processes that take place during the brain regionalization, mainly because its slow development allows to perform detailed developmental and evolutionary studies. Noteworthy, this study forms part of a broad project that aims to know how the brain of chondrichthyans becomes patterned along its axis.
The specific aims of this thesis are:

1) To perform a primary analysis of the development of *S. canicula* hypothalamus from early stages to mid-gestation characterizing the main histogenetic territories, boundaries and surrounding tissues of the whole hypothalamus, according to the assumptions of such territories defined by the updated prosomeric framework for the mouse. The results of this study are presented in chapter 1 entitled **"Prosomeric organization of the hypothalamus in an elasmobranch, the catshark *Scyliorhinus canicula*".**

2) To deepen in further prosomeric molecular subdivisions in the alar hypothalamus; to better define the molecular alar-basal boundary (**ABB**) and; to obtain some insights on the evolution of the alar hypothalamus by comparative analysis. The results of this study are presented in chapter 2 entitled **"Prosomeric organization of the hypothalamus in an elasmobranch, the catshark *Scyliorhinus canicula*".**

**3)** To look for further prosomeric molecular subdivisions in the basal hypothalamus; to test if new data on gene expression patterns support our previous observations and; to obtain some insights on the evolution of this region by comparative analysis. The results of this study are presented in chapter 3 entitled **"The shark basal hypothalamus: molecular prosomeric subdivisions and evolutionary trends".**

# Chapter 1

# Prosomeric organization of the hypothalamus in an elasmobranch, the catshark *Scyliorhinus canicula*

The results of the present work are published in Santos-Durán GN, Menuet A, Lagadec R, Mayeur H, Ferreiro-Galve S, Mazan S, Rodríguez-Moldes I, Candal E. Prosomeric organization of the hypothalamus in an elasmobranch, the catshark *Scyliorhinus canicula* Frontiers in Neuroanatomy doi: 10.3389/fnana.2015.00037 (2015)

USC
UNIVERSIDADE
DE SANTIAGO
DE COMPOSTELA

# 1. PROSOMERIC ORGANIZATION OF THE HYPOTHALAMUS IN AN ELASMOBRANCH, THE CATSHARK *SCYLIORHINUS CANICULA*

## 1.1 INTRODUCTION

Biological diversity emerges, at least in part, through changes in development. Organisms are different because their developmental process differ and, what is more, because their developmental process also evolve (Kutschera and Niklas, 2004; Müller, 2007; Medina et al., 2011). Thus, the understanding of the development of the vertebrate brain becomes fundamental to comprehend its structure and evolution. In this context, the hypothalamus has been both a central and elusive topic. The hypothalamus is a conserved integrative center that coordinates autonomic, endocrine, and limbic responses (Sarnat and Netsky, 1981; Kandel and Schwartz, 2001; Butler and Hodos, 2005). Its development, at the base of the vertebrate forebrain (prosencephalon), involves complex patterning processes dependent on different signaling events that converge at this point. It also undergoes a complex morphological deformation during development, which misleads its topological (vs. topographic) location (Shimamura et al., 1995; Puelles and Rubenstein, 2003; Puelles, 2009; Puelles et al., 2012). As a result, the hypothalamic organization remains a matter of debate (Figdor and Stern, 1993; Puelles and Rubenstein, 2003; Shimogori et al., 2010; Diez-Roux et al., 2011; Puelles et al., 2012). Cross-species comparisons can be important to resolve this issue, and an important effort to understand the underlying unity of hypothalamic embryonic and adult organization across vertebrates has been made recently (Shimogori et al., 2010; Domínguez, 2011; Morales-Delgado et al., 2011, 2014; Moreno et al., 2012; Domínguez et al., 2013, 2014; Herget et al., 2014).

The prosomeric model (Puelles and Rubenstein, 2003; Puelles et al., 2004, 2012; Medina, 2008; Puelles, 2009) has become a key reference in such comparative studies, since it offers a mechanistic paradigm of the vertebrate brain structure and organization. Initially based on analyses of amniotes, this model defines for the first time anatomical structures as developmental hierarchical units based on specification mechanisms that determine longitudinal and transverse axis orientation, segmental structure, transcription factor expression profiles and the emergence of differential histogenetic domains (Puelles and Rubenstein, 2003; Puelles, 2009; Martínez et al., 2012).

A major interest and novelty of this model is that it puts emphasis on developmental criteria (including topological relationships among certain morphological landmarks, regulatory gene expression patterns and signaling molecules). Testing their conservation across vertebrates is a powerful approach for the correct establishment of homologies between embryonic territories beyond amniotes (Puelles and Medina, 2002). The underlying notion is that formation of the vertebrate brain involves a conserved core of highly

constrained, invariant mechanisms and genetic networks, which are the basis for homology establishment. This in no way excludes the emergence of diversifications through evolution, which are the source of the neuroanatomic diversity observed among vertebrates.

Latest updates of the model provide novel views on the organization of the rostral-most (secondary) prosencephalon, and its telencephalic and hypothalamic moieties (Puelles and Rubenstein, 2003; Pombal et al., 2009; Puelles et al., 2012). Detailed studies in different vertebrate groups are necessary to validate the model assumptions. Cartilaginous fishes or chondrichthyans are crucial in this task because they are among the most basal extant groups of gnathostomes (jawed vertebrates). Because of its phylogenetic position as the closest outgroup to osteichthyans (the other major phylum of gnathostomes, which includes bony fish and tetrapods), chondrichthyans are essential to reconstruct gnathostome ancestral characteristics through comparisons with other vertebrate models. Here we studied the molecular histogenetic organization of the hypothalamus and directly adjoining territories of an elasmobranch representative of one of the most basal extant gnathostome lineage, the catshark *Scyliorhinus canicula*, and analyzed them under the updated prosomeric framework. We have integrated data from neuroepithelial specification codes (based on the expression of catshark orthologues of *Foxg1a*, *Shh*, *Nkx2.1*, *Dlx2/5*, *Otp*, and *Tbr1*), and from the distribution of α-acetylated-tubulin immunoreactive (-ir) and TH-ir cell groups, neuron-fiber tracts (5-HT-ir) and glial-processes (GFAP-ir). In the search of conserved traits among jawed vertebrates, we compared our data in *S. canicula* with that obtained in murine models. Our analysis reveals a strikingly high degree in the conservation of hypothalamic histogenetic compartments between chondrichthyan and murine models. Furthermore, we identified some of the boundaries and confirmed some of the assumptions predicted by the prosomeric model. However, some differences and discrepancies also exist mainly concerning the neuroepithelial specification genetic codes of the basal hypothalamus (BHy). Similar studies are required in other basal species to figure out if these differences should prompt the model update or they are the consequence of shark specialization.

## 1. 2 MATERIALS AND METHODS

### 1.2.1 Experimental Animals

Some embryos of the catshark (lesser spotted dogfish; *S. canicula*) were supplied by the Marine Biological Model Supply Service of the CNRS UPMC Roscoff Biological Station (France) and the Estación de Bioloxía Mariña da Graña of the University of Santiago de Compostela. Additional embryos were kindly provided by the Aquaria of Gijón (Asturias, Spain), O Grove (Pontevedra, Spain) and the Aquarium Finisterrae (A Coruña, Spain). Embryos were staged by their external features according to Ballard et al. (1993). For more information about the relationship of the embryonic stages with body size, gestation and birth, see Table 1 in Ferreiro-Galve et al. (2010). Thirty-seven embryos from stages 12 to 31 were used in this study. Eggs from different broods were raised in seawater tanks in standard conditions of temperature (15–16◦C), pH (7.5–8.5) and salinity (35 g/L). Adequate measures were taken to minimize animal pain or discomfort. All procedures conformed to the guidelines established by the European Communities Council Directive of 22 September

2010 (2010/63/UE) and by the Spanish Royal Decree 53/2013 for animal experimentation and were approved by the Ethics Committee of the University of Santiago de Compostela.

### 1.2.2 Tissue Processing

Embryos were deeply anesthetized with 0.5% tricaine methanesulfonate (MS-222; Sigma, St. Louis, MO, USA) in seawater and separated from the yolk before fixation in 4% paraformaldehyde (PFA) in elasmobranch's phosphate buffer [EPB: 0.1Mphosphate buffer (PB) containing 1,75% urea, pH 7.4] for 48–72 h depending on the stage of development. Subsequently, they were rinsed in phosphate buffer saline (PBS), cryoprotected with 30% sucrose in PB, embedded in OCT compound (Tissue Tek, Torrance, CA, USA), and frozen with liquid nitrogen-cooled isopentane. Parallel series of sections (12–20 μm thick) were obtained in transverse and sagittal planes on a cryostat and mounted on Superfrost Plus (Menzel-Glasser, Madison, WI, USA) slides.

### 1.2.3 Single and Double Immunohistochemistry on Sections and Whole Mounts

For heat-induced epitope retrieval, sections were pre-treated with 0.01 M citrate buffer (pH 6.0) for 30 min at 95◦C and allowed to cool for 20–30min at room temperature (RT). Sections were then rinsed twice in 0.05 M Tris-buffered saline (TBS; pH 7.4) for 5 min each and incubated overnight with the primary antibody (rabbit anti-serotonin [anti-5-HT] polyclonal antiserum, DiaSorin, Immunostar, Hudson, WI, USA, diluted 1:5000; polyclonal rabbit anti-Sonic Hedgehog [anti-Shh], Sta. Cruz Biotechnology, Santa Cruz, CA, USA, diluted 1:300; polyclonal rabbit anti-glial fibrillary acidic protein [anti-GFAP], Dako, Glostrup, Denmark, diluted 1:500; and monoclonal mouse antityrosine hydroxilase [anti-TH], Millipore, Billerica, MA, USA, diluted 1:500). Appropriate secondary antibodies [horseradish peroxidase (HRP)-conjugated goat anti-rabbit and anti-mouse, BIORAD, diluted 1:200] were incubated for 2 h at RT. For double immunohistochemistry (IHC) experiments, cocktails of primary antibodies were mixed at optimal dilutions and subsequently detected by using mixtures of appropriate secondary antibodies. Sections were rinsed in distilled water (twice for 30 min), allowed to dry for 2 h at 37◦C and mounted in MOWIOL 4-88 Reagent (Calbiochem, MerkKGaA, Darmstadt, Germany). All dilutions were made with TBS containing 15% donkey normal serum (DNS; Millipore, Billerica, MA, USA), 0.2% Triton X-100 (Sigma) and 2% bovine serum albumin (BSA, Sigma). Double IHC with primary antibodies raised in the same species was performed as described in Tornehave et al. (2000).

For whole mounts embryos were prepared as previously described in Kuratani and Horigome (2000) with minor modifications. After fixation with 4% PFA in 0.01 M PBS at 4◦C for 2 days, embryos were washed in 0.9% NaCl in distilled water, dehydrated in graded series of methanol solutions (50, 80, 100%) and stored at −20◦C. Samples to be stained were placed on ice in 2 mL of dimethyl sulfoxide (DMSO)/methanol (1/1) until they sank. Then, 0.5 mL of 10% Triton X-100/distilled water was added, and the embryos were incubated for

30 min at RT. After washing in 0.05 M TBS with 0.1% Triton X-100 (TST, pH 7.4) the samples were sequentially blocked using spin-clarified aqueous 1% periodic acid and 5% non-fat dried milk in TST (TSTM). Primary antibody (monoclonal mouse anti-α-acetylated-tubulin, Sigma, 1:1000) was diluted in TSTM containing 0.1% sodium azide for 2–4 days at RT with gently agitation on a shaking platform. The secondary antibody HRP-conjugated goat anti-rabbit, BIORAD, dilution 1:200 in TSTM) was incubated overnight. After a final washing in TST, the embryos were pre-incubated with 0.25 mg/mL diaminobenzidine tetrahydrochloride (DAB, Sigma) in TST with 2.5 mg/mL nickel ammonium sulfate for 1 h, and then allowed to react with DAB in TST containing 2.5mg/mL nickel ammonium sulfate and 0.00075% H2O2 for 20–40 min at RT. The reaction was stopped using Tris-HCL buffered saline and specimens were post-fixed with 4% PFA overnight at 4◦C. Epidermis and mesodermic derivatives were carefully removed and specimens were rinsed in graded series of glycerol (25, 50, 75, and 100%) in order to directly observe the neural tube under the stereomicroscope.

### 1.2.4 Controls and Specificity of the Antibodies

No immunostaining was detected when primary or secondary antibodies were omitted during incubations. Controls and specificity of anti-TH and anti-5-HT were performed as described in Pose-Méndez et al. (2014). The primary anti-α-acetylated-tubulin antibody has been shown to label early differentiated neurons and their processes in the embryonic nervous system (Piperno and Fuller, 1985; Chitnis and Kuwada, 1990). The polyclonal anti-Shh antibody (Santa Cruz Biotechnology Inc, CA, USA) was raised in rabbit against the amino acids 41–200 of Shh human protein. The *in situ* hybridization (ISH) results were similar to those obtained by IHC, and therefore validate the specificity of the anti-Shh antibody used here.

### 1.2.5 *In Situ* Hybridization on Whole Mount Embryos and on Sections

We applied ISH for *ScFoxg1a*, *ScShh* (Compagnucci et al., 2013; Quintana-Urzainqui, 2013), *ScNkx2.1* (Quintana-Urzainqui et al., 2012; Quintana-Urzainqui, 2013), *ScDlx5* (Compagnucci et al., 2013; Debiais-Thibaud et al., 2013), *ScOtp* (Quintana-Urzainqui, 2013), *ScTbr1* (Quintana-Urzainqui, 2013), and *ScDlx2* (Quintana-Urzainqui et al., 2012; Compagnucci et al., 2013; Debiais-Thibaud et al., 2013; Quintana-Urzainqui, 2013) genes. These probes were selected from a collection of *S. canicula* embryonic cDNA library (mixed stages 9–22), constructed in pSPORT1, and submitted to high throughput EST sequencing. cDNA fragments were cloned in pSPORT vectors. Sense and antisense digoxigenin-UTP-labeled and fluorescein-UTP-labeled probes were synthesized directly by *in vitro* transcription using as templates linearized recombinant plasmid DNA or cDNA fragments prepared by PCR amplification of the recombinant plasmids. ISH in whole mount and on cryostat sections was carried out following standard protocols (Coolen et al., 2009). Briefly, sections were permeabilized with proteinase K, hybridized with sense or antisense probes overnight at 65◦C (in sections) or 70◦C (whole mount) and incubated with the alkalinephosphatase-coupled anti-digoxigenin and anti-fluorescein antibody (1:2000, Roche

Applied Science, Manheim, Germany) overnight at 4◦C. The color reaction was performed in the presence of BM-Purple (Roche). Control sense probes did not produce any detectable signal.

Exhaustive phylogenetic characterizations of the catshark *Dlx* gene repertoire have been previously published (Debiais-Thibaud et al., 2013), confirming the identity of *ScDlx2* and *ScDlx5*. The unambiguous identification of the catshark orthologues of *Foxg1*, *Shh*, *Nkx2.1*, *Otp*, and *Tbr1* has been also demonstrated by the group of Dr. Sylvie Mazan, which accomplished a systematic phylogenetic analysis of the corresponding vertebrate gene families, including all the vertebrate classes derived from duplications of a single ancestral chordate orthologue (Santos-Durán et al., 2015)

### 1.2.6 Image Acquisition and Analysis

Light field images were obtained with an Olympus BX51 microscope equipped with an Olympus DP71 color digital camera. *In toto* embryos were analyzed in the Olympus SZX12 stereomicroscope fitted to an Olympus DP12 color digital camera. Photographs were adjusted for brightness and contrast and plates were prepared using Adobe Photoshop CS4 (Adobe, San Jose, CA, USA).

## 1.3. RESULTS

### 1.3.1 Preliminar Considerations Concerning Vertebrate Segmental Prosencephalic Organization

The organization of the shark hypothalamus has been analyzed in the framework of the updated prosomeric model (Puelles et al., 2012). **Figure 1** summarizes the general architecture of the hypothalamus in mouse according to the updated prosomeric model (Puelles et al., 2012). This model is mainly inspired in murine data though it is usually assumed that it can be extrapolated to all vertebrates because it also integrates information from other vertebrates (Puelles and Rubenstein, 2003; Pombal et al., 2009; Puelles, 2009). Indeed, this model represents a useful developmental and comparative framework since it makes use of concepts, nomenclature and topological references that can be used across different vertebrate species.

The prosomeric model establishes that hypothalamus and telencephalon are part of the secondary prosencephalon, which is understood as a segmental unit at the rostral-most point of the neural tube, the hypothalamus being located ventral to the telencephalon and rostral to the diencephalon (see **Figure 1A**). The model also postulates that the rostral-most point of the brain, referred as the acroterminal region (At), lies at the rostral border of the secondary prosencephalon. This region is restricted to the frontal border of the neural tube where left and right alar and basal plates meet. This border expands dorso-ventrally from the rostral-most roof plate (which is telencephalic) to the rostral-most floor plate (which is hypothalamic). Thus, every structure classically considered being dorsal or ventral to these

points (see arrowheads in **Figure 1A**), should be considered as caudal in this framework. Of note, the anterior commissure, located in the rostral-most roof plate, is a clear landmark of both the dorso-ventral and rostro-caudal axis (Puelles et al., 2012; see also **Figures 1A, B**).

The secondary prosencephalon presents two true segments rostro-caudally arranged (**Figure 1B**): hp2 (rostral or terminal) and hp1 (caudal or peduncular). Each segment harbors telencephalic and hypothalamic derivatives (**Figures 1B, C**). However, the telencephalon harbors only roof and alar plates while the hypothalamus harbors alar, basal, and floor plate derivatives. The existence of these segments is supported by several genes differentially expressed in the rostro-caudal axis, the location of commissures in the roof and floor plates (anterior and retromamillary commissures, respectively), and the course of important tracts [medial forebrain bundle (mfb); lateral forebrain bundle (lfb); and fornix (fx)] running by a common path at the rostral border of hp1, through alar and basal plates. These data, in turn, support the existence of an intersegmental boundary that separates terminal and peduncular subdivisions of both telencephalon and hypothalamus, which is referred as the intrahypothalamic boundary (IHB; **Figures 1B, C**). Caudally, the secondary prosencephalon limits with the diencephalon at the hypothalamic diencephalic border (HDB), another intersegmental limit among hp1 and p3, though it should be noticed that part of the caudal limit of the secondary prosencephalon does correspond to the telencephalon (Puelles et al., 2012; see also **Figure 1C**).

The model considers the adult hypothalamic organization arranged in different histogenetic territories defined by neuroepithelial specification codes and radial units (Puelles and Medina, 2002; Puelles et al., 2012). These codes reveal that telencephalon and hypothalamus belong to different histogenetic territories being the preoptic area (POA) the unique terminal territory of the telencephalon (**Figure 1C**). Of note, the POA also harbors the anterior commissure (Puelles et al., 2012; see also **Figures 1B, C**).

### 1.3.2 *ScFoxg1a* Expression

In mice, *Foxg1* is one of the earliest transcription factors expressed specifically in the part of the neural plate that gives rise to the telencephalon and it remains expressed throughout the telencephalon during embryonic development (see Manuel et al., 2011). In an attempt to discriminate telencephalic and underlying hypothalamic domains throughout *S. canicula* development, we have analyzed the expression of *ScFoxg1a* in the developing nervous system of this species. At stage 18, *ScFoxg1a* expression was found in the dorsal-most portion of the secondary prosencephalon including the optic cup, extending from the level of the optic stalk (which is located rostrally, within the At) up to a caudal point in the roof plate, which has been tentatively identified as the dorsal border between the telencephalon and the diencephalon (**Figure 2A**). At stage 22, *ScFoxg1a* was observed in the telencephalon and in the nasal part of the optic cup (**Figure 2B**). The expression in the telencephalon was maintained until late stages of development (**Figure 2C**), which allowed identifying the border between the telencephalon and the hypothalamus.

### 1.3.3 *ScShh* Expression

*ScShh* expression was detected during gastrulation (stage 12) in the caudal midline of the embryo (data not shown). At stage 14, during early neurulation, it has been detected in the axial mesoderm of the notochord and the prechordal plate and in the ectoderm of the caudal midline (data not shown). After the closure of the neural tube (stage 17), the signal was detected as a ventral longitudinal continuous band that extends from the caudal end of the spinal cord to the At of the forebrain, roughly at the level of the optic stalk (**Figure 2D**). As in other vertebrates (Shimamura et al., 1995), the expression of *ScShh* can be used to define the alar-basal boundary (ABB; **Figures 2E–H**). At stage 19, *ScShh* expression became downregulated in the forebrain to progressively give rise to a caudal and a rostral domain (arrow in **Figures 2E–H**). The narrow transverse and dorsally directed stripe of *ScShh*-expressing cells within the caudal domain was identified as the developing zona limitans intrathalamica (zli; arrowhead in **Figure 2G**). The rostral border of the *ScShh* caudal domain, in turn, was somewhat extended rostral to the HDB (Puelles et al., 2012), which at this stage was identified as the point where the neural tube expands to acquire the distinctive shape of the ventral hypothalamus. Therefore, the BHy appeared to be divided in three domains: two positive for *ScShh* (one rostral and other caudal) and one (intermediate) negative for *ScShh* (arrow in **Figures 2G, H**; see also Figure 5H in Compagnucci et al., 2013). Of note, the dorsal border of the rostral domain (presumably corresponding to the ABB) seems to codistribute with α-acetylatedtubulin-immunoreactive (-ir) longitudinal tracts (arrowheads in **Figure 2I**). At stage 24 (**Figure 2H**), a new domain emerged within the telencephalon. This short domain (arrowhead in **Figure 2H**) extended from a region located dorsally to the optic stalk without reaching the prospective territory of the anterior commissure (that can be identified at early development by means of α-tubulin-immunoreactivity; asterisk in **Figures 2H, I**). A clear gap of expression was observed between this telencephalic domain and the rostral hypothalamic one (**Figure 2H**). The telencephalic domain was located medially while the hypothalamic one also expanded laterally (not shown). From stage 27 onward the zli expanded dorsally toward the roof plate (arrowhead in **Figure 3A**). At stage 29 the medio-lateral histologic organization of the developing walls of the forebrain become more evident. As in previous developmental stages, Shh immunoreactivity was clearly identified in the basal plate of the diencephalon entering the caudo-ventral part of the BHy (arrow in **Figures 3A, B, B´**) and in the rostro-dorsal part of the BHy (**Figures 3A, B**), so that a clear negative gap of Shh-immunoreactivity occupied most of the caudal BHy (CBHy; **Figures 3A, B**) and part of the rostral BHy (RBHy). In the telencephalon, Shh-immunoreactivity expanded caudally beyond the prospective territory of the anterior commissure (arrowhead in **Figure 3B**; compare with **Figure 2H**). Of note, from late stage 30 onward, Shh-immunoreactivity is downregulated in the CBHy and basal diencephalon, except in the zli (data not shown).

### 1.3.4 *ScNkx2.1* Expression

The expression of *ScNkx2.1* was first detected at stage 18 in the rostro-ventral portion of the forebrain, in a longitudinal band which extended ventral to the optic stalk (arrowhead in **Figure 2J**). At stage 23 *ScNkx2.1* was expressed in most of the BHy (**Figure 2K**).

Differently from *ScShh, ScNkx2.1* delimited the ABB even in the CBHy (**Figure 2K** compare with **Figure 2G**), though a small gap of expression was observed within the caudo-ventral part of the BHy (arrow in **Figure 2K**). A second domain emerged in the telencephalon at this stage (arrowhead in **Figure 2K**). This domain was restricted to the rostral-most portion of the telencephalon and extended from a region located dorsally to the optic stalk to the prospective territory of the anterior commissure (asterisk in **Figure 2K**). A clear gap of expression was observed between the telencephalic and the hypothalamic domains. At stage 25 (**Figure 2L**), as in previous developmental stages, *ScNkx2.1* expression was lacking in a small domain located within the caudo-ventral BHy (arrow in **Figure 2L**). This region seems to fit with the rostral border of a basal α-acetylated-tubulin-ir tract [see mamillo-tegmental tract (MTT) in **Figure 2I**]. In the telencephalon, *ScNkx2.1* expression became caudally expanded beyond the prospective territory of the anterior commissure (asterisk in **Figure 2L**). At stage 29, as in previous developmental stages, *ScNkx2.1* was observed throughout most of the BHy, except in a small wedge-shaped domain within the caudo-ventral BHy (arrowhead in **Figures 3C, D**). Groups of *ScNkx2.1*-expressing cells in the caudo-ventral portion of the hypothalamus were observed along the marginal zone (arrows in **Figures 3C, C´, D**). In the telencephalon, *ScNkx2.1* expression expanded beyond the territory it occupied at previous developmental stages (asterisk in **Figure 3D**). Of note, Shh immunoreactivity was overlapping with *ScNkx2.1* expression beyond the anterior commissure (**Figure 3D**).

### 1.3.5 *ScDlx2/ScDlx5* Expression

We analyzed the expression of *ScDlx5* from stage 18 onward and the expression of *ScDlx2* from stage 29 onward. Fairly identical results were observed with both markers in the brain of *S. canicula* from stage 29 onward, so we use *ScDlx2/5* at these stages to refer indistinctly to both.

General features of *ScDlx5* expression and detailed profiles in the developing branchial arches have been previously described from stage 15 to stage 27 in Compagnucci et al. (2013) and from stage 15 to stage 25 in Debiais-Thibaud et al. (2013). We revisited these data focusing on the developing forebrain. At stage 18, *ScDlx5* expression was found in the most anterior part of the neural tube (**Figure 2M**; compare with **Figure 2A**; see also Figure 5C1 in Debiais-Thibaud et al., 2013). From stage 21 to 25, *ScDlx5* becomes mostly restricted to the anterior-most part of the telencephalon and to the olfactory placodes (**Figure 2N**; see also Figure 4G in Compagnucci et al., 2013 and Figure 5C'1 in Debiais-Thibaud et al., 2013). However, at later stages (**Figure 2O**), *ScDlx5* expression spread caudally and ventrally (arrowheads in **Figure 2O**) and reached the rostral-most portion of the optic stalk (see also Figure 9C in Debiais-Thibaud et al., 2013). This domain was fairly continuous with a longitudinal band of *ScDlx5* that crossed through the hypothalamus over the ABB (compare with **Figures 2H, L**) and entered p3 (**Figure 2O**). Therefore, this domain delineates the ABB along the hypothalamus. Of note, the longitudinal domain appeared to codistribute with α-acetylated-tubulin tracts (arrowheads in **Figure 2I**). Although both *ScDlx5* domains were continuous, a wedge-shaped area of reduced signal intensity was

observed between the dorsal (telencephalic) and the ventral (hypothalamic-diencephalic) domains (**Figure 2O**). Two bands of cells were additionally observed, which were ventrally located with respect to the longitudinal domain (arrows in **Figure 2O**). One was located at its caudal end and spread ventral-ward at the rostral end of p3. The other spread perpendicularly to the ABB from the caudo-dorsal part of the BHy up to the rostral hypothalamus (**Figure 2O**). Of note, this *ScDlx5*-expressing domain appeared to delineate *ScShh* expression in the rostral hypothalamus (compare with **Figure 2H**). This pattern became more patent at stage 29 (**Figures 3E, F**). At this stage, *ScDlx2/5*-expression was observed in the telencephalon (subpallium). The telencephalic domain is almost continuous at medial levels (black asterisk in **Figure 3F**) while a clear gap of expression was observed at the level of the anterior commissure in parasagittal sections (black asterisk in **Figure 3E**). *ScDlx2/5* expression was also observed in a longitudinal domain outlining the ABB, which crossed through the alar hypothalamus (AHy) and entered p3 (**Figure 3E**). A wedge-shaped negative domain separated the telencephalic and hypothalamic-diencephalic domains (**Figure 3E**). A transverse band of non-ventricular *ScDlx2/5*- expressing cells was observed extending ventral-ward from the alar plate (arrow in **Figures 3E, E´**), along the rostral-most p3Tg. This domain appeared to overlap with the *ScShh*-expressing domain from which the zli emerged (compare with **Figure 3A**). As observed previously, an additional domain (arrowhead in **Figures 3E, F**) cut across the BHy perpendicularly to the ABB. This pattern was maintained until late stages of development (**Figure 3M**).

### 1.3.6 *ScOtp* Expression

At stage 19, *ScOtp* signal was detected in the rhombencephalon and in the rostral-most and ventral-most portion of the optic stalk (arrowhead in **Figure 2P**) though a faint *ScOtp* expression was also observed in part of the BHy and in the AHy. At stage 25, three domains of *ScOtp* expression were observed in the forebrain. The rostral one was restricted to the rostral-most region of the forebrain, expanding ventrally from the optic stalk along the RBHy without reaching the prospective neurohypophysis. The second domain abutted the HDB at the intersection with the ABB and spread from this region up to the rostro-ventral hypothalamus. The third domain overlaid the ABB from the optic stalk up to the alar p3 and was poorly stained compared to the other two domains (arrowhead in **Figure 2Q**). From stage 28 onward these three domains were respectively identified in the RBHy (in **Figure 3G**), in an arched domain that spread from the CBHy (arrow in **Figures 3G, G´**) and in the AHy (black arrowheads in **Figure 3H**). In the BHy, a small domain containing *ScNkx2.1* alone was identified caudal to the *ScOtp*-expressing domain (arrow in **Figure 3G**).

A novel domain of non-ventricular scattered *ScOtp*-expressing cells was also detected entering p3Tg from the most caudoventral part of the BHy (arrowheads in **Figures 3G, G´´, H´**). Scattered *ScOtp*-expressing cells were observed between the alar and basal domains of the caudal hypothalamus (white arrowhead in **Figure 3H**). In the AHy, *ScOtp*-expressing cells were only observed at parasagittal levels (**Figure 3H**; compare with **Figure 3G**). Of note, non-ventricular *ScOtp*-expressing cells appeared to codistribute with the longitudinal band of *ScDlx2/5* expression over the ABB (**Figure 3H**; compare with **Figure 3F**). *ScOtp*-

expressing cells were also observed in the telencephalon (data not shown). This pattern is maintained until late stages of development. At stage 30 (**Figure 3N**), a gap of *ScOtp* expression was observed at parasagittal levels that divide the AHy in rostral and caudal domains.

### 1.3.7 *ScTbr1* Expression

*ScTbr1* signal was detected at stage 25 in dispersed cells that spread the telencephalic vesicle (**Figure 2R**), except for a rostral domain that extended from the optic stalk to the prospective territory of the anterior commissure (asterisk in **Figure 2R**). Of note, α-acetylated-tubulin-ir tracts reaching the telencephalon seem to define the boundary between telencephalic *ScTbr1* positive and negative domains (see sot in **Figure 2I**; compare with **Figure 2R**). *ScTbr1* expression was additionally observed in the dorsal most part of the alar p3, abutting the *ScDlx5* domain that entered p3 (**Figure 2R**; compare with **Figure 2O**). At stage 29, the extension of the *ScTbr1*-expressing domain became decreased in the telencephalic vesicle (not shown).

### 1.3.8 5-HT + Shh Immunoreactivity

Anti-5-HT immunoreactivity was coanalyzed with anti-Shh immunoreactivity at stage 30 to better understand the segmental organization of different fiber bundles, which in turn contributes to the understanding of the organization of the hypothalamus. Immunoreactivity for both markers was examined at stage 30 when the first 5-HT fibers reach the telencephalon (Carrera et al., 2008). Positive fibers were observed coursing parallel to the ABB (**Figure 3I**). Besides, some fibers were detected ascending throughout the AHy (white arrowhead in **Figures 3J, K**) toward the telencephalon (black arrowhead in **Figures 3J, L**) from the caudal part of the hypothalamus. This pathway seemed to concur with negative domains for *ScDlx2/5* and *ScOtp* genes at the same developmental stage (**Figures 3M, N**). A group of decussating fibers was detected close to the most caudo-ventral region of the hypothalamus (arrow in **Figures 3J, K**) that coincides with the caudal-most and ventral-most domain of *ScNkx2.1* in the BHy (**Figure 3J**; compare with **Figures 3C, D**) and also with the rostral end of the ventral-most α-acetylated-tubulin-ir tract at stage 25, that could represent a pioneering tract, the mamillo-tegmental tract (MMT in **Figure 3I**). Of note, from stage 30 onward, Shh immunoreactivity was only observed in the rostral portion of the zli but not in the caudo-ventral part of the BHy nor the diencephalic basal plate (**Figure 3J** and arrow in **Figure 3L**).

### 1.3.9 GFAP Immunoreactivity

Glial fibrillary acidic protein immunoreactivity was also analyzed in the forebrain at stage 31. Radial and longitudinal GFAP-ir processes were detected through the whole forebrain (**Figures 3O, P**). Ascending fibers to the telencephalon were detected in a similar pathway to that described above for 5-HT (black arrowhead in **Figure 3O**; compare with white arrowhead in **Figure 3K**). Some GFAP-ir processes were also observed in the same

point where 5-HT-ir fibers decussate in the caudo-ventral part of the BHy (arrow in **Figure 3O**; compare with **Figure 3K**). GFAP-ir processes were also observed in the subpallium (arrow in **Figure 3P**).

## 1.4. DISCUSSION

### 1.4.1 Alar Hypothalamus

According with the updated prosomeric model (Puelles et al., 2012; see also **Figure 4A**) the AHy, together with the telencephalon, are the rostral-most regions of the alar plate. The AHy is located ventral to the *Foxg1*-expressing telencephalon, dorsal to the BHy (which is characterized by the expression of *Nkx2.1* in its whole extension except in its caudal-most portion), and rostral to the alar p3 (characterized by the complementary expression of *Dlx* and *Tbr1* genes). Within the territory delimitated by the above-mentioned genes, two longitudinal (dorso-ventrally arranged) histogenetic domains are defined based on the complementary expression of *Dlx* and *Otp* genes. The dorsal-most domain is termed paraventricular domain (Pa), and expresses *Otp* but not *Dlx* genes. The ventral-most is the subparaventricular domain (SPa), which expresses *Dlx* genes but not *Otp*. *Dlx* is expressed beyond the HDB in the alar p3. The alar HDB is defined by the clear-cut expression among genes restricted to the AHy (*Sim1*, *Otp)* or to the alar p3 (*Lhx9*, *Arx*, *Olig2* among others). The alar p3, besides, includes the prethalamic eminence (PThE) and express genes in a complementary manner (PThE: *Tbr1*, *Lhx9*, *Gdf10*; alar p3: *Dlx* genes, *Arx*, *Gsh2*). Moreover, according with the prosomeric model both, Pa and SPa domains, present terminal (hp2) and peduncular (hp1) domains (TPa, PPa; TSPa, PSPa respectively). However these subdomains cannot be genetically identified without additional markers. Thus, the AHy presents at least four different histogenetic domains although some work on the development of hypothalamic peptidergic cells point to much more subdivision (**Figure 4A**; see also Morales-Delgado et al., 2011, 2014; Puelles et al., 2012).

In the shark, we have studied the expression of *ScFoxg1a*, *ScShh*, *ScNkx2.1*, *ScDlx2/5*, *ScOtp*, and *ScTbr1*, which allow us to identify an AHy harboring Pa-like and Spa-like histogenetic domains and their boundaries. The early expression territories of *ScFoxg1a*, *ScNkx2.1* and *ScOtp/ScTbr1* define the dorsal, ventral and caudal limits of the AHy, respectively (**Figures 2B, K, Q, R**; see also **Figure 4B**). Thus, *ScFoxg1a* was expressed from early stages of development in the presumptive telencephalon (**Figure 2C**), leading to the identification of the telencephalon-AHy border (see also **Figure 4B**). *ScNkx2.1* was expressed in most of the BHy (**Figure 2K, L**) and delineates the ABB (see also **Figure 4B**). The caudal border of the AHy could be delimited at stage 25 by the caudal-most expression of *ScOtp* at parasagittal levels (**Figure 2Q**; see also **Figure 4B**). Both *ScOtp* and *ScDlx5* were expressed from stage 25 onward within the AHy, though the intensity of the expression increases in late stages of development. At stage 29, both *ScOtp* and *ScDlx2/5* were observed in the AHy. Of note, two mutually exclusive histogenetic domains dorsoventrally arranged could be readily observed at ventricular levels (**Figures 3E, H**; see also **Figure 4B**), though non-ventricular *ScOtp*-expressing cells were also observed within the *ScDlx2/5* domain.

These observations allowed us to identify the TPa/PPalike and the TSPa/PSPa-like domains (**Figure 4B**). The former, *ScOtp*-expressing one, abutted a *ScTbr1* domain that occupied the dorsal-most part of p3 (the PThE; **Figure 4B**), which is also negative for *ScDlx2/5* (compare with **Figures 3E, E´**). The latter, *ScDlx2/5*-expressing one, as in mouse, was continuous with the transverse *ScDlx2/5*-expressing domain in p3 (**Figures 3E** and **4B**).

In the mouse, and using markers homologous to those studied here, termino-peduncular compartments can be differentiated only by the late expression of *Tbr1* in the mantle of PPa (Puelles et al., 2012). While *ScTbr1* marker did not reveal rostro-caudal differences in the shark, we discerned these compartments by means of the identification of the mfb, which coursed caudally to the IHB (see below).

### 1.4.2 Basal Hypothalamus

The BHy is the rostral-most territory of the basal and floor plates. It is located ventrally to the AHy and rostral to the basal p3 (p3Tg; **Figure 4A**). The BHy is characterized by the expression of *Nkx2.1* in its whole extension with the exception of its caudal-most region. It harbors three longitudinal domains dorso-ventrally arranged: tuberal/retrotuberal region (Tu/RTu); perimamillary/periretromamillary region (PM/PRM) and mamillary/retromamillary region (MM/RM). These domains harbor terminal and peduncular parts separated by the IHB. The peduncular domains are distinctly referred in this basal region with the prefix "retro" while the terminal lack prefix. In the mouse (**Figure 4A**), the Tu/RTu compartment is characterized by the expression of *Dlx5* although it also presents subdomains expressing *Shh* (in part of the Tu and the whole RTu); the PM/PRM is characterized by the expression of *Nkx2.1* and *Otp* although *Shh* is also expressed in the PRM; the MM only expresses *Nkx2.1* (being the caudal and ventral-most portion of the *Nkx2.1* domain) while the RM express *Shh* and other genes in a complementary manner to *Nkx2.1* (see Morales-Delgado et al., 2011, 2014; Puelles et al., 2012). The basal HDB is defined by the clear-cut expression among genes restricted to the caudal part of the hypothalamus (*Pitx2, Lhx5* among others) or to the p3Tg (*Nr5a1, Nkx6.1*; Puelles et al., 2004, 2012; Medina, 2008).

In the shark, the analysis of the expression of *ScShh, ScNkx2.1, ScDlx2/5,* and *ScOtp* highlighted the presence of Tu/RTu-like, PM/PRM-like and MM/RM-like histogenetic domains within the BHy. However, the relative organization of some of these expression territories differed between the catshark and mammals. While *ScNkx2.1* expression territories were well established in the BHy from early stages of development, the other markers analyzed here showed a more dynamic pattern through development. We chose to focus on stage 29 for the interpretation of these data, all studied markers exhibiting a strong expression at this stage, with sharp boundaries.

In mouse, according with the prosomeric model, the *Nkx2.1* territory in the basal plate located dorsal to the *Otp*, is considered to represent the Tu/RTu domain. *Dlx* genes are widely expressed in this domain (**Figure 4A** and Puelles and Rubenstein, 2003), though

some tuberal areas lack *Dlx* gene signal (Morales-Delgado et al., 2011). Accordingly, in *S. canicula*, the BHy located dorsal to the *ScOtp*-expressing domain was interpreted as the Tu/RTu-like domain (**Figure 4B**). Within this territory, *ScOtp* was expressed in a restricted stripe at the most rostro-dorsal part of the basal plate spreading ventral-ward from the ABB without reaching the neurohypophysis (see **Figures 2Q** and **4B**). *ScShh* overlapped with this domain, extended caudally and abutted a *ScDlx2/5*-expressing domain that extended from the ABB up to the neurohypophysis. Therefore, in sharks, the Tu/RTu-like domain would be composed by four subdomains: a rostro-dorsal subdomain coexpressing *ScShh*, *ScOtp* and *ScNkx2.*1; a second subdomain expressing *ScShh* and *ScNkx2.1*; a third subdomain expressing *ScDlx2/5* and *ScNkx2.1;* and a ventral subdomain expressing *ScNkx2.1* alone (compare **Figures 3C, D**; see also **Figure 4B**). As in mouse, and with the markers studied here, it was not possible to establish a clear distinction between the Tu-like and the RTu-like compartment. It is noteworthy that the Tu/RTulike compartment has a different histogenetic identity to that described in the mouse. On one hand, *ScShh* was down-regulated in a large portion of the BHy. On the other, *ScDlx2/5* expression appeared much more restricted than in mouse, and different subdomains could be delineated, including a domain expressing *ScNkx2.1* alone in midsagittal sections (**Figures 3C, D**; see also **Figure 4B**). In mouse, the single domain in the BHy that contains *Nkx2.1* expression alone was identified as the MM region. The *ScNkx2.1* expressing region ventral to *ScDlx2/5* is unlikely to correspond to the MM for two reasons. First, it is not the only compartment where we detect the expression of *ScNkx2.1* alone. Indeed, in mid-sagittal sections, a small domain can be observed ventral to *ScOtp*, which expressed *ScNkx2.1* alone (**Figures 3G´´** and **4B**). Second, the presence of a MM-like domain at this location would imply the interruption of longitudinal compartments (MM-like located dorsally to PM-like) and the redefinition of terminal domains within the BHy. Since it has been previously reported that, in mouse, some tuberal areas lack *Dlx* gene signal (Morales-Delgado et al., 2011), the most parsimonious interpretation implies that this *ScDlx2/5*-lacking region belongs to the Tu/RTu-like area and that *ScDlx2/5* cannot be used to identify the ventral border of the Tu/RTu-like domain, at least in mid-sagittal sections.

According to the prosomeric model, in mouse, adjacent to the Tu/RTu area, a distinct PM/PRM histogenetic domain exists in which *Otp* expression is selectively found. In *S. canicula*, *ScOtp* expression was observed in an arched domain that spread from the CBHy at the ABB/HDB junction and entered the rostral hypothalamus (**Figures 3G´´** and **4B**). At its caudal-most portion, this domain seems to express *ScOtp* only in the ventricular zone (asterisk in **Figures 3G´, H**; see also **Figure 4B**), while in its rostral-most portion *ScOtp* is mainly expressed on mantle cells. This *ScOtp*-expressing domain (including either ventricular or mantle cells) was therefore interpreted as a PM/PRM-like domain, where the PRM-like domain is likely to correspond to caudal *ScOtp* expression in cells at the ventricular zone, and the PM-like would mainly correspond to rostral *ScOtp* expression in mantle cells.

As in mouse, a small domain containing *ScNkx2.1* alone was identified ventral to the *ScOtp*-expressing domain (**Figures 4A, B**). This domain abutted a *ScShh*-expressing domain which expanded caudally through the diencephalic basal plate (**Figure 4B**). Based on these

expression similarities, the *ScNkx2.1* and *ScShh*-expressing territories were respectively identified as the MM-like and the RM-like domains. The caudal border of the RM-like domain abutted a transverse band of non-ventricular *ScDlx2/5*-expressing cells at the p3Tg (**Figures 3E**; see also **Figure 4B**). These *ScDlx2/5*-expressing cells are just ventral to the *ScDlx2/5*-expressing domain in the alar p3, supporting their assignment to p3Tg. Furthermore, these cells are in the same position that Pax6-ir cells in the caudal posterior tuberculum of the shark, described by Ferreiro Galve (2010) at equivalent developmental stages. Similar diencephalic basal plate *Dlx*-expressing cells have not been described in the mouse but *Dlx2*- and *Pax6*-expressing cells have been described in the basal plate of zebrafish as belonging to the preglomerular complex (p3Tg), suggesting that their presence may be an ancestral characteristic of jawed vertebrates lost in mammals (Ishikawa et al., 2007; Vernier and Wullimann, 2008). Accordingly to this, the HDB in the basal plate lie rostral to non-ventricular *ScDlx2/5*-expressing cells in p3Tg.

### 1.4.3 Posterior Tuberculum

The shark hypothalamus and the posterior tuberculum have been analyzed before, mainly under neurochemical and topographical approaches. The posterior tuberculum in chondrichthyans extends caudally from the posterior recess (or mamillary recess). This recess lies just at the caudal and ventral border of *ScNkx2.1* expression in the MM-like domain and the rostral and ventral border of *ScShh* expression in the RM-like domain (**Figures 3A, C, D**; see also **Figure 4B**). A posterior tuberculum harboring TH-ir cells has been classically related to the hypothalamus (Smeets, 1998) although modern studies addressed it as belonging to p3Tg (Carrera, 2008; Carrera et al., 2008, 2012; Ferreiro-Galve et al., 2008; Quintana-Urzainqui et al., 2012). Our present genoarchitectonic analysis suggests that the bigger part and rostral-most located portion of TH-ir cells and fibers belongs to the RM-like (*ScShh*-expressing) domain while the caudal-most located portion of these TH-ir cells and fibers belongs to p3Tg (**Figure 3B´**). Thus, the rostral-most portion of TH-ir cells should be understood as hypothalamic. This configuration seems to fit parsimoniously with the prosomeric model under the light of the following facts. TH-ir ascending fibers from the rostral posterior tuberculum to the telencephalon seem to arise from these THir hypothalamic groups (compare with Figures 4A, B in Carrera et al., 2012). As discussed below, these ascending TH-ir tracts seem to respect and follow the intersegmental boundary between hp2 and hp1 as proposed by the updated prosomeric model (Puelles et al., 2012), since they course in the most rostral part of hp1. Furthermore, equivalent cells in the posterior tuberculum and their ascending fibers to the telencephalon seem to exist across different vertebrate species (Vernier and Wullimann, 2008) and so, the situation observed in the shark is likely to occur in other vertebrates. Besides having a hypothalamic location, this TH-ir cell population seems to have a hypothalamic origin among different vertebrates. Except in reptiles and mammals, these cells emerge concurrently with those of the rostral hypothalamus in all vertebrates studied so far, supporting a conserved hypothalamic origin (Carrera et al., 2012). On the other hand, in *S. canicula*, *ScOtp* is expressed in the PM/PRM-like area from stage 25 onward (**Figure 2Q**) just before TH-ir cells emerge in the rostral posterior tuberculum (Carrera et al., 2012).

Interestingly, in zebrafish, mutants lacking *Otp* expression in the hypothalamus also lack hypothalamic and posterior tubercular TH-ir groups (Ryu et al., 2007). Finally, at late stages in *S. canicula*, as in zebrafish and mouse (Ryu et al., 2007; Puelles et al., 2012), scattered *ScOtp*-expressing cells were observed outside the ventricular zone of the PM/PRM-like region entering the marginal zone of the RM-like and p3Tg (**Figures 3H** and **4B**), which support a PM/PRM-like origin for *ScOtp*-expressing cells in p3Tg.

Thus, it appears that, among different vertebrates, at least some populations of the RM-like and p3Tg emerge from hypothalamic domains expressing *Otp*, and that TH-ir cells of the RM-like domain send ascending projections to the telencephalon caudally to the IHB.

### 1.4.4 Intrahypothalamic Boundary Identification

The updated prosomeric model proposes a secondary prosencephalon divided in two segments, hp2 and hp1, separated by the IHB. Both segments include a hypothalamic and a telencephalic counterpart (**Figure 4A**). This boundary is supported by (i) the existence of the anterior and retromamillary commissures in the roof and floor plates, respectively, (ii) the restricted expression of several genes to one or other segment, and (iii) the course of main tracts [medial forebrain bundle (mfb), lateral forebrain bundle (lfb) and fornix (fx)] separating both segments. Thus, there is a correlation among histogenetic data and fiber tract data. In fact, it was argued that the course of tracts is a powerful test for brain models since they are also guided by mechanisms related to those involved in histogenetic patterning (Puelles et al., 2012).

In the shark (**Figure 4B**), the IHB is also supported by (i) the existence of commissures in the alar and floor plates, (ii) the restricted expression of *ScShh* and *ScNkx2.1* in particular subdomains within either the rostral or the caudal segment, and (iii) the presence of different neurochemical populations of fibers, topologically homologue to those described in the model, which divide the hypothalamus in a caudal (peduncular, hp1) and a rostral (terminal, hp2) domain. Thus, we have tentatively defined an IHB-like based on genetic or histogenetic data and partial neurochemical or fiber tract data. We also discuss the congruence between the two kinds of data, when possible.

#### 1.4.4.1 The Presence of Commissures

In the roof plate, according to the prosomeric model, the IHB ends caudal to the anterior commissure. This commissure has been identified in *S. canicula* by means of α–acetylated-tubulin immunoreactivity in early embryos (**Figure 2I**) and GFAP-immunoreactivity at late development (**Figure 3P**). In the floor plate, the IHB coincides with the border between MM and RM-like subdomains. In mouse, the IHB at this point can be associated with the retromamillary commissure (also known as Forel's ventral tegmental commissure) where fx tracts cross at its rostral-most portion. This commissure seems to be continuous and indistinguishable from the prethalamic (p3Tg) commissure, a bit more caudally arranged, where fibers (partly p3Tg and partly from the raphe nuclei) cross (see Puelles et al., 2012).

Based on 5-HT-ir tracts, we have identified in *S. canicula* a conspicuous commissure rostrally located with respect to the HDB, as predicted in the frame of the prosomeric model. A hypothalamic commissure has been also identified at this point in adult chondrichthyan specimens, which has been referred as postinfundibular commissure and extends through the ventral and rostro-caudal extension of the posterior tuberculum. This postinfundibular commissure presents differential rostro-caudal connectivity and no other commissures have been described at this point, closely resembling the scenario found in the mouse. While the rostral portion (or pars superior) connects hypothalamic cell masses, fibers of the tract of the saccus vasculossus decussate in the caudal part (or pars inferior; Smeets, 1998). Previous work on the shark reveals 5-HT-ir and GAD-ir fibers crossing in the rostral and caudal extension of this commissure, respectively (Sueiro et al., 2007; Carrera, 2008). It has been proposed that these 5-HT-ir fibers belong to 5-HT-ir cells of the posterior tuberculum (Sueiro et al., 2007; Carrera, 2008) although this fact has not been confirmed. However, in mammals, on which 5-HT-ir projecting cells are only located in the brainstem, a similar commissure has been described and referred as supramamillar commissure (Botchkina and Morin, 1993) which we assumed as equivalent to the prosomeric retromamillary commissure (Puelles et al., 2004). While it remains unclear whether the postinfundibular commissure of sharks is homologous to the retromamillary commissure of mouse, it appears that its location fit with the floor plate limit of the IHB (**Figure 4B**).

1.4.4.2 Correspondence to Histogenetic Domains

Either the expression of different genes (that would help identifying different histogenetic domains) or, accordingly, the course of the IHB through the telencephalon, has not been analyzed here. In the AHy, the prosomeric model proposes that the IHB can be delineated just caudal to the optic stalk, at the caudal border of expression of genes like *Six3*, *Neurog3*, *Six6*, *Nkx2.6* or de rostral border of *Tbr1*, *Uncx4.1*, *Sim1*, *Olig2*, *Foxb1*, *Nr5a1*, which is the same point whereby the mfb, lfb, and fx course (Shimogori et al., 2010; Morales-Delgado et al., 2011, 2014; Puelles et al., 2012; see below). In the BHy, the model proposes that the IHB can be delineated just caudal to the caudal border of genes as *Nkx2.1*, *Olig2*, *Foxb1* or *Nr5a1* or de rostral border of genes as *Lmx1b*, *Lhx5*, *Ptix2*, *Lhx1*, *Lhx6*, *Lhx9*, *Arx* or *Irx5*, which is the same point whereby the fx run (Shimogori et al., 2010; Morales-Delgado et al., 2011, 2014; Puelles et al., 2012). Therefore, the PPa, PSPa, RTu, PRM, and RM domains belong to hp1, while TPa, TSPa, Tu, PM, and MM domains belong to hp2 (**Figure 4A**).

In the AHy of *S. canicula*, as discussed above, no evidence for subdivisions along the rostro-caudal axis could be found on the basis of *ScOtp* or *ScDlx2/5* expression. In the BHy, two distinct territories could be inferred from *ScNkx2.1* and *ScShh* expressions, the MM-like (rostral, *ScNkx2.1*-expressing) and the RM-like (caudal, *ScShh* expressing) domains (**Figure 4B**), which is consistent with the predictions of the prosomeric model. According to the prosomeric model, the IHB can be delineated between both domains. The other compartments (Tu/RTu and PM/PRM) are presumably divided by the IHB, but any other gene among those used here serves as a caudal (hp1) or rostral (hp2 marker, except for *ScShh*

in the Tu/RTu-like domain that, in *S. canicula* (but not in mouse) seems to be restricted to the rostral (hp2) domain.

#### 1.4.4.3 Main Tracts Coursing the Chondrichthyan Alar and Basal IHB

In the mouse, the fx is the only tract coursing from the alar to the basal plate that additionally decussates in the hypothalamic floor plate by the retromamillary commissure. The mfb is also a transverse peduncular tract whose rostral border follows the IHB (Puelles et al., 2012). In chondrichthyans, a fx counterpart has not been successfully confirmed to date (Smeets, 1998). Only a counterpart of the mfb has been described, which is referred as the basal forebrain bundle or *fasciculus basalis telencephali* in chondrichthyans literature [the sot in zebrafish literature (Smeets, 1998; Carrera, 2008; Carrera et al., 2008, 2012; Puelles et al., 2012)]. Ascending and descending projections between the telencephalon and the superior and caudal part of the inferior lobes (which probably correspond to the lateral and caudal part of the Tu/RTu-like domain defined here) have been experimentally confirmed coursing through the mfb of different adult chondrichthyans (Smeets, 1998; Hofmann and Northcutt, 2008). These facts support the existence of tracts coursing caudally to a hypothetic IHB. Interestingly, Carrera et al. (2012) have identified TH-ir fibers ascending from the posterior tuberculum to the telencephalon through the mfb, as in other vertebrates (see above; Vernier and Wullimann, 2008; Carrera et al., 2012). We argued above that the TH-ir cells of the rostral posterior tuberculum previously described as belonging to p3Tg in sharks, probably belong to what we identified here as the RM-like compartment, and that the situation observed in the shark is likely to occur in other vertebrates. Thus, TH-ir fibers likely ascending from the RM-like to the telencephalon seem to course caudally to the IHB (see above), which additionally support the identification of the rostral border of hp1. Therefore, the presence of tracts in the rostral border of the RM-like domain parsimoniously fits with the predictions of the prosomeric model respect the course of fiber tracts in the rostral border of the hp1prosomere and caudally to a hypothetic IHB (**Figure 4B**). Of note, 5-HT-ir and GAD-ir cells have been also identified in the posterior tuberculum of the shark and other vertebrates. Whether ascending projections from this source coursed to the telencephalon has not been determined to date (Barale et al., 1996; Mueller et al., 2006; Carrera, 2008; Carrera et al., 2008; Lillesaar, 2011). However, these tracts are likely to join those mfb tracts that ascend to the telencephalon just caudal to the optic stalk, indirectly drawing the boundary among the Tu-like and RTu-like.

In the alar plate, 5-HT-ir, GAD-ir, TH-ir and GFPA-ir fibers of the mfb, arising from different points of the brain, have been observed ascending to the telencephalon by a common path just caudal to the optic stalk, which could correspond to the alar IHB (Carrera, 2008; Carrera et al., 2012, **Figures 3J ,K ,O**). The most conspicuous of these tracts were 5-HT-ir tracts recognizable at stage 30 (Carrera, 2008; Carrera et al., 2008, and **Figures 3I–L** in present work). This path is also followed by GFAP-ir processes which, besides, cross at the anterior commissure (**Figures 3O, P**). Since, as reported in mouse, they coursed just caudal to the optic stalk, we propose that these tracts in *S. canicula* course caudally to the IHB, separating the TPa and TSPa (hp2) from the PPa and PSPa (hp1; **Figure 4B**). While,

with the markers used here, we cannot ascertain if this boundary in the AHy is also supported by histogenetic domains, these tracts appear to course through gaps of *ScDlx2/5* and *ScOtp* expression in the telencephalon (**Figures 3M, N**, respectively).

To summarize, our data support the conclusion that, in *S. canicula*, an IHB topologically homologous to that proposed by the updated prosomeric model, courses from the anterior commissure (in the telencephalon) to the postinfundibular commissure (in the hypothalamus) through the mfb. Note that, in contrast to mouse, the IHB in *S. canicula* can be traced by partial genetic and fiber tract evidences, since tracts coursing through the telencephalon to the floor plate have not been demonstrated. In the alar plate the mfb courses topologically caudal to the optic stalk and is known to be composed by different neurochemical systems arising from different points of the brain. In the basal plate the mfb is known to be composed, at least, of TH-ir fibers which arise upward from the rostral posterior tuberculum.

### 1.5. CONCLUSION

We have revisited and reinterpreted the organization of the developing hypothalamus in a chondrichthyan model, *S. canicula*, within a prosomeric and histogenetic framework. These data reveal striking similarities with the organization described in the mouse by means of the updated prosomeric model (Puelles et al., 2012). In the AHy we have tentatively identified TPa/PPa-like, TSPa/PSPa-like histogenetic domains and their boundaries. In the BHy we have identified similar histogenetic domains to those observed in the mouse (Tu/RTu, PM/PRM, RM/MM-like). The fact that *ScShh* was downregulated in a large portion of the BHy and *ScDlx2/5* expression was much more restricted than in mouse have allowed us to identify different subdomains within the Tu/RTu-like area. Furthermore, we have identified an IHB separating terminal and peduncular portions of telencephalon and hypothalamus, as the model predicts, based partially on genetic and fiber tract data. Altogether, these data show that the prosomeric model in its latest version provides an adequate reference to describe the molecular organization of the catshark developing hypothalamus, thus highlighting the underlying unity of this complex anatomical structure across jawed vertebrates.

**References**


Ballard, W. W., Mellinger, J., and Lechenault, H. (1993). A series of normal stages for development of *Scyliorhinus canicula*, the lesser spotted dogfish (*Chondrichthyes*: *Scyliorhinidae*). *J. Exp. Zool.* 267, 318–36.

Barale, E., Fasolo, A., Girardi, E., Artero, C., and Franzoni, M. F. (1996). Immunohistochemical investigation of gamma-aminobutyric acid ontogeny and transient expression in the central nervous system of *Xenopus laevis* tadpoles. *J. Comp. Neurol.* 368, 285–94.

Botchkina, G. I., and Morin, L. P. (1993). Development of the hamster serotoninergic system: cell groups and diencephalic projections. *J. Comp. Neurol*. 338, 405–31.

Butler, A. B., and Hodos, W. (2005). "The visceral brain: the hypothalamus and the autonomic nervous system," in *Comparative Vertebrate Neuroanatomy: Evolution and Adaptation*, eds A. B. Butler and W. Hodos (Hoboken, NJ: John Wiley & Sons), 445–67.

Carrera, I. (2008). *Desarrollo de los Sistemas Gabaérgico y Aminérgicos en el Sistema Nervioso Central de Peces Cartilaginosos*. Ph. D. thesis, Universidad de Santiago de Compostela, Compostela.

Carrera, I., Anadón, R., and Rodríguez-Moldes, I. (2012). Development of tyrosine hydroxylase-immunoreactive cell populations and fiber pathways in the brain of the dogfish *Scyliorhinus canicula*: new perspectives on the evolution of the vertebrate catecholaminergic system. *J. Comp. Neurol.* 520, 3574–03.

Carrera, I., Molist, P., Anadón, R., and Rodríguez-Moldes, I. (2008). Development of the serotoninergic system in the central nervous system of a shark, the lesser spotted dogfish *Scyliorhinus canicula*. *J. Comp. Neurol.* 511, 804–31.

Chitnis, A. B., and Kuwada, J. Y. (1990). Axonogenesis in the brain of zebrafish embryos. *J. Neurosci.* 10, 1892–1905.

Compagnucci, C., Debiais-Thibaud, M., Coolen, M., Fish, J., Griffin, J. N., Bertocchini, F., et al. (2013). Pattern and polarity in the development and evolution of the gnathostome jaw: both conservation and heterotopy in the branchial arches of the shark, *Scyliorhinus canicula*. *Dev. Biol.* 377, 428–48.

Coolen, M., Menuet, A., Chassoux, D., Compagnucci, C., Henry, S., Lévèque, L., et al. (2009). "The dogfish *Scyliorhinus canicula*, a reference in jawed vertebrates," in *Emerging Model Organisms. A Laboratory Manual*, eds R. R. Behringer, A. D. Johnson, and R. E. Rrumlauf (Cold Spring Harbor, NY: Cold Spring Harbor Laboratory Press), 431–46.

Debiais-Thibaud, M., Metcalfe, C. J., Pollack, J., Germon, I., Ekker, M., Depew, M., et al. (2013). Heterogeneous conservation of Dlx paralog coexpression in jawed vertebrates. *PLoS ONE* 8:e68182.

Diez-Roux, G., Banfi, S., Sultan, M., Geffers, L., Anand, S., Rozado, D., et al. (2011). A high-resolution anatomical atlas of the transcriptome in the mouse embryo. *PLoS Biol.* 9:e1000582.

Domínguez, L. (2011). *Organización del Hipotálamo en la Transición Anamnioamniota: Estudio Genoarquitectónico y Quimioarquitectónico.* Ph. D. thesis, Universidad Complutense de Madrid, Madrid.

Domínguez, L., González, A., and Moreno, N. (2014). Characterization of the hypothalamus of *Xenopus laevis* during development. II. The basal regions. *J. Comp. Neurol.* 522, 1102–31.

Domínguez, L., Morona, R., González, A., and Moreno, N. (2013). Characterization of the hypothalamus of *Xenopus laevis* during development. I. The alar regions. *J. Comp. Neurol.* 521, 725–59.

Ferreiro-Galve, S. (2010). *Brain and Rretina Regionalization in Sharks, Study Based on the Spatiotemporal Expression Pattern of Pax6 and other Neurochemical Markers*. Ph. D. thesis, Universidad de Santiago de Compostela, Santiago de Compostela.

Ferreiro-Galve, S., Carrera, I., Candal, E., Villar-Cheda, B., Anadón, R., Mazan, S., et al. (2008). The segmental organization of the developing shark brain based on neurochemical markers, with special attention to the prosencephalon. *Brain Res. Bull.* 75, 236–40.

Ferreiro-Galve, S., Rodríguez-Moldes, I., Anadón, R., and Candal, E. (2010). Patterns of cell proliferation and rod photoreceptor differentiation in shark retinas. *J. Chem. Neuroanat.* 39, 1–14.

Figdor, M. C., and Stern, C. D. (1993). Segmental organization of embryonic diencephalon. *Nature* 363, 630–34.

Herget, U., Wolf, A., Wullimann, M. F., and Ryu, S. (2014). Molecular neuroanatomy and chemoarchitecture of the neurosecretory preoptic hypothalamic area in zebrafish larvae. *J. Comp. Neurol.* 522, 1542–64.

Hofmann, M. H., and Northcutt, R. G. (2008). Organization of major telencephalic pathways in an elasmobranch, the thornback ray *Platyrhinoidis triseriata*. *Brain Behav. Evol.* 72, 307–25.

Ishikawa, Y., Yamamoto, N., Yoshimoto, M., Yasuda, T., Maruyama, K., Kage, T., et al. (2007). Developmental origin of diencephalic sensory relay nuclei in teleosts. *Brain Behav. Evol.* 69, 87–95.

Kandel, E., and Schwartz, J. (2001). "Sistema nervioso autónomo e hipotálamo," in *Principios de Neurociencia*, eds E. R. Kandel, J. H. Schwartz, and T. M. Jessell (Aravaca: McGraw-Hill Interamericana), 960–81.

Kuratani, S., and Horigome, N. (2000). Developmental morphology of branchiomeric nerves in a cat shark, *Scyliorhinus torazame*, with special reference to rhombomeres, cephalic mesoderm, and distribution patterns of cephalic crest cells. *Zoolog. Sci.* 17, 893–909.

Kutschera, U., and Niklas, K. J. (2004). The modern theory of biological evolution: an expanded synthesis. *Naturwissenschaften* 91, 255–76.

Lillesaar, C. (2011). The serotonergic system in fish. *J. Chem. Neuroanat.* 41, 294–308.
Manuel, M. N., Martynoga, B., Molinek, M. D., Quinn, J. C., Kroemmer, C., Mason, J. O., et al. (2011). The transcription factor Foxg1 regulates telencephalic progenitor proliferation cell autonomously, in part by controlling Pax6 expression levels. *Neural Dev.* 6, 9.

Martínez, S., Puelles, E., Puelles, S., and Echeverria, D. (2012). "Molecular regionalization of the developing neural tube," in *The Mouse Nervous System*, eds C. Watson, G. Paxinos, and L. Puelles (San Diego, CA: Academic Press), 2–18.

Medina, L. (2008). "Evolution and embryological development of the forebrain," in *Encyclopedia of Neuroscience*, eds M. D. Binder, N. Hirokawa, and U. Windhorst (Berlin: Springer-Verlag), 1172–92.

Medina, L., Bupesh, M., and Abellán, A. (2011). Contribution of genoarchitecture to understanding forebrain evolution and development, with particular emphasis on the amygdala. *Brain Behav. Evol.* 78, 216–36.

Morales-Delgado, N., Castro-Robles, B., Ferrán, J. L., Martínez-de-la-Torre, M., Puelles, L., and Díaz, C. (2014). Regionalized differentiation of CRH, TRH, and GHRH peptidergic neurons in the mouse hypothalamus. *Brain Struct. Funct.* 219, 1083–1111.

Morales-Delgado, N., Merchán, P., Bardet, S. M., Ferrán, J. L., Puelles, L., and Díaz, C. (2011). Topography of somatostatin gene expression relative to molecular progenitor domains during ontogeny of the mouse hypothalamus. *Front. Neuroanat.* 5:10.

Moreno, N., Domínguez, L., Morona, R., and González, A. (2012). Subdivisions of the turtle *Pseudemys scripta* hypothalamus based on the expression of regulatory genes and neuronal markers. *J. Comp. Neurol.* 520, 453–78.

Mueller, T., Vernier, P., and Wullimann, M. F. (2006). A phylotypic stage in vertebrate brain development: GABA cell patterns in zebrafish compared with mouse. *J. Comp. Neurol.* 494, 620–34.

Müller, G. B. (2007). Evo-devo: extending the evolutionary synthesis. *Nat. Rev. Genet.* 8, 943–49.

Piperno, G., and Fuller, M. T. (1985). Monoclonal antibodies specific for an acetylated form of alpha-tubulin recognize the antigen in cilia and flagella from a variety of organisms. *J. Cell Biol.* 101, 2085–94.

Pombal, M., Megías, M., Bardet, S. M., and Puelles, L. (2009). New and old thoughts on the segmental organization of the forebrain in lampreys. *Brain Behav. Evol.* 74, 7–19.

Pose-Méndez, S., Candal, E., Adrio, F., and Rodríguez-Moldes, I. (2014). Development of the cerebellar afferent system in the shark *Scyliorhinus canicula*: insights into the basal organization of precerebellar nuclei in gnathostomes. *J. Comp. Neurol.* 522, 131–68.

Puelles, L. (2009). "Forebrain development: prosomere model," in *Developmental Neurobiology,* ed. G. Lemke (London; Burlington, MA; San Diego, CA: Academic Press), 315–19.

Puelles, L., and Medina, L. (2002). Field homology as a way to reconcile genetic and developmental variability with adult homology. *Brain Res. Bull.* 57, 243–55.

Puelles, L., and Rubenstein, J. L. R. (2003). Forebrain gene expression domains and the evolving prosomeric model. *Trends Neurosci.* 26, 469–76.

Puelles, L., Martínez, S., Martínez-de-la-Torre, M., and Rubenstein, J. (2004). "Gene maps and related histogenetic domains in the forebrain and midbrain," in *The Rat Nervous System,* ed. G. Paxinos (San Diego, CA: Academic Press), 3–25.

Puelles, L., Martínez, S., Martínez-de-la-Torre, M. S., and Rubenstein, J. (2012). "Hypothalamus," in *The Mouse Nervous System,* eds C. Watson, G. Paxinos, and L. Puelles (San Diego, CA: Academic Press), 221–312.

Quintana-Urzainqui, I. (2013). *Development and Regionalization of the Telencephalon and Peripheral Associated Systems in the Shark Scyliorhinus canicula*. Ph. D thesis, Universidad de Santiago de Compostela, Santiago de Compostela.

Quintana-Urzainqui, I., Sueiro, C., Carrera, I., Ferreiro-Galve, S., Santos-Durán, G., Pose-Méndez, S., et al. (2012). Contributions of developmental studies in the dogfish *Scyliorhinus canicula* to the brain anatomy of elasmobranchs: insights on the basal ganglia. *Brain Behav. Evol.* 80, 127–41.

Ryu, S., Mahler, J., Acampora, D., Holzschuh, J., Erhardt, S., Omodei, D., et al. (2007). Orthopedia homeodomain protein is essential for diencephalic dopaminergic neuron development. *Curr. Biol.* 17, 873–80.

Sarnat, H. B., and Netsky, M. G. (1981). "Epithalamus and hypothalamus," in *Evolution of the Nervous System,* eds H. B. Sarnat and M. G. Netsky (Newyork, NY; Oxford: Oxford University Press), 296–320.

Shimamura, K., Hartigan, D. J., Martínez, S., Puelles, L., and Rubenstein, J. L. (1995). Longitudinal organization of the anterior neural plate and neural tube. *Development* 121, 3923–33.

Shimogori, T., Lee, D. A., Miranda-Angulo, A., Yang, Y., Wang, H., Jiang, L., et al. (2010). A genomic atlas of mouse hypothalamic development. *Nat. Neurosci.* 13, 767–75.

Smeets, W. (1998). "Cartilaginous fishes," in *The Central Nervous System of Vertebrates,* eds R. Nieuwenhuys, H. J. Ten Donkelaar, and C. Nicholson (Berlin: Springer-Verlag), 521–654.

Sueiro, C., Carrera, I., Ferreiro, S., Molist, P., Adrio, F., Anadón, R., et al. (2007). New insights on saccus vasculosus evolution: a developmental and immunohistochemical study in elasmobranchs. *Brain Behav. Evol.* 70, 187–204.

Tornehave, D., Hougaard, D. M., and Larsson, L. (2000). Microwaving for double indirect immunofluorescence with primary antibodies from the same species and for staining of mouse tissues with mouse monoclonal antibodies. *Histochem. Cell Biol.* 113, 19–23.

Vernier, P., and Wullimann, M. (2008). "Evolution of the posterior tuberculum and preglomerular nuclear complex," in *Encyclopedia of Neuroscience,* eds M. D. Binder, N. Hirokawa, and U. Windhorst (Berlin: Springer-Verlag), 1404–16.

USC
UNIVERSIDADE
DE SANTIAGO
DE COMPOSTELA

**Abbreviation list**

| | |
|---|---|
| ABB | alar-basal boundary |
| ac | anterior commissure |
| AHy | alar hypothalamus |
| At | acroterminal region |
| AP | alar plate |
| BHy | basal hypothalamus |
| BP | basal plate |
| CAHy | caudal part of the alar hypothalamus |
| CBHy | caudal part of the basal hypothalamus |
| D | diencephalon |
| F | forebrain |
| FP | floor plate |
| HDB | hypothalamo diencephalic boundary |
| hp1 | prosomere hp1 or peduncular hypothalamus |
| hp2 | prosomere hp2 or terminal hypothalamus |
| IHB | intrahypothalamic boundary |
| MM | mamillary area |
| MTT | mamillo-tegmental tract |
| mz | marginal zone |
| os | optic stalk; |
| p1 | prosomere 1 |
| p2 | prosomere 2 |
| p2Tg | tegmental part of prosomere 2 |
| p3 | prosomere 3 |
| p3Tg | tegmental part of prosomere 3 |
| P | pallium |
| PM | perimamillary area |
| POA | preoptic area |
| PPa | peduncular paraventricular area |
| PRM | periretromamillary area |
| PSPa | peduncular subparaventricular area |
| PThE | prethalamic eminence |
| RAHy | rostral part of the alar hypothalamus |
| RBHy | rostral part of the basal hypothalamus |
| Rh | rhombencephalon |
| RM | retromamillary area |
| rmc | retromamillary commissure |
| RP | roof plate |
| RTu | retrotuberal domain |
| sot | supraoptic tract |
| Sp | subpallium |
| T | telencephalon |
| TPa | terminal paraventricular area |
| TPOC | tract of the postoptic commissure |
| TSPa | terminal subparaventricular area |
| Tu | tuberal domain |
| vz | ventricular zone |

**Figure 1**. Squematic representations of the prosencephalon of early **(A)** and late **(B, C)** mouse embryo to show correspondence of longitudinal and tranverse domains in the secondary prosencephalon under the updated prosomeric model. Domains in **(A)** are illustrated according to Figure 1.1C in Martínez et al. (2012). Domains in **(B, C)** are illustrated according to Figure 8.5B in Puelles et al. (2012). **(A)** Longitudinal domains in early embryos. The arrowheads mark both the dorso-caudal and ventro-caudal limits of the acroterminal territory (At). This territory is considered the rostral-most domain of the neural tube. The dorso-caudal limit of the At can be identified caudal to the anterior commissure. **(B)** Longitudinal and transverse organization in late embryos. **(C)** Segmental organization of the secondary prosencephalon according to the prosomeric model. For abbreviations, see list.

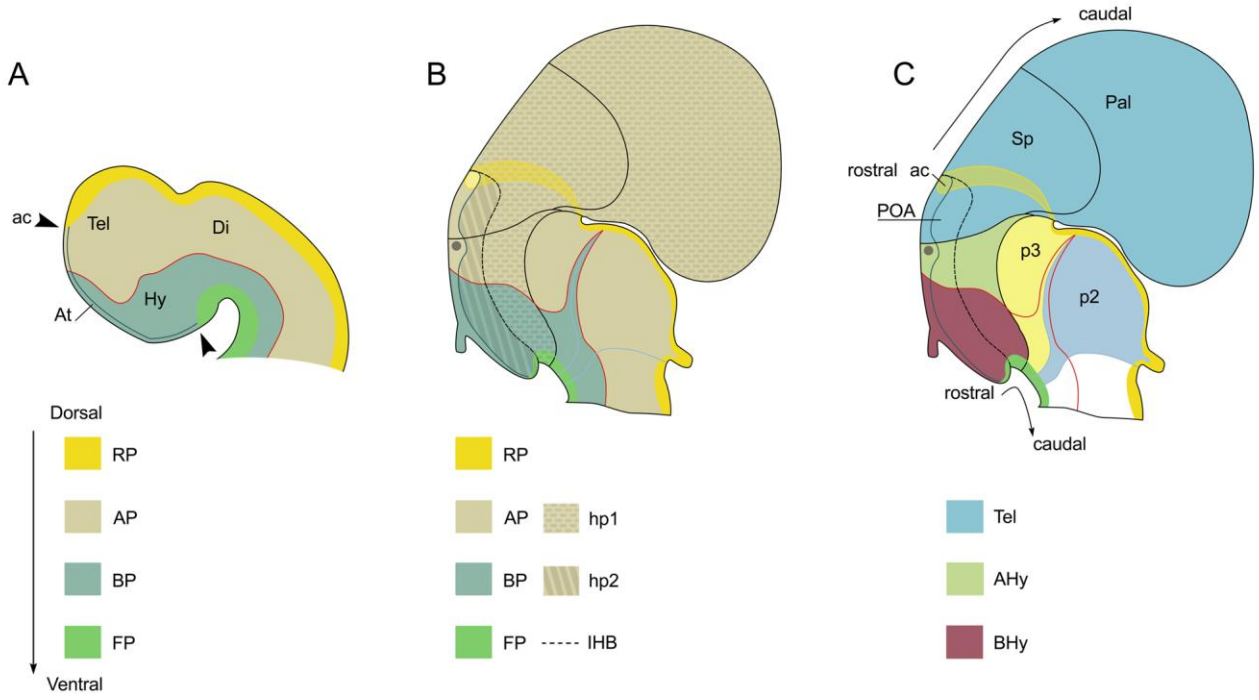
A
ac
Tel
Di
Hy
At
Dorsal
RP
AP
BP
FP
Ventral
B
RP
AP
hp1
BP
hp2
FP
IHB
C
caudal
Pal
Sp
rostral
ac
POA
p3
p2
rostral
caudal
Tel
AHy
BHy

# FIGURE 1

**Figure 2.** Regionalization of the hypothalamus and neighbor territories in embryos of *S. canicula* from stages 18–29 based on the expression pattern of *ScFoxg1a* **(A–C)**, *ScShh* **(D–H)**, *ScNkx2.1* (**J–L)**, *ScDlx5* **(M–O)**, *ScOtp* **(P, Q)**, *ScTbr1* **(R)** genes and **α**-acetylated-tubulin-immunoreactivity **(I)**. In all panels, dotted lines define the hypothalamo-telencephalic boundary (HTB), dashed lines indicate the caudal border of the secondary prosencephalon and red lines indicate the ABB. **(A–C)** *ScFoxg1a* expression in the secondary prosencephalon at indicated stages. The arrowheads in **(A)** mark the caudo-dorsal and rostro-ventral limit of *ScFoxg1a* expression. **(D–H)** *ScShh* expression at the indicated stages. The arrowhead in **(D)** marks the rostral-most point of *ScShh* expression in the forebrain. The arrows in **(E–H)** indicate the downregulation of *ScShh* expression in the hypothalamus. The arrowhead in **(G)** points to the developing zli. The arrowhead in **(H)** points to a novel domain in the telencephalon. The asterisk in **(H)** marks the prospective territory of the anterior commissure. **(I)** Anti-α-acetylated-tubulin IHC to show three sets of tracts at stage 25. These tracts are classically referred as sot, TPOC and MTT. The asterisk indicates the territory of the developing anterior commissure. The arrowheads point to the longitudinal TPOC. The arrow points to the rostral-most extension of the MTT. **(J–L)** *ScNkx2.1* expression at the indicated stages. The arrowhead in **(J)** points to the rostral-most point of *ScNkx2.1* expression at stage 18, which was restricted to a short longitudinal domain ventrally to the optic stalk. The arrow in **(K, L)** points to a small *ScNkx2.1*-negative domain at the most caudo ventral BHy. The asterisk in **(K, L)** marks the prospective territory of the anterior commissure. The arrowhead in **(K, L)** points to a domain in the telencephalon that spread rostro-caudally. **(M–O)** *ScDlx5* expression at the indicated stages. The arrowheads in **(M, N)** indicate *ScDlx5* expression in the olfactory placode and the anterior part of the telencephalon. The asterisk in **(N)** indicates the prospective territory of the anterior commissure. The arrowheads in **(O)** point to the ventral and caudal expansion of *ScDlx5* expression in the telencephalon. This domain was fairly continuous with a longitudinal band of *ScDlx5* over the ABB. The arrows in **(O)** point to *ScDlx5*-expressing domains that spread into the BHy. **(P, Q)** *ScOtp* expression at the indicated stages. The arrowhead in **(P)** indicates a restricted domain of *ScOtp* expression ventrally located with respect to the optic stalk. The expression of *ScOtp* in the hypothalamus was faint compared to that of the Rh. The white arrowhead in **(Q)** points to *ScOtp* expression in the AHy. Two additional *ScOtp*-expressing domains were observed in the BHy. **(R)** *ScTbr1* expression at stage 25 was found in part of the telencephalon and at the dorsal-most part of the rostral diencephalon (white arrowhead). The asterisk indicates the prospective territory of the anterior commissure. For abbreviations, see list

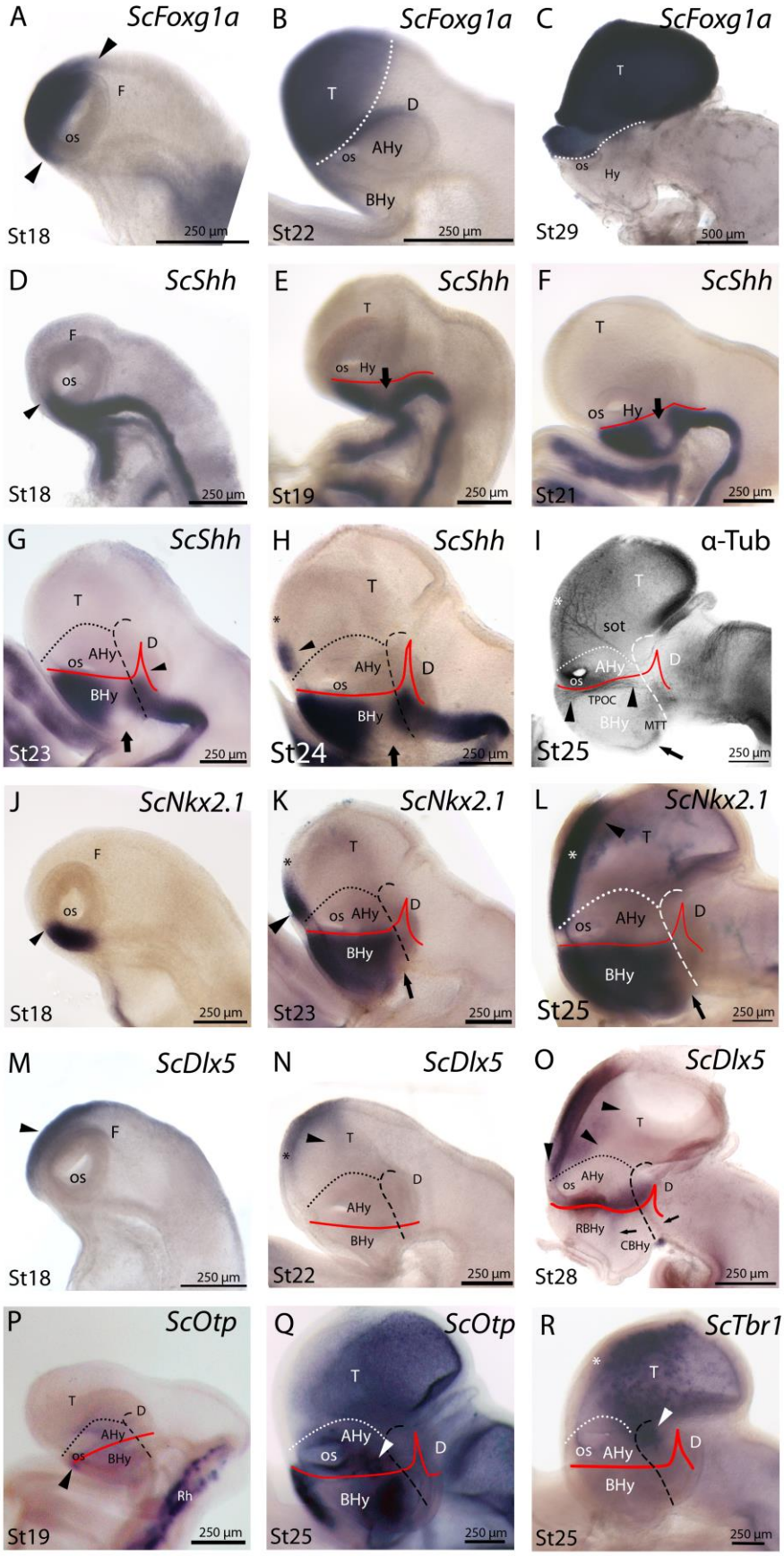
A ScFoxg1a
F
os
St18
250 µm
B ScFoxg1a
T
D
os
AHy
BHy
St22
250 µm
C ScFoxg1a
T
os
Hy
St29
500 µm
D ScShh
F
os
St18
250 µm
E ScShh
T
os Hy
St19
250 µm
F ScShh
T
os Hy
St21
250 µm
G ScShh
T
D
os
AHy
BHy
St23
250 µm
H ScShh
T
*
AHy
D
os
BHy
St24
250 µm
I α-Tub
T
*
sot
AHy
D
os
TPOC
BHy
MTT
St25
250 µm
J ScNkx2.1
F
os
St18
250 µm
K ScNkx2.1
T
*
os AHy
D
BHy
St23
250 µm
L ScNkx2.1
T
*
os
AHy
D
BHy
St25
250 µm
M ScDlx5
F
os
St18
250 µm
N ScDlx5
T
*
D
AHy
BHy
St22
250 µm
O ScDlx5
T
os
AHy
D
RBHy
CBHy
St28
250 µm
P ScOtp
T
D
AHy
os
BHy
Rh
St19
250 µm
Q ScOtp
T
AHy
os
D
BHy
St25
250 µm
R ScTbr1
*
T
os AHy
D
BHy
St25
250 µm

# FIGURE 2

**Figure 3**. Regionalization of the shark hypothalamus from stages 29–31 based on immunoreactivity to Shh **(A, B, B´, D, I–N)**, TH **(B´)**, 5-HT **(I–L)**, GFAP **(O, P)** and expression of *ScNkx2*.1 **(C, C´, D, G´´)**, *ScDlx2/5* **(E, E´, F, M)** and *ScOtp* **(G, G´, G´´, H, H´, N)** genes by means of single immunohistochemistry **(IHC; A, B, O, P)**, double IHC **(B´, I–L)**, single ISH **(C, E, E´, F, G, G´, H, H´)** and/or combined with IHC **(D, M, N)** on sagittal **(A, B, B´, C–G, G´´, H–J, M, N)** or transverse sections **(C´, E´, G´, H´, K, L, O, P)**. Image in **(G´´)** results from the overlapping of two parallel sections respectively hybridized with *ScOtp* and *ScNkx2.1* probes. Color for *ScNkx2.1* was digitally converted to brown to ease comparison. Dotted lines define the hypothalamo-telencephalic boundary (HTB), dashed lines indicate the caudal border of the secondary prosencephalon, red lines indicate the ABB and continuous black lines represent the path followed by 5-HT-ir fibers. **(A)** Shh-immunoreactivity was observed in the most caudo-ventral part of the CBHy (arrow) and in the RBHy. The arrowhead points to the zli. **(B)** Shh-immunoreactivity was observed in the telencephalon (arrowhead) beyond the territory of the anterior commissure (asterisk). The arrow points to Shh-immunoreactivity in the caudal-most CBHy. **(B´)** Detail of the squared area in **(B)** to show Shh- and TH-immunoreactivity in its most caudo-ventral part (arrow). **(C, D)** *ScNkx2.1* expression was observed in the hypothalamus and telencephalon. A detail of a transverse section at the level indicated in **(C)** is shown in **(C´)**. The arrows in **(C, C´, D)** point to *ScNkx2.1*-expressing cells in the mantle zone of the most caudo-ventral CBHy. The arrowheads in **(C, D)** indicate a wedge-shaped domain lacking *ScNkx2.1* expression. The asterisk in **(D)** indicates the territory of the anterior commissure. **(E, F)** *ScDlx2/5* expression was observed in p3 and in the secondary prosencephalon. A detail of a transverse section at the level indicated in **(D)** is shown in **(D´)**. The arrow in **(E, E´)** points to *ScDlx2/5*-expressing cells in the mantle of the p3Tg. The star in **(E, E´)** indicates the prospective territory of the PThE. The black asterisks in **(E, F)** indicate a gap of *ScDlx2/5* expression in the telencephalon. The arrowheads in **(E, F)** point to *ScDlx2/5* expression in the BHy. **(G, H)** *ScOtp* expression in the hypothalamus. Details in **(G´, H´)** correspond to transverse sections at the levels indicated in **(G, H)**. Detail in **(G´´)** correspond to the squared area in **(G)**. The arrows in **(G, G´´)** point to the ventricular domain expressing *ScOtp* in the caudal CBHy. The black arrowheads in **(G, G´´, H´)** point to *ScOtp*-expressing cells in the mantle of the most caudo-ventral part of CBHy and p3Tg. The arrow in **(G´´)** indicates a domain expressing *ScNkx2.1* alone. The white asterisks in **(G´, H)** indicate *ScOtp*-expressing cells in the mantle zone. The black arrowhead in **(H)** points to *ScOtp*-expressing cells in the AHy and the white arrowhead in **(H)** points to *ScOtp*-expressing cells between the alar and basal domains. **(I–L)** Double Shh- and 5-HT-immunoreactivity. **(K, L)** correspond to trasverse sections at the level indicated in **(J)**. 5-HT-ir fibers in **(I)** are observed in the basal plate of the secondary prosencephalon. In the rostral hypothalamus such fibers coursed among RAHy and RBHy, and were located dorsally to Shh-immunoreactivity **(I, J)**. Note the presence of 5-HT-ir fibers in the Sp **(I, J, L).** The white arrowhead in **(J, K)** points to 5-HT-ir fibers that course in the rostral CAHy. The black arrowhead in **(J, L)** points to 5-HT-ir fibers in the telencephalon. The arrow in **(J, K)** points to 5-HT-ir fibers decussating in the CBHy. The arrow in **(L)** points to the faint Shh immunoreactivity in the zli. **(M, N)** Shh IHC combined with *ScDlx2/5* expression **(M)** or *ScOtp* expression **(N)**. A gap of expression is observed between the rostral and caudal domains of *ScDlx2/5* and *ScOtp* expression, which appeared to coincide with the path followed by 5-HT-ir fibers. **(O)** GFAP-ir processes at the levelshown in **(J)**. The arrowhead points to the GFAP-ir processes among RAHy and Sp. The arrow points to the GFAP-ir processes in the CBHy. **(P)** GFAP-ir processes at the level shown in **(J)**. The arrow points to GFAP-ir processes in the Sp. For abbreviations, see list.

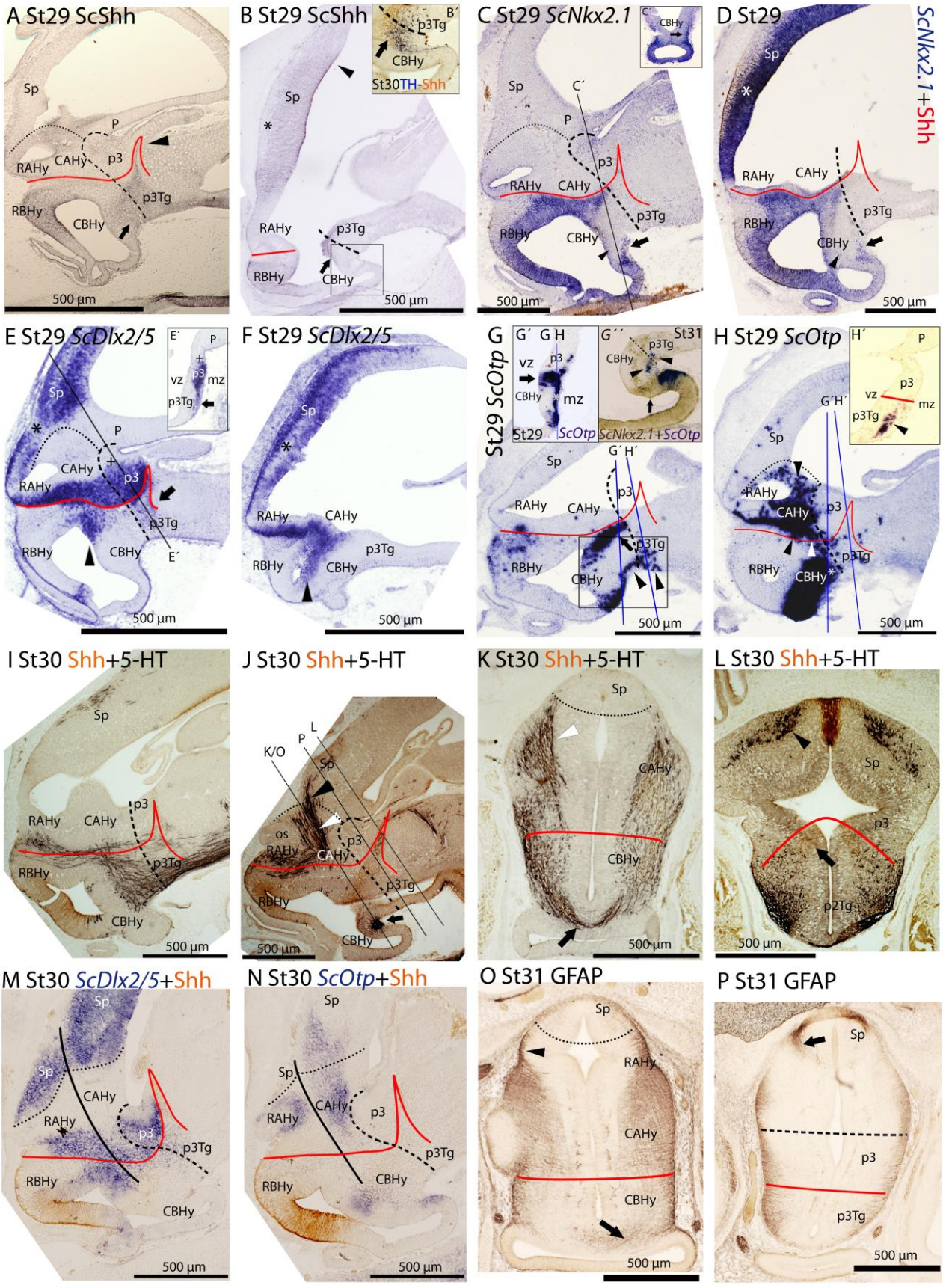
A St29 ScShh
B St29 ScShh
C St29 ScNkx2.1
D St29
ScNkx2.1+Shh
E St29 ScDlx2/5
F St29 ScDlx2/5
G St29 ScOtp
H St29 ScOtp
I St30 Shh+5-HT
J St30 Shh+5-HT
K St30 Shh+5-HT
L St30 Shh+5-HT
M St30 ScDlx2/5+Shh
N St30 ScOtp+Shh
O St31 GFAP
P St31 GFAP
Sp
P
RAHy
CAHy
p3
p3Tg
RBHy
CBHy
500 µm
St30TH-Shh
vz
mz
St29 ScOtp
ScNkx2.1+ScOtp
St31
K/O
L
os
p2Tg

. **FIGURE 3**

**Figure 4**. Schematic representation of various gene expression patterns in the forebrain of mouse **(A)** and the rostral diencephalon and hypothalamus of *S. canicula* **(B)**, and their correspondence with the updated prosomeric model (see text for details). Patterns in **(A)** are illustrated according to Figures 8.9 and 8.16 in Puelles et al. (2012). Patterns in **(B)** were mapped according to present results. Expression of *Nkx2.1* and *Otp* genes in the telencephalon has not been represented. White, green and blue dots represent non-ventricular *ScNkx2.1*-, *ScDlx2/5*-, and *ScOtp*-expressing cells, respectively. For abbreviations, see list.

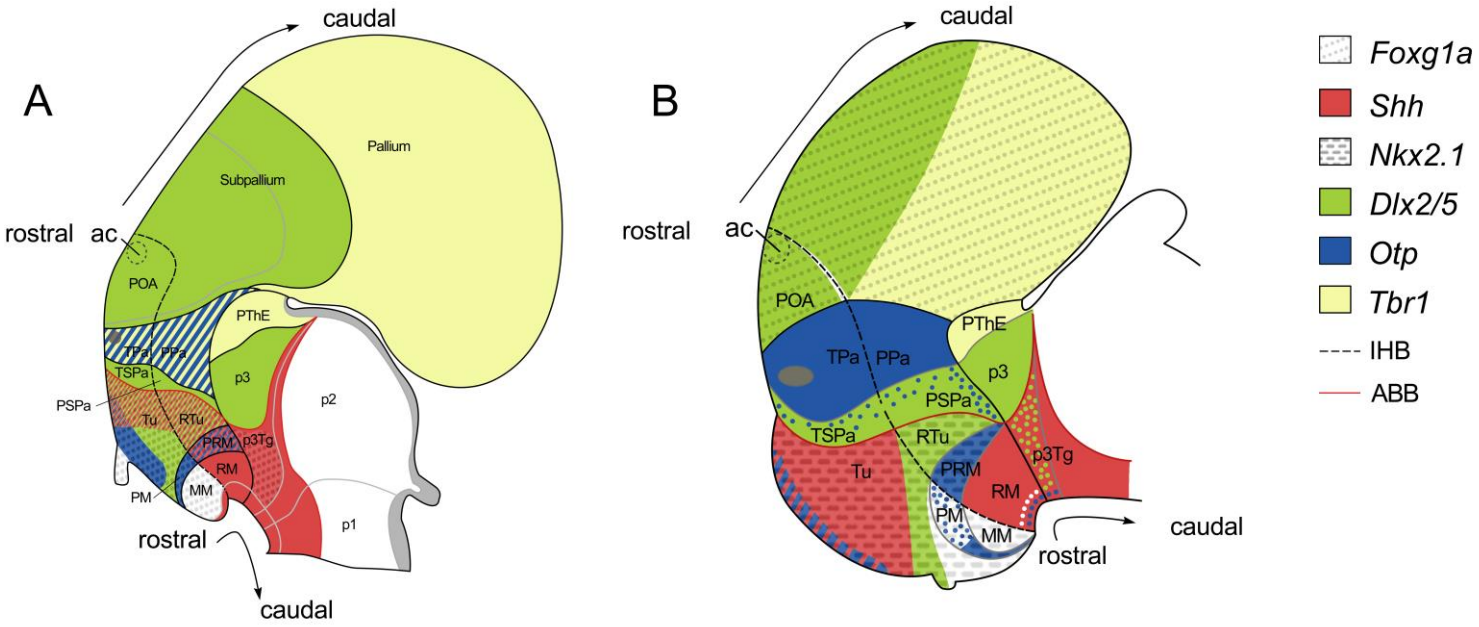




**FIGURE 4**

USC
UNIVERSIDADE
DE SANTIAGO
DE COMPOSTELA

# Chapter 2

# The shark alar hypothalamus: molecular prosomeric subdivisions and evolutionary trends

USC
UNIVERSIDADE
DE SANTIAGO
DE COMPOSTELA

# 2. The shark alar hypothalamus: molecular prosomeric subdivisions and evolutionary trends

## 2.1 INTRODUCTION

The hypothalamus is a conserved integrative center that coordinates autonomic, endocrine and limbic responses (Sarnat and Netsky, 1981; Kandel and Schwartz, 2001; Butler and Hodos, 2005). Its organization is the result of complex patterning processes that converge at the rostral-most and ventral-most point of the neural tube, which in turn, yield a complex structure that has been difficult to systematize (Shimamura et al., 1995; Puelles and Rubenstein, 2003; Puelles et al., 2004; Medina, 2008; Szabó et al., 2009; Shimogori et al., 2010; Alvarez-Bolado et al., 2012; Croizier et al., 2015). Classically, the mammalian hypothalamus has been described as consisting of a wide variety of neuronal clusters subdivided in four regions: preoptic, anterior, tuberal and mamillar (Simerly, 2004). This organization relies on conceptions that understood the brain to be organized in functional columns (also referred as "columnar models") being the hypothalamus located ventrally to the remaining diencephalon. Alternative brain conceptions have understood the brain to be divided in transverse segments (or neuromeres) yielding segmental (or neuromeric) paradigms of brain organization (Puelles, 2009). Modern segmental paradigms, as the "prosomeric model", recognizes the mentioned hypothalamic regions under an alternative mechanistic nomenclature and organization that rely on the own developmental process (Puelles and Rubenstein, 2003; Puelles, 2009; Puelles et al., 2012). Furthermore, the model also considers that these segments are organized in different histogenetic territories defined by neuroepithelial transcription factor specification codes and radial units (Puelles and Medina, 2002; Puelles et al., 2012). This paradigm understands the hypothalamus to be ventrally located with respect to the telencephalon (thus, rostral to the remaining diencephalon) forming, together, a segmental unit at the rostral-most part of the neural tube. Under these criteria the preoptic area is recognized as part of the subpallial telencephalon rather than belonging to the hypothalamus (Flames et al., 2007; Puelles et al., 2012).

The updated prosomeric model recognizes the hypothalamus to be subdivided in dorso-ventrally arranged histogenetic domains. The intrahypothalamic border (IHB) divides these histogenetic domains in rostral (hp2 or terminal) and caudal (hp1 or peduncular) portions. As a result, in the alar plate the hypothalamus presents at least four progenitor subdomains (from rostral to caudal and dorsal to ventral): terminal and peduncular paraventricular area (**TPa**, **PPa**; respectively), terminal and peduncular subparaventricular area (**TSPa**, **PSPa**; respectively) while in the basal plate there are other six. Further dorso-ventral subdivisions have also been proposed (Morales-Delgado et al., 2011, 2014; Puelles et al., 2012; Díaz et al., 2015). The relationships

among these domains and hypothalamic nucleus have been pointed: the TPa/PPa gives rise to magnocellular and parvocellular neurosecretory populations of the supraopto-paraventricular complex; the **TSPa/PSPa** will form mainly the suprachiasmatic nucleus, the anterior hypothalamic nucleus, and the subparaventricular zone, while the basal hypothalamus give rise to classical tuberal and mamillary derivatives (Morales-Delgado et al., 2011; Puelles et al., 2012). Finally, additional histogenic domains are recognized in the acroterminal territory, the rostral-most portion of the neural tube (see chapter 1), responsible of the development of structures such as the *lamina terminalis* or the optic chiasm in the alar hypothalamus.

Because of its phylogenetic position as the closest out-group to osteichthyans (the other major phylum of gnathostomes, which includes bony fish and tetrapods), chondrichthyans are essential to reconstruct gnathostome ancestral characteristics through comparisons with other vertebrate models. Recently, we have carried out a preliminary study of the molecular histogenetic organization of the hypothalamus of an elasmobranch representative, the catshark *Scyliorhinus canicula*, and we analyzed this organization under the updated prosomeric framework (see chapter 1). Such analysis revealed a strikingly high degree in the conservation of hypothalamic histogenetic compartments between chondrichthyan and murine models. Indeed, the alar expression of *ScOtp* and *ScDlx2/5* revealed apparently conserved paraventricular-like (**Pa-like**) and subparaventricular-like (**SPa-like**) progenitor domains. The basal expression of these and other markers lead to the identification of tuberal/retrotuberal-like (**Tu/RTu-like**), perimamillar/periretromamillar-like (**PM/PRM-like**) and mamillar/retromamillar-like (**MM/RM-like**) domains, apparently homologous to those described in murine models. Besides, a molecular hypothalamo-telencephalic border (**HTB**) and a hypothalamo-diencephalic border (**HDB**), matching with those described in the model, were identified in the shark, together with an intrahypothalamic border (**IHB**) defined, as in mouse (Puelles et al., 2012) based on the course of ascending tracts to the telencephalon (see chapter 1).

In such previous study (chapter 1), some histogenetic differences were also observed within particular subdomains, but the significance of which has not been explored so far. On the other hand, although many of the boundaries and assumptions predicted by the prosomeric model were confirmed in the chondrichthyan model, further dorso-ventral subdivisions and genetic evidences of rostro-caudal segmentation, particularly concerning the alar hypothalamus, have not been previously addressed. Besides, the meaning of the results observed in the shark remains unclear since trends on the evolution and development of the vertebrate hypothalamus have not been considered so far. For all these, here we have deepen in the molecular profile of the alar hypothalamus of *Scyliorhinus canicula*, with three aims: i) to look for further prosomeric molecular subdivisions, ii) to better define the molecular alar-basal boundary (**ABB**) and iii) to obtain some insights on the evolution of the alar hypothalamus by comparative analysis. To address these questions, previous data on *ScNkx2.1*, *ScDlx2/5*, *ScOtp, ScTbr1* expression and Pax6-immunoreactivity were revised jointly with new data on *ScNkx2.8*, *ScNeurog2*, *ScLhx5*, and *ScLhx9* expression and glutamic acid decarboxylase (GAD)-, TH (tyrosine hydroxylase)-, somatostatin (SS)-, and calbindin (CB)- immunoreactivity patterns. Further details on the rostro-

caudal and dorso-ventral molecular organization of the alar hypothalamus obtained with these markers support the existence of subdomains similar to those proposed by the prosomeric model. Terminal and peduncular subdivisions were defined in the Pa-like (TPa-like and PPa-like, respectively) and SPa-like (TSPa-like and PSPa-like, respectively) while a dorso-ventral subdivision could only be proposed in the SPa-like (SPaD-like and SPaV-like, respectively). Noteworthy, in the stages considered, the markers here studied did not reveal further details of the acroterminal territory in the alar hypothalamus, which should be considered in posterior works with additional genes and/or substances.

## 2.2 MATERIALS AND METHODS

### 2.2.1. Experimental animals

Some embryos of the catshark (lesser spotted dogfish; *S. canicula*) were supplied by the Marine Biological Model Supply Service of the CNRS UPMC Roscoff Biological Station (France) and the Estación de Bioloxía Mariña da Graña of the University of Santiago de Compostela. Additional embryos were kindly provided by the Aquaria of Gijón (Asturias, Spain), O Grove (Pontevedra, Spain) and Finisterrae (A Coruña, Spain). Embryos were staged by their external features according to Ballard et al. (1993). For more information about the relationship of the embryonic stages with body size, gestation and birth, see Table 1 in Ferreiro-Galve et al. (2010). Fifty embryos from stages 18 to 32 were used in this study. Eggs from different broods were raised in seawater tanks in standard conditions of temperature (15-16 ºC), pH (7.5-8.5) and salinity (35 g/L). Adequate measures were taken to minimize animal pain or discomfort. All procedures conformed to the guidelines established by the European Communities Council Directive of 22 September 2010 (2010/63/UE) and by the Spanish Royal Decree 53/2013 for animal experimentation and were approved by the Ethics Committee of the University of Santiago de Compostela.

### 2.2.2. Tissue processing

Embryos were deeply anesthetized with 0.5 % tricaine methane sulfonate (MS-222; Sigma, St. Louis, MO) in seawater and separated from the yolk before fixation in 4 % paraformaldehyde (PFA) in elasmobranch's phosphate buffer [EPB: 0.1 M phosphate buffer (PB) containing 1,75 % urea, pH 7.4] for 48-72 h depending on the stage of development. Subsequently, they were rinsed in phosphate buffer saline (PBS), cryoprotected with 30 % sucrose in PB, embedded in OCT compound (Tissue Tek, Torrance, CA), and frozen with liquid nitrogen-cooled isopentane. Parallel series of sections (12-20 µm thick) were obtained in transverse planes on a cryostat and mounted on Superfrost Plus (Menzel-Glasser, Madison, WI, USA) slides.

### 2. 2.3. Single and double immunohistochemistry on sections

For heat-induced epitope retrieval, sections were pre-treated with 0.01 M citrate buffer (pH 6.0) for 30 min at 95 ºC and allowed to cool for 20–30 min at room temperature (RT). Sections were then rinsed twice in 0.05 M Tris-buffered saline (TBS; pH 7.4) for 5 min each and incubated overnight with the primary antibody (rabbit anti-Pax6 [anti-Pax6] polyclonal antiserum, Covance, Emeryville, CA, diluted 1:400; polyclonal rabbit anti-Sonic Hedgehog [anti-Shh], Sta. Cruz Biotechnology, Santa Cruz, CA, diluted 1:300; polyclonal rabbit anti-doublecortin [anti-DCX] Cell Signaling; diluted 1:300–500; polyclonal rabbit anti-glutamate decarboxylase 65/67 Kda [anti-GAD], Millipore, Temecula, CA, diluted 1:600; monoclonal rat anti-somatostatin [anti-SS], Millipore, Temecula, CA, diluted 1:50; polyclonal rabbit anti-calbindin D-28k [anti-CB] Swant, Marly, Switzerland, diluted 1:1000; monoclonal mouse anti-tyrosine hydroxilase [anti-TH], Millipore, Billerica, MA, diluted 1:500; rabbit anti-serotonin [anti-5-HT] polyclonal antiserum, DiaSorin, Immunostar, Hudson, WI, diluted 1:5000). Appropriate secondary antibodies (horse radish peroxidase [HRP]-conjugated goat anti-rabbit and anti-mouse, BIORAD, diluted 1:200; and horse radish peroxidase [HRP]-conjugated rabbit anti-rat, Thermo SCIENTIFIC, diluted 1:50) were incubated for 2h at RT. For double immunohistochemistry experiments, cocktails of primary antibodies were mixed at optimal dilutions and subsequently detected by using mixtures of appropriate secondary antibodies. For immunofluorescence appropriate secondary antibodies were used ($DAR^{546}$ [Alexa 546-conjugated donkey anti-rabbit] Molecular Probes Eugene, OR diluted 1:100). Sections were rinsed in distilled water (twice for 30 min), allowed to dry for 2 h at 37 ºC and mounted in MOWIOL 4-88 Reagent (Calbiochem, MerkKGaA, Darmstadt, Germany). All dilutions were made with TBS containing 15 % donkey normal serum (DNS; Millipore, Billerica, MA), 0.2 % Triton X-100 (Sigma) and 2 % bovine serum albumin (BSA, Sigma). Double immunohistochemistry with primary antibodies raised in the same species was performed as described in Tornehave et al. (2000).

### 2.2.4. Controls and specificity of the antibodies

No immunostaining was detected when primary or secondary antibodies were omitted during incubations. Controls and specificity of anti-TH, anti-5-HT and anti-DCX were performed as described in Pose-Méndez et al. (2014). Controls and specificity of anti-Pax6 were performed as described in Quintana-Urzainqui et al., (2014). The polyclonal anti-Shh antibody (Santa Cruz Biotechnology Inc, CA) was raised in rabbit against the amino acids 41-200 of Shh human protein. The *in situ hybridization* (ISH) results were similar to those obtained by immunohistochemistry (IHC), and therefore validate the specificity of the anti-Shh antibody used here. The polyclonal anti-GAD antibody was raised against a synthetic peptide with the amino acid sequence [C]DFLIEEIERLGQDL from rat glutamate decarboxylase (GAD65; C-terminus residues [Cys] +572-585). The monoclonal anti-SS antibody was raised against synthetic 1-14 cyclic somatostatin conjugated to bovine thyroglobulin using carbodiimide. The polyclonal anti-CB antibody was raised against recombinant rat calbindin D-28k.

### 2.2.5. *In situ* hybridization on sections

We applied *in situ* hybridization for *ScOtp* (Quintana-Urzainqui, 2013; see also chapter 1), *ScDlx2* (Quintana-Urzainqui et al., 2012, 2015; Compagnucci et al., 2013; Debiais-Thibaud et al., 2013; Quintana-Urzainqui, 2013; see also chapter 1), *ScDlx5* (Compagnucci et al., 2013; Debiais-Thibaud et al., 2013; see also chapter 1), *ScLhx9* (Quintana-Urzainqui, 2013; Pose-Méndez et al., 2015), *ScLhx5*, *ScNkx2,* (Quintana-Urzainqui et al., 2012; Quintana-Urzainqui, 2013; see also chapter 1), *ScNkx2.8*, *ScTbr1* (Quintana-Urzainqui, 2013; see also chapter 1), and *ScNeurog2* genes. These probes were selected from a collection of *S. canicula* embryonic cDNA library (mixed stages S9 to S22), constructed in pSPORT1, and submitted to high throughput EST sequencing. cDNA fragments were cloned in pSPORT vectors. Sense and antisense digoxigenin-UTP-labeled and fluorescein-UTP-labeled probes were synthesized directly by *in vitro* transcription using as templates linearized recombinant plasmid DNA or cDNA fragments prepared by PCR amplification of the recombinant plasmids. ISH in whole mount and on cryostat sections was carried out following standard protocols (Coolen et al., 2009). Briefly, sections were permeabilized with proteinase K, hybridized with sense or antisense probes overnight at 65 ºC and incubated with the alkaline phosphatase-coupled anti-digoxigenin and anti-fluorescein antibody (1:2000, Roche Applied Science, Manheim, Germany) overnight at 4 ºC. The color reaction was performed in the presence of BM-Purple (Roche). Control sense probes did not produce any detectable signal.

### 2.2.6. Image acquisition and analysis

Light field images were obtained with an Olympus BX51 microscope equipped with an Olympus DP71 color digital camera. Fluorescent sections were photographed with an epifluorescence photomicroscope Olympus AX70 fitted with an Olympus DP70 color digital camera. Photographs were adjusted for brightness and contrast and plates were prepared using Adobe Photoshop CS4 (Adobe, San Jose, CA).

## 2.3 RESULTS

### 2.3.1 *ScOtp* expression

An overview of the expression of *ScOtp* in the hypothalamus of *S. canicula* from early to late stages of development has been previously reported (see also chapter 1). In the basal plate, *ScOtp* has been identified in distinctive histogenetic domains (Tu-like and PM/PRM-like), co-distributing with *ScShh* and/or *ScNkx2.1* markers, while in the alar plate *ScOtp* is mainly expressed in the Pa-like territory, being a reliable marker of this histogenetic domain. To deepen in the genoarchitectonic profile of this compartment, in this study we have checked the expression of *ScOtp* mainly by the analysis of transverse sections through the hypothalamus of embryos from stage 29 to 32.

At stage 29, *ScOtp* is expressed in the surroundings of the optic stalk and caudally beyond, in what mainly represents the Pa-like histogenetic domain, as seen in sagittal (**Figure 1A**) and transverse (**Figures 1B-C**) sections. *ScOtp* is recognized in individual cells in the TPa-like domain (**Figure 1B**) mostly located in the marginal zone (blue arrowhead in **Figure 1B**) but also scattered through the ventricular zone. Similarly, in the PPa-like (**Figure 1C**), *ScOtp* is mainly expressed in the marginal zone (blue arrowheads in **Figure 1C**), while scarce *ScOtp*-expressing cells are observed in the ventricular zone. Furthermore, *ScOtp*-expressing cells are recognized in the marginal zone of territories dorsal and ventral with respect to the TPa/PPa-like domain, which formed a continuous stream with the marginal *ScOtp*-expressing cells of this domain. Particularly noticeable are the strings of *ScOtp*-expressing cells that extended dorsal to the TPa-like domain into the subpallial territory (black arrowheads in **Figures 1A, B**) and dorsal to the rostral-most portion of the PPa-like domain into the pallium (red arrowheads in **Figures 1A, C**). *ScOtp*-expressing cells are also observed in the marginal zone ventral to the TPa/PPa-like domain. These cells cannot be observed at the rostral-most TSPa-like domain (**Figure 1B**) but they spread just caudal from this point into the remaining TSPa/PSPa-like domain (yellow arrowheads in **Figures 1A´, C**). Of note, these ventral *ScOtp*-expressing cells are distributed into the dorsal-most marginal zone of TSPa/PSPa-like domains (yellow arrowhead in **Figure 1C**) but they spread through the SPa-like by late stage 29 (not shown).

This basic pattern is maintained until later stages of development (**Figure 1D**) with minor modifications. *ScOtp* is abundantly expressed in radial domains from the ventricular to the marginal zone at stage 32 and also in juveniles (data not shown).

### 2.3.2. *ScDlx2*/*ScDlx5* expression

The expression of *ScDlx5* from stage 18 onwards and the expression of *ScDlx2* from stage 29 onwards have been previously reported in (see also chapter 1). Fairly identical results have been observed with both markers in the brain of *S. canicula* from stage 29 onwards, so we use *ScDlx2/5* at these stages to refer indistinctly to both. However, differences are also observed which will be commented where appropriate (see below). Here we reexamine these data to additionally analyze the expression of *ScDlx2/5* from stage 29 to 32. We further characterize the ABB and possible dorso-ventral and rostro-caudal subdomains of the alar hypothalamus, mainly by the analysis of transverse sections through the hypothalamus.

At stage 29, in the alar plate of the secondary prosencephalon and rostral diencephalon, *ScDlx2/5* is expressed in the subpallium, the SPa-like and in the alar p3, while in the basal plate it is also expressed in some subdivisions of Tu-like and RTu-like (**Figure 1E-G**; see also chapter 1). Between the expression domains of *ScDlx2/5* in the subpallium and SPa-like there is a negative wedge-shaped domain spreading from the optic stalk to the pallium that contains the territory of Pa-like and the adjacent prethalamic eminence (PThE) of the diencephalic region (**Figure 1E**; see

also chapter 1). On transverse sections, the expression of *ScDlx2/5* in the SPa-like can be recognized ventrally to the optic stalk (**Figure 1F**). Interestingly, in the subpallium, *ScDlx2/5* expression occupies the whole ventricular wall while in the SPa-like it does not (**Figures 1F-G**). In the PSPa-like, the expression of *ScDlx2/5* expands ventrally into Tu/RTu-like domains (green arrowhead in **Figure 1G**) although the extent of the ventricular expression differs between both territories. The ventricular expression of *ScDlx2/5* between the SPa-like and alar p3 also differs (data not shown).

Noteworthy, from stage 29 onwards, *ScDlx2* but not *ScDlx5*-expressing cells are observed in the marginal zone of the TPa-like domain (white arrowheads in **Figure 1F´**), which is negative for *ScDlx5* expression. These cells form a continuous string with the positive *ScDlx2/5* domain in the subpallium. At this stage, this cells run through the same path where GAD-ir fibers and cells are observed (compare white arrowheads in **Figures 1F´-F´´**).

This pattern is maintained until stage 31 (compare **Figures 1H and E**). At this stage, marginal *ScDlx2*-expressing cells form a continuous stripe between the subpallium and the TSPa-like domain (white arrowheads in **Figure 1I**). In parasagital sections, 5-HT-ir fibers can be recognized ascending to the telencephalon through the alar hypothalamus (**Figure 1J**). From this stage, *ScDlx2/5* expression is recognizable in the subventricular zone of the SPa-like (data not shown). At stage 32, *ScDlx2/5* expression is maintained both in the alar and basal hypothalamus (data not shown).

### 2.3.3 *ScTbr1* expression

*ScTbr1* expression has been described from stage 25 in chapter 1, revealing that, though *ScTbr1* is not expressed in any region of the alar hypothalamus at such stages, it is a useful marker to define its boundaries. Here we examine the detailed expression of *ScTbr1* from stage 29 to 32 in order to know if such usefulness remains throughout development.

At stage 29, *ScTbr1* remains being expressed in the pallium and PThE (**Figures 2A-C**; see also Figure 6B in chapter 1). Such expression abuts dorsal and caudally the PPa-like but not the TPa-like domain (**Figures 2A-C**; also compare red arrowheads in Figures 2A, C and 1A, C). Its expression is roughly complementary to that of *ScDlx2/5* in the telencephalon and alar p3 (Figure 2A´; also compare **Figure 2A, C** with 1E, G; see also Figure 6B in chapter 1). Note that the expression of both genes, in turn, is complementary to the ventricular domains of *ScOtp* in the TPa/PPa-like (Figure 2A´; also compare **Figures 2A**, 1E, with 1A). Together, the distinct but complementary expression of *ScTbr1*, *ScDlx2/5* and *ScOtp* domains allow to define the whole alar plate of the secondary prosencephalon and alar p3.

From stage 31 this pattern is maintained in the alar hypothalamus, and minor modifications were observed involving the telencephalon (see Quintana-Urzainqui, 2013).

### 2.3.4 *ScNeurog2* expression

At stage 29, *ScNeurog2* is expressed in restricted domains of the alar and basal plates of the prosencephalon and rostral diencephalon (**Figures 2D-G**). In the alar plate, *ScNeurog2* is expressed in the ventricular zone of the TPa/PPa-like domain and dorso-caudally beyond (**Figures 2D-G**), in the pallium and PThE. *ScNeurog2* is less intensely expressed in the TPa-like than in the PPa-like (**compare Figures 2F, G**). *ScNeurog2* expression matches the ventricular domains of *ScOtp* in the TPa/PPa-like domain (compare **Figures 2D-G** with **Figures 1A-C**) and abuts the *ScDlx2/5*-expressing TSPa/PSPa-like domain (compare **Figures 2D-G** with **Figure 1E-G**). At difference with *ScOtp, ScNeurog2*-expressing cells are not observed in the marginal zones of the TPa/PPa-like domain or surrounding territories. This basic pattern is maintained until stage 30. At stage 31, *ScNeurog2* is dowregulated in the alar hypothalamus although it is maintained in the pallium (not shown).

### 2.3.5. Pax6 immunoreactivity

In the shark, the basic segmental organization of the forebrain has been approached from mid-gestation to late stages of development based on Pax6-immunoreactivity by Ferreiro-Galve et al. (2008). Besides, *ScPax6* expression, which matched Pax6-immunoreactivity, was analyzed in the whole brain from early to late stages of development through development by Ferreiro-Galve (2010). However, any of these studies have been made under the updated prosomeric model (in fact, the alar hypothalamus as such, was not considered in those studies). Here we revisited this data on the context of the updated prosomeric model from stage 28 until stage 32.

At stage 28, Pax6-immunoreactivity is observed in the ventricular zone of a longitudinal domain continuous from the alar hypothalamus to the dorso-caudal regions of the pallium (**Figures 2H-J**) and the alar p3 including the PThE (data not shown). Pax6-immunoreactivity is fairly opposed to the *ScDlx2/5*-expressing TSPa/PSPa-like domain (compare Figure 2H with Figure 1E), though some overlapping exists between both markers at ventricular levels in the dorsal and ventral part of this domain (see black arrows in **Figures 2I, J**). Besides, Pax6- ir cells are observed in the marginal zone of a restricted area of the PSPa-like domain (black arrowheads in **Figure 2H, J**).

From stage 29 onwards, those marginal Pax6- ir cells additionally form a stream continuous through the diencephalon, being also abundant in the p3Tg (**Figure 2K;** see also Ferreiro-Galve, 2010). Marginal Pax6-ir cells in the PSPa are continuous with those that populate the basal hypothalamus following the proposed course of IHB (**Figure 2K**; see also Figure 6B in chapter 1).

This basic pattern is maintained until late stages of development but Pax6-immunoreactivity is intense in cells that populate the mantle zone of alar and basal plates in the

prosencephalon. However, they are especially abundant in the TPa-like, rostral diencephalon and pallium (for review see Ferreiro-Galve et al., 2008 and Ferreiro-Galve, 2010).

### 2.3.6 *ScLhx9* expression

*ScLhx9* expression has been previously reported in the meso-isthmo-cerebellar region of *S. canicula* from stage 25 to stage 27 (Pose-Méndez et al. 2015). Here, we report that at these stages, *ScLhx9* is also expressed in restricted domains of the secondary prosencephalon and rostral diencephalon. From stage 29 onwards (present results), *ScLhx9* is expressed in restricted domains of the secondary prosencephalon and rostral diencephalon, i.e. it is expressed dorsal, ventral and caudal to the alar hypothalamus but not in it, as can be seen in sagittal (**Figure 3A-C´, E**) and transverse section through the hypothalamus (**Figures 3D**). These territories include ventricular and/or *ScLhx9*-expressing marginal cells in restricted areas of the pallium and PThE (**Figure 3A**), subpallium and basal hypothalamus (**Figure 3B**).

In the alar plate, *ScLhx9*-expressing cells are only observed in the marginal zone of the pallium and the PThE (compare **Figures 3A, D**). In the basal hypothalamus, *ScLhx9* is expressed in a restricted domain that abuts the PSPa-like domain (black arrowheads in **Figures 3A, B, D**).

This basic pattern is maintained until late stages of development (**Figure 3E**) with minor modifications concerning marginal *ScLhx9*-expressing cells in the telencephalon (see also Quintana-Urzainqui, 2013).

### 2.3.7. *ScLhx5* expression

At stage 29, the earliest we have studied, *ScLhx5* is expressed in many different restricted domains of the alar and basal plates of the prosencephalon including pallium, subpallium, alar and basal hypothalamus and alar p3, as observed in sagittal (**Figures 3F,G**) and transverse (**Figures 3H-I**) sections through the hypothalamus.

In the basal plate of stage 29 and 30, expression of *ScLhx5* is observed in a subdomain of the Tu-like domain (similar to that of Shh; see **Figures 3F-J**), and other territories of the basal hypothalamus. In the Tu-like, *ScLhx5* expression abuts the ventral border of the TSPa-like (**Figures 3H**). In the alar plate, *ScLhx5*-expressing cells are observed in the marginal zone of pallial territories dorsal to the PPa-like, similar to *ScLhx9* (red arrowhead in **Figure 3I**; compare with *ScLhx9* in Figure 3D and also with *ScTbr1* expression in Figure 2C). From this stage, *ScLhx5* it is also expressed in the alar p3 and PThE (**Figure 3G**).

At stage 31 (**Figures 3J-J´**), *ScLhx5* is expressed in the subventricular zone and mantle of the Pa-like domain. Of note, it is more extensively expressed in the TPa-like than in the PPa-like. However in the PPa-like, a noticeable string of cells continuous with that of the alar p3 is

observed (black arrowhead in **Figure 3J´**). At stage 32, intense *ScLhx5* signal has been only observed in the telencephalon while it decreases in the hypothalamus (data not shown).

### 2.3.8. *ScNkx2.1* expression

*ScNkx2.1* expression and its comparison with that of *Shh* have been previously reported from early stages of development up to stage 29 in chapter 1. The expression of any of these markers is observed in the alar hypothalamus; however they are useful to determine boundaries with neighbor territories of the basal hypothalamus and/or the subpallium. Here, we have additionally analyzed the expression of *ScNkx2.1* from stage 29 to 32 to further characterize the alar-basal boundary later in development and the possible dorso-ventral and rostro-caudal subdomains of the alar hypothalamus, mainly by the analysis of transverse sections through the hypothalamus. With the same aim, we have comparatively analyzed *ScNkx2.1* expression and Shh-immunoreactivity at stage 29.

At stage 29, *ScNkx2.1* is expressed ventral to the optic stalk through the basal hypothalamus except in the RM-like compartment (not shown), forming a sharp limit with the proposed ABB (see continuous red line in **Figures 4A-C**; see also chapter 1). Furthermore, *ScNkx2.1* and Shh-immunoreactivity co-distribute in the Tu-like region (**Figures 4B, C**), though Shh-immunoreactivity does not match the dorsal border of *ScNkx2.1* expression. Dorsal to the alar hypothalamus, *ScNkx2.1* expression and Shh-immunoreactivity also co-distributes in the subpallium (data not shown; see Quintana-Urzainqui, 2013). In the subpallium, any of these markers abuts the alar hypothalamus (**Figures 4A-B**).

This basic pattern is maintained until late stages of development being downregulated in the basal hypothalamus at stage 32 (data not shown).

### 2.3.9. *ScNkx2.8* expression

The expression of *Nkx2.8* orthologue has not been described during the brain development of other vertebrates. However, its expression pattern fairly coincides with those of other ABB markers such as *Nkx2.2* or *Nkx2.9* (Puelles et al., 2012). To characterize *ScNkx2.8* expression here we analyze: i) the expression patterns of *ScNkx2.8* through development and ii) particularly the expression of *ScNkx2.8* at stage 25 combined with anti-doublecortin (DCX) immunohistochemistry to identify pioneering tracts.

The expression of *ScNkx2.8* has been analyzed from stage 18 until late stages of development. At stage 18 *ScNkx2.8* is expressed in a longitudinal band that spreads caudally from the rostral-most point of the neural tube without reaching the spinal cord (**Figure 4D**). The expression is more intense in a restricted domain ventrally to the optic stalk (arrowhead in **Figure 4D**). This intense domain closely resembles that of *ScNkx2.*1 at the same developmental stage

(see Figure 4J in chapter 1). This pattern is fairly maintained at stage 21, but in the rostral prosencephalon, *ScNkx2.8* expands ventrally in the prospective territory of the basal hypothalamus (**Figure 4E**). The expression is extended through the whole basal hypothalamus except in its caudal and ventral-most portion, a pattern that also closely resembles that of *ScNkx2.1* at early stages of development (arrowhead in **Figure 4E**; see also Figure 4K in chapter 1). At this stage, the expression expands up to the spinal cord (**Figure 4E**). At stage 23 the expression is downregulated in the basal hypothalamus except in a rostral subdomain (black arrowhead in **Figure 4F**). Of note, the expression observed before in the longitudinal axis is maintained, and is continuous with the rostral subdomain (**Figure 4F**). Besides, *ScNkx2.8* expression is slightly downregulated in a restricted territory rostral to the diencephalon (white arrowhead in **Figure 4F**). Noteworthy, *ScShh* is also donwregulated at this point at the same developmental stage (see **Figures 4E-F** in chapter 1).

At stage 25, the expression of *ScNkx2.8* combined with DCX-immunoreactivity reveals a co-distribution of *ScNkx2.8*-expressing cells with pioneering tracts as the postoptic commissure tract (TPOC). On transverse sections this tracts are observed as round dots at the marginal zone of *ScNkx2.8* domains (see **Figure 4G** and white arrowhead in **Figure 4G´**). At this point, TPOC have been observed in *S. canicula*, which course at the convergence of the alar and basal plates (compare Figures 4G, G´ with Figure 4I in chapter 1).

From stage 28 onwards, two dorso-ventrally arranged subdomains can be differentiated through the longitudinal expression of *ScNkx2.8*, being the dorsal more intense than the ventral one (see continuous red line in **Figures 4H, I**). In the hypothalamus, *ScNkx2.8* expression is observed in a region ventral to the optic stalk (**Figure 4H**), bordering the territory where the basal expression of *ScNkx2.1* (**Figure 4B**) and the alar expression of *ScDlx2/5* (see **Figure 1F**) abut. The dorsal intense domain is expressed in the ventral-most TSPa/PSPa-like domain (**Figures 4H, I**). The ventral less intense domain is expressed in the Tu/RTu-like domain (**Figures 4H, I**).

Furthermore, the expression of *ScNkx2.8* combined with Shh-immunoreactivity reveals that Shh-immunoreactivity in the basal hypothalamus abuts *ScNkx2.8* expression (i.e., the Tu/RTu-like domain) and therefore does not abut the TSPa/PSPa-like domain (**Figures 4H**).

The mentioned pattern is maintained in later stages of development. However, the expression in the forebrain becomes downregulated (although still recognizable) from stage 31 onwards (data not shown).

### 2.3.10 GAD-immunoreactivity.

GAD immunoreactivity was previously analyzed during the brain development of sharks by Carrera et al., (2008) and Carrera (2008), and in combination with other markers by Ferreiro-Galve et al., (2008). However it was not examined under the current prosomeric model. In the present work, GAD-immunoreactivity has been particularly analyzed at stage 30 to test if the

segmental organization described by gene expression patterns at similar stages is congruent with that deduced by means of neurochemical markers.

At stage 30, in the alar plate, GAD-immunoreactivity is observed in the subpallium and TSPa/PSPa-like domain, in a pattern that resembles that of *ScDlx2/5* (**Figure 5A**; compare with Figure 1E). Similarly to *ScDlx2/5*, GAD-immunoreactivity is reduced in a wedge-shaped territory that extends from the TPa/PPa-like domain to the pallium and PThE [**Figure 5A**; compare with Figure 1E; see also Carrera, (2008)]. Furthermore, it is also more broadly observed in the Tu/RTu-like (**Figure 5A**) than in other compartments of the basal hypothalamus (see also Carrera, 2008).

### 2.3.11 SS-immunoreactivity

We have analyzed somatostatin-immunoreactivity since this marker has been useful to identify subdomains and limits of the basal hypothalamus in other vertebrates and due to the fact that *Otp* is involved in the specification of SS-expressing cells (Morales-Delgado et al., 2011; Dominguez et al., 2015). SS-immunoreactivity is detected in the TSPa-like domain (arrowhead in **Figure 5B**) but not in other domains of the alar hypothalamus. SS-immunoreactivity is also observed in the subpallium, Tu-like, alar and basal p3 (**Figures 5B, C**) and PRM-like domain (not shown) while it is absent in the pallium and remaining compartments of the basal hypothalamus (**Figures 5B, C**).

### 2.3.12. CB immunoreactivity.

Calbindin immunoreactivity has been analyzed in the brain of adult sharks by Rodríguez-Moldes et al. (1990) revealing conspicuous cell populations in prosencephalic derivatives. Since, in mammals, CB appears to be a good marker of the Pa domain (Puelles et al., 2012), here we have analyzed the distribution of CB-immunoreactivity in the alar hypothalamus of selected embryonic stages under the updated prosomeric framework. Such distribution is similar to that described in adults (Rodríguez-Moldes et al., 1990). At stage 30 CB-immunoreactivity is observed in different regions of the alar and basal plates of the prosencephalon and in p3, but not in the alar hypothalamus or in the pallium (**Figure 5D**). Main clusters are found in the subpallium (not shown), Tu-like and PThE territories (arrowhead in **Figure 5D**) but dispersed cells can be observed in the remaining territories mentioned above (**Figure 5D**).

### 2.3.13. TH-immunoreactivity.

The segmental organization of TH-immunoreactivity was previously analyzed during the development of shark by Carrera et al., (2012) and in combination with other markers by Ferreiro-Galve et al., (2008). As the updated prosomeric model proposes important changes concerning the hypothalamus organization, here we re-examine TH-immunoreactivity

particularly at stage 30 to test if the segmental organization described by gene expression patterns at similar stages is congruent with that obtained by neurochemical markers.

At stage 30, TH-immunoreactivity is observed in the basal hypothalamus, basal p3 (p3Tg) and subpallium, in the TSPa/PSPa-like, the pallium, or alar p3 (**Figure 5E**). TH-immunoreactivity is seen in fibers that course ventrally to the SPa-like but dorsally to the Shh-ir Tu-like domain in the basal hypothalamus (arrowheads in **Figure 5E**). At the end of stage 30, TH-immunoreactivity is observed in cells at the SPa-like (Figure 2A in Chapter 4 in Carrera, 2008).

## 2.4 DISCUSSION

### 2.4.1. Boundaries and borders

In a previous work, we have defined the dorsal, caudal and ventral limits of the shark alar hypothalamus based on the expression of *ScFoxg1a*, *ScOtp*, *ScTbr1*, *ScDlx2/5*, *ScNkx2.1*, and *ScShh* in the framework of the updated prosomeric model (see chapter 1). Here we review this data and present new genetic and neurochemical evidences that further support these boundaries.

The dorsal limit between hypothalamus and telencephalon, the hypothalamo-telencephalic border (**HTB**), has been previously characterized based on the complementary expression of *ScFoxg1a* in the telencephalon and *ScOtp* in the TPa/TPa-like domain (see chapter 1). Here we add that the combined expression of *ScOtp*, GAD/*ScDlx2/5* and *ScTbr1*/*Lhx9* outlines such limit. The TPa-like abuts *ScDlx2/5* dorsal expression while the remaining PPa-like mainly abuts *ScTbr1* (Figure 6A-B). Noteworthy, at stage 29 the PPa-like is mainly in contact with the pallium while in other vertebrates both territories are in contact just by a thin corridor (Puelles and Rubenstein, 2003; Moreno et al., 2012; Puelles et al., 2012; Domínguez et al., 2013), situation that is also observed in the shark beyond stage 31, after a further development of the subpallium over the pallium (Figures 6B,7A, B). The border defined by *ScTbr1* is also well defined by *ScLhx9*-expressing cells located in the marginal zone of *ScTbr1* territories (see Figure 6A). The pattern of GAD-immunoreactivity fairly respect the defined HTB matching the same border as *ScDlx2/5* (compare Figures 5A and 1E; see also Figures 6A, C), as expected having into account that *Dlx2/5* genes are involved in the genetic specification of GABAergic cells (Anderson et al., 1999) and that in *S. canicula*, as in other vertebrates, the expression pattern of the *Dlx2* in the subpallium matches with that of GABAergic cells (Quintana-Urzainqui et al., 2012, 2015).

Of note, in mouse, CB-immunoreactivity is found in the TPa/PPa also defining the HTB (Puelles et al., 2012). However, CB-immunoreactivity is not detected in shark, neither in embryos (Figures 5D, 6C) nor in adults (Rodríguez-Moldes et al., 1990).

The present results support that the hypothalamo-diencephalic border (**HDB**) of *S. canicula* is defined by the complementary expression of *ScTbr1* in the PThE and *ScOtp* in the caudal PPa-like (compare Figures 2A and 1E; Figure 6A) as previously noticed (see chapter 1). Now, we show that this border can be also defined based on the single expression of *ScLhx5* in the whole alar p3 (Figure 6B). The expression of *ScLhx9* is also useful to define the limit between the caudal PPa-like and the PThE (Figure 6A). In addition, as *ScNeurog2* is continuously expressed through the TPa/PPa-like and pallium, including the PThE (Figures 2D). However, its expression lacks in the PThE in parasagittal sections (Figure 2E).Of note, structures showing SS-immunoreactivity and CB-immunoreactivity, together, define the same border as *ScLhx5* in the alar p3 (compare Figures 5C, D with 3G; see also Figures 6B, C). Strikingly, CB-immunoreactivity is restrictedly expressed in the PThE while structures showing SS-immunoreactivity are ascribed to the remaining alar p3 in a similar manner as *ScTbr1* and *ScDlx2/5* do (compare Figures 5D and 5C with 2A and 1E respectively; see also Figure 6A,C). Noteworthy, TH-immunoreactivity is observed in cells at the TSPa/PSPa-like but not in the alar p3 which also supports the HDB (Figure 6C).

Our present results support that the alar-basal boundary (**ABB**) in the shark hypothalamus is outlined by the abutted expression among *ScDlx2/5* in the alar plate and *ScNkx2.1* or *ScShh* in the rostral basal plate, as previously proposed (see chapter 1). While these markers indeed define alar and basal territories, respectively, our present results also reveal this boundary is thicker than previously considered. This fact made us to review the situation of the ABB which has been misleadingly defined through literature. In the updated prosomeric model, the ABB is defined by the longitudinal expression of *Nkx2.2* and other genes here co-expressed such as *Nkx2.9*, *Ptc* and *Gsx* (Puelles et al., 2012). A relevant aspect of this ABB is that *Nkx2.2* is expressed in restricted domains within alar and basal plates, co-distributing with *Nkx2.1* and *Lhx6/Lhx8* (in alar domains) and with *Nkx2.1* and *Lhx9* (in basal domains; Puelles et al., 2012). Of note, the expression of *Nkx2.1* in the ABB seems to correspond to mantle cells rather than ventricular domains (Puelles et al., 2012; Domínguez et al., 2015). The fact that *Nkx2.2* defines the ABB but in turn is expressed in alar and basal plates reveals that an additional concept is being implicitly used (although often not noticed, even for the authors of the model) to differ alar and basal plates. As the ABB is at the same time alar and basal, here we coin the concept "alar-basal border" (**ABBr**) to define the virtual point where alar and basal genes meet. Of note, this border should be understood to be neither alar nor basal; nothing could be over this figurative border and genes could only be dorsal or ventral to it (see Figure 6A-C).

Having into account this concept to interpret the present results, we propose that the shark ABBr is defined by the abutted expression of *ScDlx2/5* in the alar SPa-like and the basal expression of *ScNkx2.1*, *ScLhx5* and *ScLhx9* (see Figure 6A, B). On the other hand, we assume that the expression of *ScNkx2.8* in the territory between the Pax6-ir alar SPa-like and the Shh-ir

basal plate of the rostral hypothalamus define the ABB (Figure 6B). Although *Nkx2.8* is a fairly uncharacterized marker in neuroanatomical studies, our present observations support that the shark *Nkx2.8* orthologue is likely expressed in the ABB on the basis that i) its expression closely resembles the pattern of *Nkx2.2* in other vertebrates at the ABB (Barth and Wilson, 1995; Domínguez, 2011; Sugahara et al., 2011; Puelles et al., 2012), ii) it co-distributes with the TPOC, which is also assumed to define the ABB [see Figure 4G-G´; (Barth and Wilson, 1995; Shimamura et al., 1995; Puelles et al., 2012)]; and iii) it is expressed in alar and basal plates, as shown by *Nkx2.2* in the mouse (see Figures 4H-I; see also Puelles et al., 2012; 2015).

### 2.4.2 Prosomeric compartments and subcompartments of the alar hypothalamus.

Based on the alar complementary expression of *ScOtp* and *ScDlx2/5*, we have previously identified the shark alar hypothalamus harboring a Pa-like and SPa-like domains and tentatively defined its rostro-caudal subdivision by the course of the medial forebrain bundle (mfb) through the rostral border of hp1, just caudal to the optic stalk (see chapter 1). However we did not find molecular evidences of further rostro-caudal or dorso-ventral subdivisions. Here we deepen in the genoarchitectonic profile of the shark alar hypothalamus providing molecular insights of their dorso-ventral and rostro-caudal subdivisions besides further histogenetic implications of the markers expressed.

#### 2.4.2.1 Pa-like: Genoarchitectonic profile and further prosomeric subdivisions

We have previously characterized the shark Pa-like by the expression of *ScOtp* and the lack of *ScDlx2/5* (see chapter 1). Here we show that in this domain, similarly to that reported in tetrapods (Stoykova et al., 1996; Medina, 2008; Abellán et al., 2010; Osório et al., 2010; Puelles et al., 2012; Domínguez et al., 2013, 2015), *ScOtp* co-distribute with Pax6, *ScNeurog2* and *ScLhx5* but differently not with *ScTbr1*, differing the situation observed in mouse (see Figure 7A, B; Puelles et al., 2012; Ferran et al., 2015). Of note, cells expressing *ScNkx2.8*, a gene with a similar expected distribution to *Nkx2.2* in mammals (see above), have not been observed in shark beyond the ABB. Further molecular rostro-caudal subdivisions have been described in the Pa of some tetrapods based on markers restrictedly expressed in the terminal or peduncular Pa (TPa, PPa; respectively; Figure 7A; Domínguez et al., 2013, 2015; Ferran et al., 2015; Puelles and Rubenstein, 2015). Rostro-caudal and dorso-ventral subdivisions have been also established based on the identification of different peptidergic progenitor subdomains (Morales-Delgado et al., 2011, 2014; Puelles et al., 2012). Strikingly, in the shark, while *ScOtp*, *ScNeurog2*, and Pax6 are similarly observed through the Pa-like, *ScLhx5* presents a differential rostro-caudal expression. From stage 30 onwards, it seems to be more abundantly expressed in the terminal Pa-like (TPa-like) than the peduncular Pa-like (PPa-like) forming an evident border (see Figure 3J, J'; see also Figure 7B). Of note, this abundant *ScLhx5*-expressing subdomain is rostral to the 5-HT-ir tracts that course along the mfb (compare Figure 3J, J' with 1J). Since these tracts were

suggested to course to the telencephalon caudally to the IHB, through the rostral-most portion of the hp1 prosomere (Puelles et al., 2012; see chapter 1), we interpret that the abundantexpression of *ScLhx5* in the TPa-like correctly defines this compartment and the IHB, evidencing molecular rostro-caudal differences in the Pa-like (Figure 7B; see also Figure 6B in chapter 1; see also Puelles et al., 2012). Noteworthy, *Lhx5* has been also described to be more abundantly expressed in the rostral supraoptoparaventricular region (SPV; equivalent to the Pa-like; Domínguez et al., 2015). Taking all these considerations together, we interpret that the shark Pa presents a similar genoarchitectonic profile and further molecular rostro-caudal subdivisions to that observed in the mouse and proposed by the prosomeric model. However, further dorso-ventral subdivision could not be addressed in the present work. Finally, as discussed below, these traits seem to be acquired before the anamniote-amniote transition, earlier than previously considered (Domínguez et al., 2015).

#### 2.4.2.2 Tangential migrations involving the Pa-like and amygdala-like derivates

In the mouse, tangentially migrations involving the hypothalamus as source and/or recipient territory have been characterized from time ago by means of immunohistochemistry, autoradiography and *in situ* hybridization techniques (Morales-Delgado et al., 2011; Puelles et al., 2012; Morales-Delgado et al., 2014; Croizier et al., 2015; Díaz et al., 2015). The study of some of these intra-hypothalamic migrations led to the identification of three dorso-ventral progenitor subdomains (with their respective rostro-caudal subdivisions) in the Pa of the mouse (Morales-Delgado et al., 2011, 2014; Puelles et al., 2012). Furthermore, tangentially migrated cells derived from the Pa have been also described as contributing to extra-hypothalamic territories such as the amygdala. These cells expressing *Otp*/*Lhx5* transcription factors have been described to contribute to both the subpallial bed nucleus of the stria terminalis-like (BNST) and the medial amygdala-like (MA) in the mouse (Medina et al., 2011). In other vertebrates, similar *Otp*-expressing cells have been described as colonizing amygdala-related territories (Bardet et al., 2008; Medina et al., 2011).

Although further studies using tract-tracing techniques should be needed to confirm it, in the present study we have identified putative pathways of tangential migrations based on the spatio-temporal patterns of different markers widely used to identify tangentially migrating neurons, including cells expressing *ScDlx2*, *ScOtp* and cells showing Pax6-immunoreactivity. These cells seem to involve the alar hypothalamus as source or recipient territories, leading to further characterize the SPa-like but not the Pa-like domain. Because the specification process that lead to the expression of these genes is different from those of their recipient territories, we interpret that these cells in fact could have migrated tangentially as also suggested by Morales-Delgado et al., (2011) in mouse. Our observations support the existence in shark of cells that appear to migrate from the alar hypothalamus (*ScOtp*-expressing) as well as cells possibly

migrating within or into the alar hypothalamus (*ScOtp*-expressing; *ScDlx2*-expressing; Pax6-ir) which in both cases affect the SPa-like domain (see below).

The presence of *ScOtp*-expressing cells in the mantle of the rostral *ScDlx2/5*-positive subpallium forming a continuous stream with those in the mantle of the also *ScOtp*-expressing TPa-like (black arrowheads in Figures 1A, B, D; see also Figure 7B), suggests the existence of a migratory pathway from the Pa to the subpallium. Such *ScOtp*-expressing cells emanating from

Pa-like territories could contribute to form amygdala-related structures. Similarly, a migratory pathway of *ScOtp*-expressing cells from the Pa to the pallium may be suggested on the basis of the existence of the stream of *ScOtp*-expressing marginal cells that extends from the PPa-like to dorsal-most levels (see red arrowheads in Figures 1A, C), which can be identified as pallial territories (negative for *ScDlx2/5* but positive for Pax6-immunoreactivity and *ScTbr1* expression; see red arrowheads in Figures 1A, 1E, 2A, 2H; see also Figure 7B). Because this pallial territory, as described by Quintana-Urzainqui (2013) at later stages, also presents marginal *ScLhx9*-expressing cells, these *ScOtp*-expressing cells likely to belong to amygdaloid structures related to the ventral pallium.

Our observations in the shark appear to reveal similar tangentially migrated *Otp*-expressing cells to those described in the mouse and other vertebrates (Bardet et al., 2008; Medina et al., 2011). Thus, although our results require further confirmation, we suggest that *ScOtp*-expressing cells emanating from Pa-like territories could contribute to form amygdala-related structures. Particularly, the population found in subpallial territories of *S. canicula* could give rise to amygdaloid structures related to the BNST while that found in the *ScLhx9*-expressing pallium could form amygdaloid structures related to the MA. We cannot ascertain whether this likely migrating cells emerge form TPa or PPa-like although in mouse they seem to be born in the TPa-like (Morales-Delgado et al., 2011). Nevertheless, more studies are needed to firmly demonstrate what seems likely, i.e., that *ScOtp* amygdala-related structures are, at least, an early acquisition of gnathostome vertebrates.

2.4.2.3 Considerations about the pallial-like genoarchitectonic profile of the Pa-like territory

In mouse, Pax6 is expressed in a broad territory on which the co-distribution with other markers led to the identification of different subdomains in the pallium (Figure 7A; see also Stoykova et al., 1996; Medina et al., 2004, 2011; Medina, 2008; Puelles et al., 2012). In the shark, a similar analysis on pallial subdivision was made from stage 31 onwards by Quintana-Urzainqui (2013). In the present work we stress that Pax6 defines a continuous ventricular domain spreading in two axes: rostro-caudal, from the optic to the alar p3; and dorso-ventral, from the pallial-subpallial boundary to the ABB (as previously reported by Ferreiro-Galve et al., 2008; Ferreiro Galve, 2010). In such territory, the expression of Sc*Otp*, Sc*Neurog2*, Sc*Tbr1*,

Sc*Lhx5*, Sc*Lhx9* in the ventricular zone (v), subventricular zone (s) and/or the mantle zone (m) defines different sub-divisions inside the mentioned Pax6-positive territory (present results) in the pallium and beyond : TPa-like (Pax6v/*ScOtp*vm/ScNeurog2vs/abundant *ScLhx5*m); PPa-like (Pax6v/*ScOtp*vm/*ScNeurog2*vs/*ScLhx5*m) ventral pallium (Pax6v/*ScTbr1*s/*ScLhx9*m); lateral pallium (Pax6v/*ScTbr1*s/*ScNeurog2*vs); medial pallium (Pax6v/*ScTbr1*s/*ScLhx9v*); dorsal pallium (Pax6vm*/ScTbr1s*), PThE (Pax6v/*ScNeurog2vs/ScTbr1*s/*ScLhx5*vm/*ScLhx9*m), and some subdivisions of the alar p3 (Pax6v/*ScLhx5*vm) (Figure 6A, 7B). This analysis suggests that the TPa/PPa-like has a pallial-like genoarchitecture.

These observations support two ideas. On one hand, the fact that the TPa/PPa-like expresses genes related to the pallium, while the preoptic area (defined in terms of molecular specification codes) express genes like *Dlx, Nkx2.1* or *Shh* related to the subpallium (see Flames et al., 2007; Bardet et al., 2010), support previous observations in other vertebrates that these domains belong to different histogenetic territories (Bulfone et al., 1993; Puelles et al., 2000; Flames et al., 2007). On the other hand, the fact that markers expressed in the pallium are also expressed in the Pa-like and PThE suggests that the last territories are subdomains of an expanded pallial-like territory. Noteworthy, the fact that in the updated prosomeric model nor the Pa neither the HTB reach the HDB at the roof plate (see Figure 8.5B in Puelles et al., 2012) implicitly support the continuity among Pa, PThE and pallium. As discussed in chapter 1, *ScFoxg1* is expressed in the pallium and subpallium also defining the HDB, highlighting a discontinuity between the telencephalon and the alar hypothalamus. However, the loss of the ventral but not the dorsal telencephalon in *Foxg1* null mutant mice (Xuang et al., 1995; Martynoga et al., 2005) supports that this marker is required for the development of the subpallium but maybe not for all the telencephalon questioning its reliability as telencephalic marker. The lack of Pax6 in the supraoptoparaventricular area (SPV; equivalent to the Pa) of amphibians could be against such continuity among pallium, Pa-like and PThE (Dominguez et al., 2013; 2015). Nevertheless, Pax6 donwregulation in the Pa-like of amphibians could be an acquired trait since, likely, it is expressed in other anamniotes (see below). Together, our unorthodox proposal should be considered as an open question to deep in future studies.

2.4.2.4. SPa-like: further prosomeric subdivisions

We have previously identified the shark SPa-like domain by the expression of *ScDlx2/5* and the lack of *ScOtp,* and characterized its rostro-caudal subdivisions by the course of the mfb through the rostral border of hp1 (see chapter 1). Our present results suggest that the shark SPa-like present a dorso-ventral regionalization (SPaD-like and SPaV-like, respectively) resembling that proposed for the mouse, where dorso-ventral (dorsal SPa [SPaD] or supraliminal and ventral SPa [SPaV] or liminal) and rostro-caudal (the terminal TSPa and the peduncular PSPa) subdivisions have been defined on the basis of the complementary or partial overlapping of specific genes as *Dlx2, Nkx2.1* and*Nkx2.2*, among others (Morales-Delgado et al., 2011; Puelles

et al., 2012; Díaz et al., 2015; see also Figure 7B) Besides, a rostro-caudal regionalization based on the differential distribution of presumed tangentially migrated cells lead us to propose the existence of terminal (TSPa-like) and peduncular (PSPa-like) subdomains by the intersection of dorso-ventral and rostro-caudal differences (TSPaD-like and TSPaV-like; PSPaD-like and PSPaV-like, respectively; see below).

The dorso-ventral regionalization of the shark Spa-like is rather evident. A **SPaD**-like can be defined by the co-distribution of *ScDlx2/5* and Pax6, ventral beyond the Pa-like (see continuous and dashed black lines in Figures 1F, G, 2I, J respectively; see also Figure 7B). In this subdomain, Pax6-immunoreactivity is not detected through the whole ventricular surface and characteristically shows a weak labelling (see black arrow in Figures 2I-J; see also Figure 7B), which appears to be common in regions where *Pax6* and *Dlx* co-distribute (like the pallium-subpallium boundary; see below). On the other hand, a **SPaV**-like can be defined in shark by the ventricular co-distribution of *ScDlx2/5* and *ScNkx2.8* (compare Figures 1F, G with 4H, I; see also Figure 6B, 7B). As discussed above, *ScNkx2.8* defines the ABB, being expressed in the alar and basal plates. Thus, as also exposed above, the expression of *ScNkx2.8* in the ABB abuts dorsally with ventricular Pax6-ir cells in the SPaD-like domain (compare Figures 4H, I with 2I-J; see also Figures 6B, 7B) and ventrally with cells showing Shh-immunoreactivity in the rostral basal hypothalamus (Figure 4H; see also Figures 6B, 7B). Of note, *ScNkx2.8* also presents a dorso-ventral regionalization being more intensely expressed in the dorsal and alar domain than in the ventral and basal domain (see Figures 4H, I). The ventral rim of the alar plate can be identified by the expression of *ScLhx9* in a band comparable to the subliminal domain described in mouse (Figures 3A-E; see also Figures 6B, 7A-B) or by the expression *ScLhx5* or *ScNkx2.1* in the basal plate (Figures 3F, H-J and Figures 4A-C; see also Figures 6A, 7A-B). Taking all together, the dorso-ventral compartmentalization in the shark SPa-like seems evident, but differences with that described in mammals are noted, especially in the SPaV-like compartment (compare Figures 7A and B).

#### 2.4.2.5 Tangential migrations involving the SPa-like and basal hypothalamus

In the Pa-like, *ScOtp* expression is continuous with *ScOtp*-expressing cells into the marginal zone of the SPaD-like (see yellow arrowheads in Figures 1A´, C, D; see also Figure 7B) excepting at the rostral-most portion of the TSPa-like (see Figure 1B). However, by late stage 29 these *ScOtp*-expressing cells are observed in the subventricular zone of the *ScDlx2/5*-positive SPaD/SPaV-like (data not shown). Taking into account their spatio-temporal distribution, as argued above, we consider that such *Otp*-expressing cells may have migrated tangentially from the Pa-like to the SPa-like. Similar *Otp*-positive cells have been also observed in the SPa of the mouse (Bardet et al., 2008; Morales-Delgado et al., 2011). Moreover, *Otp*, has been involved in the development of the catecholaminergic phenotype in the zebrafish hypothalamus (Del Giacco

et al., 2006; 2008; Blechman et al., 2007; Ryu et al.; 2007), suggesting a correlation among Sc*Otp*-expressing cells and TH-ir cells in the SPa-like of the shark (compare Figures 6C and 7B).

Furthermore, a rostro-caudal regionalization in the SPa-like domain can be distinguished based on cells showing Pax6-immunoreactivity presumed to be tangentially migrated cells. These cells are observed in the mantle zone of Pax6- and *ScDlx2/5*-positive ventricular domains in the SPaD-like (black arrowheads in Figure 2H, J; compare with Figures 1F, G; see also Figure 7B). Similar Pax6-positive cells can be observed at the pallial-subpallial boundary, in the mantle of the dorsal lateral ganglionic eminence (LGE) and other *Dlx* territories pointing that the presence of Pax6-ir cells in the mantle is common in regions where *Pax6* and *Dlx* co-distribute (Flames et al., 2007; Ferreiro-Galve et al., 2008; Ferreiro Galve, 2010; Medina et al., 2011; Quintana-Urzainqui, 2013). Although at stage 28, these cells seem to occupy both the PSPaD-like and the PSPaV-like (Figure 2J) they are only be observed caudal to the TSPa-like forming a continuous stream with diencephalic marginal Pax6-ir cells (black arrowheads in Figures 2H, J; agreeing with previous descriptions in Ferreiro-Galve (2010) although using a different terminology). Noteworthy, similar cells have been found in the mouse addressed to the "posterior entopeduncular area" which parsimoniously fit with the updated hp1 prosomere (see Figures 7A-B) (Stoykova et al., 1996; Puelles et al., 2012). From stage 30 onwards these cells spread into the hypothalamic basal plate (white arrowheads in Figure 2K) forming a strikingly stream that closely describes the IHB proposed in chapter 1). Besides, these cells apparently reach the MM/RM-like border, and thus, the hp2/hp1 limit (Puelles et al., 2012; see chapter 1), which again fits with the model. Thus we interpret that these Pax6-ircells are caudal to the IHB likely accompanying tracts coursing by the rostral border of hp1 (of note, the updated model provided an explanatory framework for this observation). In fact, Pax6 expression has been involved in the correct pathfinding of different tracts systems through the prosencephalon by means of both, indirect and local mechanisms, which supports this idea (Mastick et al., 1997; Vitalis et al., 2000; Jones et al., 2002; Prestoz et al., 2012). Taking together these observations, we interpret that a TSPa-like can be differentiated from a PSPa-like based on these cells both in the mouse and the shark (see Figure 7B; see also Stoykova et al., 1996; Puelles et al., 2012).

Finally, we also have observed a group of *ScDlx2*-expressing cells continuous with the subpallium in the marginal zone of the TPa-like (arrows Figure 1F´). As discussed above, since *Dlx* and *Otp* expression are the result of different developmental processes we interpret that these cells migrate tangentially. Of note, at later stages and in an equivalent position, *ScDlx2*-expressing cells form a continuous string among the *ScDlx2/5* expressing subpallium and the TSPa-like domain suggesting the existence of at least one telencephalic-hypothalamic stream (arrowheads in Figure 1I; see Figure 7B). Noteworthy, Tripodi et al. (2004) and Shimogori et al. (2010) respectively detected COUP-TF-expressing and *Foxg1*-expressing cells likely emanating from the ventral telencephalon into the anterior hypothalamus. Furthermore, one of those

migrating streams described by Tripodi et al. (2004) seems to course from the subpallium to the suprachiasmatic region (equivalent to the SPa) through the marginal anterior hypothalamus (equivalent to the Pa) resembling that observed in the shark (see their Figure 6B). Thus, the existence of a tangential telencephalic-hypothalamic stream could be conserved among vertebrates similarly to other migrations that have been recently identified in the telencephalon of the shark (Quintana-Urzainqui et al. 2015).

### 2.4.3 Evo-Devo considerations concerning the alar hypothalamus.

We have revisited our previous observations about *ScNkx2.1*, *ScDlx2/5*, *ScOtp*, *ScTbr1* expression and Pax6-immunoeactivity and we have additionally analyzed *ScNkx2.8*, *ScNeurog2*, *ScLhx5* and *ScLhx9* expression to better characterize the genoarchitectonic organization of the shark alar hypothalamus and neighboring territories. Our analysis reveals that the data described for the chondrychthyan model, *S. canicula*, globally fit with the general assumptions and further details of the prosomeric model together with an important part of the data described in mouse (see above; see also Puelles et al., 2012; see chapter 1). Besides, for the genes studied and compared here, our data also reveal a strikingly degree of conservation of expression in the compartments (Pa-like, SPa-like) among both models. These facts support the early acquisition of these traits in development and evolution, which explain the similarities observed across vertebrates at a certain level of analysis, being also the base of the establishment of homologies (Puelles and Medina, 2002). Differences are also observed but mainly addressed to the identity (rostro-caudal; ventro-dorsal) of subcompartments, which could explain local differences in proliferation and differentiation patterns across organisms, yielding different morphologies and neuronal subtypes.

To better understand the evolutionary meaning of these observations, here we have comparatively reviewed our findings with data described in other vertebrates. A similar analysis was made by other authors in the context of precedent prosomeric conceptions (Wullimann et al., 2005; van den Akker et al., 2008; Osório et al., 2010; Domínguez, 2011; Moreno and González, 2011; Moreno et al., 2012; Domínguez et al., 2013) and a recent work reviewed data on the anamniote-amniote transition under the updated paradigm (Domínguez et al., 2015). The analysis of our data in shark, based on comparing the presence/absence of expression of certain genes in equivalent topological regions, disagree with some of their interpretations concerning some acquisitions at the anamniote-amniote transition. To shed light on this matter, we have performed a further review of available results in bony fishes and agnathans to better know the anamniote scenario. We are aware of the difficulties to carry out such comparison, mainly because of the scarce number of detailed works specifically addressing the alar hypothalamus. Furthermore, establishing comparisons and homologies among vertebrates results misleading since, depending on the animal model, the brain organization paradigm and/or the version of the prosomeric model considered, the progenitor domains are referred under a plethora of different names [the Pa-like for example can be also named as preoptic region/area; supraoptoparaventricular area, preoptic supraoptoparaventricular region, optoeminential region or paraventricular region, posterior intrahypothalamic diagonal, among others, while the SPa-like region can be referred as preoptic area/region, suprachiasmatic area/region, anterior intrahypothalamic diagonal;

suprachiasmatic/anterior hypothalamus posterior area or hypothalamic cell cord/ posterior entopeduncular area, among other names (Wullimann and Rink, 2001; Bardet et al., 2008; Shimogori et al., 2010; Puelles et al., 2012; Domínguez et al., 2014, 2015; Herget et al., 2014; Manoli et al., 2014)]. In addition, comparisons could also be misleading even working under the same paradigm due to differences in axis interpretation. As an example, in amphibians and reptiles, Domínguez et al., (2015) describe rostro-caudal (but not dorso-ventral) subcompartments. However, an interpretation of such subdomains as dorso-ventral would reflect a more parsimonious course of the IHB.

#### 2.4.3.1 Vertebrate Pa-like

The available information about the expression of selected Pa markers in vertebrates as mouse, chick, *Xenopus*, zebrafish and lamprey reveals the following scenario: *Otp* is suggested to be expressed in the Pa-like of all the vertebrates studied so far, *Lhx5* seem to be expressed only in tetrapods, and *Pax6* and *Neurog2* seem to be an amniote acquisition (Wullimann et al., 2005; Joly et al., 2007; Osório et al., 2010; Domínguez, 2011; Moreno and González, 2011; Moreno et al., 2012; Domínguez et al., 2013; 2015). Our present data in a shark representative of basal gnathostomes support the early acquisition of *Otp* and also reveal an acquisition of *Neurog2*, *Pax6* and *Lhx5* earlier than previously suggested.

The expression of *Lhx5* has been clearly reported in the Pa of amniotes (Abellán et al., 2010; Shimogori et al., 2010). In *Xenopus*, *Lhx5* expression has been described in the "rostral supraoptoparaventricular area" (Domínguez et al., 2013, 2015), a territory that could be related to the Pa. Our results in shark clearly show *Lhx5* expression in the Pa-like of a gnathostome fish. As far as we know there are no similar reports in other fishes, although *Lhx5* expression has been recently described in the "preoptic supraoptoparaventricular area" of zebrafish (Manoli et al., 2014), a territory that could be equivalent to the Pa domain. Moreover, the possibility that *Lhx5*-like expression in Pa-like territory happened earlier than the gnathostome emergence should be taken into account. The expression of *Lhx1/5* has been described in the prosencephalon of *Lampreta fluviatilis* by Osorio et al., (2005) and, although a detailed description about its possible expression in the Pa-like territory is lacking, a close inspection of their Figure 5B supports this possibility. Besides, *Lhx1/5* has been clearly described in the magnocellular preoptic nucleus of *Petromyzon marinus* in later stages of development (Osório et al., 2006). Taking together these observations, we interpret that, likely, *Lhx5*-like expression was early acquired in the Pa-like of vertebrates.

Pax6 has been described in the alar hypothalamus of amniotes (Stoykova and Gruss, 1994; Li et al., 1994; Stoykova et al., 1996; Puelles et al, 2000; Moreno et al., 2012; see also Robertshaw et al., 2013 and their supplemental material) but not in *Xenopus* (Bachy et al., 2002; Moreno et al., 2008). The expression of Pax6 in shark (Ferreiro-Galve et al., 2008; Ferreiro-Galve, 2010; present results) supports an early acquisition in basal gnathostomes. Furthermore, in zebrafish, Pax6-immunoreactivity has been shown in the caudal-most preoptic area (Wullimann and Rink, 2001; Wullimann and Mueller, 2004), which could correspond to what we interpret as the updated Pa-like domain. Similarly, the distribution of cells showing Pax6-immunoreactivity

in the trout *Salmo trutta fario* (unpublished observations) is compatible with this idea. In lampreys, *Pax6* is likely to be expressed in the Pa-like (Figure 7C) although differentially among different species (Murakami et al., 2001; Derobert et al., 2002; Uchida et al., 2003; Osorio et al., 2005; Sugahara et al. 2011). As in other vertebrates, its expression is located among dorsal and ventral *Dlx1/6* expression patterns (see "TE" and "TH" in Figure 6B of Murakami et al., 2001). In *Lethentheron japonicum*, developing supraoptic tracts (SOT) tracts to the telencephalon appear to divide the mentioned Pax6 domain in rostral and caudal portions (see Figures 2B, 4C2, C3 in Suzuki et al., 2015; see also Barreiro et al., 2008), which support the SOT as to belonging to the mfb, as suggested by Puelles et al. (2012), resembling the situation observed in the shark (see chapter 1). Sugahara et al. (2011) also demonstrated that *Pax6* expression in the rostral secondary prosencephalon of *Lethenteron japonicum* seems to be regulated by *Shh* and *Fgf* pathways. Noteworthy, the inhibition of such pathways performed by Sugahara et al. (2011) yield an *Pax6* expression pattern similar to that found in *Lampetra japonica* by Murakami (2001) (compare Figures 5E and 7E in the first, with 7E in the second). Thus, *Pax6* seems to be acquired but differentially expressed in lampreys. Together, all this data point that a Pax6 expressing Pa-like domain seems to be present in early vertebrates being an early conserved trait of vertebrates.

Members of the *neurogenin* family have been reported in the forebrain of different vertebrate groups, including lampreys ( Wullimann et al., 2005; Guérin et al., 2009; Nieber et al., 2009; Osório et al., 2010; Robertshaw et al, 2013). There are no doubts of its expression in the Pa of amniotes. In mouse, *Neurog2* expression has been described in the supraoptic/paraventricular and anterior hypothalamus (equivalent to the updated Pa domain), in the prethalamic eminence and in the pallium (Medina et al., 2004; Osório et al., 2010; Puelles et al., 2012). In chick, there are no detailed data reporting *Neurog2* expression in the Pa-like. Nevertheless, *Neurog2* expression has been detected in a domain equivalent to the Pa-like during a short developmental window (see Robertshaw et al., 2013 and their supplemental material). Our results showing that *ScNeurog2* is expressed in the Pa-like of cartilaginous fishes reveals that the presence of *neurogenin* in the Pa-like could be an early acquisition of gnathostomes although it has not been evidenced in other anamiotes. In *Xenopus*, *Ngnr1* (*neurogenin related 1*), the closest to mammalian *Neurog2* (Nieber et al., 2009; Osório et al., 2010), is not expressed in the preoptic area (Wullimann et al., 2005; Osório et al., 2010), a region that appeared to be equivalent to the updated Pa-like. This fact is likely related to the absence of Pax6 in the Pa-like (Medina, 2008; Moreno et al., 2008, 2009; Domínguez et al., 2013). In zebrafish, only one *neurogenin* (*Neurog1*) has been identified and it is expressed in the pallium and prethalamic eminence but not in the preoptic area (Wullimann and Mueller, 2004; Jeong et al., 2006; Osório et al., 2010) which, in these fishes appears to be the area equivalent to the updated Pa-like domain. In agnathans, there are no data about *Ngn2* but the possibility that other members of the *neurogenin* family as *Ngn1* and *NeuroD2*, which are abundantly expressed through the larval brain of the lamprey (Guérin et al., 2009), are expressed in the alar hypothalamus must not be discharged.

#### 2.4.3.2. Vertebrate SPa-like

The expression of *Dlx*, *Arx* and *Islet* genes in the SPa-like of vertebrates seems to be a common and early acquired trait since such expression has been documented in all vertebrates

studied so far (Domínguez, 2011; Martínez-de-la-Torre et al., 2011; Moreno et al., 2012; Domínguez et al., 2013, 2015; Herget et al., 2014). Variability across vertebrate groups involves the co-expression, or not, with other genes such as *Nkx2.2*, *Shh* and *Nkx2.1* in the SPa-like (Domínguez, 2011; Moreno and González, 2011; Moreno et al., 2012; Domínguez et al., 2013).

In lampreys, *Nkx2.1* and *Nkx2.2* are likely to co-distribute with *Dlx* in the SPa-like while not with *Hh* (homologues of *Shh*) (Myojin et al., 2001; Sugahara et al., 2011; also reviewed in Moreno and González, 2011 and Domínguez et al., 2015). In zebrafish *Nkx2.1*, *Shh* and *Nkx2.2* are also likely to co-distribute without subdividing the SPa-like domain (Barth and Wilson, 1995; Rohr et al., 2001; van den Akker et al., 2008; Domínguez et al., 2013). However, data on zebrafish *Nkx2.1* expression must be taken with care since, recently, the orthologues previously defined as *Nkx2.1a* and *Nkx2.1b* have been renamed as *Nkx2.4b* and *Nkx2.1* respectively (Manoli et al., 2014).

Furthermore, two subcompartments have also been described in the *Dlx*-expressing alar hypothalamus of different tetrapods based on *Nkx2.2*, *Nkx2.1* and *Shh* expression(Domínguez, 2011; Moreno et al., 2012; Domínguez et al., 2013, 2015). One subdomain seems to co-express *Nkx2.1*, *Nkx2.2* and *Shh* while the other not. From amphibians to mammals, the domain expressing these markers seems to be almost reduced in favor of the other (Domínguez, 2011; Moreno et al., 2012; Domínguez et al., 2013). In amphibians and reptiles these subdomains were defined as rostro-caudal (Domínguez et al., 2013; 2015), however, a dorso-ventral interpretation was made in other vertebrates. Taking these into account, it can be concluded that in tetrapods the SPa-like is divided in dorso-ventral subdomains (SPaD-like and SPaV-like) as the updated prosomeric model proposes (Puelles et al., 2012; Domínguez et al., 2013, 2015). With all, there seems to be a tendency to the reduction of *Nkx2.2* and *Nkx2.1* from the SPa-like in favor of the formation and or reduction of dorso-ventral compartments from fishes to mammals.

Strikingly, the data obtained in the shark apparently contradict this tendency. On one hand, only *ScNkx2.8* expression (likely to match *Nkx2.2* expression in mammals) seems to be expressed in the SPa-like while *ScNkx2.1* and *ScShh*/Shh-immunoreactivity seem to be absent, resembling a situation closer to mammals than to other vertebrate groups. In mammals, *Nkx2.1* seems to be expressed only in mantle cells of the alar hypothalamus (Shimogori et al., 2010; Puelles et al., 2012) further supporting this idea. This fact can be explained by the size of the shark pallium compared with that of other fishes. The balance among *Pax6*/*Nkx2.1* is believed to regulate the size of alar/basal compartments (van den Akker et al., 2008; Domínguez, 2011; Moreno et al., 2012; Puelles et al., 2012; Domínguez et al., 2013). Thus, the expanded expression of Pax6 in the shark could determine a bigger pallium over the basal hypothalamus and, consequently, a *ScNkx2.1* restriction. Noteworthy, the basal restriction of *Nkx2.1* and the co-distribution of *Dlx/Pax6* in a hypothetic SPa-like could also be an ancestral trait as claimed by Murakami et al., (2001).

On the other hand, our data also support the existence of dorso-ventral subcompartments based on Pax6-immunoreactivity or *ScNkx2.8* co-distribution with *ScDlx2/5* but not with Sc*Shh* or Sc*Nkx2.1*. This fact raises the possibility that dorso-ventral compartments could also be

addressed in fishes. Finally, as in shark, a population of *Pax6*-positive cells restricted to the PSPa-like and continuous into the hypothalamus and the diencephalon have also been described in mouse (Stoykova et al., 1996). Populations of Pax6-positive cells have also been described in zebrafish under other prosomeric conceptions that could also support a rostro-caudal regionalization of the SPa-like in bony fishes (Wulliman and Rink, 2001; Wulliman and Mueller, 2004).

## 2.5 CONCLUSIONS

Our present data suggest the existence of further molecular rostro-caudal and dorso-ventral subdivisions in the alar hypothalamus of the shark as proposed by the prosomeric model and observed in the mouse. A detailed comparative review of data among different vertebrates reveals a striking degree of conservation for the markers studied here, although there are also differences. Concerning the shark ABB, we have coined the concept of ABBr to solve the difficulties of establishing this territory based on the blurred definitions of the literature. We propose the ABB as the physical domain of *ScNkx2.8* expression, while the ABBr as the virtual line defined by the alar or basal expression of *ScDlx2/5* or *ScNkx2.1*, respectively. Besides, based on *ScOtp* expression we have identified amydala-related structures derived from the hypothalamus. This revisited comparative analysis also supports that a Pa-like positive for *Otp*, *Neurog2*, *Pax6*, *Lhx5* and a SPa-like positive for *Dlx*, *Nkx2.8*/*Nkx2.2* were already present before agnathan-gnathostome transition.

## References


Abellán, A., Vernier, B., Rétaux, S., and Medina, L. (2010). Similarities and differences in the forebrain expression of Lhx1 and Lhx5 between chicken and mouse: Insights for understanding telencephalic development and evolution. *J. Comp. Neurol.* 518, 3512–28.

Anderson, S., Mione, M., Yun, K., and Rubenstein, J. L. (1999). Differential origins of neocortical projection and local circuit neurons: role of Dlx genes in neocortical interneuronogenesis. *Cereb. Cortex* 9, 646–54.

Álvarez-Bolado, G., Paul, F. A., and Blaess, S. (2012). Sonic hedgehog lineage in the mouse hypothalamus: from progenitor domains to hypothalamic regions. *Neural Dev.* 7, 4.

Bachy, I., Berthon, J., and Rétaux, S. (2002). Defining pallial and subpallial divisions in the developing *Xenopus* forebrain. *Mech. Dev.* 117, 163–72.

Ballard, W. W., Mellinger, J., and Lechenault, H. (1993). A series of normal stages for development of *Scyliorhinus canicula*, the lesser spotted dogfish (*Chondrichthyes*: *Scyliorhinidae*). *J. Exp. Zool.* 267, 318–36.

Bardet, S. M., Ferrán, J. L. E., Sanchez-Arrones, L., and Puelles, L. (2010). Ontogenetic expression of sonic hedgehog in the chicken subpallium. *Front. Neuroanat.* 4.

Bardet, S. M., Martinez-de-la-Torre, M., Northcutt, R. G., Rubenstein, J. L. R., and Puelles, L. (2008). Conserved pattern of OTP-positive cells in the paraventricular nucleus and other hypothalamic sites of tetrapods. *Brain Res. Bull.* 75, 231–5.

Barreiro-Iglesias, A., Villar-Cheda, B., Abalo, X.-M., Anadón, R., and Rodicio, M. C. (2008). The early scaffold of axon tracts in the brain of a primitive vertebrate, the sea lamprey. *Brain Res. Bull.* 75, 42–52.

Barth, K. a, and Wilson, S. W. (1995). Expression of zebrafish nk2.2 is influenced by sonic hedgehog/vertebrate hedgehog-1 and demarcates a zone of neuronal differentiation in the embryonic forebrain. *Development* 121, 1755–68.

Blechman, J., Borodovsky, N., Eisenberg, M., Nabel-Rosen, H., Grimm, J., and Levkowitz, G. (2007). Specification of hypothalamic neurons by dual regulation of the homeodomain protein Orthopedia. *Development* 134, 4417–26.

Bulfone, A., Martinez, S., Marigo, V., Campanella, M., Basile, A., Quaderi, N. et al. (1999). Expression pattern of the Tbr2 (Eomesodermin) gene during mouse and chick brain development. *Mech. Dev.* 84, 133–38.

Butler, A. B., and Hodos, W. (2005). "The visceral brain: the hypothalamus and the autonomic nervous system," in *Comparative Vertebrate Neuroanatomy: Evolution and Adaptation*, eds A. B. Butler and W. Hodos (Hoboken, NJ: John Wiley & Sons), 445–67.

Candal E1, Anadón R, Bourrat F, Rodríguez-Moldes I. Cell proliferation in the developing and adult hindbrain and midbrain of trout and medaka (teleosts): a segmental approach. Brain Res Dev Brain Res. 2005 Dec 7;160(2):157-75. Epub 2005 Oct 19

Candal, E. (2002) Proliferation and cell death in the brain and retina of teleosts: ralation to OI-KIP and reelin expression

Carrera, I. (2008). *Desarrollo de los Sistemas Gabaérgico y Aminérgicos en el Sistema Nervioso Central de Peces Cartilaginosos*. Ph. D. thesis, Universidad de Santiago de Compostela, Compostela.

Carrera, I., Anadón, R., and Rodríguez-Moldes, I. (2012). Development of tyrosine hydroxylase-immunoreactive cell populations and fiber pathways in the brain of the dogfish *Scyliorhinus canicula*: new perspectives on the evolution of the vertebrate catecholaminergic system. *J. Comp. Neurol.* 520, 3574–603.

Carrera, I., Ferreiro-Galve, S., Sueiro, C., Anadón, R., and Rodríguez-Moldes, I. (2008). Tangentially migrating GABAergic cells of subpallial origin invade massively the pallium in developing sharks. *Brain Res. Bull.* 75, 405–9.

Compagnucci, C., Debiais-Thibaud, M., Coolen, M., Fish, J., Griffin, J. N., Bertocchini, D., et al. (2013). Pattern and polarity in the development and evolution of the gnathostome jaw: both conservation and heterotopy in the branchial arches of the shark, *Scyliorhinus canicula*. *Dev. Biol.* 377, 428–48.

Coolen, M., Menuet, A., Chassoux, D., Compagnucci, C., Henry, S., Lévèque, L., et al. (2009). "The dogfish *Scyliorhinus canicula*, a reference in jawed vertebrates," in *Emerging Model Organisms. A Laboratory Manual,* edsR. R. Behringer, A. D. Johnson, and R. E. Rrumlauf (Cold Spring Harbor, NY: Cold Spring Harbor Laboratory Press), 431–46.

Croizier, S., Chometton, S., Fellmann, D., and Risold, P. (2015). Characterization of a mammalian prosencephalic functional plan. 8, 1–13.

Debiais-Thibaud, M., Metcalfe, C. J., Pollack, J., Germon, I., Ekker, M., Depew, M., et al. (2013). Heterogeneous conservation of Dlx paralog co-expression in jawed vertebrates. *PLoS One* 8, e68182.

Derobert, Y., Baratte, B., Lepage, M., and Mazan, S. (2002). Pax6 expression patterns in *Lampetra fluviatilis* and *Scyliorhinus canicula* embryos suggest highly conserved roles in the early regionalization of the vertebrate brain. *Brain Res. Bull.* 57, 277–80.

Díaz, C., Morales-Delgado, N., and Puelles, L. (2015). Ontogenesis of peptidergic neurons within the genoarchitectonic map of the mouse hypothalamus. *Front. Neuroanat.* 8, 1–19.

Domínguez, L. (2011). *Organización del Hipotálamo en la Transición Anamnio- amniota: Estudio Genoarquitectónico y Quimioarquitectónico.* Ph. D. thesis, Universidad Complutense de Madrid, Madrid.

Domínguez, L., González, A., and Moreno, N. (2014). Characterization of the hypothalamus of *Xenopus laevis* during development. II. The basal regions. *J. Comp. Neurol.* 522, 1102–31.

Domínguez, L., González, A., and Moreno, N. (2015). Patterns of hypothalamic regionalization in amphibians and reptiles: common traits revealed by a genoarchitectonic approach. *Front. Neuroanat.* 9, 3.

Domínguez, L., Morona, R., González, A., and Moreno, N. (2013). Characterization of the hypothalamus of *Xenopus laevis* during development. I. The alar regions. *J. Comp. Neurol.* 521, 725–59.

Ferrán, J. L., Puelles, L., and Rubenstein, J. L. R. (2015). Molecular codes defining rostrocaudal domains in the embryonic mouse hypothalamus. *Front. Neuroanat.* 9.

Ferreiro Galve, S. (2010). *Brain and retina regionalization in sharks, study based on the spatiotemporal expression pattern of pax6 and other neurochemical markers.* Ph. D. thesis, Universidad Santiago de Compostela, Compostela.

Ferreiro-Galve, S., Carrera, I., Candal, E., Villar-Cheda, B., Anadón, R., Mazan, S., et al. (2008). The segmental organization of the developing shark brain based on neurochemical markers, with special attention to the prosencephalon. *Brain Res. Bull.* 75, 236–40.

Ferreiro-Galve, S., Rodríguez-Moldes, I., Anadón, R., and Candal, E. (2010). Patterns of cell proliferation and rod photoreceptor differentiation in shark retinas. *J. Chem. Neuroanat.* 39, 1–14.

Flames, N., Pla, R., Gelman, D. M., Rubenstein, J. L. R., Puelles, L., and Marín, O. (2007). Delineation of multiple subpallial progenitor domains by the combinatorial expression of transcriptional codes. *J. Neurosci.* 27, 9682–95.

Frowein, J. v, Campbell, K., and Götz, M. (2002). Expression of Ngn1, Ngn2, Cash1, Gsh2 and Sfrp1 in the developing chick telencephalon. *Mech. Dev.* 110, 249–52.

Del Giacco, L., Pistocchi, A., Cotelli, F., Fortunato, A. E., and Sordino, P. (2008). A peek inside the neurosecretory brain through Orthopedia lenses. *Dev. Dyn.* 237, 2295–303.

Del Giacco, L., Sordino, P., Pistocchi, A., Andreakis, N., Tarallo, R., Di Benedetto, B., et al. (2006). Differential regulation of the zebrafish orthopedia 1 gene during fate determination of diencephalic neurons. *BMC Dev. Biol.* 6, 50.

Guérin, A., d'Aubenton-Carafa, Y., Marrakchi, E., Da Silva, C., Wincker, P., Mazan, S., et al. (2009). Neurodevelopment genes in lampreys reveal trends for forebrain evolution in craniates. *PLoS One* 4, e5374.

Herget, U., Wolf, A., Wullimann, M. F., and Ryu, S. (2014). Molecular neuroanatomy and chemoarchitecture of the neurosecretory preoptic-hypothalamic area in zebrafish larvae. *J. Comp. Neurol.* 522, 1542–64.

Jeong, J.-Y., Einhorn, Z., Mercurio, S., Lee, S., Lau, B., Mione, M., et al. (2006). Neurogenin1 is a determinant of zebrafish basal forebrain dopaminergic neurons and is regulated by the conserved zinc finger protein Tof/Fezl. *Proc. Natl. Acad. Sci. U. S. A.* 103, 5143–48.

Joly, J. S., Osório, J., Alunni, A., Auger, H., Kano, S., and Rétaux, S. (2007). Windows of the brain: Towards a developmental biology of circumventricular and other neurohemal organs. *Semin. Cell Dev. Biol.* 18, 512–24.

Jones, L., López-Bendito, G., Gruss, P., Stoykova, A., and Molnár, Z. (2002). Pax6 is required for the normal development of the forebrain axonal connections. *Development* 129, 5041–52.

Kandel, E., and Schwartz, J. (2001).“Sistema nervioso autónomo e hipotálamo,”in *Principios de Neurociencia*, eds E. R. Kandel, J. H. Schwartz, and T. M. Jessell (Aravaca: McGraw-Hill Interamericana), 960–81.

Li, H. S., Yang, J. M., Jacobson, R. D., Pasko, D., and Sundin, O. (1994). Pax-6 is first expressed in a region of ectoderm anterior to the early neural plate: implications for stepwise determination of the lens. *Dev. Biol.* 162, 181–94.

Manoli, M., Driever, W., and Scholpp, S. (2014). during development of the zebrafish hypothalamus , preoptic region , and pallidum. 8, 1–16.

Martínez-de-la-Torre, M., Pombal, M. A., and Puelles, L. (2011). Distal-less-like protein distribution in the larval lamprey forebrain. *Neuroscience* 178, 270–84.

Martynoga, B., Morrison, H., Price, D. J., and Mason, J. O. (2005). Foxg1 is required for specification of ventral telencephalon and region-specific regulation of dorsal telencephalic precursor proliferation and apoptosis. *Dev. Biol.* 283, 113–27.

Mastick, G. S., Davis, N. M., Andrew, G. L., and Easter, S. S. (1997). Pax-6 functions in boundary formation and axon guidance in the embryonic mouse forebrain. *Development* 124, 1985–97.

Medina, L. (2008). "Evolution and embryological development of the forebrain," in *Encyclopedia of Neuroscience*, eds M. D. Binder, N. Hirokawa, and U. Windhorst (Berlin: Springer-Verlag), 1172–92.

Medina, L., Bupesh, M., and Abellán, A. (2011). Contribution of genoarchitecture to understanding forebrain evolution and development, with particular emphasis on the amygdala. *Brain. Behav. Evol.* 78, 216–36.

Medina, L., Legaz, I., González, G., De Castro, F., Rubenstein, J. L. R., and Puelles, L. (2004). Expression of Dbx1, Neurogenin 2, Semaphorin 5A, Cadherin 8, and Emx1 distinguish ventral and lateral pallial histogenetic divisions in the developing mouse claustroamygdaloid complex. *J. Comp. Neurol.* 474, 504–23.

Morales-Delgado, N., Castro-Robles, B., Ferrán, J. L., Martinez-de-la-Torre, M., Puelles, L., and Díaz, C. (2014). Regionalized differentiation of CRH, TRH, and GHRH peptidergic neurons in the mouse hypothalamus. *Brain Struct. Funct.* 219, 1083–111.

Morales-Delgado, N., Merchán, P., Bardet, S. M., Ferrán, J. L., Puelles, L., and Díaz, C. (2011). Topography of Somatostatin Gene Expression Relative to Molecular Progenitor Domains during Ontogeny of the Mouse Hypothalamus. *Front. Neuroanat.* 5, 10.

Moreno, N., and González, A. (2011). The non-evaginated secondary prosencephalon of vertebrates. *Front. Neuroanat.* 5, 12.

Moreno, N., Domínguez, L., Morona, R., and González, A. (2012). Subdivisions of the turtle *Pseudemys scripta* hypothalamus based on the expression of regulatory genes and neuronal markers. *J. Comp. Neurol.* 520, 453–78.

Moreno, N., González, A., and Rétaux, S. (2009). Development and evolution of the subpallium. *Semin. Cell Dev. Biol.* 20, 735–43.

Moreno, N., Rétaux, S., and González, A. (2008). Spatio-temporal expression of Pax6 in *Xenopus* forebrain. *Brain Res.* 1239, 92–9.

Murakami, Y., Ogasawara, M., Sugahara, F., Hirano, S., Satoh, N., and Kuratani, S. (2001). Identification and expression of the lamprey Pax6 gene: evolutionary origin of the segmented brain of vertebrates. *Development* 128, 3521–31.

Myojin, M., Ueki, T., Sugahara, F., Murakami, Y., Shigetani, Y., Aizawa, S., et al. (2001). Isolation of Dlx and Emx gene cognates in an agnathan species, *Lampetra japonica*, and

their expression patterns during embryonic and larval development: Conserved and diversified regulatory patterns of homeobox genes in vertebrate head evolution. *J. Exp. Zool.* 291, 68–84.

Nieber, F., Pieler, T., and Henningfeld, K. a. (2009). Comparative expression analysis of the Neurogenins in *Xenopus tropicalis* and *Xenopus laevis. Dev. Dyn.* 238, 451–8.

Osório, J., Mazan, S., and Rétaux, S. (2005). Organisation of the lamprey (*Lampetra fluviatilis*) embryonic brain: insights from LIM-homeodomain, Pax and hedgehog genes. *Dev. Biol.* 288, 100–12.

Osório, J., Megías, M., Pombal, M. A., and Rétaux, S. (2006). Dynamic expression of the LIM-homeodomain gene Lhx15 through larval brain development of the sea lamprey (*Petromyzon marinus*). *Gene Expr. Patterns* 6, 873–8.

Osório, J., Mueller, T., Rétaux, S., Vernier, P., and Wullimann, M. F. (2010). Phylotypic expression of the bHLH genes Neurogenin2, NeuroD, and Mash1 in the mouse embryonic forebrain. *J. Comp. Neurol.* 518, 851–71.

Pose-Méndez, S., Candal, E., Adrio, F., and Rodríguez-Moldes, I. (2014). Development of the cerebellar afferent system in the shark *Scyliorhinus canicula*: insights into the basal organization of precerebellar nuclei in gnathostomes. *J. Comp. Neurol.* 522, 131–68.

Pose-Méndez, S., Candal, E., Mazan, S., and Rodríguez-Moldes, I. (2015). Genoarchitecture of the rostral hindbrain of a shark: basis for understanding the emergence of the cerebellum at the agnathan-gnathostome transition. *Brain Struct. Funct.* Jan 1 [Epub ahead of print]

Prestoz, L., Jaber, M., and Gaillard, A. (2012). Dopaminergic axon guidance: which makes what? *Front. Cell. Neurosci.* 6, 32.

Puelles, L. (2009). "Forebrain development: prosomere model," in *Developmental Neurobiology*, ed. G. Lemke (London; Burlington, MA; SanDiego, CA: Academic Press), 315–19.

Puelles, L., and Medina, L. (2002). Field homology as a way to reconcile genetic and developmental variability with adult homology. *Brain Res. Bull.* 57, 243–55.

Puelles, L., and Rubenstein, J. L. R. (2015). A new scenario of hypothalamic organization: rationale of new hypotheses introduced in the updated prosomeric model. *Front. Neuroanat.* 9.

Puelles, L., and Rubenstein, J. L. R. (2003). Forebrain gene expression domains and the evolving prosomeric model. *Trends Neurosci.* 26, 469–76.

Puelles, L., Kuwana, E., Puelles, E., Bulfone, A., Shimamura, K., Keleher, J., et al. (2000). Pallial and Subpallial Derivatives in the Embryonic Chick and Mouse Telencephalon, Traced by the Expression of the Genes Dlx-2 , Emx-1 , Nkx-2 . 1 , Pax-6 , and Tbr-1. 438, 409–38.

Puelles, L., Martínez, S., Martínez-de-la-Torre, M., and Rubenstein, J. (2004). "Gene maps and related histogenetic domains in the forebrain and midbrain," in *The Rat Nervous System*, ed. G. Paxinos (San Diego, CA: Academic Press), 3–25.

Puelles, L., Martínez, S., Martínez-de-la-Torre, M. S.,and Rubenstein, J. (2012). "Hypothalamus," in *The Mouse Nervous System*, eds C. Watson, G. Paxinos, and L. Puelles (San Diego, CA: Academic Press), 221–312.

Quintana-Urzainqui, I. (2013). *Development and regionalization of the telencephalon and peripheral associated systems in the shark Scyliorhinus canicula*. Ph. D. thesis, Universidad de Santiago de Compostela, Compostela.

Quintana-Urzainqui, I., Rodríguez-Moldes, I., and Candal, E. (2014). Developmental, tract-tracing and immunohistochemical study of the peripheral olfactory system in a basal vertebrate: insights on Pax6 neurons migrating along the olfactory nerve. *Brain Struct. Funct.* 219, 85–104.

Quintana-Urzainqui, I., Rodríguez-Moldes, I., Mazan, S., and Candal, E. (2015). Tangential migratory pathways of subpallial origin in the embryonic telencephalon of sharks: evolutionary implications. *Brain Struct. Funct.* 220, 2905-26

Quintana-Urzainqui, I., Sueiro, C., Carrera, I., Ferreiro-Galve, S., Santos-Durán, G., Pose-Méndez, S., et al. (2012). Contributions of developmental studies in the dogfish *Scyliorhinus canicula* to the brain anatomy of elasmobranchs: insights on the basal ganglia. *Brain. Behav. Evol.* 80, 127–41.

Robertshaw, E., Matsumoto, K., Lumsden, A., and Kiecker, C. (2013). Irx3 and Pax6 establish differential competence for Shh-mediated induction of GABAergic and glutamatergic neurons of the thalamus. *Proc. Natl. Acad. Sci. U. S. A.* 110, E3919–26.

Rodríguez-Moldes, I., Timmermans, J. P., Adriaensen, D., De Groodt-Lasseel, M. H., Scheuermann, D. W., and Anadon, R. (1990). Immunohistochemical localization of calbindin-D28K in the brain of a cartilaginous fish, the dogfish (*Scyliorhinus canicula L.*). *Acta Anat. (Basel).* 137, 293–302.

Rohr, K. B., Barth, K. A., Varga, Z. M., and Wilson, S. W. (2001). The Nodal pathway acts upstream of Hedgehog signaling to specify ventral telencephalic identity. *Neuron* 29, 341–51.

Ryu, S., Mahler, J., Acampora, D., Holzschuh, J., Erhardt, S., Omodei, D., et al. (2007). Orthopedia Homeodomain Protein Is Essential for Diencephalic Dopaminergic Neuron Development. *Curr. Biol.* 17, 873–80.

Sarnat, H. B., and Netsky, M. G. (1981). "Epithalamus and hypothalamus, "in *Evolution of the Nervous System*, eds H. B. Sarnat and M. G. Netsky (Newyork, NY; Oxford: Oxford University Press), 296–320.

Shimamura, K., Hartigan, D. J., Martinez, S., Puelles, L., and Rubenstein, J. L. (1995). Longitudinal organization of the anterior neural plate and neural tube. *Development* 121, 3923–33.

Shimogori, T., Lee, D. A., Miranda-Angulo, A., Yang, Y., Wang, H., Jiang, L., et al. (2010). A genomic atlas of mouse hypothalamic development. *Nat. Neurosci.* 13, 767–75.

Simerly, R. B. (2004). "Anatomical Substrates of Hypothalamic Integration," in *The Rat Nervous System*, ed. G. Paxinos (San Diego, CA: Academic Press), 336–51.

Stoykova, A., and Gruss, P. (1994). Roles of Pax-genes in developing and adult brain as suggested by expression patterns. *J. Neurosci.* 14, 1395–412.

Stoykova, A., Fritsch, R., Walther, C., and Gruss, P. (1996). Forebrain patterning defects in Small eye mutant mice. *Development* 122, 3453–65.

Sugahara, F., Aota, S., Kuraku, S., Murakami, Y., Takio-Ogawa, Y., Hirano, S., et al. (2011). Involvement of Hedgehog and FGF signalling in the lamprey telencephalon: evolution of regionalization and dorsoventral patterning of the vertebrate forebrain. *Development* 138, 1217–26.

Suzuki, D. G., Murakami, Y., Escriva, H., and Wada, H. (2015). A comparative examination of neural circuit and brain patterning between the lamprey and amphioxus reveals the evolutionary origin of the vertebrate visual center. *J. Comp. Neurol.* 523, 251–61.

Szabó, N.-E., Zhao, T., Cankaya, M., Theil, T., Zhou, X., and Alvarez-Bolado, G. (2009). Role of neuroepithelial Sonic hedgehog in hypothalamic patterning. *J. Neurosci.* 29, 6989–7002.

Tornehave, D., Hougaard, D. M., and Larsson, L. (2000). Microwaving for double indirect immunofluorescence with primary antibodies from the same species and for staining of mouse tissues with mouse monoclonal antibodies. *Histochem. Cell Biol.* 113, 19–23.

Tripodi, M., Filosa, A., Armentano, M., and Studer, M. (2004). The COUP-TF nuclear receptors regulate cell migration in the mammalian basal forebrain. *Development* 131, 6119–29.

Uchida, K., Murakami, Y., Kuraku, S., Hirano, S., and Kuratani, S. (2003). Development of the adenohypophysis in the lamprey: evolution of epigenetic patterning programs in organogenesis. *J. Exp. Zool. B. Mol. Dev. Evol.* 300, 32–47.

Van den Akker, W. M. R., Brox, A., Puelles, L., Durston, A. J., and Medina, L. (2008). Comparative functional analysis provides evidence for a crucial role for the homeobox gene Nkx2.1/Titf-1 in forebrain evolution. *J. Comp. Neurol.* 506, 211–23.

Vitalis, T., Cases, O., Engelkamp, D., Verney, C., and Price, D. J. (2000). Defect of tyrosine hydroxylase-immunoreactive neurons in the brains of mice lacking the transcription factor Pax6. *J. Neurosci.* 20, 6501–16.

Wullimann, M. F., and Mueller, T. (2004). Identification and Morphogenesis of the Eminentia Thalami in the Zebrafish. *J. Comp. Neurol.* 471, 37–48.

Wullimann, M. F., and Rink, E. (2001). Detailed immunohistology of Pax6 protein and tyrosine hydroxylase in the early zebrafish brain suggests role of Pax6 gene in development of dopaminergic diencephalic neurons. *Dev. Brain Res.* 131, 173–91.

Wullimann, M. F., Rink, E., Vernier, P., and Schlosser, G. (2005). Secondary neurogenesis in the brain of the African clawed frog, *Xenopus laevis*, as revealed by PCNA, Delta-1, Neurogenin-related-1, and NeuroD expression. *J. Comp. Neurol.* 489, 387–402.

Xuan, S., Baptista, C. A., Balas, G., Tao, W., Soares, V. C., and Lai, E. (1995). Winged helix transcription factor BF-1 is essential for the development of the cerebral hemispheres. *Neuron* 14, 1141–52.

**Abbreviation list.**

| | |
|---|---|
| ABB | alar-basal boundary |
| ABBr | alar-basal border |
| AHy | alar hypothalamus |
| ap2 | prosomere 2, alar part |
| ap3 | prosomere 3, alar part |
| BHy | basal hypothalamus |
| D | diencephalon |
| F | forebrain |
| H | hindbrain |
| HDB | hypothalamo-diencephalic border |
| hp1 | prosomere hp1 or peduncular |
| hp2 | prosomere hp2 or terminal |
| HTB | hypothalamo-telencephalic border |
| IHB | intrahypothalamic border |
| M | mesencephalon |
| m | mantle expression |
| MM | mamillary area |
| mz | mantle zone |
| os | optic stalk |
| p3 | prosomere 3 |
| p3Tg | tegmental part of prosomere 3 |
| P | pallium |
| Pa | paraventricular area |
| PBHy | peduncular basal hypothalamus |
| PM | perimamillary area |
| PPa | paraventricular area, peduncular part |
| PRM | periretromamillary area |
| PSPa | subparaventricular area, peduncular part |
| PSPaD | subparaventricular area, peduncular and dorsal part |
| PSPaV | subparaventricular area, peduncular and ventral part |
| PThE | prethalamic eminence (ap3) |
| R | rhombencephalon |
| RM | retromamillary region |
| RTu | retrotuberal region |
| s | subventricular expression |
| sc | spinal cord |
| SlBHy | basal hypothalamus, subliminal part |
| SIPBHy | basal hypothalamus, subliminal and peduncular part |
| SITBHy | basal hypothalamus, subliminal and terminal part |
| Sp | subpallium |
| SPa | subparaventricular region |
| SPaD | subparaventricular region, dorsal part |
| SPaV | subparaventricular region, ventral part |
| T | telencephlalon |
| TBHy | basal hypothalamus, terminal part |
| TPa | paraventricular region, terminal part |
| TSPa | subparaventricular area, terminal part |
| TSPaD | subparaventricular area, terminal and dorsal part |
| TSPaV | subparaventricular area, terminal and ventral part |
| Tu | tuberal region |
| v | ventricular expression |
| vz | ventricular zon |

**Figure 1.** Regionalization of the alar hypothalamus and neighbor territories in embryos of *S. canicula* at stages 29-31 based on the expression of *ScOtp* **(A-D)** and *ScDlx2/5* **(E-J)** expression and GAD **(F´´)** and 5-HT immunoreactivity **(J)** by means of single *in situ* hybridization **(A-F´,G-I)** and/or combined with immunohistochemistry **(F´´, J)** on sagittal **(A, D, E, H-J)** or transverse **(B-C, F-G)** sections. Continuous red line: alar-basal border (ABBr). Dashed red line: IHB. Grey line: HTB. Continuous black line divides dorso-ventral division of the alar hypothalamus into Pa-like (dorsal) and SPa-like (ventral). Dashed black line represents subdivisions inside the SPa-like into SPa dorsal (SPaD) and ventral (SPaV). **(A-D)** *ScOtp* expression in the Pa-like at indicated stages. *ScOtp* labeling in the SPa-like corresponds to marginal cells. Black arrowheads point *ScOtp*-expressing cells in the subpallium. Red arrowheads point *ScOtp*-expressing cells in the pallium. Blue arrowheads point marginal *ScOtp*-expressing cells in the Pa-like. Yellow arrowheads point *ScOtp*-expressing cells ventral to the Pa-like. **(A´)** Detail of a region equivalent to that squared area in (A) to show *ScOtp*-expressing cells ventral to the Pa-like rostrally. **(E-J)** *ScDlx2/5* expression in the subpallium, SPa-like and alar p3 at indicated stages. Red arrowhead points lack of expression in the pallium. White arrowheads point *ScDlx2*-expressing (F´) cells and GAD-ir cells (F´´) in the marginal zone of the Pa-like. Green arrowhead in G points *ScDlx2/5* expression in the RTu. (J) Detail of a region equivalent to that squared in I. Arrows point 5-HT-ir tracts coursing in the marginal Pa-like and SPa-like. For abbreviations, see list.

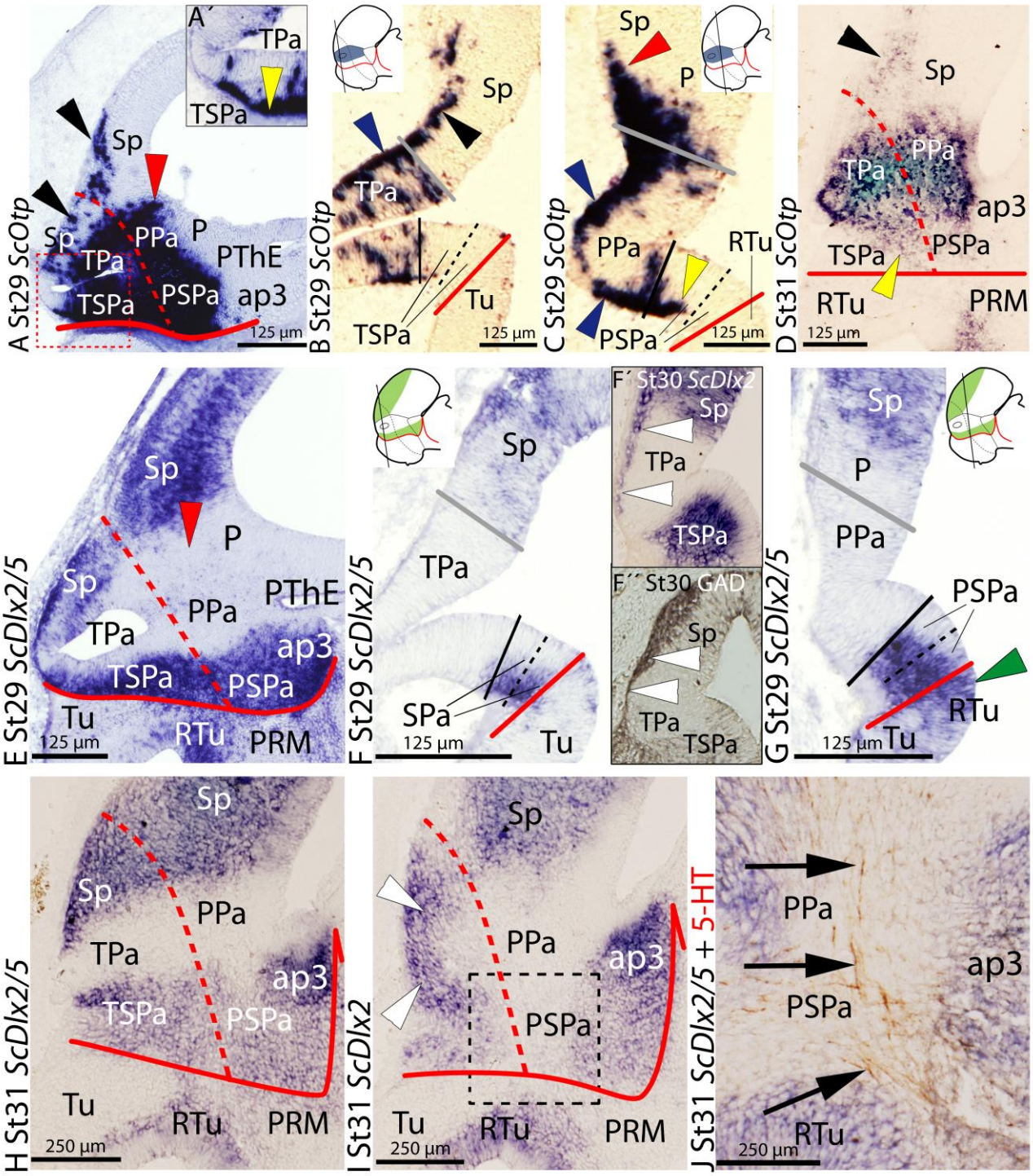
A´
TPa
TSPa
Sp
Sp
PPa
P
TPa
PThE
TSPa
PSPa
ap3
125 µm
A St29 ScOtp
Sp
TPa
TSPa
Tu
125 µm
B St29 ScOtp
Sp
P
PPa
RTu
PSPa
125 µm
C St29 ScOtp
Sp
PPa
TPa
ap3
TSPa
PSPa
RTu
PRM
125 µm
D St31 ScOtp
Sp
P
Sp
PPa
TPa
PThE
ap3
TSPa
PSPa
RTu
PRM
Tu
125 µm
E St29 ScDlx2/5
Sp
TPa
SPa
125 µm
Tu
F St29 ScDlx2/5
F´ St30 ScDlx2
Sp
TPa
TSPa
F´´ St30 GAD
Sp
TPa
TSPa
Sp
P
PPa
PSPa
RTu
125 µm
Tu
G St29 ScDlx2/5
Sp
Sp
PPa
TPa
ap3
TSPa
PSPa
Tu
RTu
PRM
250 µm
H St31 ScDlx2/5
Sp
PPa
ap3
PSPa
Tu
RTu
PRM
250 µm
I St31 ScDlx2
PPa
PPa
ap3
PSPa
PSPa
ap3
RTu
250 µm
J St31 ScDlx2/5 + 5-HT

# FIGURE 1

**Figure 2.** Regionalization of the alar hypothalamus and neighbor territories in embryos of *S. canicula* at stages 29-31 based on the expression of *ScTbr1* **(A-C),** *ScDlx2/5* **(A´)** *ScNeurog2* **(D-G)** and Pax6-immunoreactivity **(H-K)** by means of single *in situ* hybridization on sections **(A-G)** and single immunoenzyme staining **(H-J)** or immunofluorescence (**K)** on sagittal **(A, D, E, K)** or transverse **(B, C, F, G, I-J)** sections. Image **(A´)** result from overlapping of two parallel sections hybridized with *ScTbr1* and *ScDlx2/5*. **(A-C)** *ScTbr1* expression in the pallium and PThE. Red arrowhead points rostral-most expression in the pallium. (A´) The complementary expression of *ScTbr1* and *ScDlx2/5* defines the Pa-like domain. **(D-G)** *ScNeurog2* expression in the Pa-like and pallium. Note that Figures D, E present artifacts corresponding to broken tissue. Red arrowhead points the rostral-most pallium lacking *ScNeurog2***. (H-K)** Pax6-immunoreactivity at indicated stages. Red arrowhead points to marginal Pax6-immunoreactivityat the rostral-most pallium. Black and white arrowheads point marginal Pax6-ir cells in the peduncular SPa-like (PSPa-like) and peduncular basal hypothalamus. Arrows point and/or low Pax6-ir intensity dorsal and ventral to the Pa-like. Note that the stream of Pax6-ir cells in **(K)** closely follows the IHB. For other labels, see legend Figure 1. For abbreviations, see list.

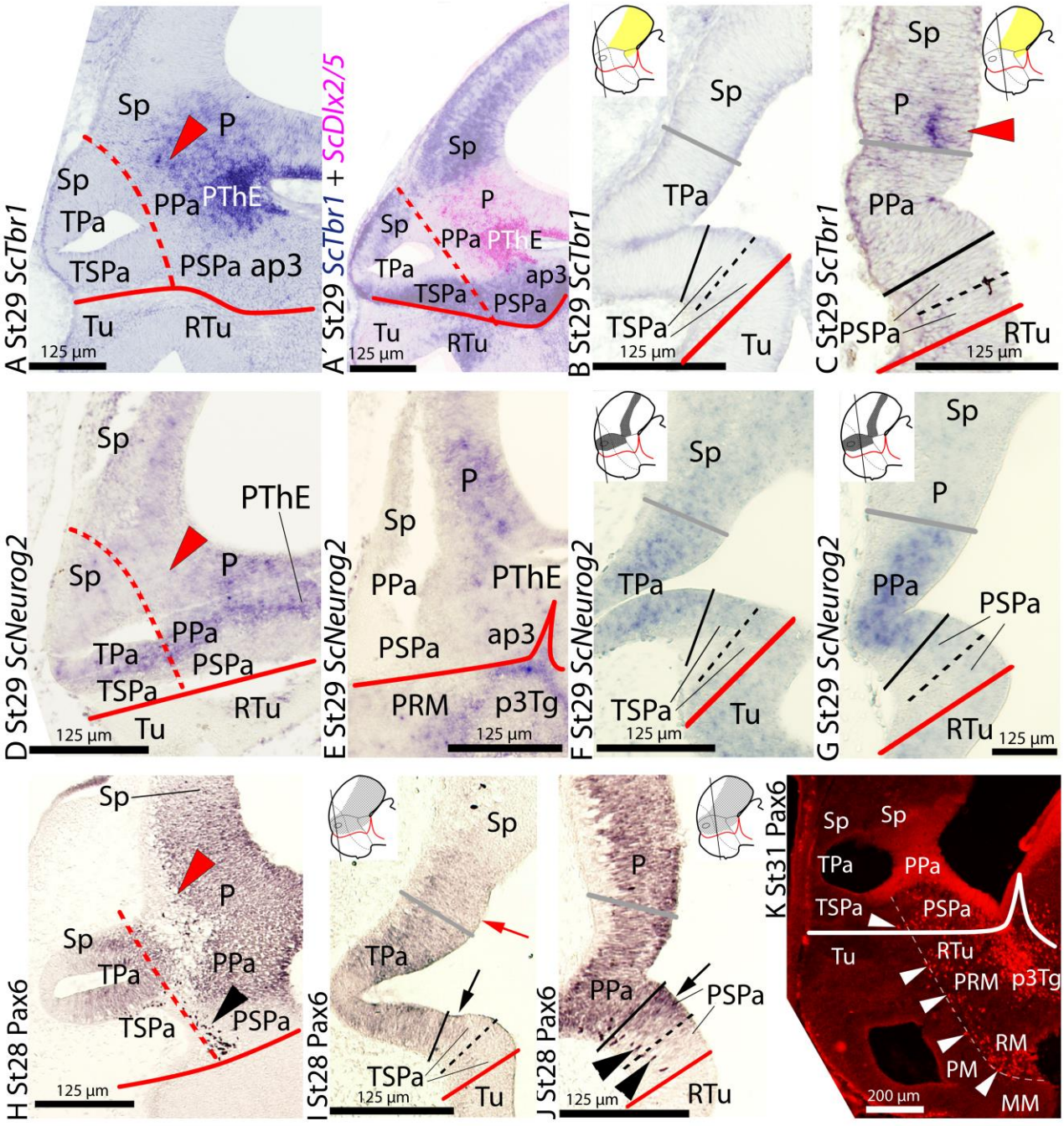
A St29 ScTbr1
Sp
P
Sp
PPa
PThE
TPa
TSPa
PSPa ap3
Tu
RTu
125 µm
A´ St29 ScTbr1 + ScDlx2/5
Sp
P
Sp
PPa PThE
TPa
ap3
TSPa
PSPa
Tu
RTu
125 µm
B St29 ScTbr1
Sp
TPa
TSPa
Tu
125 µm
C St29 ScTbr1
Sp
P
PPa
PSPa
RTu
125 µm
D St29 ScNeurog2
Sp
PThE
Sp
P
PPa
TPa
PSPa
TSPa
RTu
125 µm
Tu
E St29 ScNeurog2
P
Sp
PPa
PThE
PSPa
ap3
PRM
p3Tg
125 µm
F St29 ScNeurog2
Sp
TPa
TSPa
Tu
125 µm
G St29 ScNeurog2
Sp
P
PPa
PSPa
RTu
125 µm
H St28 Pax6
Sp
P
Sp
TPa
PPa
TSPa
PSPa
125 µm
I St28 Pax6
Sp
TPa
TSPa
125 µm
Tu
J St28 Pax6
P
PPa
PSPa
125 µm
RTu
K St31 Pax6
Sp
Sp
TPa
PPa
TSPa
PSPa
Tu
RTu
PRM
p3Tg
RM
PM
MM
200 µm

# FIGURE 2

**Figure 3.** Regionalization of the alar hypothalamus and/or neighbor territories in embryos of *S. canicula* at stages 29-31 based on the expression of *ScLhx9* **(A-E),** and *ScLhx5* **(F-J)** on sagittal **(A-C´, E-G, J)** or transverse **(D, H-I)** sections. Some of them were double labeled for immunohistochemistry against Shh **(E, G, H-J). (A-E)** *ScLhx9* expression in the limits of the alar hypothalamus, pallium, prethalamic eminence and basal hypothalamus, at indicated stages. Black arrowhead points *ScLhx9* expression in the basal hypothalamus just ventral to the SPa-like. Red arrowhead points *ScLhx9*-expressing cells in the pallium. **(C)** Section medial to (B). **(C´)** Detail of the squared region in (C) showing absence of *ScLhx9* expression from the rostral-most alar hypothalamus. **(F-J)** *ScLhx5*-expression in different regions of the prosencephalon including the alar hypothalamus. **(I)** Red arrowhead points *ScLhx5*-expressing cells in the pallium. **(J´)** Sagital section lateral to (J). Black arrowhead points a string of *ScLhx5*-expressing cells extending along the alar hypothalamus (PPa) and alar p3. For other labels, see legend Figure 1. For abbreviations, see list.

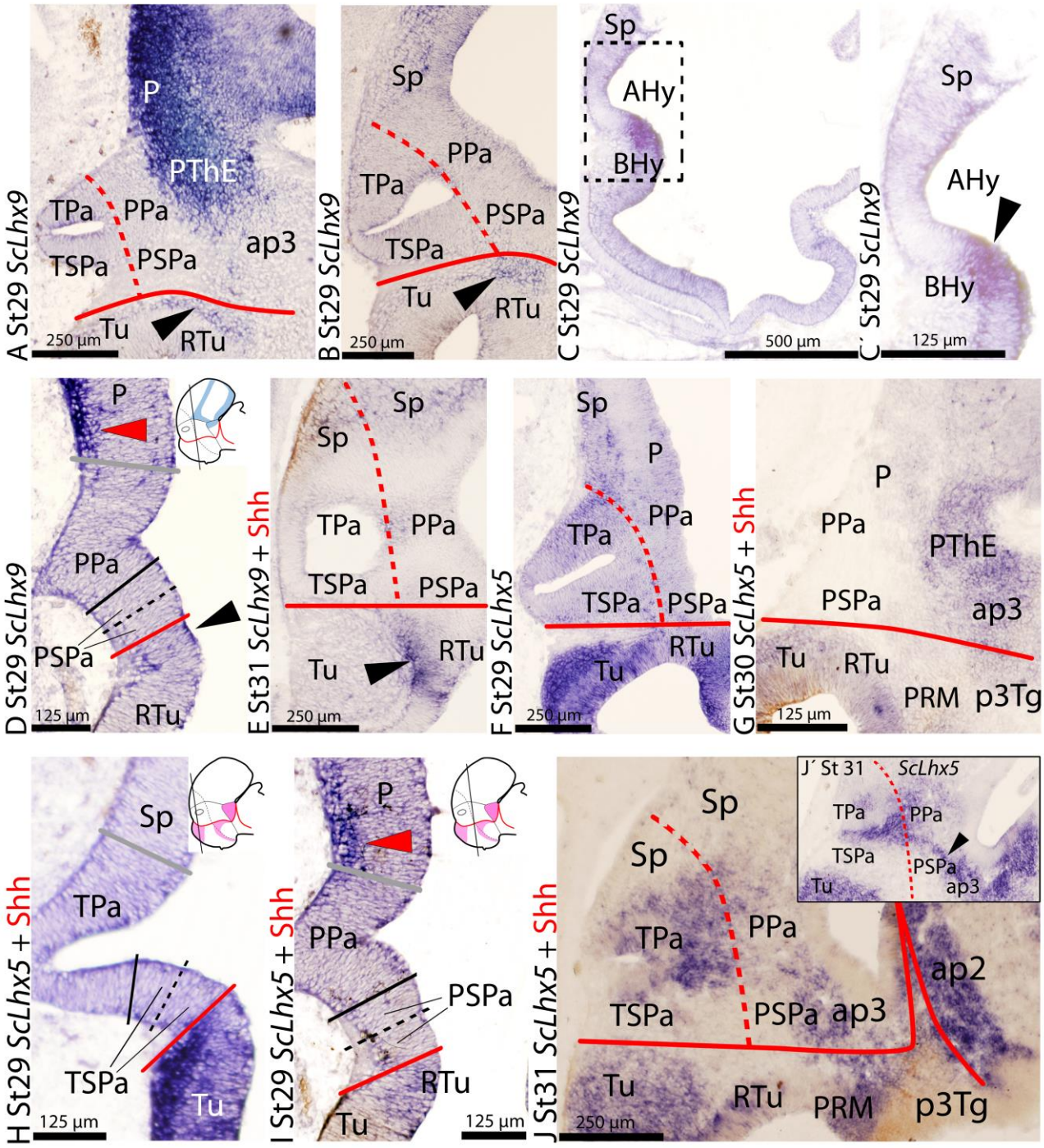
A St29 ScLhx9
P
PThE
TPa
PPa
TSPa
PSPa
ap3
Tu
RTu
250 µm
B St29 ScLhx9
Sp
PPa
TPa
PSPa
TSPa
Tu
RTu
250 µm
C St29 ScLhx9
Sp
AHy
BHy
500 µm
C´ St29 ScLhx9
Sp
AHy
BHy
125 µm
D St29 ScLhx9
P
PPa
PSPa
RTu
125 µm
E St31 ScLhx9 + Shh
Sp
Sp
TPa
PPa
TSPa
PSPa
Tu
RTu
250 µm
F St29 ScLhx5
Sp
P
PPa
TPa
TSPa
PSPa
RTu
Tu
250 µm
G St30 ScLhx5 + Shh
P
PPa
PThE
PSPa
ap3
Tu
RTu
PRM
p3Tg
125 µm
H St29 ScLhx5 + Shh
Sp
TPa
TSPa
Tu
125 µm
I St29 ScLhx5 + Shh
P
PPa
PSPa
RTu
Tu
125 µm
J St31 ScLhx5 + Shh
J´ St 31
ScLhx5
TPa
PPa
TSPa
PSPa
Tu
ap3
Sp
Sp
TPa
PPa
ap2
TSPa
PSPa
ap3
Tu
RTu
PRM
p3Tg
250 µm

# FIGURE 3

**Figure 4.** Regionalization of the alar hypothalamus and neighbor territories in embryos of *S. canicula* at stages 18-29 based on the expression of *ScNkx2.1* **(A-C)** and *ScNkx2.8* **(D-I)** on sagittal **(A)** and transverse **(B, C, G, H, I)** sections and single whole mounts *in situ* hybridizations **(D-F)**. Some sections were double labeled for immunohistochemistry against Shh **(B, C, H)** and DCX **(G, G´). (A-C)** *ScNkx2.1* expression at indicated stages. **(D-I)** *ScNkx2.8* expression at indicated stages. Arrowhead in **D** points prospective basal hypothalamus. Arrowhead in E points lack of *ScNkx2.8* expression at the caudal-most basal hypothalamus. Black arrow in F points *ScNkx2.8* expression at the rostral-most basal hypothalamus and white arrowhead points downregulation at the caudal basal hypothalamus. **(G´)** Detail of the squared region in **(G).** Arrowhead in G' points DCX-irfibers of the TPOC seen as round dots in transverse section. For other labels, see legend Figure 1. For abbreviations, see list.

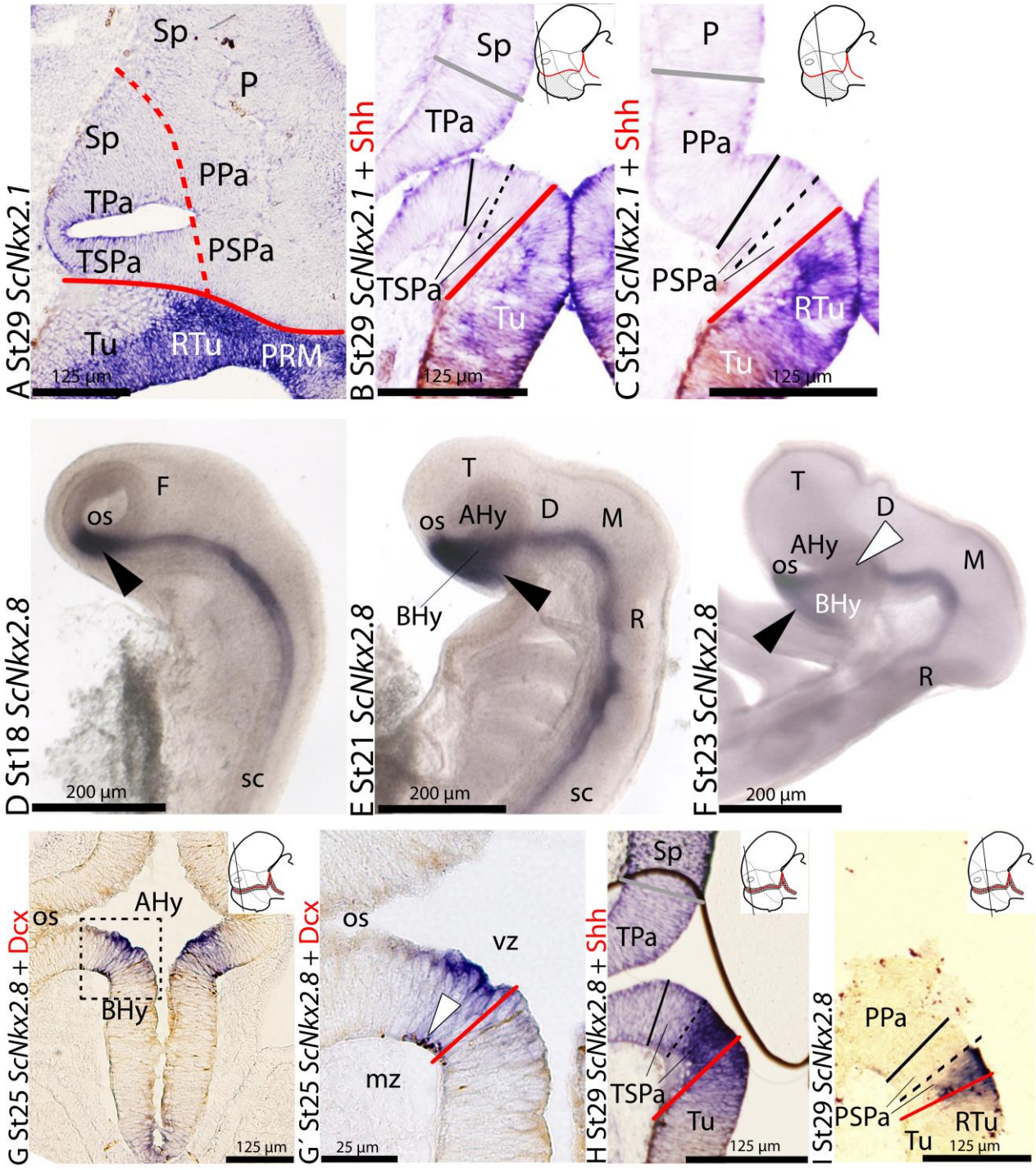
A St29 ScNkx2.1
Sp
P
PPa
TPa
PSPa
TSPa
Tu
RTu
PRM
125 µm
B St29 ScNkx2.1 + Shh
Sp
TPa
TSPa
Tu
125 µm
C St29 ScNkx2.1 + Shh
P
PPa
PSPa
RTu
Tu
125 µm
D St18 ScNkx2.8
F
os
200 µm
sc
E St21 ScNkx2.8
T
os
AHy
D
M
BHy
R
200 µm
sc
F St23 ScNkx2.8
T
D
AHy
os
M
BHy
R
200 µm
G St25 ScNkx2.8 + Dcx
os
AHy
BHy
125 µm
G´ St25 ScNkx2.8 + Dcx
os
vz
mz
25 µm
H St29 ScNkx2.8 + Shh
Sp
TPa
TSPa
Tu
125 µm
I St29 ScNkx2.8
PPa
PSPa
RTu
Tu
125 µm

# FIGURE 4

**Figure 5.** Regionalization of the alar hypothalamus and neighbor territories in embryos of *S. canicula* at stage 30 based on GAD **(A),** SS **(B-C)**, CB **(D)**, and TH **(E)** immunoreactivities by means of single **(A, D)** or double **(B, C, E)** immunohistochemistry on sagittal sections. Continuous red line represents the ABBr. Dashed red line represents IHB. Section (A) is more medial that the other sections. Arrowhead in B points SS-immunoreactivity in the terminal SPa-like (TSPa-like). Arrow in B points SS-immunoreactivity in fibers. Arrowhead in D points restricted CB-immunoreactivity in the PThE. For abbreviations, see list.

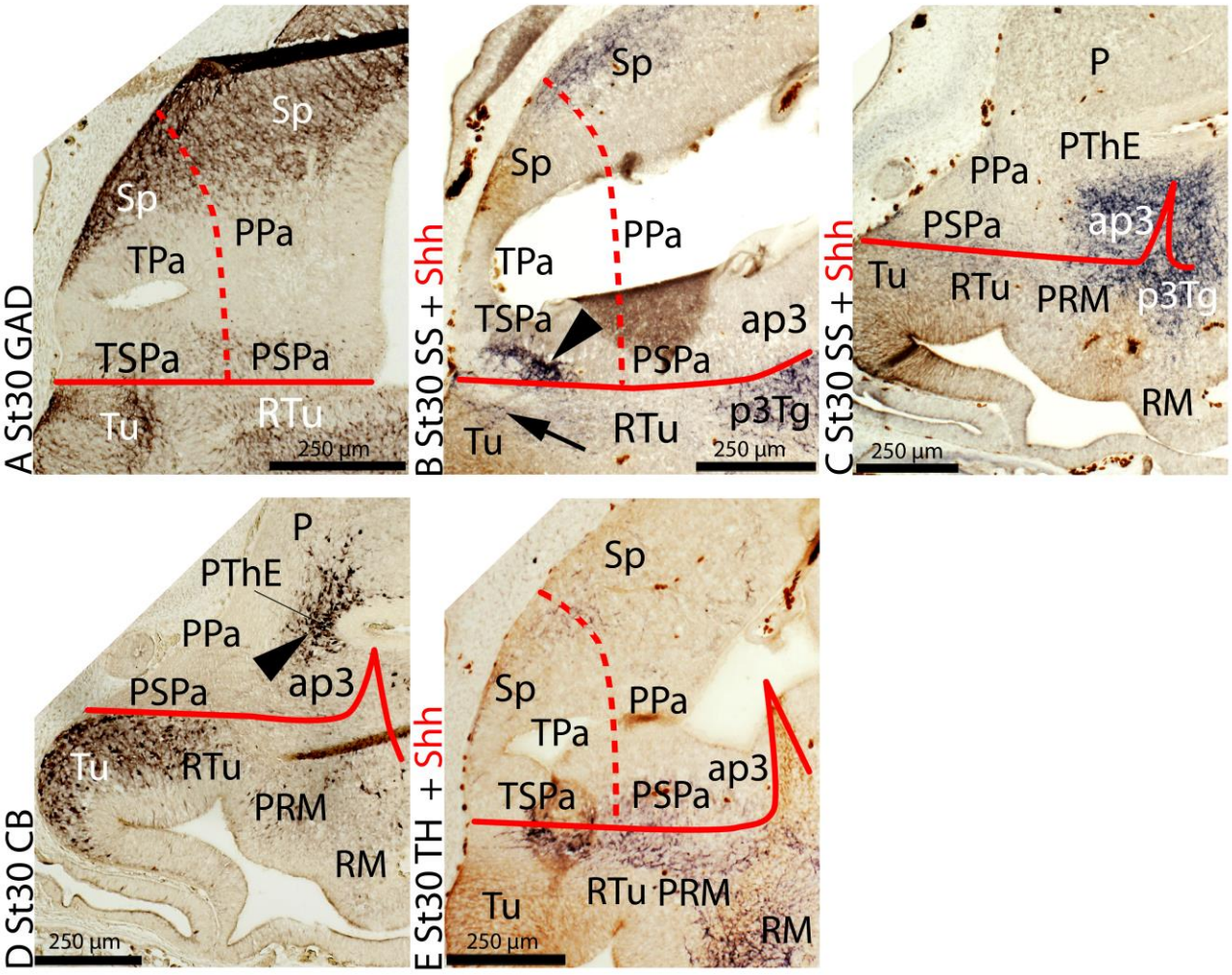
A St30 GAD
Sp
Sp
PPa
TPa
TSPa
PSPa
Tu
RTu
250 µm
B St30 SS + Shh
Sp
Sp
PPa
TPa
TSPa
ap3
PSPa
Tu
RTu
p3Tg
250 µm
C St30 SS + Shh
P
PThE
PPa
PSPa
ap3
Tu
RTu
PRM
p3Tg
RM
250 µm
D St30 CB
P
PThE
PPa
PSPa
ap3
Tu
RTu
PRM
RM
250 µm
E St30 TH + Shh
Sp
Sp
PPa
TPa
TSPa
PSPa
ap3
Tu
RTu PRM
RM
250 µm

# FIGURE 5

**Figure 6.** Schematic representation of various gene expression and neurochemical immunoreactive patterns in the telencephalon, hypothalamus and rostral diencephalon of *S. canicula* at stage 29. **(A)** Domains and subdomains defined by *ScOtp*, *ScDlx2/5*, *ScNeurog2*, *ScLhx9*, *ScTbr1* and *ScNkx2.1* expression patterns. Some of these genes define subdivisions in the pallium. **(B)** Domains and subdomains defined by *ScOtp*, *ScDlx2/5*, *ScLhx5*, *ScLhx9*, *ScNkx2.8* and Shh-immunoreactivity. **(C)** Domains and subdomains defined by immunoreactivity to GAD, SS, CB and TH. Asterisk stress that immunoreactive patterns have not been represented. Continuous red line represents ABBr. Discontinuous black line represents IHB. For abbreviations, see list.

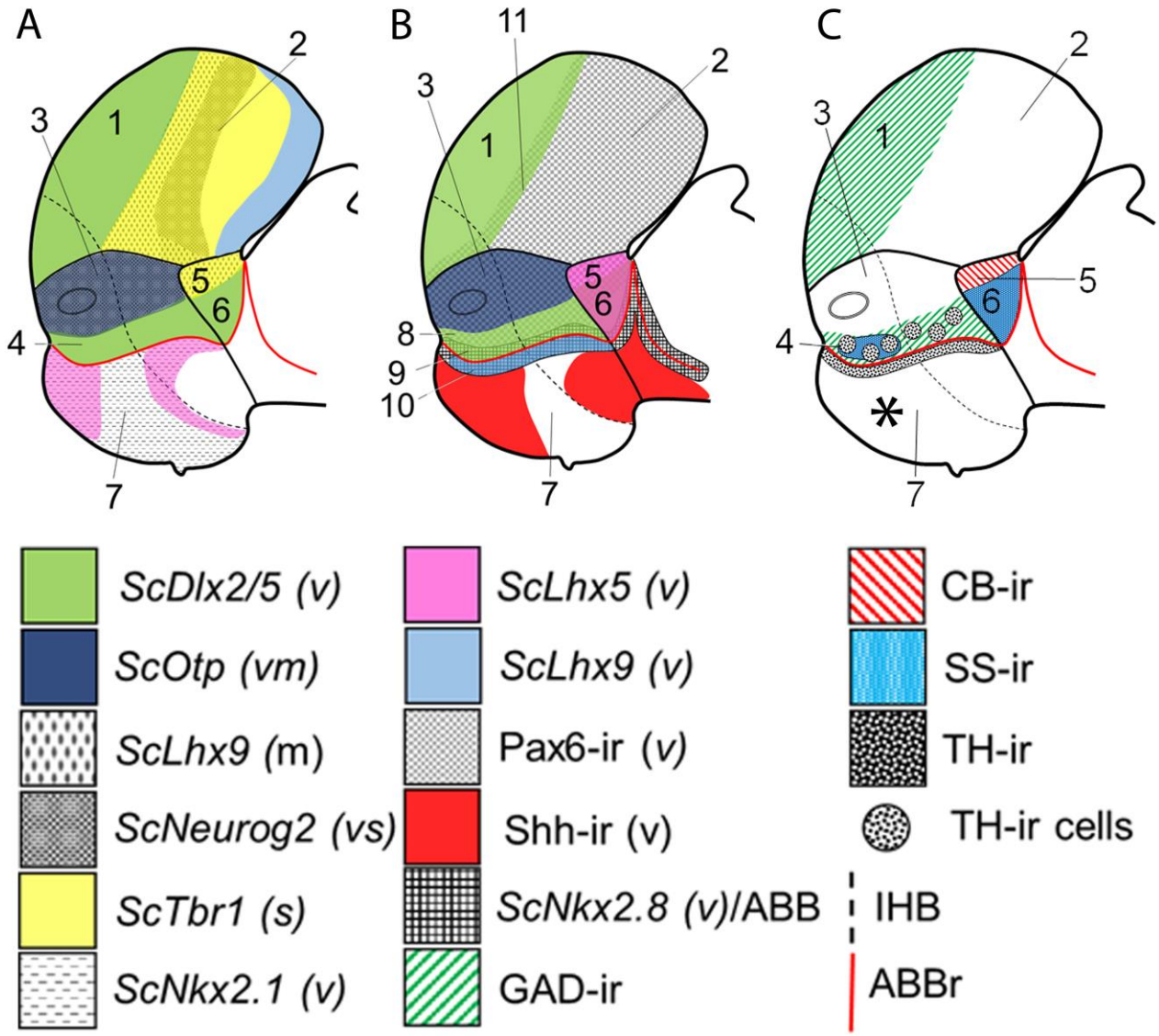


1. Subpallium
2. Pallium
3. Pa-like
4. SPa-like
5. PThE
6. Alar p3
7. Basal hypothalamus
8. SPaD-like
9. SPaV-like
10. SIBHy
11. Pallium-Subpallium boundary

**FIGURE 6**

**Figure 7.** Schematic representation of various gene expression patterns in the telencephalon, hypothalamus and rostral diencephalon of **(A)** *S. canicula* at stage 31 **(B)** developing mouse adapted from Puelles et al. (2012) **(C)** lamprey adapted from Martínez-de-la-Torre (2011). Domains and subdomains defined by *Otp*, *Dlx2*, *Pax6*, *Neurog2*, *Lhx9*, *Lhx5*, *Tbr1*, *Nkx2.8*, *Nkx2.2*, *Shh*, *Hh* and *Nkx2.1* orthologues. Continuous red line represents ABBr. Discontinuous black line represents IHB. For abbreviations, see list.

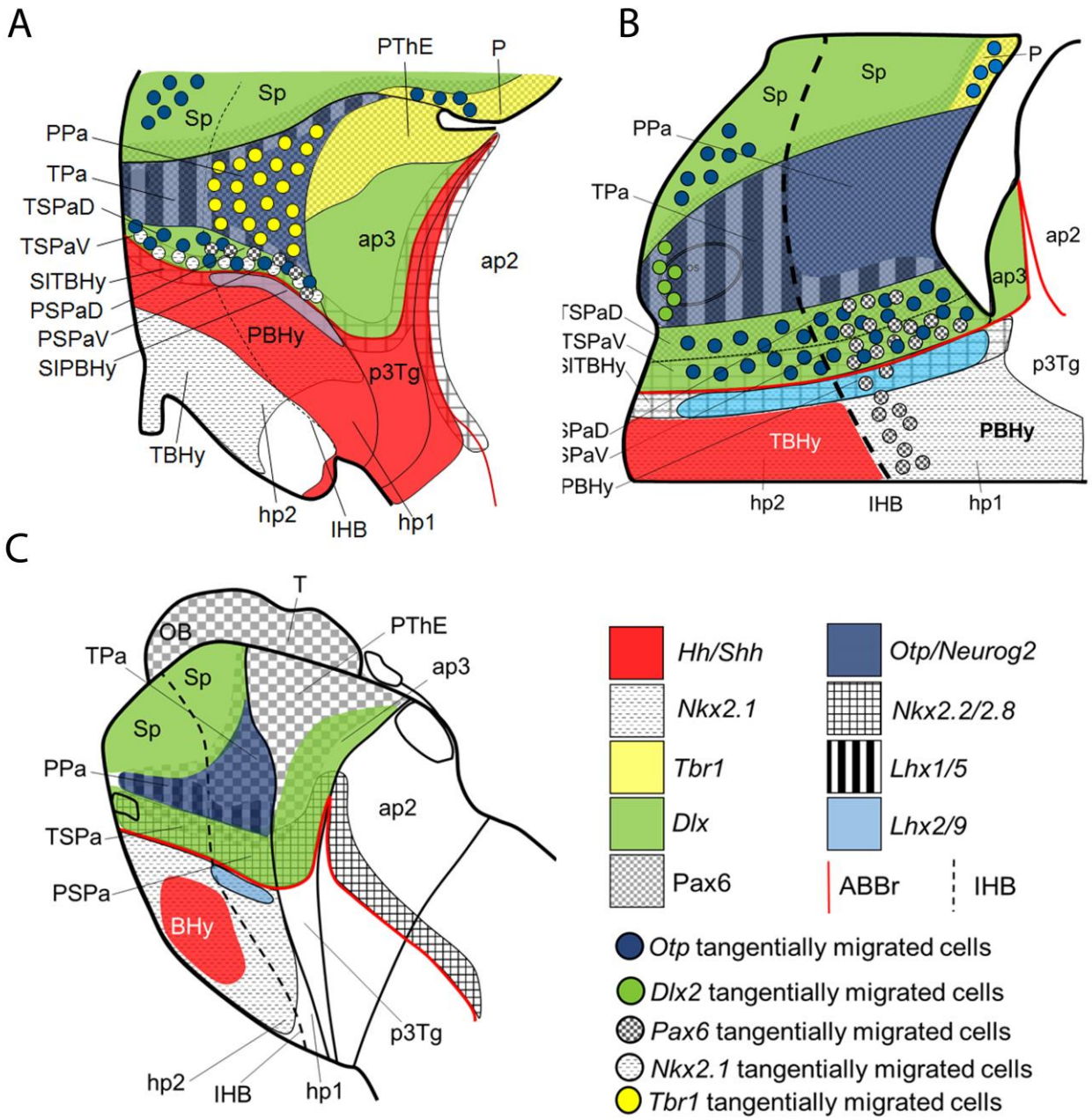
A
PThE
P
Sp
Sp
PPa
TPa
TSPaD
TSPaV
SITBHy
PSPaD
PSPaV
SIPBHy
ap3
ap2
PBHy
p3Tg
TBHy
hp2
IHB
hp1
B
Sp
Sp
P
PPa
TPa
ap2
ap3
TSPaD
TSPaV
SITBHy
p3Tg
TBHy
PBHy
hp2
IHB
hp1
C
T
OB
PThE
TPa
Sp
ap3
Sp
PPa
ap2
TSPa
PSPa
BHy
p3Tg
hp2
IHB
hp1
Hh/Shh
Nkx2.1
Tbr1
Dlx
Pax6
Otp/Neurog2
Nkx2.2/2.8
Lhx1/5
Lhx2/9
ABBr
IHB
Otp tangentially migrated cells
Dlx2 tangentially migrated cells
Pax6 tangentially migrated cells
Nkx2.1 tangentially migrated cells
Tbr1 tangentially migrated cells

# FIGURE 7

USC
UNIVERSIDADE
DE SANTIAGO
DE COMPOSTELA

# Chapter 3

# The shark basal hypothalamus: molecular prosomeric subdivisions and evolutionary trends.

USC
UNIVERSIDADE
DE SANTIAGO
DE COMPOSTELA

# 3. The shark basal hypothalamus: molecular prosomeric subdivisions and evolutionary trend

## 3.1 INTRODUCTION

The hypothalamus is an important physiologic center of the brain that integrates information from limbic, endocrine and autonomic sources to elaborate different kinds of homeostatic and behavioral responses such as feeding or reproduction (Sarnat & Netsky, 1981; Kandel and Schwartz, 2001; Butler and Hodos, 2005). Its organization has been elusive for neuroanatomists since it is the result of complex patterning processes that converge at the rostral-most and ventral-most point of the neural tube (Shimamura et al., 1995; Puelles and Rubenstein, 2003; Puelles et al., 2004; Medina, 2008; Szabó et al., 2009; Shimogori et al., 2010; Alvarez-Bolado et al., 2012; Croizier et al., 2015). It is well known that the prechordal plate and the notochord have a significant influence in the patterning and histogenesis of the vertebrate hypothalamus and prosencephalon; however, their roles are not well understood yet (Shimamura et al., 1995; García-Calero et al., 2008; Puelles et al., 2012; Puelles and Rubenstein, 2003; 2015). Other inductive tissues and/or signaling centers are also assumed to take part in hypothalamic development with an even less understood participation in this process (Kapsimali et al., 2004; Lee et al., 2006; Medina, 2008; Shimogori et al., 2010; Sugahara et al., 2011; Szabó et al., 2009; Wolf & Ryu, 2013).

The classical organization of the hypothalamus (for a review see Simerly, 2004) is based on columnar conceptions of the brain supported by functional components of the cranial and spinal nerves (Puelles, 2009; Puelles et al., 2012; Puelles and Rubenstein, 2015). This interpretation states that the hypothalamus belongs to the diencephalon, located under the thalamus, and consists of a wide variety of neuronal clusters subdivided in four regions: preoptic, anterior, tuberal and mamillar (see General Introduction). Modern interpretations based on molecular developmental data, including the prosomeric model, understand the hypothalamus as being located under the telencephalon, forming together a developmental unit known as the secondary prosencephalon (Puelles and Rubenstein, 2003).

Although a big effort has been made to develop the prosomeric framework in the mouse for biomedical purposes (*Allen Developing Mouse Brain Atlas;* http://developingmouse.brain-map.org/), it has been pointed that, to date, its statements and nomenclature seems to be mainly used in developmental studies rather than in studies involving adult anatomy and/or a clinical scope (Croizier et al., 2015). Nevertheless, to date, the model has proven to be a suitable tool for comparative studies and it has been adopted by an important part of the comparative, developmental and evo-devo (evolution and development) communities in neuroscience (Medina, 2008; Pombal et al., 2009; Osório et al.,

2010; Martínez-de-la-Torre et al., 2011; Medina et al., 2011; Moreno et al., 2012; Domínguez et al., 2013; 2015; Manoli et al., 2014). In fact, in the field of comparative studies, on which one has to deal with both divergent and conserved neural structures, the model became a really useful tool since it offers a mechanistic systematized organization and nomenclature, topologically comparable among vertebrates (Puelles and Medina, 2002; Puelles and Rubenstein, 2003, 2015). Noteworthy, the updating of the model occurs by a feedback process among hypothesis formulation and their testing in different vertebrates (Puelles and Rubenstein, 2003, 2015; Pombal et al., 2009; Martínez-de-la-Torre et al., 2011; Puelles et al., 2012). As a result, the model incorporates common trends in brain development and evolution rather than divergences. Thus, testing the recently updated assumptions of the model (Puelles et al., 2012) by the evo-devo community is a work that will provide new insights to understand vertebrate brain evolution, will deliver feedback to the prosomeric model and, ultimately, will help to mammalian brain systematization.

The comparative analysis of the progenitor domains under updated or precedent prosomeric conceptions suggests that the vertebrate hypothalamus presents homologue histogenetic domains (Moreno et al., 2012; Domínguez et al., 2013; 2014; 2015; chapter 1). Of note, the histogenetic domains within the alar hypothalamus seem to be more conserved than those of the basal hypothalamus ( chapter 1). This correlation is extended at the morphological level. While the vertebrate alar hypothalamus has a more conserved morphological structure, the basal hypothalamus presents more divergences (Butler and Hodos, 2005). In the basal hypothalamus of the mouse, the relationship among these domains and hypothalamic nucleus have been pointed: the tuberal/retrotuberal (**Tu/RTu**) and the mammillar/retromammillar (**MM/RM**) domains give rise to classical tuberal and mamillary derivatives, while the novel perimamillar/periretromamillar (**PM/PRM**) domain gives rise to clusters addressed to tuberal and/or mammillary regions in the classic nomenclature (Morales-Delgado et al., 2011; Puelles et al., 2012). Indeed, although the existence of homologue domains has been described in other vertebrates, their correspondence with adult structures is unclear in many cases.

Cartilaginous fishes or chondrichthyans are a good model to address the correspondence among histogenetic domains, their morphological outcome, and the evolution of both for several reasons. On one hand, as in mammals, the adult elasmobranch basal hypothalamus has been divided into tuberal and mammilar regions (see Section 3.1 in General Introduction). The tuberal region presents conserved structures, like the tracts of the hypothalamic-hypophyseal system, a median eminence, or the neurohypophysis, lateral tuberal nucleus**,** and also other structures that are only present in the tuberal hypothalamus of gnathostome fishes such as the inferior hypothalamic lobes and the saccus vasculosus. On the caudal and classical mammillary region, mammillary derivatives are mostly occupied by functionally integrated structures that form two continuous circumventricular organs: the posterior recess organ, caudally, and its rostrolateral continuation, the paraventricular organ. Caudally beyond the mammillary recess there is an rich and conserved catecholaminergic structure known as the posterior tuberculum, that has been recently ascribed to the prosomeric retromamillary area in chapter 1 although it was also addressed to the diencephalon (Vernier & Wullimann, 2008). On the other hand, chondricthyans are also a relevant model because they are among the most basal extant groups of gnathostomes (jawed vertebrates). Because of its phylogenetic position as the closest out-group to osteichthyans (the other major phylum of gnathostomes, which includes bony fish and tetrapods), chondrichthyans are essential to

reconstruct gnathostome ancestral characteristics through comparisons with other vertebrate models.

Recently, we have carried out a preliminary study of the molecular histogenetic organization of the hypothalamus of an elasmobranch representative, the catshark *Scyliorhinus canicula*, and we analyzed this organization under the updated prosomeric framework (chapter 1). This analysis revealed a strikingly high degree in the conservation of hypothalamic histogenetic compartments between chondrichthyan and murine models (chapter 1). The basal expression of *ScNkx2.1*, *ScDlx2/5*, *ScShh* and *ScOtp* led to the identification of tuberal/retrotuberal-like (**Tu/RTu-like**), perimamillar/periretromamillar-like (**PM/PRM-like**) and mamillar/retromamillar-like (**MM/RM-like**) domains, apparently homologous to those described in murine models. Besides, a molecular hypothalamo-telencephalic border (**HTB**) and a hypothalamo-diencephalic border (**HDB**), matching with those described in the prosomeric model, were identified in the shark. An intrahypothalamic border (**IHB**) was also defined, as in mouse (Puelles et al., 2012), based on the course of ascending tracts to the telencephalon (chapter 1). Furthermore, a comparative analysis of the histogenetic domains and their adult morphological outcome was not addressed.

Although many of the boundaries and assumptions predicted by the prosomeric model were confirmed in the chondrichthyan model, further dorso-ventral subdivisions and genetic evidences of rostro-caudal segmentation, particularly concerning the basal hypothalamus, have not been previously addressed. Besides, the meaning of the results observed in the shark remains unclear since trends on the evolution and development of the vertebrate hypothalamus have not been considered so far. Here we deepen in the molecular profile of the basal hypothalamus of *Scyliorhinus canicula*, with three aims: i) to look for further prosomeric molecular subdivisions, ii) to test if new data on gene expression patterns support our previous observations and iii) to obtain some insights on the evolution of this region by comparative analysis. To address these questions, previous data on *ScNkx2.1*, *ScDlx2/5*, *ScOtp* and *ScShh*/Shh-immunoreactivity expression were revised jointly with new data on *ScLhx5*, *ScEmx2*, *ScLmx1b*, *ScPitx2*, *ScPitx3a*, *ScFoxa1*, *ScFoxa2*, *and ScNeurog2* expression and serotonin (5-HT)-, cell proliferating nuclear antigen (PCNA)-, glutamic acid decarboxylase (GAD)-, tyrosine hydroxylase (TH)-, somatostatin (SS)-, calbindin (CB)- and glial fibrillary acidic protein (GFAP)- immunoreactivity patterns.

## 3.2. MATERIALS AND METHODS

### 3.2.1 Experimental animals

Some embryos of the catshark (lesser spotted dogfish; *S. canicula*) were supplied by the Marine Biological Model Supply Service of the CNRS UPMC Roscoff Biological Station (France) and the Estación de Bioloxía Mariña da Graña (Galicia, Spain). Additional embryos were kindly provided by the Aquaria of Gijón (Asturias, Spain), O Grove (Pontevedra, Spain) and Finisterrae (A Coruña, Spain). Embryos were staged by their external features according to Ballard et al. (1993). For more information about the relationship of embryonic stages with

body size, gestation and birth, see Table 1 in Ferreiro-Galve et al. (2010). Sixtynine embryos from stages 28 to 32 were used in this study. Eggs from different broods were raised in seawater tanks in standard conditions of temperature (15-16 ºC), pH (7.5-8.5) and salinity (35 g/L). Adequate measures were taken to minimize animal pain or discomfort. All procedures conformed to the guidelines established by the European Communities Council Directive of 22 September 2010 (2010/63/UE) and by the Spanish Royal Decree 53/2013 for animal experimentation and were approved by the Ethics Committee of the University of Santiago de Compostela.

### 3.2.2. Tissue processing

Embryos were deeply anesthetized with 0.5 % tricaine methane sulfonate (MS-222; Sigma, St. Louis, MO) in seawater and separated from the yolk before fixation in 4 % paraformaldehyde (PFA) in elasmobranch's phosphate buffer [EPB: 0.1 M phosphate buffer (PB) containing 1,75 % urea, pH 7.4] for 48-72 h depending on the stage of development. Subsequently, they were rinsed in phosphate buffer saline (PBS), cryoprotected with 30 % sucrose in PB, embedded in OCT compound (Tissue Tek, Torrance, CA), and frozen with liquid nitrogen-cooled isopentane. Parallel series of sections (12-20 μm thick) were obtained in transverse planes on a cryostat and mounted on Superfrost Plus (Menzel-Glasser, Madison, WI, USA) slides.

### 3.2.3. Single and double immunohistochemistry on sections and whole mounts

For heat-induced epitope retrieval, sections were pre-treated with 0.01 M citrate buffer (pH 6.0) for 30 min at 95 ºC and allowed to cool for 20–30 min at room temperature (RT). Sections were then rinsed twice in 0.05 M Tris-buffered saline (TBS; pH 7.4) for 5 min each and incubated overnight with the primary antibody (polyclonal rabbit anti-Sonic Hedgehog [anti-Shh], Sta. Cruz Biotechnology, Santa Cruz, CA, diluted 1:300; polyclonal rabbit anti-serotonin [anti-5-HT] DiaSorin, Immunostar, Hudson, WI, diluted 1:5000; monoclonal mouse anti-proliferating cell nuclear antigen [anti-PCNA] Sigma, St Louis, MO, diluted 1:500; polyclonal sheep anti-GAD65/67 [anti-GAD 1440] kindly provided by Dr. E. Mugnaini, diluted 1:20000; monoclonal mouse anti-tyrosine hydroxilase [anti-TH], Millipore, Billerica, MA, diluted 1:500; monoclonal rat anti-somatostatin [anti-SS], Millipore, Temecula, CA, diluted 1:50; polyclonal rabbit anti-calbindin D-28k [anti-CB] Swant, Marly, Switzerland, diluted 1:1000, polyclonal rabbit anti-glial fibrillary acidic protein [anti-GFAP], Dako, Glostrup, Denmark, diluted 1:500). Appropriate secondary antibodies (horseradish peroxidase [HRP]-conjugated goat anti-rabbit and anti-mouse, BIORAD, diluted 1:200; and horse radish peroxidase [HRP]-conjugated rabbit anti-rat, Thermo SCIENTIFIC, diluted 1:50) were incubated for 2h at RT. For double immunohistochemistry experiments, cocktails of primary antibodies were mixed at optimal dilutions and subsequently detected by using mixtures of appropriate secondary antibodies. Sections were rinsed in distilled water (twice for 30 min), allowed to dry for 2 h at 37 ºC and mounted in MOWIOL 4-88 Reagent (Calbiochem, MerkKGaA, Darmstadt, Germany). All dilutions were made with TBS containing 15 % donkey normal serum (DNS; Millipore, Billerica, MA), 0.2 % Triton X-100 (Sigma) and 2 % bovine serum albumin (BSA, Sigma). Double immunohistochemistry with primary antibodies raised in the same species was performed as described in Tornehave et al. (2000).

For whole mounts embryos were prepared as previously described in Kuratani and Horigome, (2000) with minor modifications. After fixation with 4 % PFA in 0.01 M PBS at 4 ºC for 2 days, embryos were washed in 0.9 % NaCl in distilled water, dehydrated in graded series of methanol solutions (50 %, 80 %, 100 %) and stored at -20 ºC. Samples to be stained were placed on ice in 2 ml of dimethyl sulfoxide (DMSO)/methanol (1/1) until they sank. Then, 0.5 ml of 10 % Triton X-100/distilled water was added, and the embryos were incubated for 30 min at RT. After washing in 0.05 M TBS with 0.1 % Triton X-100 (TST, pH 7.4) the samples were sequentially blocked using spin-clarified aqueous 1 % periodic acid and 5 % non-fat dried milk in TST (TSTM). Primary antibody (polyclonal rabbit anti-Sonic Hedgehog [anti-Shh], Sta. Cruz Biotechnology, Santa Cruz, CA, diluted 1:300) was diluted in TSTM containing 0.1 % sodium azide for 2 to 4 days at RT with gently agitation on a shaking platform. The secondary antibody (horseradish peroxidase [HRP]-conjugated goat anti-rabbit, BIORAD, diluted 1:200 in TSTM) was incubated overnight. After a final washing in TST, the embryos were pre-incubated with 0.25 mg/mL diaminobenzidine tetrahydrochloride (DAB, Sigma) in TST with 2.5 mg/mL nickel ammonium sulfate for 1 h, and then allowed to react with DAB in TST containing 2.5 mg/mL nickel ammonium sulfate and 0.00075 % $H_2O_2$ for 20-40 min at RT. The reaction was stopped using Tris-HCl buffered saline and specimens were post-fixed with 4 % PFA overnight at 4 ºC. Epidermis and mesodermic derivatives were carefully removed and specimens were rinsed in graded series of glycerol (25 %, 50 %, 75 % and 100 %) in order to directly observe the neural tube under the stereomicroscope.

### 3.2.4. Controls and specificity of the antibodies

No immunostaining was detected when primary or secondary antibodies were omitted during incubations. Controls and specificity of anti-TH and anti-5-HT were performed as described in Pose-Méndez et al. (2014). The monoclonal anti- PCNA antibody specifically labels proliferating cells in the brain, retina and olfactory epithelium of this species (Rodríguez-Moldes et al., 2008; Ferrando et al., 2010; Ferreiro-Galve et al., 2010; Quintana-Urzainqui et al., 2012). The polyclonal anti-Shh antibody (Santa Cruz Biotechnology Inc, CA) was raised in rabbit against the amino acids 41-200 of the human Shh protein. The *in situ* hybridization (ISH) results were similar to those obtained by immunohistochemistry (IHC), and therefore validate the specificity of the anti-Shh antibody used here. The polyclonal anti-GAD antibody was raised against a synthetic peptide with the amino acid sequence [C]DFLIEEIERLGQDL from rat glutamate decarboxylase (GAD65; C-terminus residues [Cys] +572-585). The monoclonal anti-SS antibody was raised against synthetic 1-14 cyclic somatostatin conjugated to bovine thyroglobulin using carbodiimide. The polyclonal anti-CB antibody was raised against recombinant rat calbindin D-28k. The polyclonal anti-GFAP antibody is a purified immunoglobulin fraction of rabbit antiserum generated to bovine spinal cord GFAP. This antibody has been previously used as a glial immunohistochemical marker in *S. caninula* (Wasowicz et al. 1999; Sueiro et al. 2007), though neuronal precursors in the retina were also found to be GFAP-immunoreactive (-ir) (personal communication).

### 3.2.5 *In situ* hybridization on sections and whole mounts

We applied *in situ* hybridization for *ScOtp* (Quintana-Urzainqui, 2013; chapter 1), *ScDlx2* (Quintana-Urzainqui et al., 2012a, 2014b; Compagnucci et al., 2013; Debiais-Thibaud et al., 2013; Quintana-Urzainqui, 2013; chapter 1), *ScDlx5* (Compagnucci et al., 2013; Debiais-Thibaud et al., 2013; chapter 1), *ScNkx2.1* (chapter 1), *ScLhx5*, *ScEmx2* (Derobert et al., 2002), *ScLmx1b* (Pose-Méndez et al., 2015), *ScPtix2* (Lagadec et al., 2015), *ScPtix3a*, *ScFoxa1*, *ScFoxa2*, and *ScNeurog2* genes. These probes were selected from a collection of *S. canicula* embryonic cDNA library (mixed stages S9 to S22), constructed in pSPORT1, and submitted to high throughput EST sequencing. Selected cDNA fragments were cloned in pSPORT vectors. Sense and antisense digoxigenin-UTP-labeled and fluorescein-UTP-labeled probes were synthesized directly by *in vitro* transcription using as templates linearized recombinant plasmid DNA or cDNA fragments prepared by PCR amplification of the recombinant plasmids. *In situ* hybridization in whole mount and on cryostat sections was carried out following standard protocols (Coolen et al., 2009). Briefly, sections were permeabilized with proteinase K, hybridized with sense or antisense probes overnight at 65 ºC and incubated with the alkaline phosphatase-coupled anti-digoxigenin and anti-fluorescein antibody (1:2000, Roche Applied Science, Manheim, Germany) overnight at 4 ºC. The color reaction was performed in the presence of BM-Purple (Roche). Control sense probes did not produce any detectable signal.

#### 3.2.6 Image acquisition and analysis

Light field images were obtained with an Olympus BX51 microscope equipped with an Olympus DP71 color digital camera. Fluorescent sections were photographed with an epifluorescence photomicroscope Olympus AX70 fitted with an Olympus DP70 color digital camera. Photographs were adjusted for brightness and contrast and plates were prepared using Adobe Photoshop CS4 (Adobe, San Jose, CA).

## 3.3. RESULTS

### 3.3.1. *ScNkx2.1*, *ScOtp* and *ScDlx2*/*ScDlx5 expression.* Comparison with *ScShh*/Shh-immunoreactivity

An overview of the expression of *ScShh*, *ScNkx2.1*, *ScOtp* and *ScDlx2*/*ScDlx5* in the basal hypothalamus of *S. canicula* mainly in early stages of development has been previously described in chapter 1.

To further characterize possible dorso-ventral and rostro-caudal subdomains and the acroterminal territory (the rostral-most domain of the neural tube) of the basal hypothalamus, here we review the data to deepen in the genoarchitectonic profile of the basal hypothalamus. A detailed comparative analysis of the expression of such gene markers in sagittal and transverse sections is presented from stages 29 to 32, when the basic mature cytoarchitecture and organization of the basal hypothalamus is achieved and all structures of the adult hypothalamus are clearly recognized.

3.3.1.1 *ScShh*-expression/Shh-immunoreactivity.

As described in **chapter 1,** from stage 29 onwards, Shh-immunoreactivity is observed in a limited part of the rostral and dorsal Tu-like domain and broadly detected within the RM-like domain and extending from here along the diencephalic basal plate (see Figures 1A-C; see also chapter 1). Shh-immunoreactivity is observed in the Tu-like without reaching the SPa-like domain (Figure 1B; see also chapter 2). However, it is not observed in the midline (acroterminal territory) just dorsal to the developing adenohypophysis (black arrowhead in Figure 1B). Caudally, Shh-immunoreactivity is only observed in a portion of the RM-like domain but not at its dorsal-most and ventral-most portions (arrowheads in Figure 1C). From stage 30, Shh-immunoreactivity is still detected but becomes reduced compared to previous stages RM-like and p3Tg (arrowheads in Figure 1D; see also chapter 1).

3.3.1.2 *ScNkx2.1* expression

From stage 29 onwards, *ScNkx2.1* is expressed ventral to the optic stalk through the whole basal hypothalamus except in the RM-like compartment (see Figures 1E-H). While *ScNkx2.1* and Shh-immunoreactivity co-distribute in part of the Tu-like domain (Figure 1F), Shh-immunoreactivity does not match the dorsal border of *ScNkx2.1* expression (black arrow in Figure 1F). *ScNkx2.1* is additionally expressed in the acroterminal territory dorsal to the adenohypophysis, in contrast to Shh (arrowhead in Figure 1F). *ScNkx2.1* expression in the MM-like abuts the RM-like, but it does not meet Shh-immunoreactivity since it is absent from the ventral-most portion of RM-like, which creates a gap between both markers (Figure 1G; also compare Figures 1A, E; see also chapter 1). Of note, *ScNkx2.1* expression forms a clear-cut border among the positive MM-like and the negative RM-like domain that is more evident on sagittal sections (Figure 1H), though, as noted in chapter 1, *ScNkx2.1*-expressing cells can be detected in the mantle of the RM-like domain (black arrowhead in Figure 1G, H).

3.3.1.3 *ScOtp* expression

In the basal plate, *ScOtp* has been identified in Tu-like and PM/PRM-like domains. From stage29 onwards *ScOtp* is expressed in the rostral-most basal plate of the Tu-like domain, from the optic stalk to the primordial neurohypophysis (Figure 1I). Specifically, it is restricted to the acroterminal territory of the Tu-like domain just dorsal to the adenohypophysis (Figure 1I; arrowhead in Figure 1J). In the PM/PRM domain *ScOtp* expression abuts the RM-like but not necessarily the Shh-immunoreactivity of this domain (Figure 1K). In the PM-like, *ScOtp* is also expressed in the acroterminal territory acroterminal territory (Figure 1I´). Note that the expression of *ScOtp* in the PM-like faces the MM-like (Figure 1L). Marginal *ScOtp*-expressing cells can be recognized in the RM-like (black arrowheads in Figures 1K, L) and p3Tg (not shown). This pattern is maintained until stage 32.

3.3.1.4 *ScDlx2*/*ScDlx5* expression

In the basal plate *ScDlx2/5* is intensely expressed in a restricted subdomain of the Tu/RTu-like and the p3Tg domains (Figure 1M). In the hypothalamus, it is expressed in a subdomain spreading from the RTu-like to the neurohypophysis (Figures 1M-N). Rostrally, *ScDlx2/5* expression of in the basal hypothalamus co-distributes with Shh-immunoreactivity in a subdomain of the Tu-like (Figure 1N). Note that neither *ScDlx2/5* expression nor Shh-immunoreactivity can be observed in the acroterminal territory co-extensive with the adenohypophysis (arrowhead in Figure 1N). Caudal and dorsal to this domain, *ScDlx2/5* expression in the RTu-like almost abuts Shh-immunoreactivity of the RM-like although a gap exists (arrow Figure 1O). In the most caudo-ventral part of Tu-like, individual and dispersed *ScDlx2/5*-expressing cells can be recognized almost reaching the rostral and ventral-most part of the PM-like (arrowheads in Figure 1M, O) including the primordium of the saccus vasculosus. These cells are less intense but still observable at stage 31 (arrowhead in Figure 1P). At stage 32 the basic pattern described for *ScDlx2/5* is maintained although reduced in intensity (see below). Of note, *ScDlx2/5* expression in the Tu-like can be ascribed to the lateral inferior lobes of adult shark hypothalamus but not to other regions.

### 3.3.2 *ScLhx5* expression

From stage 29 onwards, in the basal plate, *ScLhx5* is observed in subdomain of the dorsal-most and rostral-most Tu-like domain (Figure 1Q-T). *ScLhx5* expression also can be observed in the PM/PRM-like and MM-like domains (Figures 1Q-T). Note that *ScLhx5* expression in the MM-like domain describes a clear-cut border with the RM-like domain (Figure 1T), though *ScLhx5*-expressing cells can be recognized in the mantle of the RM-like domain (arrowheads in Figures 1 S-T).

### 3.3.3 *ScEmx2* expression

The expression of *ScEmx2* has been analyzed by Derobert et al., (2002) in the brain and related tissues from early stages of development (stage 19) until midgestation stages (stages 28-30). Here we analyze the detailed expression of *ScEmx2* in the basal hypothalamus from stage 29 until stage 31. From stage 29 onwards, *ScEmx2* is expressed in the basal hypothalamus in a well-defined domain spreading into part of rostral and ventral-most Tu-like domain, the PM/PRM-like and the MM-like domains (Figure 2A-D). Of note, it expression lacks in midline domains of the Tu-like (acroterminal territory) such as the neurohypophysis (Figue 2A) and saccus vasculosus (Figure 2B, C) but is present immediately caudal to the last (Figure 2D, E).

A comparison of *ScEmx2* expression with other markers reveals several correlations. We compared *ScEmx2* expression patterns with the presence of 5-HT-immunoreactive (-ir) cells since the hypothalamus of the shark is known to harbor circumventricular organs rich in 5-HT-immunoreactivity. This comparison revealed that the expression of *ScEmx2* highly correlates with the presence of 5-HT-ir cells at this point of the brain (Figures 2F-J compare

with Figures 2A-E). Faint 5-HT-immunoreactivity is also found beyond (but close to) *ScEmx2*-expresing domains like the RTu-like (Figure 3J) and the RM-like (Figure 3I, J).

Furthermore, we compared *ScEmx2* expression patterns with the presence of PCNA-immunoreactive (-ir) cells (Figures 2K-O). PCNA-ir cells define proliferative zones that are separated by non-proliferative (PCNA-immunonegative) ventricular regions, which are believed to define important segmental boundaries (Candal et al., 2005). Of note, the caudal border of *ScEmx2* expression in the MM-like domain (arrowhead in Figure 2A; arrow in Figure 2D) correlates with a domain of reduced PCNA-immunoreactivity in the ventricular zone (arrowhead in Figures 2K; arrow in Figure 2N)). The caudal border of *ScEmx2* expression in the PRM-like domain also correspond with a domain of restricted PCNA-immunoreactivity (compare arrowheads in Figures 2E, O). Thus, a band of reduced or negative proliferation seems to spread from the rostral and dorsal border of the RM-like (Figure 2M-O), p3Tg and zli (not shown).

Finally, we compared *ScEmx2* expression with that of other markers of the basal hypothalamus to better understand its organization. A comparison with Shh-immunoreactivity (Figure 2P) revealed that the *ScEmx2*-expressing domain is fairly complementary to Shh in which respects the PRM-like and RM-like domains (compare Figures 2A, P). Besides, this *ScEmx2*-expressing domain includes the caudal domain expressing *ScLhx5* in the PM/PRM-like and MM-like (compare Figures 2A, Q; also compare Figures 2C, R) and *ScOtp* in the PM/PRM-like (compare Figures 2C, S).Of note, *ScEmx2*, *ScLhx5* and *ScOtp* define consecutive more restricted domains (compare Figures 2C, R, S). Morevoer, the expression of *ScEmx2* abuts that of *ScDlx2/5* in dorsal and caudal positions (RTu-like domain; compare Figures 2E, 1O) while they co-distribute in more rostral and ventral positions (compare arrowheads in Figure 2B, 1M).

### 3.3.4 *ScLmx1b, ScPitx2, ScPitx3a, ScFoxa1, ScFoxa2* and *ScNeurog2* as markers of the RM

*ScFoxa1* and *ScFoxa2* are expressed in fairly the same spatial and temporal patters in the regions and stages considered in this study and thus are conjointly referred as *ScFoxa1/2*.

At stage 29 *ScLmx1b, ScPitx2, ScPitx3a, ScFoxa1/2* and *ScNeurog2* are expressed in a similar pattern spreading caudally from RM-like into the diencephalon including the zli in the case of *ScPitx2, ScPitx3a, ScFoxa1/2* and *ScNeurog2* (Figures 3A-D). On transverse sections the expression of these genes dorsally abut the PRM-like (Figures 3E-H). Rostrally these markers also abut the MM-like (arrowheads in Figures 3E-H). From stage 29 onwards this general pattern persists although some differences emerge. At stage 31, *ScLmx1b* becomes downregulated being restricted to the floor plate (Figure 3I) while Shh-immunoreactivity is still found in the basal plate (arrowheads in Figure 3I). At later stages *ScPtix2* is still expressed in the pattern (Figure 3J) observed at stage 29, while *ScPtix3a* is restrictedly expressed in the caudal-most diencephalon (not shown). In the case of *ScFoxa1/2*, there is slight dorsal and ventral downregulation but the main pattern persists through RM-like and

diencephalon (Figure 3K). From stage 30 onwards, *ScNeurog2* becomes donwregulated in the mentioned territories although it can be recognized in the zli and habenula (data not shown). Finally, *ScLmx1b*, *ScPtix2* and *ScFoxa1/2* still present a sharp border of expression that abuts the MM-like domain at this developmental stage (arrowheads in Figures 3L-N).

### 3.3.5 GAD immunoreactivity

GAD-immunoreactivity was previously analyzed during the brain development of sharks by Carrera et al., 2008 and in combination with other markers by Ferreiro-Galve et al., 2008. Besides, its expression in the alar hypothalamus has been analyzed under the current prosomeric model (see chapter 2). Here GAD-immunoreactivity was particularly analyzed in the basal hypothalamus at stage 30 to test if the segmental organization described by gene expression patterns at similar stages is congruent with that deduced by means of neurochemical markers.

GAD immunoreactive structures can be observed in the basal hypothalamus in a pattern that closely resembles that of *ScDlx2/5* (compare Figures 4A and 1M). GAD-immunoreactivity is detected in the RTu-like domain and in a restricted portion of the Tu-like domain (Figure 4A). Note that GAD-immunoreactive (-ir) cells are also observed in the saccus vasculosus (see Sueiro et al., 2007 and arrowhead in Figure 4A). Besides, GAD-immunoreactivity was not observed in the RM-like domain or p3Tg although GAD-ir fibers were detected coursing through these domains (Figure 4A).

### 3.3.6 TH + Shh immunoreactivity

The distribution of TH-immunoreactivity has been well characterized in *S. canicula* under precedent segmental frameworks in Ferreiro-Galve et al., 2008 and Carrera et al., 2012. Besides it has been previously examined under the current prosomeric model in the alar hypothalamus (see chapter 2) but not in the basal hypothalamus. TH-immunoreactivity was specifically analyzed at stage 30 to assess if the pattern of expression of neurochemical markers support the segmental organization defined above by means of gene expression patterns.

At stage 30, TH-immunoreactivity was observed in the RM-like and p3Tg just ventral to Shh-immnunoreactivity (Figure 4B). This pattern coincides with the expression of *ScLmx1b*, *ScPitx2*, *ScPitx3a*, *ScFoxa1*, *ScFoxa2* and *ScNeurog2* genes in the same domains. Individual TH-immunoreactive cells were also observed in the dorsal and rostral-most Tu-like and the ventral and caudal-most Tu-like close to the PM-like (data not shown). At stage 32, TH-immunoreactivity can be abundantly detected through the RM-like, p3Tg and zli (Figure 4C), which again resembles the pattern of the above mentioned gene markers.

### 3.3.7 CB immunoreactivity

Calbindin-immunoreactivity has been analyzed in adult sharks by Rodríguez-Moldes et al. (1990) and in the alar hypothalamus under the updated prosomeric framework (see

chapter 2). The pattern of CB-immunoreactivity was analyzed in the basal hypothalamus to check whether it coincides with territories defined by the gene markers used here. At stage 29 abundant CB- immunoreactivity can be recognized in the rostral and dorsal-most Tu-like (arrowhead in Figure 4D), in a pattern that seems to coincide with that of GAD-immunoreactivity in the Tu-like domain (compare with Figure 4A). More dispersed groups of CB-immunoreactive (-ir) cells can be observed in the RTu-like, PRM-like and p3Tg (Figure 4D). Of note, CB-immunoreactivity has not been detected in the caudal and ventral-most Tu-like, PM-like and MM-like (Figure 4D).

#### 3.3.8 SS + Shh immunoreactivity

Somatostatin-immunoreactivity has been analyzed jointly with Shh-immunoreactivity at stage 30 to get a better comprehension of its segmental organization in the alar hypothalamus (see chapter 2). Here we analyze its distribution at stage 30 since SS has been described as a useful marker to define the caudal border of the prosomeric hypothalamus (Morales-Delgado et al., 2011). Scarce SS-immunoreactivity can be observed in the rostral and dorsal-most Tu-like (arrow in Figure 4E). Another reduced group can be observed in the RM-like on parasagittal sections (arrow in Figure 4F). Finally, SS-immunoreactivity can also be abundantly observed in the alar p3 and p3Tg (Figure 4F-G).

#### 3. 3.9. GFAP immunoreactivity

GFAP-immunoreactivity was analyzed at stage 29 and 30. Radial and longitudinal GFAP- immunoreactivity processes were detected through the whole hypothalamus (Figures 4H, H´). Of note, GFAP-immunoreactivity was particular abundant in the neurohypophysis and saccus vasculosus (Figures 4H, H´).

### 3.4. DISCUSSION

#### 3.4.1 Basal hypothalamus-diencephalic boundary

In a previous work, we defined the basal **hypothalamus-diencephalic boundary (HDB)** of *S. canicula* by the clear-cut border between *ScOtp*- and *ScNkx2.1*-expression in the **PRM-like** and the distribution of *ScDlx2/5*-expressing cells in the basal portion of the **p3Tg** (chapter 1; see also Figure 5 A, C, D). Our present results using more genetic and neurochemical markers have contributed to shed light on this boundary.

The location of SS-immunoreactive (-ir) neurons in the p3Tg (separately from those of the RM-like) in *S. canicula* supports the limit between the RM-like and the p3Tg as it has been proposed in mouse (Morales-Delgado et al., 2011), which reinforces our previous identification of a HDB similar to that observed in mammals.

However, our data also support alternative interpretations of the HDB. It is striking that all the genes expressed in the RM-like –*ScLmx1b*, *ScPitx2a*, *ScPitx3a*, *ScFoxa1*,

*ScFoxa2*, *ScNeurog2*– share a similar pattern, being expressed caudally beyond this domain into the basal plate of the diencephalon an even in the zli. Besides, these markers also display a clear-cut border with genes expressed in the *ScNkx2.1*-expressing hypothalamus such as *ScOtp*, *ScLhx5* and *ScEmx2* (Figure 5A, C, D, E). Since boundaries are characterized by different expression patterns on each of its sides (Dahman et al., 2011), our data suggest on one hand that there is no boundary between the RM-like and p3Tg (Figure 5A, E), and on the other, that a boundary exists between the RM-like domain and every other part of the basal hypothalamus. In this line, the expression of *ScNkx2.1*, *ScEmx2* and *ScOtp* was continuous between the terminal and peduncular portions of the basal hypothalamus, which argues against the existence of a boundary (the IHB) at this point.

### 3.4.2 Prosomeric compartments and subcompartments of the basal hypothalamus

In a previous work, we have identified the shark basal hypothalamus harboring a Tu/RTu-like, PRM/PM-like and MM/RM-like domains based on the basal expression of *ScNkx2.1*, *ScShh*, *ScOtp* and *ScDlx2/5* (see chapter 1; Figure 5A). Such study has revealed homologue domains in mouse and shark, but also the existence of different subdomains. The present work further analyzes a number of markers that has revealed that the genoarchitecture of the catshark basal hypothalamus is more complex than previously described, which allow recognizing dorso-ventral subdivisions.

The analysis of gene expression patterns and chemical markers has allowed to additionally identify the basal acroterminal region and to characterize different subdomains within this territory (Figure 5B). The acroterminal domain (which, according the prosomeric model is the territory corresponding to the rostral-most point of the brain; reviewed in chapter 1) seems responsible for the development of structures such as the optic chiasm in the alar plate or the neurohypophysis in the basal plate (Puelles et al., 2012; Puelles and Rubenstein, 2015; Ferrán et al., 2015). In addition, in non-acroterminal territories, the differential expression of *ScEmx2* in relation to the other genetic markers has led us to recognize three main dorso-ventral territories and their subdivisions in the basal hypothalamus (see Figures 5A-D). For simplicity, subdomains are named according to the updated prosomeric model nomenclature and identified with numbers from dorsal to ventral: rostro-dorsal subdomains lacking *ScEmx2* (Figure 5C); ventral subdomains expressing *ScEmx2* (Figure 5D) and ventro-caudal subdomains lacking *ScEmx2* (Figure 5E). Moreover, these *Emx2* subdivisions present a high correlation with the distribution of three neurochemical markers: the negative dorsal domain seem to correspond mainly with a GAD-ir territory (see Figure 5F, compare with 5A, C); the positive one seems to correspond mainly with 5-HT-immunoreactivity (see Figure 5F; compare with Figure 5A, D); while the negative caudal one seems to be mainly TH-ir (see Figure 5F; compare with Figure 5A, E). Noteworthy, these main subdivisions do not agree neither our previous histogenetic analysis of the basal hypothalamus nor the prosomeric model (see chapter 1). However, they seem to have morphological significance at later stages (Figure 6).

3.4.2.1 The basal acroterminal domain (*ScShh* negative)

The acroterminal domain involves the alar and basal plate spreading from the rostral-most roof plate to the rostral-most floor plate (see chapter 1). We have tentatively defined different subdomains in the basal acroterminal region. We have identified at least 6 subdomains named from 1-6 from dorsal to caudal (BAt1-6; Figure 5B). Of note, some of these acroterminal subdomains are negative for markers broadly expressed in the Tu-like, i.e, patterns in the acroterminal (medial) domain do not necessarily match those found in more lateral regions (compare Figures 5A, B). The two dorsal-most domains (**BAt1-2**) are positive for *ScNkx2.1* (Figure 1F) and *ScOtp* (Figure 1J) but only BAt1 shows expression of *ScLhx5* (Figure 5B). Furthermore, *ScOtp* co-distributes with *ScNkx2.8* (Figure 1J, J´; see also chapter 1 and 2, respectively). In addition, BAt1 in its dorsal-most portion contains cells immunoreactive to GAD, TH, and SS, and fibers immunoreactive to 5-HT around stage 30 (not shown). Strikingly, we did not detect any neurochemical marker in the other subdomains of the acroterminal region around these stages. Instead, a portion of BAt2 shows intense GFAP-immunoreactivity from stage 29 onward. BAt1-2 subdomains are negative for other gene markers broadly expressed in the Tu-like such as *ScDlx2/5* and Shh (Compare Figure 1J with 1N and 5A with 5B). Of note, at later stages *ScLhx5* is absent from the midline (arrowhead in Figure 2R). Noteworthy, **BAt1-2** are almost co-extensive with the developing adenohypophysis (Figure 5B), which in part is co-extensive with negative subdomains for *ScDlx2/5*-expression and Shh-immunoreactivity (Figure 1 N). Of note, these gaps are as wide as the adenohypophysis, which has been noted in other vertebrates even for different adenohypophysis sizes (see Figure 2N in Manning et al., 2006), suggesting a role for the adenohypophysis in the local patterning of the hypothalamus at this point. In turn, either these gaps and *ScNkx2.8*-expression in shark are wider than the medio-lateral extension of *ScOtp*-expression, which suggests the existence of additional medio-lateral subdomains (Figure 1J, J´).

**BAt3** (the acroterminal region at the level of the neurohypophysis) is also Shh-immunonegative and also expresses *ScNkx2.1* (see Figure 4C in chapter 1), but differently from BAt1-2, it expresses *ScDlx2/5* (Figure 1M, 5B). GFAP-ir cells are also observed in this subdomain (Figure 4H').

Ventrally to BAt3, we identified **BAt4** as a subdomain that corresponds to the primourdium of the saccus vasculosus (Figure 5B; see also Van De Kamer & Shuurmans, 1957; Sueiro et al., 2007). The initial tiny domain expands becoming morphologically distinguishable (stage 29, Figures 1E, I; stage 30, Figures 1F, 4E; stage 32 Figure 2F. This domain is characterized by the expression of *ScNkx2.1* and dispersed *ScDlx2/5*-expressing cells (Figure 1M). Since *ScDlx2/5* is involved in the development of GABAergic phenotype (Anderson et al., 1999), its expression in the saccus vasculosus could explain the existence of GABAergic cells at this point (Sueiro et al., 2007). Moreover, from stage 29 onwards BAt4 (the developing saccus vasculosus), differentially show intense GFAP-immunoreactivity not observable in more caudal subdomains (Figure 4H, H'; see also Sueiro et al., 2007). Finally,

BAt4 is also characterized by lack of *ScEmx2* (Figures 2B, C) and 5-HT immunoreactivity (see Figure 2F-H) which, however, are present in more caudal acroterminal subdomains (Figure 2D, E, J; see also BAt5 in Figure 5B) and in lateral (non-acroterminal) domains (Figure 5A, D, F). Noteworthy, the tip of the notochord has been described to reach the primordium of the saccus vasculosus (BAt4)(Figure 4H; see also Figure 1 in Van De Kamer & Shuurmans, 1957) suggesting a causal relationship to saccus vasculosus development. This idea is implicitly supported by the concept of the acroterminal region, since particular signaling events are thought to be involved in the development of several structures (lamina terminalis, optic chiasma, neurohypophysis) addressed to this territory (Puelles et al., 2012, Puelles and Rubenstein, 2015).

BAt4 shares with the domain ventral to it (**BAt5**) *ScNkx2.1* expression, dispersed *ScDlx2/5*-expressing cells and GAD-immunoreactivity. However, as commented above, BAt5 differentially presents a lack GFAP-immunoreactivity and the presence of *ScEmx2* expression (Figure 2D, E; see also Figure 5B) besides 5-HT-immunoreactivity (Figure 2J) at late stages of development. The ventral-most acroterminal domain is **BAt6** which express *ScNkx2.1*, *ScEmx2*, *ScOtp* and *ScLhx5*, but not *ScDlx2/5* (see Figure 5B). However, we cannot discard that this territory could be interpreted as the floor plate of the MM-like (Figure 5D) that in mouse (but not in shark; compare Figures 7A, 7B) differentially expresses *Shh* (see Figure 8.9B in Puelles et al., 2012).

#### 3.4.2.2 Rostro-dorsal subdomains (*ScEmx2* negative)

We have identified six subdomains dorsal to those co-expressing *ScEmx2* (Figure 5C). As commented above, these domains also are mainly positive for GAD (Figure 4A, Figure 5F). Five of them belong to Tu-like (Tu1-5) and one to the RTu-like (RTu1) (Figure 5C). Of note a subdomain belonging to the caudal and ventral-most Tu-like, Tu6, presents dispersed *ScDlx2/5*-expressing and GAD-ir cells. This subdomain lies within the *ScEmx2* expressing domain, and thus is discussed below (see also Figure 5D).

The dorsal and rostral-most domain is **Tu1** and expresses markers like *ScNkx2.1* and *ScLhx5* (Figure 5C). Caudally to it, we have distinguished a similar domain lacking *ScLhx5* but expressing *ScDlx2/5*, named as **Tu2** (Figure 5C). These two subdomains belong to the basal portion of the ABB and so, they lack *ScShh* (Figure 5C) and they express *ScNkx2.8* and *ScLhx9* (see also chapter 2). More ventrally, two subdomains, **Tu3** and **Tu4**, appear as the ventral extension of Tu1 and Tu2 respectively, since they share with them either *ScLhx5* or *ScDlx2/5* expression. However, they express *ScShh* (Figure 5C) and lack *ScNkx2.8* and *ScLhx9* expression (see also chapter 2). The expression of *ScLhx5* in the Tu1/Tu3 appears complementary to that of *ScDlx2/5* in Tu2/Tu4 (Figures 5C, 6A). Complementary patterns among *Dlx* and *Lhx5* have been previously described in the mouse forebrain (Sheng et al., 1997), which suggests a conserved inhibitory relationship between both genes. Noteworthy, CB-immunoreactivity has been detected in the *ScLhx5*-expressing Tu1/Tu3 (Figure 5F, 6A). Faint immunoreativity for 5-HT and SS has also been observed in these domains (Figure 5F),

not appearing related to the genetic subdomains here identified. Moreover, a small domain ventral (and caudal) to Tu4, which expressed *ScNkx2.1* and *ScDlx2/5* but was negative to Shh-immunoreactivity, was referred as **Tu5** (Figure 5C, 6A). The dorsal and caudal-most subdomain identified is **RTu1** (Figure 5C, 6B), which expresses the same genes as Tu2 and Tu5 (*ScNkx2.1*, *ScDlx2/5*; see Figure 5C) and shows CB-immunoreactivity (Figure 5F).

3.4.2.3 Ventral subdomains (*ScEmx2* positive)

This domain is characterized by a nested expression of *ScEmx2, ScLhx5* and *ScOtp* in the caudal and ventral *ScNkx2.1*-expressing hypothalamus (Figure 5D). As result, six ventral subdomains are observed (Figure 5D). All the domains share *ScNkx2.1* and *ScEmx2* expression besides the richness in 5-HT-immunoreactivity over other neurochemical markers, mostly at later stages (see also Carrera et al., 2008) (Figure 5F).

The rostral and dorsal-most subdomain, referred as Tu6, was previously identified as the rostral and ventral-most domain of the Tu-like characterized by the expression of *ScEmx2* and a dispersed distribution of *ScDlx2/5*-expressing and GAD-ir cells (see chapter 1; see also Figure 5D, F).More ventrally, we referred as **PM1** a domain characterized by *ScNkx2.1*/*ScEmx2*/*ScLhx5* expression. Ventral to PM1, we identified **PM2** (the PM-like of chapter 1) as the subdomain that expresses *ScNkx2.1/ScEmx2/ScLhx5/ScOtp.* Ventral to PM2 we identified **MM1** (MM-like of chapter 1), which expresses *ScNkx2.1/ScEmx2/ScLhx5* but not *ScOtp* (Figure 5D). Of note, the markers expressed in the MM1 (MM-like), show a clear-cut border with those expressed in the RM-like domain (Figures 5D-E). In the dorsal and caudal-most portion of this *ScEmx2*-expressing domain we have identified the caudal continuation of PM1 and PM2referred as **PRM1** and **PRM2** respectively (Figure 5D). The dorsal-most is referred as PRM1 and expresses *ScNkx2.1*/*ScEmx2*/*ScLhx5* (Figure 5D) while the ventral one, PRM2 (the PRM-like in chapter 1) also expresses *ScOtp* (Figure 5D). This subdomain may be also supported by the restricted CB-immunoreactivity at this point (Figure 5F).

3.4.2.4 Ventro-caudal subdomains (*ScEmx2* negative)

Of note, in this *ScEmx2*-negative territory neither *ScNkx2.1* nor other markers expressed in more dorsal and rostral subdomains could be detected, excepting Shh (Figure 5E; compare with Figures 5A-D). Besides, although differences through development also exist, almost all the markers expressed here present a similar pattern being continuously detected from the RM-like into the basal plate of the diencephalon and, in many cases, also in the zli (see Figure 5E; see also Figure 3A-D). Another common feature of these markers is that they present a clear-cut border of expression between the RM-like and the remaining subdomains of the basal hypothalamus (Figure 5E). Besides the lack of *ScEmx2*, these domains are rich in TH-immunoreactivity, mostly at late stages of development (Figure 5E) and SS-immunoreactivity is significant in some subdomains (Figure 5F).

We have identified three dorso-ventral subdomains in the ventral and caudal-most point of the basal hypothalamus here referred as **RM1**, **RM2** and **RM3** (Figure 5E), which fairly correspond to the previously defined RM-like territory (chapter 1; see also Figure 5E). The dorsal-most domain, RM1, may be defined based on lack of Shh-immunoreactivity at stage 29 and the expression of *ScLmx1b*/*ScPitx2*/*ScPitx3a*/*ScFoxa1*/*ScFoxa2*/*ScNeurog2* (Figure 5E). In the RM2, these markers co-distribute with Shh-immunoreactivity while the ventral-most domain, RM3, is again characterized by the lack of Shh-immunoreactivity (Figure 5E). Of note, from stage 30 onwards, *ScPitx2* is expressed in the whole RM-like (Figure 3J, M) but the downregulation of other genes suggest the existence of even four dorso-ventral domains. The dorsal-most contains only *ScPitx2*; ventral to it a *ScPitx2*-expressing domain co-distributes with Shh-immunoreactivity (compare Figure 3J with 1D); the next co-distributes with *ScFoxa1/2* (Figure 3K, N) while the ventral-most co-distributes with *ScLmx1b* (Figure 3I, L). The remaining markers, *ScPitx3a* and *ScNeurog2*, became completely dowregulated from the RM-like at these stages. Of note, we also detected SS-ir cells in the marginal zone of the rostral-most border of the RM-like (Figure 4E, 5F). These cells do not support the mentioned dorso-ventral organization but could have a relationship with tracts projecting to the telencephalon since they are located adjoining that was previously defined by us as a boundary (see chapter 1), where they co-distribute with Pax6-ir cells (see Figure 3N in chapter 2).

### 3.4.3 Alternative segmental organization of the basal hypothalamus: proposal based on evo-devo considerations

Our data reveal that *S. canicula* shares with other vertebrates many expression patterns of genes involved in the histogenesis of the basal hypothalamus, but also reveal a complex scenario for homologies establishment and subdomain identity (Figure 7). We interpret that expression of such genes is organized into three main histogenetic domains (a rostro-dorsal unit lacking *ScEmx2* [Figures 7A, B]; a ventral unit expressing *ScEmx2* [Figures 7C, D] and a ventro-caudal unit lacking *ScEmx2* [Figures 7E, F]), which not necessarily coincide with those of the updated prosomeric model (Puelles et al., 2012; Puelles and Rubenstein, 2015). These domains seem to respect certain common rules across vertebrates but they give rise to complex and different histogenetic units, which makes difficult the establishment of homologies. The main point of our proposal is that Tu6, the PM/PRM and the MM form a histogenetic unit. Such interpretation is supported by the following observations in the shark: i) the patterns of gene expression here observed (Tu6/PRM/PM/MM) seem to be different from those present in both the Tu/RTu-like and the RM-like, (Figure 7G-H); ii) *ScOtp*, *ScEmx2*, *ScLhx5* and *ScNkx2.1* are continuously expressed across the hp2/hp1 boundary but they do not enter the RM-like domain suggesting that Tu6/PRM/PM/MM-like do not belong to the same histogenic unit that RM-like; iii) gene expression patterns in Tu6/PRM/PM/MM-like present a fairly nested organization in relation to the RM-like (Figure 5D), similar to that observed in many diencephalic genes with respect to the zli (Vieira et al., 2005). We hypothesize that this is a conserved trait (see below). Of note, in mouse, the expression of genes like *Pitx2* and *Neurog2* extends from the MM into the RM (Figure 7C-D), which argues

against these domains belonging to different histogenic units. However, this fact could be understood as a trait acquired in the course of vertebrate evolution.

We think these domains may be also recognized in mouse and other vertebrates. Comparisons with data described in other vertebrates (though considering a rather different group of genes), will complement recent revisions about data on the anamniote-amniote transition under the updated paradigm (Domínguez et al., 2015), which in turn may contribute to better understand the evolutionary meaning of these observations.

#### 3.4.3.1 Evidence from comparison with amniotes

We have mainly compared the expression patterns between two models –shark and mouse– in terms of the updated prosomeric paradigm. In mouse, different works have addressed the expression of the orthologous genes to those here considered mainly under a prosomeric framework, although not necessarily the updated one: *Shh*, *Nkx2.1*, *Dlx5*, *Otp* (Morales-Delgado et al., 2011, 2014; Puelles et al., 2012), *Lhx5* (Abellán et al., 2010; Szabó et al., 2009; Puelles et al., 2012), *Emx2* (Shimamura et al., 1995; Suda et al., 2001; Szabó et al., 2009), *Lmx1b* (Asbreuk et al., 2002; Martinez-Ferre et al., 2012; Puelles et al., 2012), *Pitx2* (Martin et al. 2004; Puelles et al., 2012); *Foxa1* (Diez-Roux et al., 2011; Martínez-Ferre et al., 2012; Puelles et al., 2012); *Foxa2*; and *Neurog2* (Osorio et al., 2010; Puelles et al., 2012). The patterns of all of them are available in the mouse developmental Allen Brain Atlas. We have drafted these patterns around mouse stage 13.5 mainly from Allen Brain Atlas and other reports (see above), and we compared them with data in shark around stage 29 (present results). The expression of some of the genes analyzed in shark as *Nkx2.1*, *Shh*, *Otp*, *Dlx*, *Emx2*, *Foxa2*, has been studied in birds (Manning et al., 2006 Bardet et al., 2008, 2010; García-Calero et al., 2008; Abellán et al., 2010). Because all these expression patterns appeared to describe a scenario similar to that of mammals (reviewed in Domínguez et al., 2014, 2015), we have considered the differences observed between shark and mouse transposable to birds.

In both, mouse and shark, the **Tu/RTu** is characterized by the expression of *Nkx2.1*, *Dlx2/5* and *Otp* (Figure 7A-B; see also chapter 1). However, differences in sub-compartmentation emerge while considering additional markers. In mouse, *Lhx5* is broadly expressed in the basal hypothalamus before stage 13.5 (Szabó et al., 2009; Abellán et al., 2010; Allen Brain Atlas). Nevertheless, after this stage, it becomes downregulated and restrictedly expressed in non-Tu/RTu domains (Figure 7A). In shark, *ScLhx5* is expressed in the dorsal-most Tu-like from stage 29-31 (Figure 7B). Besides, in the mouse, the expression of *Shh* is restricted to the dorsal and caudal-most Tu and RTu (Figure 7A) while in *S. canicula* it is fairly expressed in the whole Tu-like but absent in the RTu-like (Figure 7B). Noteworthy, the differential spatial distribution of Shh between both models leads to the emergence of a subdomain in the mouse Tu (asterisk in Figure 7A) containing *Dlx2/5* alone, which is not present in shark (Figure 7B). Finally, in mouse, *Emx2* is absent from the Tu/RTu while in shark it is expressed in Tu6 (Figure 7A, B). This analysis reveals that different subdomains

can be defined in different organisms even when considering the same markers in part because the number of subdomains will depend on the number and the class of genes studied, which raises non trivial questions concerning homologies establishment. Moreover, the subdivisons sketched in the shark Tu/RTu-like do not seem to support the same prosomeric dorso-ventral microzones (dorsal, intermedian and ventral) proposed in mouse on the basis of the combined expression of different gene markers (Puelles et al., 2012, Puelles and Rubenstein, 2015; Ferrán et al., 2015).

The **PM/PRM** is characterized in both models by *Otp* and *Lhx5* expression (Figure 7C-D). Of note, in shark, this compartment also expresses Sc*Emx2* (Figure 7C-D). Noteworthy, the PRM-like of shark lacks *Shh* expression in contrast to mouse (Figure 7C-D).

Respecting the **MM/RM, in both species** there seem to be a common tendency on which genes expressed in the RM, like *Lmx1b* or *Foxa1*, appear to form a clear-cut border of expression with respect to those expressed in the MM (and even in the PRM-like) as *Nkx2.1*, *Emx2* (see Figure 6L in Shimamura et al., 1995) and Lhx5 (see Figures 7E-F). However, in mouse this rule seems to be ignored by patterns like *Pitx2* and *Neurog2* since they are expressed in both domains (Figure 7E-F). Of note, the expression of *Neurog2* in previous stages seems to be restricted to the RM (termed as p3Tg in Figure 2B-B´ in Osorio et al., 2010).

We have found more genes defining the border between the PRM/RM and between the MM/RM domains than genes commonly expressed in both the MM and RM in mouse and other vertebrates. This organization fits with the *ScEmx2*-positive/negative domains we defined in shark (Figure 5, 7H) which in mouse is likely to be represented by genes expressed in the PM/PRM/MM like *Sim1* and *Otp* (Morales-Delgado et al., 2014; Puelles et al., 2012) (Figure 7G-H).

#### 3.4.3.2 Evidence from comparison with anamniotes

An exhaustive comparison of data in the basal hypothalamus based on the updated prosomeric model cannot be made to date due to the scarce number of detailed works specifically addressing this question. Nevertheless, a recent work reviewed data on the anamniote-amniote transition under the updated paradigm (Domínguez et al., 2015). However, this paper considers a rather different group of genes for comparisons from those used in the present work. Our analysis is tentatively made by comparing the presence/absence of expression in equivalent topological regions to the vertebrate basal hypothalamus. However, we must have into account that the expression of similar genes in similar positions does not necessarily mean the existence of homologue domains. Thus, establishing comparisons and homologies among vertebrates could result misleading. Furthermore, depending on the animal model, the brain organization paradigm and/or the version of the prosomeric model considered, the progenitor domains are referred under a plethora of names (tuberal, tubero-mamillar, mamillary band, supramamillary, tubero terminal, retromamillar, subliminal, diagonal band and intermediate hypothalamus; Bardet et al., 2008; Shimogori et al., 2010; Szabó et al., 2009; Puelles et al., 2012; Domíngez et al., 2014, 2015; Manoli & Driever, 2014) adding an extra level of complexity.

Taking into account studies in lampreys dealing with the expression of *Nkx2.1*, *Dlx*, *HhB* (Shh orthologue), *Lhx1/5*, *EmxB (Emx2 orthologue)* and *PitxA* (*Pitx2* orthologue) genes in the rostral-most prosencephalon (Murakami et al., 2001; Myonjin et al., 2001; Ogasawara et al., 2001; Uchida et al., 2003; Osorio et al., 2005, 2006; Guerin et al., 2009; Tank et al., 2009; Kano et al., 2010; Martinez-de-la-Torre et al., 2011; Sugahara et al., 2011), we may recognize in the basal hypothalamus a dorsal/rostral and round domain expressing *Nkx2.1* that likely harbors *Dlx*, *HH* and *Lhx1/5* subdomains (Figure 8A; see also Murakami et al., 2001; Ogasawara et al., 2001; Uchida et al., 2003; Osorio et al., 2005, 2006; Kano et al., 2010; Martinez-de-la-Torre et al., 2011; Sugahara et al., 2011), a situation which resembles that observed in the shark Tu/RTu-like (compare with Figures 5, 7). Ventro-caudally to *Dlx*, a reduced band of *EmxB* and *Lhx1/5* expression (Figure 8A) together with a strong downregulation of *HhB* at this point, (see also Murakami et al., 2001; Myonjin et al., 2001; Ogasawara et al., 2001; Uchida et al., 2003; Osorio et al., 2005, 2006; Guerin et al., 2009; Kano et al., 2010; Sugahara et al., 2011; Tank et al., 2009), supports the possibility that this domain represent the lamprey PRM/PM/MM-like. Differently from other vertebrates, these ventro-caudal genes (*Lhx1/5*, *EmxB*) are expressed in a continuous vertical band (perpendicular to the ABB and parallel to the zli) (see Figure 8). Caudal to this band, a vertical domain expresses *HhB* (Figure 8), *PitxA* (see Figure 4 in Uchida et al., 2003) which could represent the RM-like domain. It is very persuading to propose a shift in this angle from 180º to 90º degrees from lampreys to amniotes (see below). Noteworthy, a change in the angle described between genes expressed in the zli and those expressed just rostral or caudal to it has been proposed to explain morphological differences among species of cichlid fishes (Sylvester et al., 2010). These expression patterns in lampreys support the existence of alternative histogenetic domains in the basal hypothalamus and also support that changes in *Hh/Shh* expression in the caudo-ventral hypothalamus could influence the expression and morphogenesis of the *Emx2* positive hypothalamus located just adjacent to it.

Although the expression of the genes analyzed in shark and their topological positions seem to be conserved in Actinopterygians, differences exist that could have yielded different histogenetic domains. In zebrafish, the expression of *Nkx2.1*, *Otp*, *Dlx*, *Shh*, *Lhx5*, *Emx2*, *Lmx1b*, *Pitx3*, *Neurog1*, and *Foxa2* (also referred as axial or *HNF3β*) (Barth & Wilson, 1995; Hauptman & Gester, 2000; Mathieu et al., 2002; Kapsimali et al., 2004; Jeong et al., 2006; Filippi et al., 2007, 2012; ; Ryu et al., 2007; Del Giacco et al., 2008; Osorio et al., 2010; Yang et al., 2012; Lauter et al., 2013; Wolf & Ryu, 2013; Manoli & Driever, 2014) reveals that the genoarchitecture of the dorso-rostral hypothalamus is more conserved than its caudo-ventral portion. Particularly, the expression of *Nkx2.1*, *Shh*, *Dlx2*, *Otp* and *Lhx5* (Hauptman & Gester, 2000; Ryu et al., 2007; Manoli & Driever, 2014) appears to define histogenetic subdomains really similar to those described in shark in the Tu/RTu-like (present results). However, differences are noted caudo-ventrally. As in shark, *Otp* is expressed as a subdomain in the intermediate portion of the large *Emx2*-expressing domain, which is also positive for *Nkx2.1* (see aslo Figure 2 D´´ and 2E´´in Wolf & Ryu, 2013). However, in contrast to shark, this domain also expresses *Shh* (see also Figure 2N in Wolf & Ryu, 2013) resembling the situation of mouse (see above). Caudo-ventral to this point, the patterns of genes like *Shh*, *Lmx1b*, *Pitx3*, *Neurog1* and *Foxa2* (Barth & Wilson, 1995; Hauptman & Gester, 2000; Mathieu et al., 2002; Jeong et al., 2006; Filippi et al., 2007; Ryu et al., 2007; Del Giacco et al., 2008; Osorio et al., 2010; Yang et al., 2012; Lauter et al., 2013; Manoli & Driever, 2014) show an organization similar to that observed in shark. Noteworthy, differently from that observed in

shark, *Lhx5* seems to be expressed caudally to *Nkx2.1* rather than co-distributing with it (see also Lauter et al., 2013). Furthermore, in contrast to shark, *Foxa2* seems to not reach the rostral-most border of Shh in a hypothetic RM-like (see also Lauter et al., 2013; Hauptman & Gester, 2000).

The basal hypothalamus of the amphibian *Xenopus laevis* has been recently characterized including data of *Nkx2.1, Shh and Otp* orthologues (Dominguez et al., 2010, 2014, 2015) and also of *Neurog* (Wulliman et al., 2005; Osorio et al., 2010;) and *Lhx5* (Bachy et al., 2001) ortologues. The *X. laevis* rostro-dorsal domain expressing *Nkx2.1*, *Shh*, *Otp* and *Isl1* (Dominguez et al., 2015) likely represents the Tu/RTu-like of shark (present results), but differently, this domain lacks *Lhx5* expression (see Bachy et al., 2001). In this Tu/RTu-like, two rostro-caudal subdomains were identified in *X. laevis* based on *Nkx2.2 vs. Isl1* and *Otp* expression (Dominguez et al., 2014) that, due to their relative extension, resemble those observed in shark based on *ScLhx5 vs.ScDlx2/5* (Figure 5C). In contrast to fishes, in amphibians *Shh* expression is continuous from the zli to the basal hypothalamus (Dominguez et al., 2010), which could mean that *Shh* is expressed (as in mouse) in a hypothetic RTu-like. Strikingly, more detailed works have failed to find *Shh* co-distribution with *Otp* (Dominguez et al., 2014, 2015). Ventrally to the *Xenopus* Tu/RTu-like [corresponding to the rostral and caudal tuberal region (RT/CT), of Domínguez et al., 2015], *Nkx2.1* and *Otp* expressions define a domain [mammillary region (M) in Domínguez et al., 2015] that could be homologous to the shark PM/PRM/MM-like. Ventrally to it, a subdomain was described expressing *Shh* (Dominguez et al., 2015), that could represent the RM-like domain of shark. The expression of *Neurog* genes has been described in the p3Tg under former prosomeric assumptions (Osorio et al., 2010) but their adscription to a RM-like domain cannot be discarded under the last recapitulation of the model. Noteworthy, the expression of *Shh* and *Nkx2.1* also has been described in the p3Tg which is supported also by other authors (Van Den Akker et al., 2008) although seems non-parsimonious in relation with the alternative segmental proposal for the basal hypothalamus.

### 3.4.4 Clues to understand basal hypothalamic organization among vertebrates: Insights from chondricthyans and mouse defective for neural Shh

Our comparative analysis suggests that Shh-dowregulation in part of the hypothalamus seems to be both a common but also a divergent trait among vertebrate brains (depending on how this downregulation take place; see below). Of note, this downregulation also seems to be fairly complementary (or partially complementary) to the increase of *Emx2* expression in the peduncular hypothalamus among different vertebrates (see below; see also Mathieu et al., 2002; Kapsimali et al., 2004; Manning et al., 2006; Wolf and Ryu, 2013).

It is a remarkable fact that the phenotype of certain mutant mice lacking neural *Shh* in the hypothalamic neuroepithelium is characterized by an array of collateral defects (Szabó et al., 2009; Blaess et al., 2015) that resemble certain traits of gene expression observed in shark. **First**, while in wild mice *Emx2* is restricted to MM (Figure 7A), the lack of *Shh* triggers *Emx2* upregulation (see Figure 4 in Szabó et al., 2009; note that hypothalamic regions are not named according to the prosomeric framework), which could be related to the presence of *ScEmx2* in the PM-like and part of the Tu-like of sharks, where expression of *ScShh* is

restricted with respect to mouse (Figure 7B). **Second**, the lack of neural Shh reduces the proliferation in the rostral and ventral-most hypothalamus (see Figure 4 and 6 in Szabó et al., 2009). Of note, in the shark, the neural walls of *ScEmx2*-expressing hypothalamus (lacking *ScShh*) also seem less developed than those expressing *ScShh* (see Figure 4 and 6 in Szabó et al., 2009 compare with our Figures 4A-J). Moreover, the expression of *Otp* becomes completely downregulated in the PM/PRM of mutants (see Figure S2E-F in Szabó et al., 2009), which again fits the situation observed in shark. We believe this fact is also related with the thin -and maybe shifted- *ScOtp* expressing domain (see Figures 7C-D). Of note, *Pitx2* is expressed in the MM/RM in wild mice being dramatically dowregulated in mutants (see Figure 3K-L in Szabó et al., 2009). In sharks, the fact that *ScPitx2* is expressed in the RM-like and caudally beyond but not in the MM-like (Figure 7E-F), also could be correlated with a lack of Shh signaling.

These facts support the idea of changes in midline signaling centers/pathways as important driving forces in evolution (Retaux and Kano, 2010; Sugahara et al., 2011). Furthermore, these and other lines of evidence (see Kapsimali et al., 2004; Manning et al., 2006) suggest the existence of a conserved inverse relationship between *Shh* and *Emx2* that shapes the evolution of the vertebrate basal hypothalamus (see also below). Furthermore, we think that these data also support the significance of our *ScEmx2*-positive/negative domains and the existence of an alternative hypothetic PM/PRM/MM histogenetic domain in shark and other vertebrates (see below).

### 3.4.5 Alternative interpretation of the caudal border of the hypothalamus and secondary prosencephalon

The updated prosomeric model proposes the existence of two intersegmental boundaries affecting the hypothalamus and secondary prosencephalon (Puelles et al., 2012; Puelles and Rubenstein, 2015). The IHB separates segments of the secondary prosencephalon (hp2/hp1), while the HDB separates the secondary prosencephalon from the rostral-most segment of the caudal prosencephalon (hp1/p3). These boundaries have been defined according the observation of several expression patterns and other traits like the course of important tracts (Puelles et al., 2012; Puelles and Rubenstein, 2015). In chapter 1, we assumed these boundaries as plausible defining them on similar evidences. However, in this chapter we met evidences suggesting the existence of an important boundary that does not fit neither the IHB nor the HDB (present results). This fact make us to look for further evidences supporting -or not- our observations.

Boundaries have been described to display a reduction or delay in proliferation, which results in constrictions between bulges or segments (Larsen et al., 2001; Puelles and Rubenstein, 2003). Among other signs, boundaries can be detected by markers associated to cell cycle arrest (Candal, 2002; Baek et al., 2006) or by the absence of proliferation markers like PCNA (Candal et. al., 2005). We have analyzed PCNA-immunoreactivity in embryos at stage 31, which were chosen because the presence of discontinuities in ventricular

proliferation in the neuroepithelium. An area of reduced proliferation was detected at the level of the MM/RM-like boundary (arrowheads in Figures 3R-S) continuous along the PRM/RM-like boundary (arrowhead in Figure 3T). This PCNA-negative band coincides with the border between genes complementarily expressed in the MM-like/PRM-like and in the MM-like/RM-like domains (compare arrowheads in Figures 3D with N). Thus, this PCNA-negative band does not support neither the basal HDB nor the IHB but in turn could represent an alternative course of the basal HDB. Furthermore, strikingly, in the alar plate, this band is continuous with the zli (not shown), which separates genes continuously expressed in the alar hypothalamus and p3 from those expressed in the remaining prosencephalon (see chapter 1; see also Larsen et al., 2001; Lim and Golden, 2007; Martinez et al., 2012). Together, these facts suggest a complete reinterpretation of the HDB (alar/basal).

The review of the boundary concept in the literature (reviewed in Dahmann et al., 2011; Cavodeassi and Hourat, 2012; Kiecker and Larsen, 2012; see also Larsen et al., 2001, Puelles et al., 2012) suggests that, among others, boundaries share several features related to their development or function: i) they emerge between sharp domains of expression of transcription factors (likely selector genes); ii) at these points expression of signaling molecules is turned on, acting as local or secondary organizers; iii) they show slower proliferation and a delay or absence of neurogenesis; iv) they behave as lineage restriction boundaries; v) they display boundary receptor activity (cadherins, ephrins); and/or v) they are supported by the course of transverse tracts.

In the alar plate, these features are well known to be satisfied at the p3/p2 boundary (the zli) but not at the hp1/p3 (HDB) (Dahmann et al., 2011; Cavodeassi and Hourat, 2012; Kiecker and Larsen, 2012). In the basal plate, as discussed above, the course of prosomeric boundaries as defined by the updated prosomeric model does not necessarily match other boundary criteria. However, several lines of evidence suggest a continuation along the rostral border of the RM-like. **First**, the expression patterns of transcription factors in RM-like are markedly different from that found in Tu6/PM/MM/PRM-like in shark and other vertebrates. **Second**, a PCNA-negative band was observed in shark at this point (see above). **Third**, different signaling molecules like *Shh/HhB* and *Wnts* are expressed close to this boundary. *Shh/HhB* expression in basal vertebrates respect this boundary. However *Shh* upregulation in the *Nkx2.1*-expressing hypothalamus of tetrapods could mask this evidence. Besides**,** *Wnt* genes, which have been described in transverse bands of expression within rhombomeric boundaries (Riley et al., 2004), are also conserved and continuously expressed from the zli into the rostral basal plate apparently following the course of the rostral limit of RM, even among distant vertebrates (compare Figure 7A-C in Guerin et al., 2009 with 1J in Sugahara et al., 2011; see also Figure 3X in Quinlan et al., 2009; note that this nomenclature has not been used by these authors). Noteworthy these expression patterns almost spread from alar-to-basal plates apparently fulfilling the "complete" criteria of prosomeric boundaries (Puelles and Rubenstein, 2003; 2015; Puelles et al., 2012). **Fourth**, the distribution of different groups of boundary molecules, some of them overlapping with *Wnt8* expression also support this interpretation (see Figure 5 in Larsen et al., 2001; Figure 4B in García-Calero et al., 2006), as

they were described to course in the caudal limit of *Nkx2.1*-expression in the hypothalamic basal plate (García-Calero et al., 2006). **Fifth**, this boundary could also be supported by the transverse course of the mamillothalamic tract (Figdor and Stern, 1993) which has been described in different vertebrates including *S. canicula* (Ware et al., 2014; 2015). Together, all these evidences support a boundary coursing the alar/basal plates from the zli to the rostral border of RM-like rather than at hp1/p3 (HDB) or p3/2. Such boundary fairly fits with that described by Figdor and Stern (1993) among D1/D2 segments. This interpretation would include the alar p3 (besides prethalamic eminence) but exclude the RM-like from the secondary prosencephalon.

Such interpretative differences could be due to differences in *Shh* expression in the hypothalamus across vertebrates. In amniotes, *Shh* is fairly continuously expressed from the RM-like to the Tu-like (Puelles et al., 2012) blurring this boundary. These differences could also rely on how prosomeric model understands some boundaries. Although the model integrates different kind of data, implicitly it understands some boundaries as defined by a kind of combinatorial selector code, as it happens in rhombomeres. A combinatorial definition could have multiple interpretations which in part explain differences among updates (Puelles and Rubenstein, 1993; 2003; 2015; Puelles et al., 2012). However, other evidences support common rules acting in the field rostral to the zli (Larsen et al., 2001; Baek et al., 2006; reviewed in Beccari et al., 2014), which argue against the existence of certain hypothalamic boundaries. The expression of genes like *Dlx*, *Arx*, *Foxd1* (Shimogori et al., 2010) continuous through the alar hypothalamus and alar p3 also suggest this idea. Furthermore, in the basal plate, the logic of histogenetic domains (i.e. Tu/RTu; PM/PRM; MM/RM) and segmental boundaries also should imply the existence of markers commonly expressed between the MM/RM that instead define a sharp border with p3Tg. Such markers have not been described in the prosomeric model. In amniotes, genes expressed in the RM are frequently continuously expressed in the diencephalic basal plate. More rarely, some genes like *Pitx2*, *Neurog2* and *Shh* are also expressed in the MM. These markers do not reach the MM of basal vertebrates suggesting that rostralization is acquired through vertebrate evolution. This could be associated to differences in prechordal/notochordal signaling or their relative position among vertebrates, a source of variability that has not been considered.

#### 3.4.5.1 Other histogenetic landmarks

Our proposal as a HDB coursing from the zli through the rostral border of RM-like, indirectly argues against the existence of a HDB between the alar hypothalamus and the alar p3 8see above). The work of Szabó et al., (2009) with Shh mutant mice reveals interesting data in this regard. In spite of the loss of different p3 and PThE markers, *Lhx5* is still expressed in the PThE and alar hypothalamus (Szabó, et al., 2009). This fact suggests a compartmentation inside the secondary prosencephalon. Of note, this last evidence reinforce our previous observation on *Pax6* expression as an important histogenetic territory inside the secondary prosencephalon (Figure 9D; see also Figure 6B in chapter 2). The limits defined by *Pax6* are also respected by genes expressed inside this territory such as *Otp*, *Neurog2* and

*Tbr1* among others, and genes expressed in neighbor territories of the supallium and other alar hypothalamus subdivisions (Figure 9D; see also Figure 6B in chapter 2). This affirmation argues against the expression patterns of *Foxg1* as marker of the telencephalon and its function as an important player in telencephalic development (see chapter 1). Nevertheless, we think that more genes support the boundaries defined by Pax6 than the hypothalamo-telencephalic boundary defined by *Foxg1* (Figure 9D).

In contrast with that reported by Szabó et al., (2009), the mice mutants described by Shimogori et al. (2010) present a normal specification in the alar p3. The fact that the mutants described by Szabó et al. still express Shh in the preoptic area while those of Shimogori et al. do not, suggests that a right balance among rostro-dorsal and ventro-caudal Shh signaling is required for correct alar p3 development. We did reflect this trait in our alternative proposal since the phenotype shown by Szabó et al., (2009), but not that of Shimogori et al., (2010), resembles conserved traits observed in vertebrates: at least some Shh expression in the rostro-dorsal hypothalamus is present, either it belongs to the hypothalamus or to the preoptic area (see Figure 9E; see also below).

Furthermore, we think that these results, together with data observed in shark (present results), evidence an important area of Shh influence that extends from the preoptic area to the ventral-most Tu-like (Figure 9E). This limit would explain the reciprocal requirement of Shh for the development of the subpallium (Medina, 2008; Sugahara et al., 2011) and the development of the rostro-dorsal basal hypothalamus (Szabó et al., 2009). We think this influence of Shh could also explain rostro-caudal differences in the alar hypothalamus since Shh also controls the expression of genes like *Pax6* (Sugahara et al., 2011). Of note, this limit resembles the caudal limit of p6 of early prosomeric versions (Puelles and Rubenstein, 1993). However, this would not be a limit between segments.

Finally, concerning the IHB we think that rostro-caudal differences can be observed at least in the alar hypothalamus, although here we have not found more evidence than the course of the medial forebrain bundle (chapter 1), the distribution of Pax6-ir cells in the basal hypothalamous (chapter 2) and the lack of Shh in the RTu-like (chapter 1; present results). Thus, the existence of an intersegmental boundary defined as a combinatorial code, as other prosomeric boundaries, seems plausible. However, the existence of intersegmental limit supported by other boundary properties seems less plausible in the secondary prosencephalon. Our present data do not support such interpretation. Nevertheless, this assumption has to be taken with care. We were able to identify PCNA-negative band that could fit with the IHB in the alar hypothalamus (and in the subpallial midline). However, we fail to follow it in the basal plate and/or to be supported by other defining traits of boundaries.

## 3.5. CONCLUSION

In the present work we test our previous analysis on the prosomeric organization of the basal hypothalamus (see chapter 1) of the shark by further analyzing other markers. These data suggest that the basal hypothalamus organized in three main histogenetic domains mainly

based in the expression or lack of *ScEmx2* or the richness or not of 5-HT-immunoreactivity. Such analysis do not support our previous segmental organization for the shark basal hypothalamus according to the updated prosomeric model (see chapter 1). Furthermore, a comparison with orthologue markers expressed in the basal hypothalamus of the mouse suggests that although the expression patters are conserved define different histogenetic domains among vertebrates. Moreover, our comparative analysis suggest that the three domains defined in shark are likely observed in other vertebrates. Finally, the expression of *ScOtp*, *ScLhx5* and *ScEmx2* in the *ScNkx2.1*-positive hypothalamus define a clear-cut border with *ScLmx1b*, *ScPitx2*, *ScPitx3a*, *ScFoxa1*, *ScFoxa2*, *ScNeurog2*, which are expressed in the RM-like and diencephalic basal plate. This fact, do not support the HDB. Negative PCNA-immunoreactivity observed through the rostral border of RM-like and zli suggest an alternative interpretation of the caudal boundary of the hypothalamus also affecting the whole secondary prosencephalon. Different lines of evidence support such alternative interpretation.

## References


Abellán, A., Vernier, B., Rétaux, S., and Medina, L. (2010). Similarities and differences in the forebrain expression of Lhx1 and Lhx5 between chicken and mouse: Insights for understanding telencephalic development and evolution. *J. Comp. Neurol.* 518, 3512–28

Álvarez-Bolado, G., Paul, F. A., and Blaess, S. (2012). Sonic hedgehog lineage in the mouse hypothalamus: from progenitor domains to hypothalamic regions. *Neural Dev.* 7, 4.

Anderson, S., Mione, M., Yun, K., and Rubenstein, J. L. (1999). Differential origins of neocortical projection and local circuit neurons: role of Dlx genes in neocortical interneuronogenesis. *Cereb. Cortex* 9, 646–54

Asbreuk, C. H. J., Vogelaar, C. F., Hellemons, A., Smidt, M. P., and Burbach, J. P. H. (2002). CNS expression pattern of Lmx1b and coexpression with ptx genes suggest functional cooperativity in the development of forebrain motor control systems. *Mol. Cell. Neurosci.* 21, 410–20.

Bachy, I., Vernier, P., and Retaux, S. (2001). The LIM-homeodomain gene family in the developing *Xenopus* brain: conservation and divergences with the mouse related to the evolution of the forebrain. *J. Neurosci.* 21, 7620–9.

Baek, J. H., Hatakeyama, J., Sakamoto, S., Ohtsuka, T., and Kageyama, R. (2006). Persistent and high levels of Hes1 expression regulate boundary formation in the developing central nervous system. *Development* 133, 2467–76.

Ballard, W. W., Mellinger, J., and Lechenault, H. (1993). A series of normal stages for development of *Scyliorhinus canicula*, the lesser spotted dogfish (*Chondrichthyes*: *Scyliorhinidae*). *J. Exp. Zool.* 267, 318–36.

Bardet, S. M., Ferrán, J. L. E., Sanchez-Arrones, L., and Puelles, L. (2010). Ontogenetic expression of sonic hedgehog in the chicken subpallium. *Front. Neuroanat.* 4.

Bardet, S. M., Martinez-de-la-Torre, M., Northcutt, R. G., Rubenstein, J. L. R., and Puelles, L. (2008). Conserved pattern of OTP-positive cells in the paraventricular nucleus and other hypothalamic sites of tetrapods. *Brain Res. Bull.* 75, 231–5.

Beccari, L., Marco-Ferreres, R., and Bovolenta, P. (2013). The logic of gene regulatory networks in early vertebrate forebrain patterning. *Mech. Dev.* 130, 95–111.

Blaess, S., Szabó, N., Haddad-Tóvolli, R., Zhou, X., and Álvarez-Bolado, G. (2014). Sonic hedgehog signaling in the development of the mouse hypothalamus. *Front. Neuroanat.* 8, 156.

Barth, K. a, and Wilson, S. W. (1995). Expression of zebrafish nk2.2 is influenced by sonic hedgehog/vertebrate hedgehog-1 and demarcates a zone of neuronal differentiation in the embryonic forebrain. *Development* 121, 1755–68.

Butler, A. B., and Hodos, W. (2005). "The visceral brain: the hypothalamus and the autonomic nervous system," in *Comparative Vertebrate Neuroanatomy: Evolution and Adaptation*, eds A. B. Butler and W. Hodos (Hoboken, NJ: John Wiley & Sons), 445–67.

Candal, E., Anadón, R., Bourrat, F., and Rodríguez-Moldes, I. (2005). Cell proliferation in the developing and adult hindbrain and midbrain of trout and medaka (teleosts): a segmental approach. *Brain Res. Dev. Brain Res.* 160, 157–75.

Carrera, I., Anadón, R., and Rodríguez-Moldes, I. (2012). Development of tyrosine hydroxylase-immunoreactive cell populations and fiber pathways in the brain of the dogfish *Scyliorhinus canicula*: new perspectives on the evolution of the vertebrate catecholaminergic system. *J. Comp. Neurol.* 520, 3574–603.

Carrera, I., Ferreiro-Galve, S., Sueiro, C., Anadón, R., and Rodríguez-Moldes, I. (2008). Tangentially migrating GABAergic cells of subpallial origin invade massively the pallium in developing sharks. *Brain Res. Bull.* 75, 405–9.

Compagnucci, C., Debiais-Thibaud, M., Coolen, M., Fish, J., Griffin, J. N., Bertocchini, D., et al. (2013). Pattern and polarity in the development and evolution of the gnathostome jaw: both conservation and heterotopy in the branchial arches of the shark, *Scyliorhinus canicula*. *Dev. Biol.* 377, 428–48.

Coolen, M., Menuet, A., Chassoux, D., Compagnucci, C., Henry, S., Lévèque, L., et al. (2009). "The dogfish *Scyliorhinus canicula*, a reference in jawed vertebrates," in *Emerging Model Organisms. A Laboratory Manual*, eds R. R. Behringer, A. D. Johnson, and R. E. Rrumlauf (Cold Spring Harbor, NY: Cold Spring Harbor Laboratory Press), 431–46.

Croizier, S., Chometton, S., Fellmann, D., and Risold, P. (2015). Characterization of a mammalian prosencephalic functional plan. 8, 1–13.

Dahmann, C., Oates, A. C., and Brand, M. (2011). Boundary formation and maintenance in tissue development. *Nat. Rev. Genet.* 12, 43–55.

Debiais-Thibaud, M., Metcalfe, C. J., Pollack, J., Germon, I., Ekker, M., Depew, M., et al. (2013). Heterogeneous conservation of Dlx paralog co-expression in jawed vertebrates. *PLoS One* 8, e68182.

Del Giacco, L., Pistocchi, A., Cotelli, F., Fortunato, A. E., and Sordino, P. (2008). A peek inside the neurosecretory brain through Orthopedia lenses. *Dev. Dyn.* 237, 2295–303.

Derobert, Y., Plouhinec, J. L., Sauka-Spengler, T., Le Mentec, C., Baratte, B., Jaillard, D., et al. (2002). Structure and expression of three Emx genes in the dogfish *Scyliorhinus canicula*: functional and evolutionary implications. *Developmental Biology*, *247*(2), 390–404.

Diez-Roux, G., Banfi, S., Sultan, M., Geffers, L., Anand, S., Rozado, D., Magen, A., Canidio, E., Pagani, M., Peluso, I., et al. (2011). A high-resolution anatomical atlas of the transcriptome in the mouse embryo. *PLoS Biol.* 9, e1000582.

Domínguez, L., González, A., and Moreno, N. (2010). Sonic hedgehog expression during *Xenopus* laevis forebrain development. *Brain Res.* 1347, 19–32.

Domínguez, L., González, A., and Moreno, N. (2014). Characterization of the hypothalamus of *Xenopus laevis* during development. II. The basal regions. *J. Comp. Neurol.* 522, 1102–31.

Domínguez, L., González, A., and Moreno, N. (2015). Patterns of hypothalamic regionalization in amphibians and reptiles: common traits revealed by a genoarchitectonic approach. *Front. Neuroanat.* 9, 3.

Domínguez, L., Morona, R., González, A., and Moreno, N. (2013). Characterization of the hypothalamus of *Xenopus laevis* during development. I. The alar regions. *J. Comp. Neurol.* 521, 725–59.

Ferrando S., Gallus L., Gambardella C., Ghigliotti L., Ravera S., Vallarino M., et al. (2010) Cell proliferation and apoptosis in the olfactory epithelium of the shark *Scyliorhinus canicula*. J Chem Neuroanat 40:293–300

Ferrán, J. L., Puelles, L., and Rubenstein, J. L. R. (2015). Molecular codes defining rostrocaudal domains in the embryonic mouse hypothalamus. *Front. Neuroanat.* 9.

Ferreiro-Galve, S., Rodríguez-Moldes, I., Anadón, R., and Candal, E. (2010). Patterns of cell proliferation and rod photoreceptor differentiation in shark retinas. *J. Chem. Neuroanat.* 39, 1–14.

Ferreiro-Galve, S., Carrera, I., Candal, E., Villar-Cheda, B., Anadón, R., Mazan, S., et al. (2008). The segmental organization of the developing shark brain based on neurochemical markers, with special attention to the prosencephalon. *Brain Res. Bull.* 75, 236–40.

Figdor, M. C., and Stern, C. D. (1993). Segmental organization of embryonic diencephalon. *Nature* 363, 630–34.

Filippi, A., Dürr, K., Ryu, S., Willaredt, M., Holzschuh, J., and Driever, W. (2007). Expression and function of nr4a2, lmx1b, and pitx3 in zebrafish dopaminergic and noradrenergic neuronal development.

Filippi, A., Jainok, C., and Driever, W. (2012). Analysis of transcriptional codes for zebrafish dopaminergic neurons reveals essential functions of Arx and Isl1 in prethalamic dopaminergic neuron development. *Dev. Biol.* 369, 133–149.

García-Calero, E., de Puelles, E., and Puelles, L. (2006). EphA7 receptor is expressed differentially at chicken prosomeric boundaries. *Neuroscience* 141, 1887–97.

García-Calero, E., Fernández-Garre, P., Martínez, S., & Puelles, L. (2008). Early mammillary pouch specification in the course of prechordal ventralization of the forebrain tegmentum. *Developmental Biology*, *320*(2), 366–77.

Guérin, A., d'Aubenton-Carafa, Y., Marrakchi, E., Da Silva, C., Wincker, P., Mazan, S., et al. (2009). Neurodevelopment genes in lampreys reveal trends for forebrain evolution in craniates. *PLoS One* 4, e5374.

Hauptmann, G., and Gerster, T. (2000). Regulatory gene expression patterns reveal transverse and longitudinal subdivisions of the embryonic zebrafish forebrain. *Mech. Dev.* 91, 105–118.

Jeong, J.-Y., Einhorn, Z., Mercurio, S., Lee, S., Lau, B., Mione, M., et al. (2006). Neurogenin1 is a determinant of zebrafish basal forebrain dopaminergic neurons and is regulated by the conserved zinc finger protein Tof/Fezl. *Proc. Natl. Acad. Sci. U. S. A.* 103, 5143–5148.

Kandel, E., and Schwartz, J. (2001).“Sistema nervioso autónomo e hipotálamo,”in *Principios de Neurociencia*, eds E. R. Kandel, J. H. Schwartz, and T. M. Jessell (Aravaca: McGraw-Hill Interamericana), 960–81.

Kano, S., Xiao, J.-H., Osório, J., Ekker, M., Hadzhiev, Y., Müller, F., et al. (2010). Two lamprey Hedgehog genes share non-coding regulatory sequences and expression patterns with gnathostome Hedgehogs. *PLoS One* 5, e13332.

Kapsimali, M., Caneparo, L., Houart, C., & Wilson, S. W. (2004). Inhibition of Wnt/Axin/beta-catenin pathway activity promotes ventral CNS midline tissue to adopt hypothalamic rather than floorplate identity. *Development (Cambridge, England)*, *131*(23), 5923–33.

Kiecker, C., and Lumsden, A. (2012). The role of organizers in patterning the nervous system. *Annu. Rev. Neurosci.* 35, 347–67. doi:10.1146/annurev-neuro-062111-150543.

Kuratani, S., and Horigome, N. (2000). Developmental morphology of branchiomeric nerves in a cat shark, *Scyliorhinus torazame*, with special reference to rhombomeres, cephalic mesoderm, and distribution patterns of cephalic crest cells. *Zoolog. Sci.* 17, 893–909.

Lagadec, R., Laguerre, L., Menuet, A., Amara, A., Rocancourt, C., Péricard, P., et al. (2015). The ancestral role of nodal signalling in breaking L/R symmetry in the vertebrate forebrain. *Nature Communications*, *6*, 6686.

Larsen, C. W., Zeltser, L. M., and Lumsden, A. (2001). Boundary formation and compartition in the avian diencephalon. *J. Neurosci.* 21, 4699–711.

Lauter, G., Söll, I., and Hauptmann, G. (2013). Molecular characterization of prosomeric and intraprosomeric subdivisions of the embryonic zebrafish diencephalon. *J. Comp. Neurol.* 521, 1093–1118.

Lee, J. E., Wu, S.-F., Goering, L. M., & Dorsky, R. I. (2006). Canonical Wnt signaling through Lef1 is required for hypothalamic neurogenesis. *Development*, *133*(22), 4451–4461.

Manning, L., Ohyama, K., Saeger, B., Hatano, O., Wilson, S. A., Logan, M., and Placzek, M. (2006). Regional morphogenesis in the hypothalamus: a BMP-Tbx2 pathway coordinates fate and proliferation through Shh downregulation. *Dev. Cell* 11, 873–85.

Manoli, M., Driever, W., and Scholpp, S. (2014). during development of the zebrafish hypothalamus , preoptic region , and pallidum. 8, 1–16.

Martin, D. M., Skidmore, J. M., Philips, S. T., Vieira, C., Gage, P. J., Condie, B. G., Raphael, Y., Martinez, S., and Camper, S. A. (2004). PITX2 is required for normal development of neurons in the mouse subthalamic nucleus and midbrain. *Dev. Biol.* 267, 93–108.

Martinez-Ferre, A., and Martinez, S. (2012). Molecular regionalization of the diencephalon. *Front. Neurosci.* 6, 73. doi:10.3389/fnins.2012.00073.

Martínez-de-la-Torre, M., Pombal, M. A., and Puelles, L. (2011). Distal-less-like protein distribution in the larval lamprey forebrain. *Neuroscience* 178, 270–84.

Mathieu, J., Barth, A., Rosa, F. M., Wilson, S. W., and Peyriéras, N. (2002). Distinct and cooperative roles for Nodal and Hedgehog signals during hypothalamic development. *Development* 129, 3055–65.

Medina, L. (2008). "Evolution and embryological development of the forebrain," in *Encyclopedia of Neuroscience*, eds M. D. Binder, N. Hirokawa, and U. Windhorst (Berlin: Springer-Verlag), 1172–92.

Medina, L., Bupesh, M., and Abellán, A. (2011). Contribution of genoarchitecture to understanding forebrain evolution and development, with particular emphasis on the amygdala. *Brain. Behav. Evol.* 78, 216–36.

Morales-Delgado, N., Merchán, P., Bardet, S. M., Ferrán, J. L., Puelles, L., and Díaz, C. (2011). Topography of Somatostatin Gene Expression Relative to Molecular Progenitor Domains during Ontogeny of the Mouse Hypothalamus. *Front. Neuroanat.* 5, 10

Morales-Delgado, N., Castro-Robles, B., Ferrán, J. L., Martinez-de-la-Torre, M., Puelles, L., and Díaz, C. (2014). Regionalized differentiation of CRH, TRH, and GHRH peptidergic neurons in the mouse hypothalamus. *Brain Struct. Funct.* 219, 1083–111.

Moreno, N., Domínguez, L., Morona, R., and González, A. (2012). Subdivisions of the turtle *Pseudemys scripta* hypothalamus based on the expression of regulatory genes and neuronal markers. *J. Comp. Neurol.* 520, 453–78.

Murakami, Y., Ogasawara, M., Sugahara, F., Hirano, S., Satoh, N., and Kuratani, S. (2001). Identification and expression of the lamprey Pax6 gene: evolutionary origin of the segmented brain of vertebrates. *Development* 128, 3521–31.

Myojin, M., Ueki, T., Sugahara, F., Murakami, Y., Shigetani, Y., Aizawa, S., et al. (2001). Isolation of Dlx and Emx gene cognates in an agnathan species, *Lampetra japonica*, and their expression patterns during embryonic and larval development: Conserved and diversified regulatory patterns of homeobox genes in vertebrate head evolution. *J. Exp. Zool.* 291, 68–84.

Ogasawara, M., Shigetani, Y., Suzuki, S., Kuratani, S., and Satoh, N. (2001). Expression of thyroid transcription factor-1 (TTF-1) gene in the ventral forebrain and endostyle of the agnathan vertebrate, *Lampetra japonica*. *Genesis* 30, 51–8.

Osório, J., Mazan, S., and Rétaux, S. (2005). Organisation of the lamprey (*Lampetra fluviatilis*) embryonic brain: insights from LIM-homeodomain, Pax and hedgehog genes. *Dev. Biol.* 288, 100–12.

Osório, J., Megías, M., Pombal, M. A., and Rétaux, S. (2006). Dynamic expression of the LIM-homeodomain gene Lhx15 through larval brain development of the sea lamprey (*Petromyzon marinus*). *Gene Expr. Patterns* 6, 873–8.

Osório, J., Mueller, T., Rétaux, S., Vernier, P., and Wullimann, M. F. (2010). Phylotypic expression of the bHLH genes Neurogenin2, NeuroD, and Mash1 in the mouse embryonic forebrain. *J. Comp. Neurol.* 518, 851–71.

Pombal, M. A., Megías, M., Bardet, S. M., & Puelles, L. (2009). New and old thoughts on the segmental organization of the forebrain in lampreys. *Brain, Behavior and Evolution*, *74*(1), 7–19.

Pose-Méndez, S., Candal, E., Adrio, F., and Rodríguez-Moldes, I. (2014). Development of the cerebellar afferent system in the shark *Scyliorhinus canicula*: insights into the basal organization of precerebellar nuclei in gnathostomes. *J. Comp. Neurol.* 522, 131–68.

Pose-Méndez, S., Candal, E., Mazan, S., and Rodríguez-Moldes, I. (2015). Genoarchitecture of the rostral hindbrain of a shark: basis for understanding the emergence of the cerebellum at the agnathan-gnathostome transition. *Brain Struct. Funct.* Jan 1 [Epub ahead of print]

Puelles, L., Martínez, S., Martínez-de-la-Torre, M. S.,and Rubenstein, J. (2012). "Hypothalamus," in *The Mouse Nervous System*, eds C. Watson, G. Paxinos, and L. Puelles (San Diego, CA: Academic Press), 221–312.

Puelles, L., Martínez, S., Martínez-de-la-Torre, M., and Rubenstein, J. (2004). "Gene maps and related histogenetic domains in the forebrain and midbrain," in *The Rat Nervous System*, ed. G. Paxinos (San Diego, CA: Academic Press), 3–25.

Puelles, L. (2009). "Forebrain development: prosomere model," in *Developmental Neurobiology*, ed. G. Lemke (London; Burlington, MA; SanDiego, CA: Academic Press), 315–19.

Puelles, L., and Medina, L. (2002). Field homology as a way to reconcile genetic and developmental variability with adult homology. *Brain Res. Bull.* 57, 243–55.

Puelles, L., and Rubenstein, J.L.R. (1993) Expression patterns of homeobox and other putative regulatory genes in the embryonic mouse forebrain suggest a neuromeric organization. *Trends Neurosci*. 16, 472-79.

Puelles, L., and Rubenstein, J. L. R. (2003). Forebrain gene expression domains and the evolving prosomeric model. *Trends Neurosci.* 26, 469–76.

Puelles, L., and Rubenstein, J. L. R. (2015). A new scenario of hypothalamic organization: rationale of new hypotheses introduced in the updated prosomeric model. *Front. Neuroanat.* 9.

Quinlan, R., Graf, M., Mason, I., Lumsden, A., and Kiecker, C. (2009). Complex and dynamic patterns of Wnt pathway gene expression in the developing chick forebrain. *Neural Dev.* 4, 35.

Quintana-Urzainqui, I. (2013). *Development and regionalization of the telencephalon and peripheral associated systems in the shark Scyliorhinus canicula*. Ph. D. thesis, Universidad de Santiago de Compostela, Compostela.

Quintana-Urzainqui, I., Rodríguez-Moldes, I., and Candal, E. (2014a). Developmental, tract-tracing and immunohistochemical study of the peripheral olfactory system in a basal vertebrate: insights on Pax6 neurons migrating along the olfactory nerve. *Brain Struct. Funct.* 219, 85–104.

Quintana-Urzainqui, I., Rodríguez-Moldes, I., Mazan, S., & Candal, E. (2014b). Tangential migratory pathways of subpallial origin in the embryonic telencephalon of sharks: evolutionary implications. *Brain Structure and Function*.

Quintana-Urzainqui, I., Sueiro, C., Carrera, I., Ferreiro-Galve, S., Santos-Durán, G., Pose-Méndez, S., et al. (2012a). Contributions of developmental studies in the dogfish *Scyliorhinus canicula* to the brain anatomy of elasmobranchs: insights on the basal ganglia. *Brain. Behav. Evol.* 80, 127–41.

Quintana-Urzainqui I, Rodrı´guez-Moldes I, Candal E (2012b) Developmental, tract-tracing and immunohistochemical study of the peripheral olfactory system in a basal vertebrate: insights on Pax6 neurons migrating along the olfactory nerve. Brain Struct Funct.

Rétaux, S., and Kano, S. (2010). Midline signaling and evolution of the forebrain in chordates: a focus on the lamprey Hedgehog case. *Integr. Comp. Biol.* 50, 98–109.

Riley, B. B., Chiang, M.-Y., Storch, E. M., Heck, R., Buckles, G. R., and Lekven, A. C. (2004). Rhombomere boundaries are Wnt signaling centers that regulate metameric patterning in the zebrafish hindbrain. *Dev. Dyn.* 231, 278–91.

Rodríguez-Moldes I., Ferreiro-Galve S., Carrera I., Sueiro C., Candal E., Mazan S., et al. (2008) Development of the cerebellar body in sharks: spatiotemporal relations of Pax6 expression, cell proliferation and differentiation. *Neurosci Lett* 432:105–110

Rodríguez-Moldes, I., Timmermans, J. P., Adriaensen, D., De Groodt-Lasseel, M. H., Scheuermann, D. W., and Anadon, R. (1990). Immunohistochemical localization of calbindin-D28K in the brain of a cartilaginous fish, the dogfish (*Scyliorhinus canicula L.*). *Acta Anat. (Basel).* 137, 293–302.

Ryu, S., Mahler, J., Acampora, D., Holzschuh, J., Erhardt, S., Omodei, D., et al. (2007). Orthopedia homeodomain protein is essential for diencephalic dopaminergic neuron development. *Curr. Biol.* 17, 873–80.

Sarnat, H. B., and Netsky, M. G. (1981). "Epithalamus and hypothalamus, "in *Evolution of the Nervous System*, eds H. B. Sarnat and M. G. Netsky (Newyork, NY; Oxford: Oxford University Press), 296–320.

Sheng, H. Z., Bertuzzi, S., Chiang, C., Shawlot, W., Taira, M., Dawid, I., et al. (1997). Expression of murine Lhx5 suggests a role in specifying the forebrain. *Dev. Dyn.* 208, 266–277.

Shimamura, K., Hartigan, D. J., Martinez, S., Puelles, L., and Rubenstein, J. L. (1995). Longitudinal organization of the anterior neural plate and neural tube. *Development* 121, 3923–33.

Shimogori, T., Lee, D. A., Miranda-Angulo, A., Yang, Y., Wang, H., Jiang, L., et al. (2010). A genomic atlas of mouse hypothalamic development. *Nat. Neurosci.* 13, 767–75.

Simerly, R. B. (2004). "Anatomical Substrates of Hypothalamic Integration," in *The Rat Nervous System*, ed. G. Paxinos (San Diego, CA: Academic Press), 336–51.

Suda, Y., Hossain, Z. M., Kobayashi, C., Hatano, O., Yoshida, M., Matsuo, I., et al. (2001). Emx2 directs the development of diencephalon in cooperation with Otx2. *Development* 128, 2433–50.

Sueiro, C., Carrera, I., Ferreiro, S., Molist, P., Adrio, F., Anadón, R., and Rodríguez-Moldes, I. (2007). New insights on Saccus vasculosus evolution: a developmental and immunohistochemical study in elasmobranchs. *Brain. Behav. Evol.* 70, 187-204.

Sugahara, F., Aota, S., Kuraku, S., Murakami, Y., Takio-Ogawa, Y., Hirano, S., et al. (2011). Involvement of Hedgehog and FGF signalling in the lamprey telencephalon: evolution of regionalization and dorsoventral patterning of the vertebrate forebrain. *Development* 138, 1217–26.

Sylvester, J. B., Rich, C. A., Loh, Y.-H. E., van Staaden, M. J., Fraser, G. J., and Streelman, J. T. (2010). Brain diversity evolves via differences in patterning. *Proc. Natl. Acad. Sci. U. S. A.* 107, 9718–23.

Szabó, N.-E., Zhao, T., Cankaya, M., Theil, T., Zhou, X., and Alvarez-Bolado, G. (2009). Role of neuroepithelial Sonic hedgehog in hypothalamic patterning. *J. Neurosci.* 29, 6989–7002.

Tornehave, D., Hougaard, D. M., and Larsson, L. (2000). Microwaving for double indirect immunofluorescence with primary antibodies from the same species and for staining of mouse tissues with mouse monoclonal antibodies. *Histochem. Cell Biol.* 113, 19–23.

Uchida, K., Murakami, Y., Kuraku, S., Hirano, S., and Kuratani, S. (2003). Development of the adenohypophysis in the lamprey: evolution of epigenetic patterning programs in organogenesis. *J. Exp. Zool. B. Mol. Dev. Evol.* 300, 32–47.

Van den Akker, W. M. R., Brox, A., Puelles, L., Durston, A. J., and Medina, L. (2008). Comparative functional analysis provides evidence for a crucial role for the homeobox gene Nkx2.1/Titf-1 in forebrain evolution. *J. Comp. Neurol.* 506, 211–23.

Van de Kamer, J. C., and Shuurmans, A. J. (1953). Development and structure of the saccus vasculosus of *Scylliorhinus caniculus* (L.). *J. Embryol. Exp. Morphol*. 1, 85-96.

Vernier, P., and Wullimann, M. (2008). "Evolution of the posterior tuberculum and preglomerular nuclear complex," in *Encyclopedia of Neuroscience,* eds M. D. Binder, N. Hirokawa, and U. Windhorst (Berlin: Springer-Verlag), 1404–16.

Vieira, C., Garda, A.-L., Shimamura, K., and Martinez, S. (2005). Thalamic development induced by Shh in the chick embryo. *Dev. Biol.* 284, 351–63.

Ware, M., Dupé, V., and Schubert, F. R. (2015). Evolutionary Conservation of the Early Axon Scaffold in the Vertebrate Brain. *Dev. Dyn.*

Ware, M., Waring, C. P., and Schubert, F. R. (2014). Development of the Early Axon Scaffold in the Rostral Brain of the Small Spotted Cat Shark ( *Scyliorhinus canicula* ) Embryo. *Int. Sch. Res. Not.* 2014, 1–8.

Wasowicz M., Ward R., Repérant J. (1999). An investigation of astroglial morphology in Torpedoand Scyliorhinus. J Neurocytol 28:639-653

Wolf, A., and Ryu, S. (2013). Specification of posterior hypothalamic neurons requires coordinated activities of Fezf2, Otp, Sim1a and Foxb1.2. *Development* 140, 1762–73.

Wullimann, M. F., Rink, E., Vernier, P., and Schlosser, G. (2005). Secondary neurogenesis in the brain of the African clawed frog, *Xenopus laevis*, as revealed by PCNA, Delta-1, Neurogenin-related-1, and NeuroD expression. *J. Comp. Neurol.* 489, 387–402.

Yang, N., Dong, Z., and Guo, S. (2012). Fezf2 Regulates Multilineage Neuronal Differentiation through Activating Basic Helix-Loop-Helix and Homeodomain Genes in the Zebrafish Ventral Forebrain. *J. Neurosci.* 32, 10940–10948.

**Abbreviation list**

| | |
|---|---|
| ABB | alar-basal boundary |
| ABBr | alar-basal border |
| Ah | adenohypophysis |
| AHy | alar hypothalamus |
| ap3 | prosomere 3, alar part |
| BAt | basal acroterminal subdomain |
| hp1 | prosomere hp1 or peduncular |
| hp2 | prosomere hp2 or terminal |
| IHB | intrahypothalamic boundary |
| MM | mamillary area |
| Nh | neurohypophysis |
| Nt | notochord |
| OB | olfactory bulbs |
| P | pallium |
| p3Tg | prosomere 3, tegmental part |
| Pa | paraventricular area |
| PM | perimamillar area |
| PRM | periretromamillar area |
| PSPa | subparaventricular area, peduncular part |
| PThE | prethalamic eminence (ap3) |
| RM | retromamillary area |
| RTu | retrotuberal area |
| Sp | subpallium |
| SPa | subparaventricular area |
| Sv | saccuss vasculosus |
| TPa | paraventricular area, terminal part |
| TSPa | subparaventricular area, terminal part |
| Tu | tuberal area |
| zli | zona limitans intrathalamica |

**Figure 1.** Regionalization of the basal hypothalamus and neighbor territories in embryos of *S. canicula* at stages 29-31 based on the immunoreactivity to Shh **(A-D),** and expression of *ScNkx2.1* **(E-H),** *ScOtp* **(I-L)**, ScNkx2.8 **(J´),** *ScDlx2/5* **(M-P)** and *ScLhx5* (**Q-T**) by means of immunohistochemistry **(A-D),** and *in situ* hybridization **(H-J, L, M, P, Q, S, T)** on sagittal **(A, D, E, H, I, L, M, P, Q, R, T)** or transverse **(B, C, F, G, I´, J, J´, K, N, O, S)** sections. Some *in situ* sections were double labeled for immunohistochemistry against Shh **(E-G, K, N, O, R)**. **(A-D)** Shh-immunoreactivity in the Tu and RM. Note also the continuity of labeling along the p3Tg and the zli. Black arrowhead in B points the lack of labeling in the acroterminal region. Arrowhead in C marks the absence of Shh-immunoreactivity in the ventral-most portion of RM. Arrowheads in D show weak Shh-immunoreactivity in RM, p3Tg and zli at stage 30. **(E-H)** *ScNkx2.1* expression in the different territories of the basal hypothalamus excepting the RM. Black arrowhead in F points the acroterminal region showing *ScNkx2.1* expression and absence of Shh-immunoreactivity. Arrows point different distribution of Shh-immunoreactivity and *ScNkx2.1* expression. Arrowheads in G and H point *ScNkx2.1*-expressing cells in the RM mantle. Arrow in G point points dorsal-most distribution of Shh-immunoreactivity. (**I-L**) *ScOtp* expression in regions of the Tu-like and PM/PRM-like domains. Arrowhead in I shows the expression of *ScOtp* in the MM abutting the negative RM. Arrowhead in J points the restricted *ScOtp* expression in the midline of the acroterminal region. Arrowheads in I, K and L indicate *ScOtp*-expressing cells in the mantle of RM region that lacks Shh-immunoreactivity. (**M-P**) *ScDlx2/5* expression in restricted regions of the Tu/RTu-like. Note also intense labeling in ap3. Arrowheads in M, O and P indicate dispersed *ScDlx2/5*-expressing cells in the caudo-ventral part of Tu-like. Arrowhead in N marks the acroterminal region lacking *ScDlx2/5* expression (and Shh immunoreactivity). (**Q-T**) *ScLhx5* expression in the Tu-like, PM/PRM-like and MM-like domains. Arrowhead in S points *ScLhx5*-expressing cells in the mantle of the RM-like domain. For abbreviations, see list.

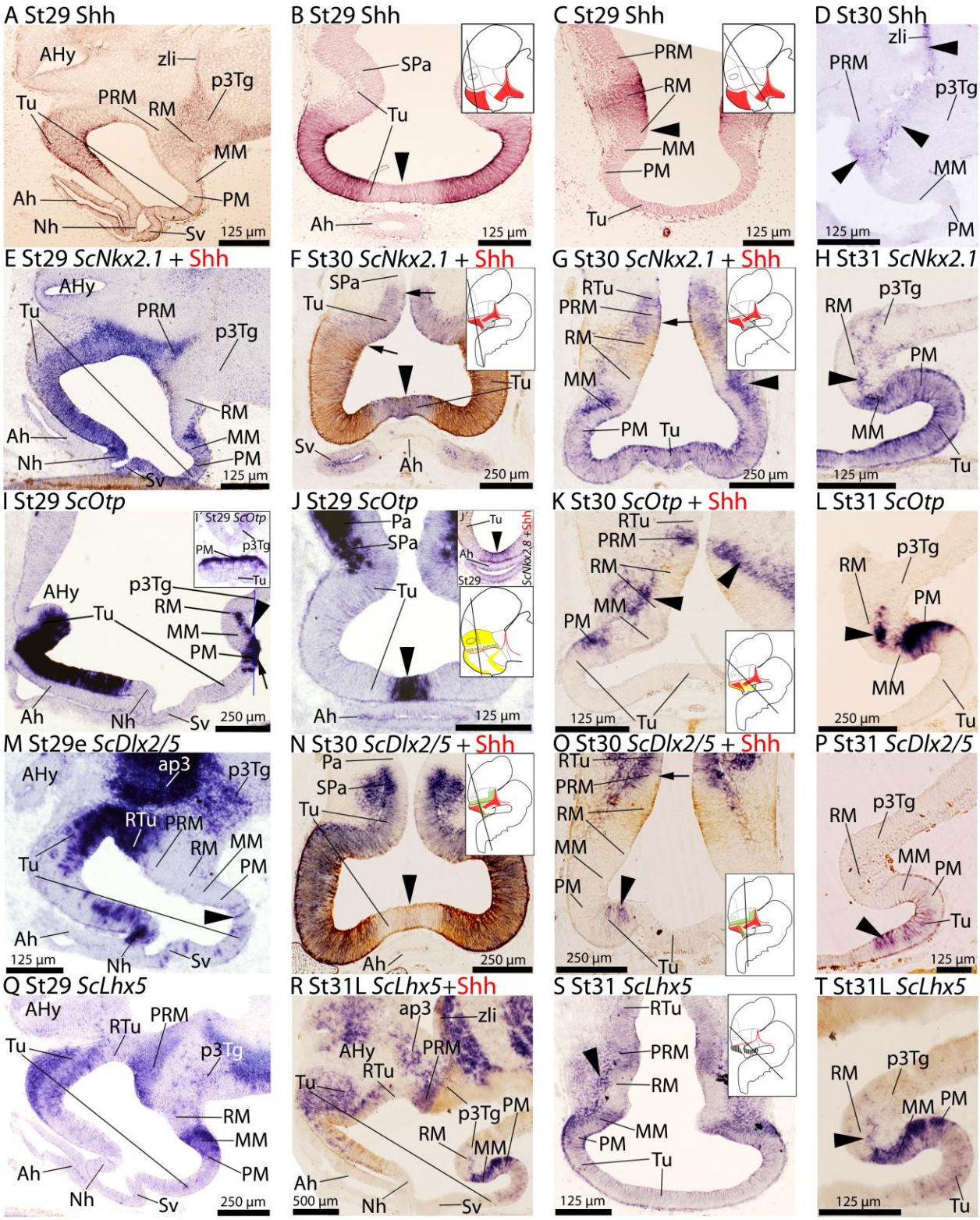
A St29 Shh
AHy
zli
p3Tg
Tu
PRM
RM
MM
Ah
PM
Nh
Sv
125 µm
B St29 Shh
SPa
Tu
Ah
125 µm
C St29 Shh
PRM
RM
MM
PM
Tu
125 µm
D St30 Shh
zli
PRM
p3Tg
MM
125 µm
PM
E St29 ScNkx2.1 + Shh
AHy
Tu
PRM
p3Tg
RM
Ah
MM
Nh
PM
Sv
125 µm
F St30 ScNkx2.1 + Shh
SPa
Tu
Tu
Sv
Ah
250 µm
G St30 ScNkx2.1 + Shh
RTu
PRM
RM
MM
PM
Tu
250 µm
H St31 ScNkx2.1
p3Tg
RM
PM
MM
125 µm
Tu
I St29 ScOtp
I' St29 ScOtp
PM
p3Tg
Tu
AHy
Tu
p3Tg
RM
MM
PM
Ah
Nh
Sv
250 µm
J St29 ScOtp
Pa
SPa
Tu
J'
Tu
Ah
ScNkx2.8 +Shh
St29
Ah
125 µm
K St30 ScOtp + Shh
RTu
PRM
RM
MM
PM
125 µm
Tu
L St31 ScOtp
p3Tg
RM
PM
MM
250 µm
Tu
M St29e ScDlx2/5
AHy
ap3
p3Tg
RTu
PRM
RM
MM
Tu
PM
Ah
125 µm
Nh
Sv
N St30 ScDlx2/5 + Shh
Pa
SPa
Tu
Ah
250 µm
O St30 ScDlx2/5 + Shh
RTu
PRM
RM
MM
PM
250 µm
Tu
P St31 ScDlx2/5
RM
p3Tg
MM
PM
Tu
125 µm
Q St29 ScLhx5
AHy
RTu
PRM
Tu
p3Tg
RM
MM
Ah
PM
Nh
Sv
250 µm
R St31L ScLhx5+Shh
ap3
zli
AHy
PRM
RTu
Tu
p3Tg
PM
RM
MM
Ah
500 µm
Nh
Sv
S St31 ScLhx5
RTu
PRM
RM
MM
PM
Tu
125 µm
T St31L ScLhx5
RM
p3Tg
MM
PM
125 µm
Tu

**FIGURE 1**

**Figure 2.** Regionalization of the basal hypothalamus and neighbor territories in embryos of *S. canicula* at stages 29-32 based on the expression of *ScEmx2* **(A-E)**, *ScLhx5* **(Q,R)**, *ScOtp* **(S)** and *ScDl2/5* **(T)**, and the immunoreactivity to 5-HT (**F-J**), PCNA (**K-O**) and Shh (**P**) on whole mounts (A,P,Q) and in sagittal (F, K) and transverse (B-E, G-J, L-O, R-T) sections. **(A-E)** *ScEmx2* expression through the caudo-ventral Tu-like, PM/PRM-like and MM-like domains. Note the absence of expression in the RM-like domain and in the rostral part of the acroterminal territory. **(A)** Lateral view of a whole mount. Arrowhead marks the caudal border of the *ScEmx2* expression in the MM-like. Note the shark limit with the negative RM-like domain. **(B-E)** Sequence of sections from ventral (B) to dorsal (E) levels of the basal hypothalamus. Arrowhead in B points intense ScEmx2 expression in the ventral Tu-like. Arrows in D mark as the *ScEmx2* expression in the MM-like and PRM-like border the negative territory of the RM-like. Arrowhead in E points the caudal border of *ScEmx2* expression in the PRM-like. **(F-J)** 5-HT immunoreactivity in sections at equivalent levels to that of shown in A-E to comparatively show that the distribution of 5-HT-immunoreactivity in the circumventricular organs almost matches with that of *ScEmx2* expression. For labels of arrowheads, see B and E. **(K-O)** PCNA-immunoreactivity in sections at equivalent levels to that of showed in A-E and in F-J. Arrowheads indicate discontinuities in PCNA-immunoreactivity. **(P)** Lateral view of a whole mount embryo stained for Shh-immunoreactivity to show the complementary pattern to that of *ScEmx2* expression. **(Q, R)** Lateral view of a whole mount embryo (Q) and transverse section (R) showing that the caudal domain of *ScLhx5* corresponding to PM/PRM-like and MM-like, codistribute with *ScEmx2* (compare Q with A and R with C). **(S)** *ScOtp* expression in restricted territories of PM/PRM-like and MM-like domains. Compare with expressions of *ScLhx5* in R and *ScEmx2* in C to notice that different subdomains can be identified in PM/PRM-like and MM-like comparing these three markers. **(T)** *ScDlx2/5* expression at stage 32 is reduced at the dorsal-most levels of the Tu-like domain and absent in its caudo-ventral region. For abbreviations, see list.

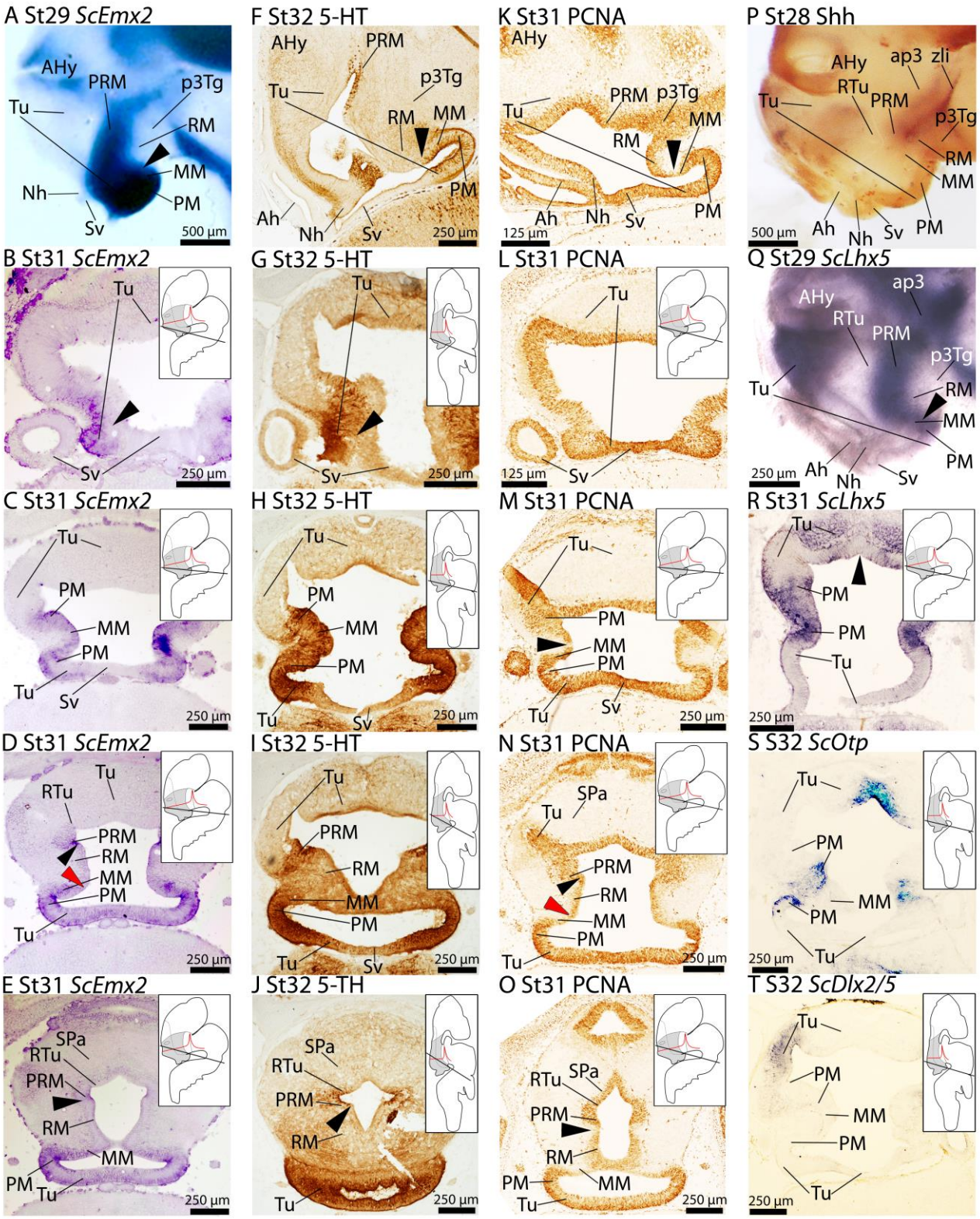
A St29 ScEmx2
AHy
PRM
p3Tg
Tu
RM
MM
Nh
PM
Sv
500 µm
F St32 5-HT
AHy
PRM
p3Tg
Tu
RM
MM
PM
Ah
Nh
Sv
250 µm
K St31 PCNA
AHy
PRM
p3Tg
Tu
MM
RM
Ah
Nh
Sv
PM
125 µm
P St28 Shh
AHy
ap3
zli
RTu
Tu
PRM
p3Tg
RM
MM
500 µm
Ah
Nh
Sv
PM
B St31 ScEmx2
Tu
Sv
250 µm
G St32 5-HT
Tu
Sv
250 µm
L St31 PCNA
Tu
125 µm
Sv
Q St29 ScLhx5
AHy
ap3
RTu
PRM
p3Tg
Tu
RM
MM
PM
250 µm
Ah
Nh
Sv
C St31 ScEmx2
Tu
PM
MM
PM
Tu
Sv
250 µm
H St32 5-HT
Tu
PM
MM
PM
Tu
Sv
250 µm
M St31 PCNA
Tu
PM
MM
PM
Tu
Sv
250 µm
R St31 ScLhx5
Tu
PM
PM
Tu
250 µm
D St31 ScEmx2
Tu
RTu
PRM
RM
MM
PM
Tu
250 µm
I St32 5-HT
Tu
PRM
RM
MM
PM
Tu
Sv
250 µm
N St31 PCNA
SPa
Tu
PRM
RM
MM
PM
Tu
250 µm
S S32 ScOtp
Tu
PM
MM
PM
250 µm
Tu
E St31 ScEmx2
SPa
RTu
PRM
RM
MM
PM
Tu
250 µm
J St32 5-TH
SPa
RTu
PRM
RM
Tu
250 µm
O St31 PCNA
RTu
SPa
PRM
RM
PM
MM
Tu
250 µm
T S32 ScDlx2/5
Tu
PM
MM
PM
250 µm
Tu

**FIGURE 2**

**Figure 3.** Regionalization of the basal hypothalamus and neighbor territories in embryos of *S. canicula* at stages 29-31 based on the expression of *ScLmx1b* **(A, E, I, L)**, *ScPitx2a* **(B, F, J, M)**, *ScFoxa1/2* **(C, G, K, N)** and *ScNeurog2* **(D, H)** in sagittal (A-D, I-N) and transverse (E-H) sections. Some *in situ* sections were double labeled for immunohistochemistry against Shh (I). (**A-D**) Equivalent sagittal sections of embryos at stage 29 showing the similar pattern of expression of *ScLmx1b, ScPitx2a, ScFoxa1/2* and *ScNeurog2*. Insets in B and C show similar results with *ScPitx3a* and *ScFoxa1*. (**E-H**) Transverse equivalent sections showing that in any case, the expression of *ScLmx1b, ScPitx2a, ScFoxa1/2* and *ScNeurog2* is restricted to the RM. Arrowheads points the sharp limit where the expression of these genes is abutting the negative MM-like. (**I-N**) Panoramic views (I-K) and details (L-N) of sagittal sections to show similar patterns of expression of *ScLmx1b, ScPitx2a and ScFoxa1/2* in the RM and *ScNeurog2*. Arrowheads point the region where the expression of such genes abuts the negative MM-like. For abbreviations, see list.

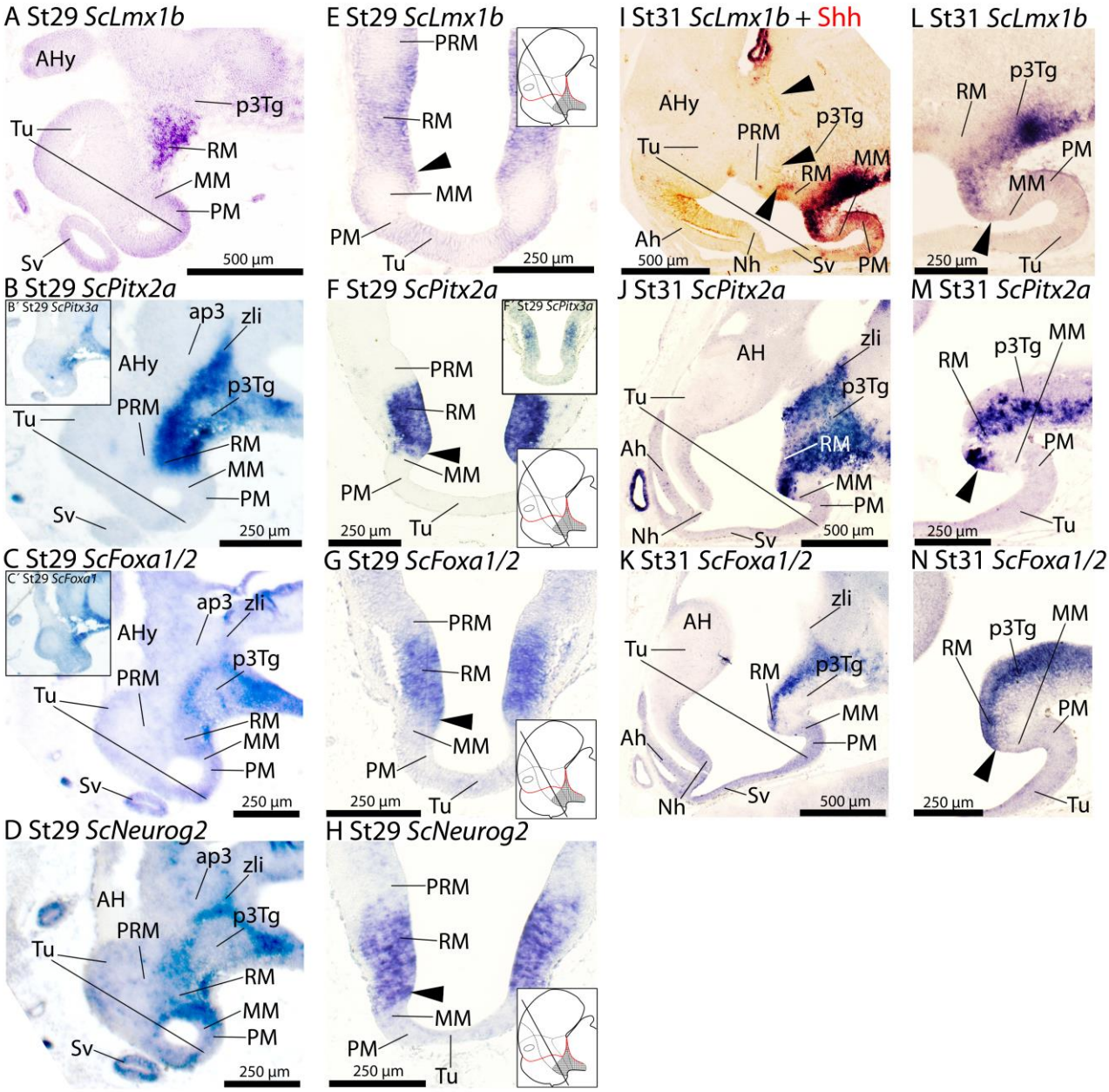
A St29 ScLmx1b
AHy
p3Tg
Tu
RM
MM
PM
Sv
500 µm
E St29 ScLmx1b
PRM
RM
MM
PM
Tu
250 µm
I St31 ScLmx1b + Shh
AHy
p3Tg
Tu
PRM
RM
MM
Ah
Nh
Sv
PM
500 µm
L St31 ScLmx1b
RM
p3Tg
PM
MM
250 µm
Tu
B St29 ScPitx2a
B´ St29 ScPitx3a
ap3
zli
AHy
p3Tg
PRM
Tu
RM
MM
PM
Sv
250 µm
F St29 ScPitx2a
F´ St29 ScPitx3a
PRM
RM
MM
PM
250 µm
Tu
J St31 ScPitx2a
AH
zli
p3Tg
Tu
Ah
RM
MM
PM
Nh
Sv
500 µm
M St31 ScPitx2a
RM
p3Tg
MM
PM
250 µm
Tu
C St29 ScFoxa1/2
C´ St29 ScFoxa1
ap3
zli
AHy
p3Tg
PRM
Tu
RM
MM
PM
Sv
250 µm
G St29 ScFoxa1/2
PRM
RM
MM
PM
250 µm
Tu
K St31 ScFoxa1/2
AH
zli
Tu
RM
p3Tg
MM
Ah
PM
Nh
Sv
500 µm
N St31 ScFoxa1/2
RM
p3Tg
MM
PM
250 µm
Tu
D St29 ScNeurog2
ap3
zli
AH
PRM
p3Tg
Tu
RM
MM
PM
Sv
250 µm
H St29 ScNeurog2
PRM
RM
MM
PM
250 µm
Tu

# FIGURE 3

**Figure 4.** Regionalization of the basal hypothalamus and neighbor territories in embryos of *S. canicula* at stage 30 and 32 based on GAD **(A),** TH **(B-C)**, CB **(D)**, SS (E-G), and GFAP **(E)** immunoreactivities on sagittal sections. Some sections were double labeled for immunohistochemistry against Shh (B, E-G). For abbreviations, see list.

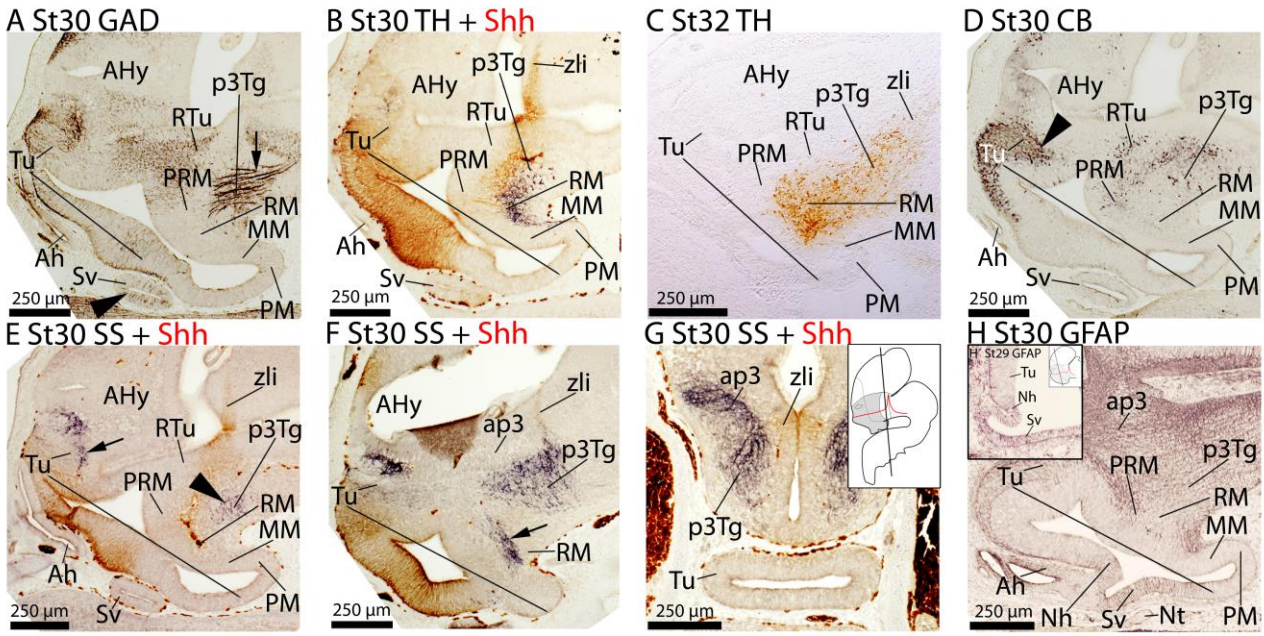
A St30 GAD
AHy
p3Tg
RTu
Tu
PRM
RM
MM
Ah
Sv
250 µm
PM
B St30 TH + Shh
p3Tg
zli
AHy
RTu
Tu
PRM
RM
MM
Ah
Sv
250 µm
PM
C St32 TH
AHy
p3Tg
zli
RTu
Tu
PRM
RM
MM
250 µm
PM
D St30 CB
AHy
RTu
p3Tg
Tu
PRM
RM
MM
Ah
Sv
250 µm
PM
E St30 SS + Shh
zli
AHy
RTu
p3Tg
Tu
PRM
RM
MM
Ah
250 µm
Sv
PM
F St30 SS + Shh
zli
AHy
ap3
p3Tg
Tu
RM
250 µm
G St30 SS + Shh
ap3
zli
p3Tg
Tu
250 µm
H St30 GFAP
H' St29 GFAP
Tu
Nh
Sv
ap3
PRM
p3Tg
Tu
RM
MM
Ah
250 µm
Nh
Sv
Nt
PM

# FIGURE 4

**Figure 5.** Schematic representations of various gene expression and neurochemical immunoreactive patterns defining domains and subdomains in the basal hypothalamus of *S. canicula* around stage 29 and 30. The expression of some of these markers is also represented in the telencephalon, alar hypothalamus and rostral diencephalon. Figures **(A, C-F)** reflect markers expressed in lateral sections while (B) reflects markers expressed in the midline (acroterminal territory). **(A)** Gene expression markers and subdomains of the basal hypothalamus. **(B)** Gene expression markers and subdomains of the acroterminal territory. **(C)** Gene expression markers and subdomains of the rostro-dorsal domain lacking *ScEmx2*-expression**. (D)** Gene expression patterns and subdomains in the *ScEmx2*-expressing hypothalamus**. (E)** Gene expression patters and subdomains of the caudo-ventral domains lacking *ScEmx2*-expression. **(F)** Distribution of neurochemical substances. The scheme includes data from stage beyond 30. Continuous red line represents ABBr. Discontinuous black line represents IHB. For abbreviations, see list.

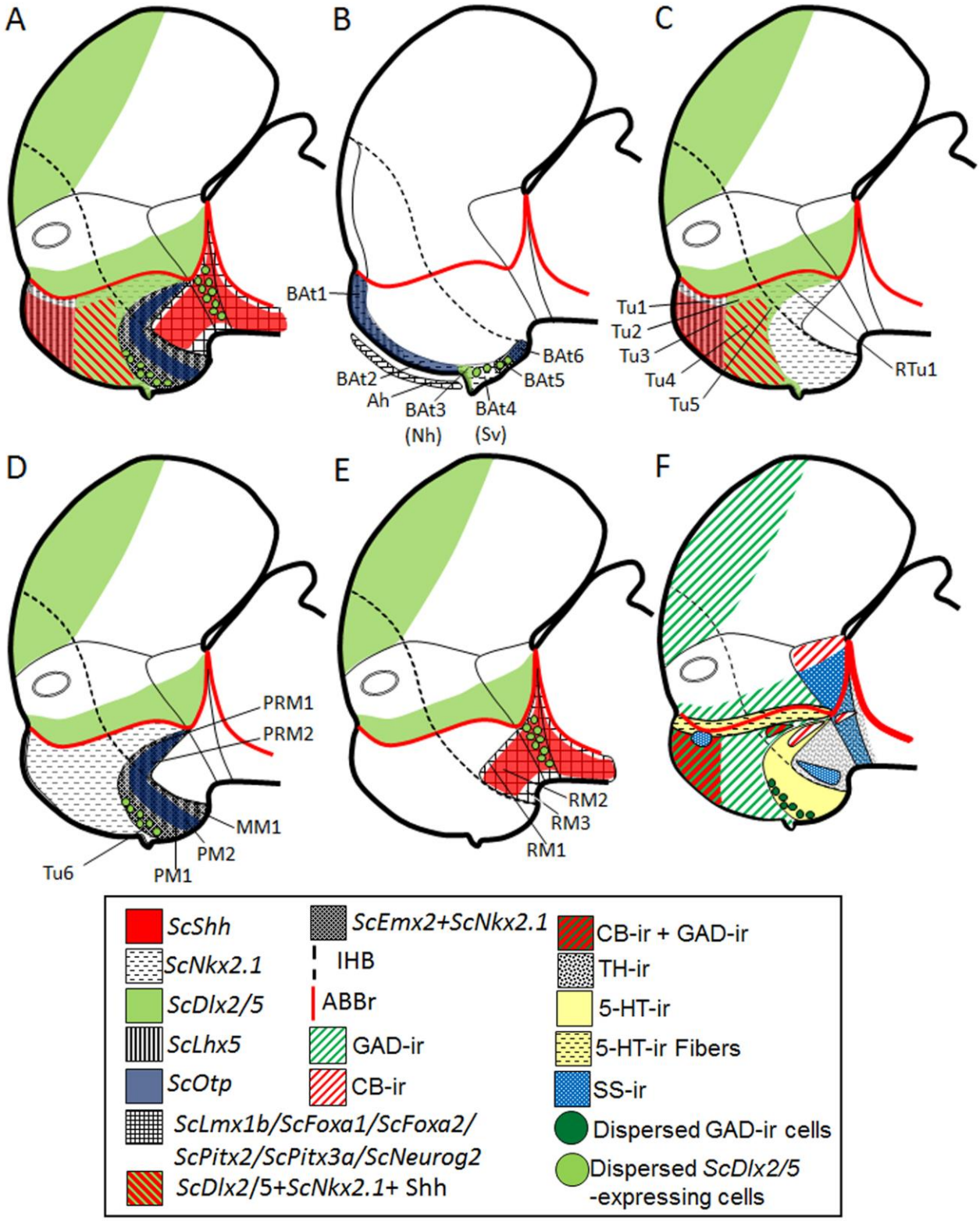
A
B
C
BAt1
BAt2
Ah
BAt3
(Nh)
BAt4
(Sv)
BAt5
BAt6
Tu1
Tu2
Tu3
Tu4
Tu5
RTu1
D
E
F
PRM1
PRM2
MM1
PM2
PM1
Tu6
RM2
RM3
RM1
ScShh
ScNkx2.1
ScDlx2/5
ScLhx5
ScOtp
ScLmx1b/ScFoxa1/ScFoxa2/
ScPitx2/ScPitx3a/ScNeurog2
ScDlx2/5+ScNkx2.1+ Shh
ScEmx2+ScNkx2.1
IHB
ABBr
GAD-ir
CB-ir
CB-ir + GAD-ir
TH-ir
5-HT-ir
5-HT-ir Fibers
SS-ir
Dispersed GAD-ir cells
Dispersed ScDlx2/5
-expressing cells

**FIGURE 5**

**Figure 6**. Schematic representations of the domains and subdomains of the basal hypothalamus of embryos at stages 30 and 31 based on gene expression and neurochemical markers indicated transverse **(A, B)** and sagittal **(C)** sections. **(A)** Transverse representation of the rostral subdomains. The level of the section is represented with blue line in (C). **(B)** Transvers representation of caudal subdomains. The level of the section is represented with blue line in (C). **(C)** Saggital representation of several expression patterns. The representation also reflects the ventriculum. For abbreviations, see list.

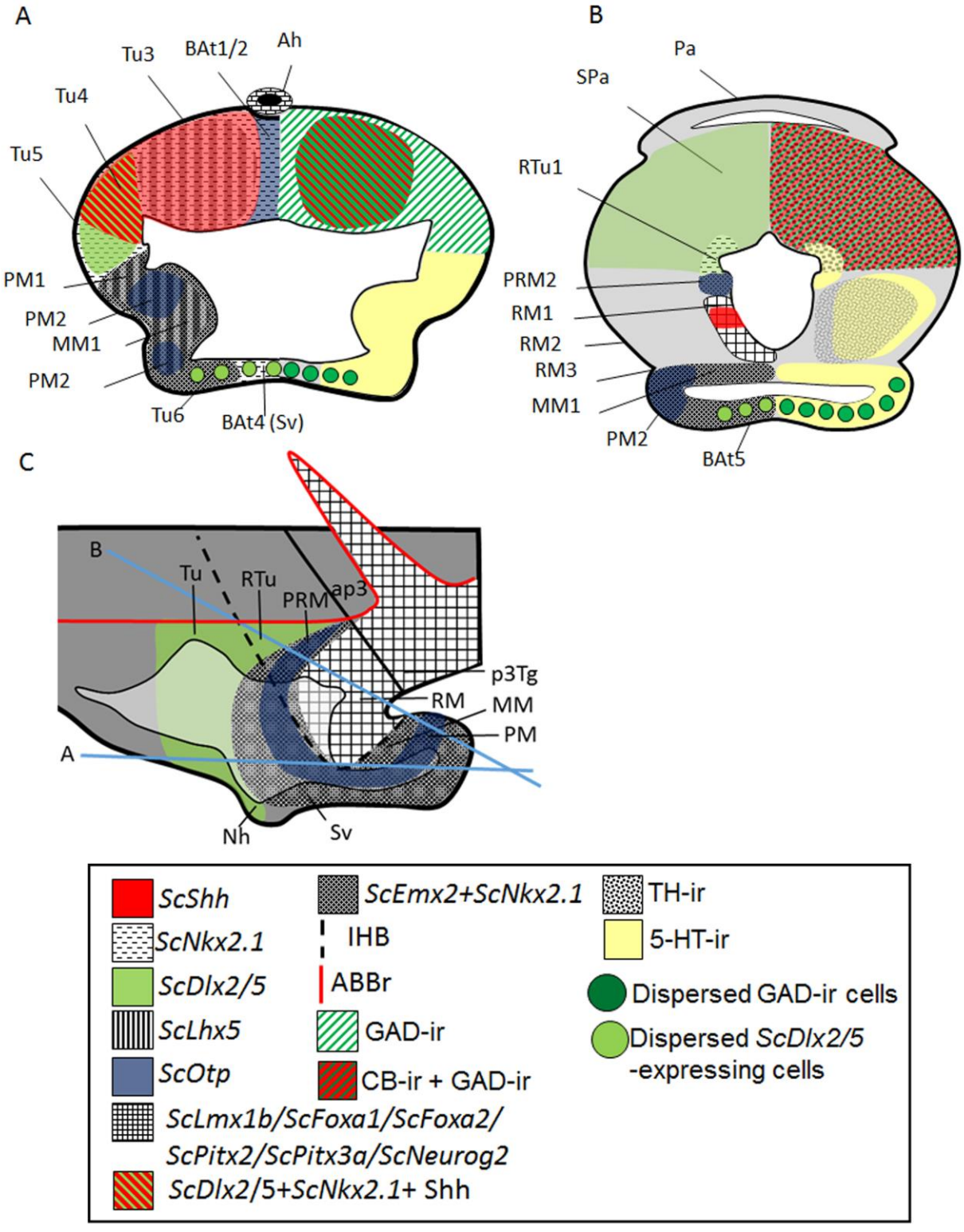
A
Tu3
BAt1/2
Ah
Tu4
Tu5
PM1
PM2
MM1
PM2
Tu6
BAt4 (Sv)
B
Pa
SPa
RTu1
PRM2
RM1
RM2
RM3
MM1
PM2
BAt5
C
B
Tu
RTu
PRM
ap3
p3Tg
RM
MM
PM
A
Nh
Sv
ScShh
ScNkx2.1
ScDlx2/5
ScLhx5
ScOtp
ScLmx1b/ScFoxa1/ScFoxa2/
ScPitx2/ScPitx3a/ScNeurog2
ScDlx2/5+ScNkx2.1+ Shh
ScEmx2+ScNkx2.1
IHB
ABBr
GAD-ir
CB-ir + GAD-ir
TH-ir
5-HT-ir
Dispersed GAD-ir cells
Dispersed ScDlx2/5
-expressing cells

# FIGURE 6

**Figure 7.** Schematic representations of the expression patterns of various genes in the basal hypothalamus around E13,5 mouse **(A, C, E, G)** and stage 29 *S. canicula* **(B, D, F, H)**, and their correspondence with the updated prosomeric model (A-F). **(G)** and **(H)** represent the organization of the three main histogenetic domains proposed for the basal hypothalamus. This domains do not support the updated prosomeric organization. Data of mouse come mainly from the Allen Brain Atlas. For abbreviations, see list.

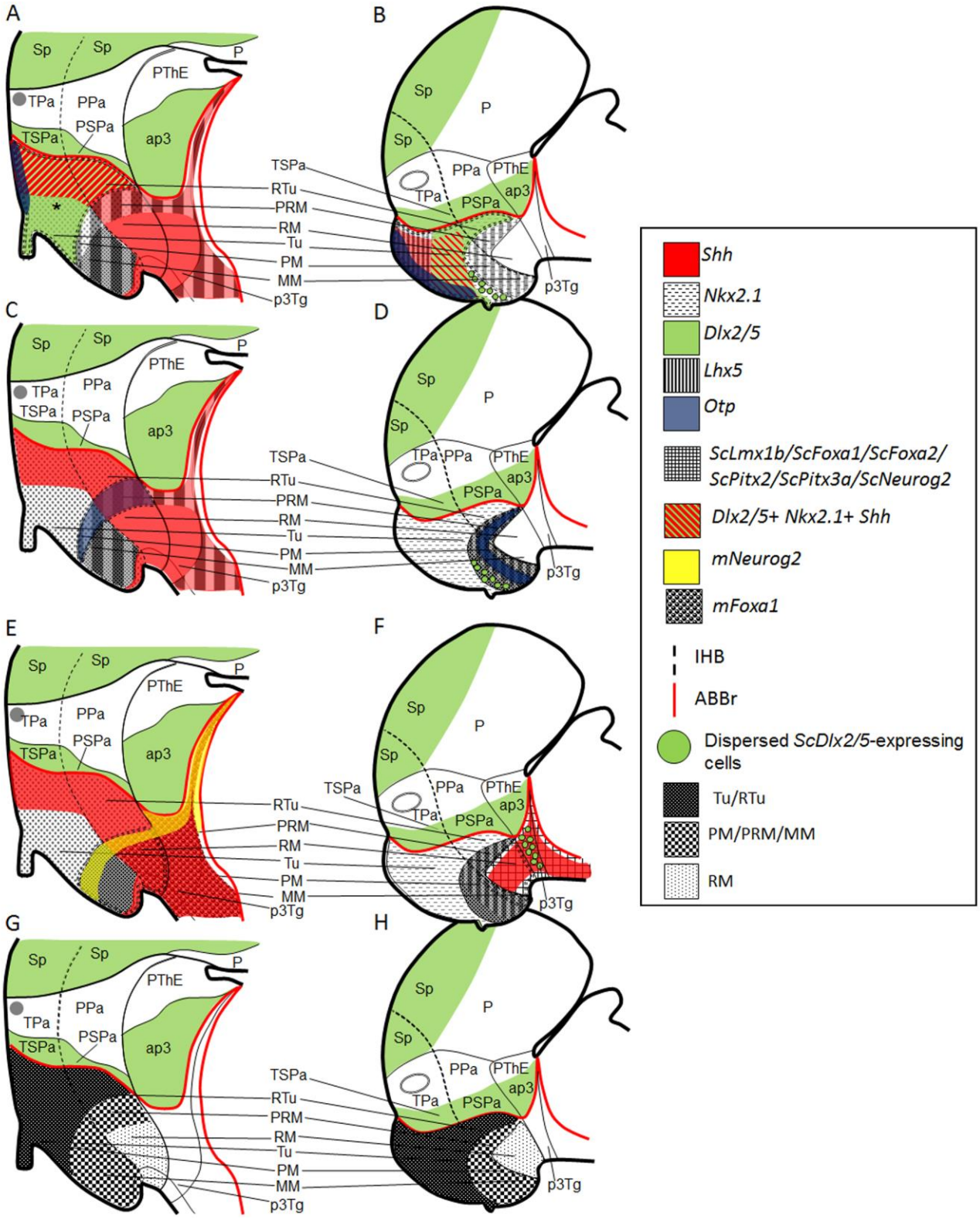
A
B
C
D
E
F
G
H
Sp
P
PThE
TPa
PPa
PSpa
TSPa
ap3
RTu
PRM
RM
Tu
PM
MM
p3Tg
Shh
Nkx2.1
Dlx2/5
Lhx5
Otp
ScLmx1b/ScFoxa1/ScFoxa2/
ScPitx2/ScPitx3a/ScNeurog2
Dlx2/5+ Nkx2.1+ Shh
mNeurog2
mFoxa1
IHB
ABBr
Dispersed ScDlx2/5-expressing cells
Tu/RTu
PM/PRM/MM
RM

**FIGURE 7**

**Figure 8.** Schematic representations of the expression pattern of various genes in the prosencephalon of lamprey based on data available in the literature (see text for details). For abbreviations, see list.

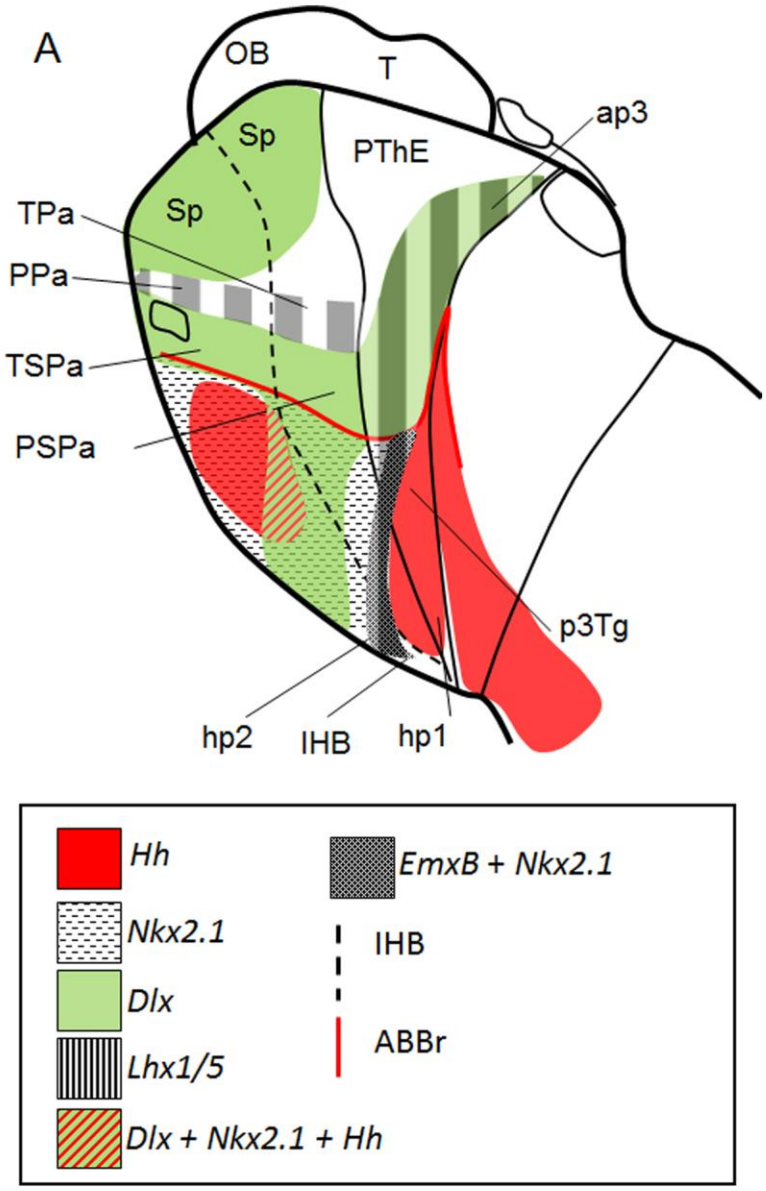
A
OB
T
ap3
Sp
PThE
Sp
TPa
PPa
TSPa
PSPa
p3Tg
hp2
IHB
hp1
Hh
EmxB + Nkx2.1
Nkx2.1
IHB
Dlx
ABBr
Lhx1/5
Dlx + Nkx2.1 + Hh

# FIGURE 8

USC
UNIVERSIDADE
DE SANTIAGO
DE COMPOSTELA

# GENERAL DISCUSSION

USC
UNIVERSIDADE
DE SANTIAGO
DE COMPOSTELA

# GENERAL DISCUSSION

This work pursues to understand the morphological evolution of the vertebrate hypothalamus. In order to recognize *how* has it changed through evolution first we had to define *what* we understood by hypothalamus (Northcutt, 2002; Butler and Hodos, 2005). Since the study of developmental transcription factors and signaling molecules offers a good way to stablish meaningful comparisons and correct homologies, we took an *evo-devo* approach (Van Valen, 1982; Gilbert et al., 1996; Abouheif, 1997; Puelles and Medina, 2002; Hall, 2003) also looking for a definition of hypothalamus in those terms. With these aims in mind, we have made use of the prosomeric model framework since it has been a useful comparative tool that also offers a well-defined concept of hypothalamus (Puelles et al., 2012; Puelles and Rubenstein, 2003, 2015). We focused on the catshark *Scyliorhinus canicula*, a species representative of basal gnathostomes (Coolen et al., 2009), as a biological model to understand the evolution of the vertebrate hypothalamus, and we analyze this material by means of immunohistochemistry and *in situ* hybridization techniques.

The adult hypothalamus of chondrichthyans has been extensively studied during last decades by means of different techniques, such as electron microscopy, radioimmunoassays, immunohistochemistry, *in situ* hybridization and tract tracing, in order to gain knowledge about its neurochemical organization and connectivity (Smeets, 1983; Smeets and Boord, 1985; Rodríguez-Moldes and Anadón, 1987; Vallarino and Ottonello, 1987; Vallarino et al., 1988a, 1988b, 1989, 1990a, 1990b, 1991, 1992, 1994; Stuesse and Cruce, 1992; Molist et al. 1992, 1993; Rodríguez-Moldes et al., 1993a, 1993b; D´Antonio et al., 1995; Meurling et al., 1996; Smeets, 1998; Anadón et al., 2000; Teijido et al., 2002; Hofmann and Northcutt, 2008, 2012; Quintana-Urzainqui, 2013). The development of the embryonic hypothalamus of cartilaginous fishes has been also analyzed as part of different works during last years (Carrera et al, 2005, 2008a, 2008b, 2012; Carrera, 2008; Ferreiro Galve, 2010; Quintana-Urzainqui et al., 2012, 2013) and even some studies have been addressed to the development of specific hypothalamic systems (Sueiro et al., 2007). However, although the segmental organization of the shark prosencephalon has been analyzed under precedent prosomeric conceptions (Ferreiro-Galve et al., 2008; Carrera et al., 2012), studies were lacking that were focused on the development of the whole chondrichthyan hypothalamus, formal molecular and/or developmental definitions of this structure and updated segmental frameworks.

In this monograph, we firstly examined the expression of *ScFoxg1a*, *ScShh*, *ScNkx2.1*, *ScDlx2/5*, *ScOtp*, *ScTbr1* genes and patterns of immunoreactivity to different substances (TH, 5-HT and GFAP-ir) from early to late development, to identify the limits of the hypothalamus

in a shark and tentatively define its regionalization. This led us to sketch the hypothalamo-telencephalic border (**HTB**) and the hypothalamo-diencephalic border (**HDB**), the dorsal and caudal limits of the hypothalamus, respectively. Besides, we have identified longitudinal histogenetic domains homologue to those proposed by the prosomeric model based on the expression of: *ScOtp* (**Pa-like**), *ScDlx2/5* (**SPa-like**) in the alar plate; and **Tu/RTu-like** (*ScNkx2.1+ScDlx2/5+ScShh+ScOtp*), **PM/PRM-like** (*ScNkx2.1+ScOtp*) and **MM/RM-like** (*ScNkx2.1+ScShh*) in the basal plate. Besides, we found evidences of the intrahypothalamic border (**IHB**) in the alar plate by the course of 5-HT-immunoreactive tracts to the telencephalon through the medial forebrain bundle. Furthermore, our data revealed a strikingly degree of conservation among data obtained in the shark and mouse. Of note, while the alar hypothalamus seemed more conservative, the basal hypothalamus presents some differences mainly regarding the extension of *ScShh* and *ScDlx2/5* expression in this territory. Moreover, this work shed light on the identity of the posterior tuberculum, which had been previously addressed to the hypothalamus or to the diencephalon under different evidences (Vernier and Wullimann, 2008). Our analysis suggested that, under the updated prosomeric framework (Puelles et al., 2012; Puelles and Rubenstein, 2015), the rostral-most part of the posterior tuberculum likely corresponds to the RM-like.

In the absence of similar studies in other fishes, this primary analysis is the first to shed light on the hypothalamic organization of basal gnathostomes and also suggests that the predictions of the updated prosomeric model could be in fact extrapolated to different classes of vertebrates.

Therefore, the main histogenetic domains seem to be homologue among shark and mouse at a single level of analysis (i.e. the existence of histogenetic domains). Nevertheless, this preliminary work has raised more questions than those answered by it, mainly in the following subjects:

i) The prosomeric model and hypothalamic subdivisions: Could we identify more subdomains in the shark hypothalamus? Is the prosomeric model able to integrate the similarities or differences observed? Could other kind of models or modeling approaches improve the explanatory resolution of the prosomeric model?

ii) The conservation or divergence of the data observed in the shark: Are these traits also observable in other vertebrates? If true, what this tells us about morphological differences? If false, could the differential expression patterns explain morphological differences?

ii) Classical problems of homologies establishment: The existence of homologies at single level of analysis (domains) involves the existence of homologies at further level of analysis (subdomains)(Striedter and Northcutt, 1991; Abouheif, 1997; Striedter, 1998; Butler and Saidel, 2000; Puelles and Medina, 2002; Kleisner, 2007) Which is the best way to understand homologies of processes (Butler and Saidel, 2000; Gilbert and Bolker, 2001; Hall, 2003; Kleisner, 2007; Shubin et al., 2009) Is the study of compared expression patterns the best approach to understand morphological similarities -or differences- among vertebrates?

Thus, as next steps we tried to answer some of these points. To do so, we decided to approach the alar and basal hypothalamus separately as they seem to work as partially independent developmental units.

In the **alar hypothalamus**, on one hand, we reviewed data obtained in the first work trying to integrate it with new data on the expression of *ScLhx9*, *ScLhx5*, *ScNeurog2*, *ScNkx2.8* genes and Pax6-immunoreactivity, besides immunoreactivity to different neurochemical markers (GAD, SS, CB and TH). This analysis revealed interesting facts. **First**, it revealed that the alar hypothalamus of the shark and the mouse share various expression patterns both in the Pa-like (*ScOtp*, *ScNeurog2*, *ScLhx5 a*nd Pax6-immunoreactivity) and SPa-like (*ScDlx2/5* and *ScNkx2.8*). **Second**, we were able to identify genetic evidences of rostro-caudal (in the Pa-like and SPa-like) and dorso-ventral subdomains (in the SPa-like) based on this markers. Of note, as wee deepen in subdomain identity, the expression of these markers in the alar hypothalamus seems to be less conserved among shark and mouse than previously reported in the basis of *ScOtp*- and Sc*Dlx2/5*-expression alone. **Third**, the distribution of Pax6-immunoreactive cells in the basal hypothalamus suggests and supports the existence of an IHB separating terminal (hp2) and peduncular (hp1) subdivisions of the secondary prosencephalon, as predicted by the prosomeric model. **Fourth**, the expression of *ScOtp* and other markers inside a broader domain of Pax6-immunoreactivity led us to suggest that the Pa-like could belong to a territory more related to the pallium and alar p3 than to the SPa-like, which seems to be supported by data from different vertebrates. Of note, this novel proposal questions the course of the hypothalamus-telencephalic border (HTB). **Fifth**, these analyses also lead us to identify amygdala-related structures derived from the hypothalamus based on *ScOtp* expression. The identification of *ScOtp*-expressing cells in different domains of the telencephalon suggest that the existence of amygdaloid-like structures could be already present in early gnathostomes, though studies addressing this question still lack in other fishes (Medina et al., 2011). **Sixth**, we have reexamined the situation of the ABB in the shark as we meet difficulties to establish this territory based on the blurred definitions of the literature. We propose ABB as the domain of *ScNkx2.8*-expression while we coined the concept of ABBr as the virtual line where the alar and basal plates abut or defined by the alar or basal expression of *ScDlx2/5* or *ScNkx2.1*, respectively. This novel concept means an improvement for neuroanatomical studies being transferable to other works. **Seventh**, On the other hand, a detailed comparative review of data among different vertebrates reveal a striking degree of conservation for the markers here considered for the alar hypothalamus. Besides, this review also supports that a Pa-like positive for *Otp*, *Neurog2*, *Pax6*, *Lhx5* and a SPa-like positive for *Dlx*, *Nkx2.8*/*Nkx2.2* were already present before agnathan-gnathosme transition while other studies on which chondricthyans were not considered suggested that many of this traits were acquired during the anamniote-amniote transition (Domínguez et al., 2014, 2015). This fact stresses the relevance of our data besides the importance of including information from elasmobranches in *evo-devo* studies.

In the **basal hypothalamus**, we proceed in a similar manner as for the alar hypothalamus. On one hand, we reviewed our assumptions concerning the basal

hypothalamus trying to integrate our previous data with new data on the basal expression of *ScLhx5*, *ScEmx2*, *ScLmx1b*, *ScPitx2*, *ScPitx3a*, *ScNeurog2*, *ScFoxa1* and *ScFoxa2* genes besides to immunoreactivity to different substances including the proliferation marker PCNA. The cross data between previous information and new markers yielded a number of subdomains that goes beyond the comparative scope analysis of a single work. However, differences observed among main histogenetic compartments stress previous issues we had met on the alar hypothalamus when we deepen in the comparative analysis of subdomains: histogenetic domains that are homologue at a single level of analysis seem to not be homologue at other levels of analysis. This –again– raises the unresolved question of the correct level of analysis for homologies establishment (Striedter and Northcutt, 1991; Abouheif, 1997; Striedter, 1998; Butler and Saidel, 2000; Puelles and Medina, 2002; Kleisner, 2007).

However, this analysis also yielded other interesting results. The analysis of the expression patterns observed in shark suggests that the basal hypothalamus could be better understood as being divided into three main domains characterized by the expression –or not– of *ScEmx2* (*ScEmx2* negative: Tu/RTu-like; *ScEmx2* postive: part of the Tu-like, PM/PRM-like and MM-like; *ScEmx2* negative: RM-like). Noteworthy, this novel proposal do not support the histogenetic compartments assumed by the prosomeric model. Furthermore, unexpectedly, these results were supported by evidence from mutants mice defective for hypothalamic neural signaling (Szabó et al., 2009). In contrast to wild mice, sharks and mice mutants share a phenotype characterized by *Emx2* upregulation and *Pitx2* downregulation besides hypoplasia in a ventro-caudal region of the basal hypothalamus defective for Shh signaling. Under our point of view this suggest that, at least in some cases, the patterning process (the rules) operating among vertebrates could be essentially the same, but important differences could arise by means of divergent signaling process. Moreover, the expression patterns of *ScShh*/Shh-immunoreactivity, *ScLmx1b*, *ScPitx2*, *ScPitx3a*, *ScNeurog2*, *ScFoxa1* and *ScFoxa2* in the RM-like are continuous with those of the diencephalic basal plate suggesting that the RM-like belongs to the diencephalon rather than to the hypothalamus. In the shark, this idea is further supported by different lines of evidence including absence of PCNA in boundaries, the transversal expression of *Wnt8a* among different vertebrates, the course of certain tracts and previous segmental analysis (Figdor and Stern, 1993). Noteworthy, the comparative study of the genes here considered also seem to support this proposal. If true, our analysis would reveal an alternative interpretation of the histogenesis in the basal hypothalamus. Furthermore, this view also suggests an alternative and novel interpretation of the secondary prosencephalon that would include the alar p3 (besides the PThE) while excluding the RM-like.

To sum up, the present monograph sheds light on the histogenetic organization of the hypothalamus and neighbor territories in *S. canicula*. The key position of this model as representative of chondrichthyans and basal gnathostomes joint to the thoughtful wealth of the data here presented make this work a milestone in three key subjects: i) chondrichthyan

development and neuroanatomy; ii) vertebrate brain evolution; and iii) segmental interpretation of the forebrain (or prosomeric model feedback).

We are aware that the interpretation of our data is open to discussion and some general considerations should be taken into account:

**First**, we have just presented the analysis of a handful of genes, but it has been suggested that around 3908 genes are expressed in the prosencephalon of mammals (Martínez et al., 2012). Although it is true that the theoretical number of boundaries is far away from the number of boundaries observed (Puelles et al., 2012) we cannot claim that our observations could be applicable to other genes or to all vertebrates. Furthermore, our analysis also reveals that different interpretations could be possible even with well-known expression patterns and similar developmental frameworks.

**Second**, we are still far away to understand what do the expression patterns studied (and the maps we make) really mean and hence, how development and/or the brain really work. We hardly understand some correlations among the expression -or its lack- of a few genes in certain territories and the logic of gene regulatory networks (GRN) governing brain patterning (Beccari et al. 2013). Moreover, the correlation among these GNRs and the spatial distribution of the genes involved remain elusive. Noteworthy, the organization proposed by Puelles and collaborators in the prosomeric model (Puelles and Rubenstein 1993, 2003, 2015; Puelles et al., 2012) and in the developmental ontology (Puelles et al., 2013) likely reflect spatio-temporal traits of such networks. However, these paradigms do not explicitly reflect the relationship among the genes used to define histogenetic compartments and, as consequence, the explanatory resolution of the models is reduced. In fact, we could understand these models as undirected graphs of gene networks on which nodes but not information flux is known. Testing the logic of compartments under network approaches would provide further mechanistic evidences of the existences of boundaries, domains and subdomains.

**Third**, the era of "omics" (Shimogori et al., 2010; Diez-Roux et al., 2011; Sherwood and Duka, 2012) is providing biologist with bulks of data that not necessarily shed light on the principles governing these systems, unless a suitable approach is afforded. Having a list of the parts of a car doesn't mean that one could understand how it works. This is the main take home point of systems biology and/or complex systems theory: it's difficult to understand systems formed by multiple interacting particles from different levels of hierarchy without understanding their relationships and their dynamics (Kitano, 2002). Noteworthy, the complex systems approach could also change some paradigms in evolution since it also suggests that many conserved traits, assumed to be so due to the black-box action of natural selection, can be in fact explained by properties intrinsic to systems theory (Goodwin, 1998; Striedter, 1998; Kauffman, 2003).

Finally, as perspective, all these evidences stress that current biologists need to have some training in computation and/or mathematical modeling skills and establish collaboration

with specialist on these fields to deepen in the understanding of biology (Gilbert and Sarkar, 2000; Müller, 2007). Such approaches have been applied in the study of development, morphogenesis and evolution in a variety of systems (Chang et al., 2009; Salazar-Ciudad, 2009; Salazar-Ciudad and Jernvall, 2010; Zhu et al., 2010; Garzón-Alvarado et al., 2011; Salazar-Ciudad and Marín-Riera, 2013; Moustakas-Verho et al., 2014; Harjunmaa et al., 2014; Raspopovic et al., 2014; Reingruber and Holcman, 2014; Matamoro-Vidal et al., 2015; Salvador-Martínez and Salazar-Ciudad, 2015) to cite only some samples, yielding impressive examples in certain tissues (Salazar-Ciudad and Jernvall, 2010; Salazar-Ciudad and Marín-Riera, 2013; Harjunmaa et al., 2014) but not yet in comparative brain development. These facts suggest that, on which concerns compared neuroanatomy and the study of brain models, maybe the next big step (or the next challenge for the prosomeric model) would be to translate experimental information into a mathematical formulation. Modeling approaches have the advantage to make us think about problems in a different way. For example, if we were able to translate the prosomeric framework into a mathematical formulation, the prosomeric model would be a set of equations (on which variables or parameters can be modified to describe different vertebrate phenotypes) or it rather would be a result (a single solution)?

**References**


Abouheif, E. (1997). Developmental genetics and homology: a hierarchical approach. *Trends Ecol. Evol.* 12, 405–8.

Anadón, R., Molist, P., Rodríguez-Moldes, I., López, J. M., Quintela, I., Cerviño, M. C., Barja, P., and González, A. (2000). Distribution of choline acetyltransferase immunoreactivity in the brain of an elasmobranch, the lesser spotted dogfish (*Scyliorhinus canicula*). *J. Comp. Neurol.* 420, 139–70.

Beccari, L., Marco-Ferreres, R., Bovolenta, P. (2013). The logic of gene regulatory networks in early vertebrate forebrain patterning. *Mech Dev*. 130:95-111.

Butler, A. B., and Hodos, W. (2005). "Evolution and Variation," in *Comparative vertebrate neuroanatomy: Evolution and Adaptation*, ed. J. W. & Sons.

Butler, A. B., and Saidel, W. M. (2000). Defining sameness: historical, biological, and generative homology. *Bioessays* 22, 846–53.

Carrera, I. (2008). Desarrollo de los sistemas gabaérgico y aminérgicos en el sistema nervioso central de peces cartilaginosos. Ph.D. thesis. Universidad Santiago de Compostela, Compostela. Available at: http://hdl.handle.net/10347/2449.

Carrera, I., Anadón, R., and Rodríguez-Moldes, I. (2012). Development of tyrosine hydroxylase-immunoreactive cell populations and fiber pathways in the brain of the dogfish *Scyliorhinus canicula*: new perspectives on the evolution of the vertebrate catecholaminergic system. *J. Comp. Neurol.* 520, 3574–603.

Carrera, I., Ferreiro-Galve, S., Sueiro, C., Anadón, R., and Rodríguez-Moldes, I. (2008a). Tangentially migrating GABAergic cells of subpallial origin invade massively the pallium in developing sharks. *Brain Res. Bull.* 75, 405–9.

Carrera, I., Molist, P., Anadón, R., and Rodríguez-Moldes, I. (2008b). Development of the serotoninergic system in the central nervous system of a shark, the lesser spotted dogfish *Scyliorhinus canicula. J. Comp. Neurol.* 511, 804–31.

Carrera, I., Sueiro, C., Molist, P., Ferreiro, S., Adrio, F., Rodríguez, M. A., Anadón, R., and Rodríguez-Moldes, I. (2005). Temporal and spatial organization of tyrosine hydroxylase-immunoreactive cell groups in the embryonic brain of an elasmobranch, the lesser-spotted dogfish *Scyliorhinus canicula*. *Brain Res. Bull.* 66, 541–5.

Chang, C., Wu, P., Baker, R. E., Maini, P. K., Alibardi, L., and Chuong, C.-M. (2009). Reptile scale paradigm: Evo-Devo, pattern formation and regeneration. *Int. J. Dev. Biol.* 53, 813–26.

Coolen, M., Menuet, A., Chassoux, D., Compagnucci, C., Henry, S., Lévèque, L., et al. (2009). "The Dogfish *Scyliorhinus canicula*, a Reference in Jawed Vertebrates," in *Emerging Model Organisms*. A Laboratory Manual, eds R. R. Behringer, A. D. Johnson,

and R. E. Rrumlauf (Cold Spring Harbor, NY: Cold Spring Harbor Laboratory Press), 431-46.

D'Antonio, M., Vallarino, M., Lovejoy, D. A., Vandesande, F., King, J. A., Pierantoni, R., and Peter, R. E. (1995). Nature and distribution of gonadotropin-releasing hormone (GnRH) in the brain, and GnRH and GnRH binding activity in serum of the spotted dogfish Scyliorhinus canicula. *Gen. Comp. Endocrinol.* 98, 35–49. doi:10.1006/gcen.1995.1042.

Diez-Roux, G., Banfi, S., Sultan, M., Geffers, L., Anand, S., Rozado, D., Magen, A., Canidio, E., Pagani, M., Peluso, I., et al. (2011). A high-resolution anatomical atlas of the transcriptome in the mouse embryo. *PLoS Biol.* 9, e1000582.

Domínguez, L., González, A., and Moreno, N. (2014). Characterization of the hypothalamus of *Xenopus laevis* during development. II. The basal regions. *J. Comp. Neurol.* 522, 1102–31. doi:10.1002/cne.23471.

Domínguez, L., González, A., and Moreno, N. (2015). Patterns of hypothalamic regionalization in amphibians and reptiles: common traits revealed by a genoarchitectonic approach. *Front. Neuroanat.* 9, 3. doi:10.3389/fnana.2015.00003.

Ferreiro Galve, S. (2010). Brain and retina regionalization in sharks, study based on the spatiotemporal expression pattern of pax6 and other neurochemical markers. Ph.D. thesis, Universidad de Santiago de Compostela, Compostela. Available at: http://hdl.handle.net/10347/2835.

Ferreiro-Galve, S., Carrera, I., Candal, E., Villar-Cheda, B., Anadón, R., Mazan, S., and Rodríguez-Moldes, I. (2008). The segmental organization of the developing shark brain based on neurochemical markers, with special attention to the prosencephalon. *Brain Res. Bull.* 75, 236–40.

Figdor, M. C., and Stern, C. D. (1993). Segmental organization of embryonic diencephalon. *Nature* 363, 630–4.

Garzón-Alvarado, D. A., Martínez, A. M. R., and Segrera, D. L. L. (2011). A model of cerebral cortex formation during fetal development using reaction-diffusion-convection equations with Turing space parameters. *Comput. Methods Programs Biomed.* 104, 489–97.

Gilbert, S. F., and Bolker, J. A. (2001). Homologies of process and modular elements of embryonic construction. *J. Exp. Zool.* 291, 1-12.

Gilbert, S. F., and Sarkar, S. (2000). Embracing complexity: organicism for the 21st century. *Dev. Dyn.* 219, 1–9.

Gilbert, S. F., Opitz, J. M., and Raff, R. A. (1996). Resynthesizing evolutionary and developmental biology. *Dev. Biol.* 173, 357–72.

Goodwin, B. (1998). *Las manchas del leopardo. La evolución de la complejidad*, Eds Tusquets (Tusquets; España), 304.

Hall, B. K. (2003). Evo-Devo: evolutionary developmental mechanisms. *Int. J. Dev. Biol.* 47, 491–5.

Harjunmaa, E., Seidel, K., Häkkinen, T., Renvoisé, E., Corfe, I. J., Kallonen, A., Zhang, Z.-Q., Evans, A. R., Mikkola, M. L., Salazar-Ciudad, I., et al. (2014). Replaying evolutionary transitions from the dental fossil record. *Nature* 512, 44–8.

Hofmann, M. H., and Northcutt, R. G. (2008). Organization of major telencephalic pathways in an elasmobranch, the thornback ray *Platyrhinoidis triseriata*. *Brain. Behav. Evol.* 72, 307–25.

Hofmann, M. H., and Northcutt, R. G. (2012). Forebrain organization in elasmobranchs. *Brain. Behav. Evol.* 80, 142–51.

Kauffman, S. (2003). *Investigaciones: complejidad, autoorganización y nuevas leyes para una biología general* , Eds Tusquets (Tusquets; España), 376.

Kitano, H. (2002). Systems biology: a brief overview. *Science* 295, 1662–4.

Kleisner, K. (2007). The formation of the theory of homology in biological sciences. *Acta Biotheor.* 55, 317–40.

Martínez, S., Puelles, E., Puelles, S., and Echeverría, D. (2012). "Molecular Regionalization of the Developing Neural Tube," in *The Mouse Nervous System*, eds. C. Watson, G. Paxinos, and L. Puelles (Academic Press, 2011), 814.

Matamoro-Vidal, A., Salazar-Ciudad, I., and Houle, D. (2015). Making quantitative morphological variation from basic developmental processes: Where are we? The case of the Drosophila wing. *Dev. Dyn.* 244, 1058-73.

Medina, L., Bupesh, M., and Abellán, A. (2011). Contribution of genoarchitecture to understanding forebrain evolution and development, with particular emphasis on the amygdala. *Brain. Behav. Evol.* 78, 216–36.

Meurling, P., Rodríguez, E. M., Peña, P., Grondona, J. M., and Pérez, J. (1996). Hypophysial and extrahypophysial projections of the neurosecretory system of cartilaginous fishes: an immunocytochemical study using a polyclonal antibody against dogfish neurophysin. *J. Comp. Neurol.* 373, 400–21.

Molist, P., Rodríguez-Moldes, I., and Anadón, R. (1992). Immunocytochemical and electron-microscopic study of the elasmobranch nucleus sacci vasculosi. *Cell Tissue Res.* 270, 395–404.

Molist, P., Rodríguez-Moldes, I., and Anadón, R. (1993). Organization of catecholaminergic systems in the hypothalamus of two elasmobranch species, *Raja undulata* and

*Scyliorhinus canicula*. A histofluorescence and immunohistochemical study. *Brain. Behav. Evol.* 41, 290–302.

Moustakas-Verho, J. E., Zimm, R., Cebra-Thomas, J., Lempiäinen, N. K., Kallonen, A., Mitchell, K. L., Hämäläinen, K., Salazar-Ciudad, I., Jernvall, J., and Gilbert, S. F. (2014). The origin and loss of periodic patterning in the turtle shell. *Development* 141, 3033–9.

Müller, G. B. (2007). Evo-devo: extending the evolutionary synthesis. *Nat. Rev. Genet.* 8, 943–9.

Northcutt, R. G. (2002). Understanding vertebrate brain evolution. *Integr. Comp. Biol.* 42, 743–56.

Puelles, L., Martínez, S., Martínez-de-la-Torre M, S., and Rubenstein, J. (2012). "Hypothalamus," in *Watson C, Paxinos G, Puelles L (eds) The Mouse Nervous Systeem*, eds. C. Watson, G. Paxinos, and L. Puelles (Elsevier Academic Press, San Diego), 814.

Puelles, L., and Medina, L. (2002). Field homology as a way to reconcile genetic and developmental variability with adult homology. *Brain Res. Bull.* 57, 243–55.

Puelles, L., and Rubenstein, J.L.R. (1993) Expression patterns of homeobox and other putative regulatory genes in the embryonic mouse forebrain suggest a neuromeric organization. *Trends Neurosci*. 16, 472-79.

Puelles, L., and Rubenstein, J. L. R. (2003). Forebrain gene expression domains and the evolving prosomeric model. *Trends Neurosci.* 26, 469–76.

Puelles, L., and Rubenstein, J. L. R. (2015). A new scenario of hypothalamic organization: rationale of new hypotheses introduced in the updated prosomeric model. *Front. Neuroanat.* 9. doi:10.3389/fnana.2015.00027.

Puelles, L., Harrison, M., Paxinos, G., Watson, C. (2013). A developmental ontology for the mammalian brain based on the prosomeric model. *Trends Neurosci*. 36:570-8.

Quintana-Urzainqui, I. (2013). Development and regionalization of the telencephalon and peripheral associated systems in the shark *Scyliorhinus canicula*. Ph.D. thesis, Universidad Santiago de Compostela, Compostela. Available at: http://hdl.handle.net/10347/9269.

Quintana-Urzainqui, I., Sueiro, C., Carrera, I., Ferreiro-Galve, S., Santos-Durán, G., Pose-Méndez, S., Mazan, S., Candal, E., and Rodríguez-Moldes, I. (2012). Contributions of developmental studies in the dogfish *Scyliorhinus canicula* to the brain anatomy of elasmobranchs: insights on the basal ganglia. *Brain. Behav. Evol.* 80, 127–41.

Raspopovic, J., Marcon, L., Russo, L., and Sharpe, J. (2014). Modeling digits. Digit patterning is controlled by a Bmp-Sox9-Wnt Turing network modulated by morphogen gradients. *Science* 345, 566–70.

Reingruber, J., and Holcman, D. (2014). Computational and mathematical methods for morphogenetic gradient analysis, boundary formation and axonal targeting. *Semin. Cell Dev. Biol.* 35, 189–202.

Rodríguez-Moldes, I., and Anadón, R. (1987). Aminergic neurons in the hypothalamus of the dogfish, *Scyliorhinus canicula* L. (Elasmobranch). A histofluorescence study. *J. Hirnforsch.* 28, 685–93.

Rodríguez-Moldes, I., Manso, M. J., Becerra, M., Molist, P., and Anadón, R. (1993a). Distribution of substance P-like immunoreactivity in the brain of the elasmobranch Scyliorhinus canicula. *J. Comp. Neurol.* 335, 228–44.

Rodríguez-Moldes, I., Scheuermann, D. W., Adriaensen, D., De Groodt-Lasseel, M. H., Molist, P., and Anadón, R. (1993b). Microspectrofluorimetric study of monoamines in the hypothalamus of Scyliorhinus stellaris L. *J. Hirnforsch.* 34, 57–61.

Salazar-Ciudad, I. (2009). Looking at the origin of phenotypic variation from pattern formation gene networks. *J. Biosci.* 34, 573–87.

Salazar-Ciudad, I., and Jernvall, J. (2010). A computational model of teeth and the developmental origins of morphological variation. *Nature* 464, 583–6.

Salazar-Ciudad, I., and Marín-Riera, M. (2013). Adaptive dynamics under development-based genotype-phenotype maps. *Nature* 497, 361–4.

Salvador-Martínez, I., and Salazar-Ciudad, I. (2015). How complexity increases in development: An analysis of the spatial-temporal dynamics of 1218 genes in Drosophila melanogaster. *Dev. Biol.* doi:10.1016/j.ydbio.2015.07.003.

Sherwood, C. C., and Duka, T. (2012). Now that we've got the map, where are we going moving from gene candidate lists to function in studies of brain evolution. *Brain. Behav. Evol.* 80, 167–169.

Shimogori, T., Lee, D. A., Miranda-Angulo, A., Yang, Y., Wang, H., Jiang, L., Yoshida, A. C., Kataoka, A., Mashiko, H., Avetisyan, M., et al. (2010). A genomic atlas of mouse hypothalamic development. *Nat. Neurosci.* 13, 767–75. doi:10.1038/nn.2545.

Shubin, N., Tabin, C., and Carroll, S. (2009). Deep homology and the origins of evolutionary novelty. *Nature* 457, 818-23.

Smeets, W. J. (1983). The secondary olfactory connections in two chondrichthians, the shark *Scyliorhinus canicula* and the ray *Raja clavata*. *J. Comp. Neurol.* 218, 334–44.

Smeets, W. (1998). "Cartilaginous Fishes," in *The Central Nervous System of Vertebrates: With posters*, ed. C. Nieuwenhuys, R; Donkelaar, HJ; Nicholson (Springer Science & Business Media 1998), 2219.

Smeets, W. J., and Boord, R. L. (1985). Connections of the lobus inferior hypothalami of the clearnose skate *Raja eglanteria* (Chondrichthyes). *J. Comp. Neurol.* 234, 380–92.

Striedter, G. F. (1998). Stepping into the same river twice: homologues as recurring attractors in epigenetic landscapes. *Brain. Behav. Evol.* 52, 218–31.

Striedter, G. F., and Northcutt, R. G. (1991). Biological hierarchies and the concept of homology. *Brain. Behav. Evol.* 38, 177–89.

Stuesse, S. L., and Cruce, W. L. (1992). Distribution of tyrosine hydroxylase, serotonin, and leu-enkephalin immunoreactive cells in the brainstem of a shark, *Squalus acanthias*. *Brain. Behav. Evol.* 39, 77–92.

Sueiro, C., Carrera, I., Ferreiro, S., Molist, P., Adrio, F., Anadón, R., and Rodríguez-Moldes, I. (2007). New insights on saccus vasculosus evolution: a developmental and immunohistochemical study in elasmobranchs. *Brain. Behav. Evol.* 70, 187–204.

Szabó, N.-E., Zhao, T., Cankaya, M., Theil, T., Zhou, X., and Alvarez-Bolado, G. (2009). Role of neuroepithelial Sonic hedgehog in hypothalamic patterning. *J. Neurosci.* 29, 6989–7002.

Teijido, O., Manso, M. J., and Anadón, R. (2002). Distribution of thyrotropin-releasing hormone immunoreactivity in the brain of the dogfish *Scyliorhinus canicula*. *J. Comp. Neurol.* 454, 65–81.

Van Valen, L. M. (1982). Homology and causes. *J. Morphol.* 173, 305–12.

Vallarino, M., and Ottonello, I. (1987). Neuronal localization of immunoreactive adrenocorticotropin-like substance in the hypothalamus of elasmobranch fishes. *Neurosci. Lett.* 80, 1–6.

Vallarino, M., Andersen, A. C., Delbende, C., Ottonello, I., Eberle, A. N., and Vaudry, H. (1989). Melanin-concentrating hormone (MCH) immunoreactivity in the brain and pituitary of the dogfish *Scyliorhinus canicula*. Colocalization with alpha-melanocyte-stimulating hormone (alpha-MSH) in hypothalamic neurons. *Peptides* 10, 375–82.

Vallarino, M., Bucharles, C., Facchinetti, F., and Vaudry, H. (1994). Immunocytochemical evidence for the presence of Met-enkephalin and Leu-enkephalin in distinct neurons in the brain of the elasmobranch fish *Scyliorhinus canicula*. *J. Comp. Neurol.* 347, 585–97.

Vallarino, M., Danger, J. M., Fasolo, A., Pelletier, G., Saint-Pierre, S., and Vaudry, H. (1988a). Distribution and characterization of neuropeptide Y in the brain of an elasmobranch fish. *Brain Res.* 448, 67–76.

Vallarino, M., Feuilloley, M., Gutkowska, J., Cantin, M., and Vaudry, H. (1990a). Localization of atrial natriuretic factor (ANF)-related peptides in the central nervous system of the elasmobranch fish *Scyliorhinus canicula*. *Peptides* 11, 1175–81.

Vallarino, M., Feuilloley, M., Yon, L., Charnay, Y., and Vaudry, H. (1992). Immunohistochemical localization of delta sleep-inducing peptide (DSIP) in the brain and pituitary of the cartilaginous fish *Scyliorhinus canicula*. *Peptides* 13, 645–52.

Vallarino, M., Ottonello, I., D'Este, L., and Renda, T. (1988b). Sauvagine/urotensin I-like immunoreactivity in the brain of the dogfish, *Scyliorhinus canicula*. *Neurosci. Lett.* 95, 119–24.

Vallarino, M., Salsotto-Cattaneo, M. T., Feuilloley, M., and Vaudry, H. (1991). Distribution of FMRFamide-like immunoreactivity in the brain of the elasmobranch fish *Scyliorhinus canicula*. *Peptides* 12, 1321–8.

Vallarino, M., Viglietti-Panzica, C., and Panzica, G. C. (1990b). Immunocytochemical localization of vasotocin-like immunoreactivity in the brain of the cartilaginous fish, *Scyliorhinus caniculus*. *Cell Tissue Res.* 262, 507–513.

Vernier, P., and Wullimann, M. (2008). "Evolution of the Posterior Tuberculum and Preglomerular Nuclear Complex.," in *Encyclopedia of Neuroscience*, ed. U. Binder, MD; Hirokawa, N; Windhorst (Springer), 4398.

Zhu, J., Zhang, Y.-T., Alber, M. S., and Newman, S. A. (2010). Bare bones pattern formation: a core regulatory network in varying geometries reproduces major features of vertebrate limb development and evolution. *PLoS One* 5, e10892. doi:10.1371/journal.pone.0010892.

USC
UNIVERSIDADE
DE SANTIAGO
DE COMPOSTELA

# RESUMEN

USC
UNIVERSIDADE
DE SANTIAGO
DE COMPOSTELA

# RESUMEN

# DESARROLLO Y EVOLUCIÓN DEL HIPOTÁLAMO DE VERTEBRADOS: HALLAZGOS EN CONDRICTIOS.

## INTRODUCCIÓN

La evolución es un hecho científico. Para entender el proceso evolutivo es necesario reconocer *qué* ha cambiado entre los organismos, *cómo* ha cambiado, *cuándo* ha cambiado y *porqué* ha cambiado. Entender *qué* ha cambiado en los organismos exige compararlos bajo diferentes aproximaciones. En lo que se refiere a las ciencias morfológicas, esta tarea implica la comparación de estructuras y su origen embriológico reconociendo caracteres similares y diferentes.

El resurgimiento de las ciencias morfológicas (anatomía, embriología, paleontología) llegó con el redescubrimiento de homologías en el ADN y los genes homoebox, en *Drosophila* y en los vertebrados. Estos genes y procesos del desarrollo revelarían ser importantes mecanismos evolutivos dando lugar a una nueva disciplina conocida como *evo-devo* que reconciliaría a la biología del desarrollo (que depende de la expresión de combinaciones de genes) con la teoría de la evolución. Por tanto un enfoque *evo-devo* resulta una buena aproximación para entender la evolución morfológica.

Sin embargo, para entender el desarrollo y evolución del hipotálamo de vertebrados primero tendremos que entender qué es y cómo se forma el hipotálamo. El hipotálamo es un centro integrador altamente conservado que coordina respuestas autonómicas, endocrinas y límbicas. Al igual que otras regiones del sistema nervioso central, el hipotálamo se origina a partir del tubo neural. Este tubo se origina a partir de la placa neural, la cual se pliega sobre sí misma formando una estructura tubular en la que la capa de células más internas –el epéndimo– está formada por células proliferantes. Estas células neuroepiteliales integran señales difusibles en el espacio (a lo largo del tubo neural) y en el tiempo (durante el desarrollo). Esta integración de señales da lugar a la expresión de diferentes grupos de factores de transcripción, los cuales dirigen los principales procesos morfogenéticos a través de la regulación de la proliferación, diferenciación y migración celular. El estudio de estos factores de transcripción ha revelado la existencia de unidades histogenéticas radiales, definidas por dominios neuroepiteliales, con propiedades morfogenéticas comunes codificadas genéticamente. Estas unidades histogenéticas (y sus propiedades morfogenéticas) varían a lo largo del tubo neural en función del escenario epigenético. Entre vertebrados, las

bases del establecimiento de homologías se basa precisamente en la existencia de estas unidades histogenéticas (o dominios morfogenéticos) que expresan códigos genéticos similares debido a la existencia de escenarios epigenéticos comunes. Sin embargo, las propiedades morfogenéticas de estas unidades son similares pero no idénticas, por lo que pueden dar lugar a una estructura radial diferente.

En lo que se refiere al hipotálamo, éste se desarrolla en la parte más rostral y ventral del tubo neural en un punto donde confluyen diferentes señales difusibles. Como resultado los procesos morfogenéticos que tienen lugar en el hipotálamo son complejos dando lugar a una estructura histológica compleja cuya sistematización ha resultado esquiva. Diferentes escuelas entienden la organización del cerebro y del hipotálamo de forma distinta. La escuela columnar entiende que el cerebro está organizado en unidades histogenéticas longitudinales como extensión de los componentes funcionales de los nervios espinales y craneales. La escuela neuromérica entiende que el cerebro está organizado en unidades histogenéticas transversales debido al estudio del propio proceso del desarrollo. Los primeros entienden que el hipotálamo está situado debajo del tálamo originándose de las columnas más ventrales en este punto mientras que los segundos entienden que el hipotálamo está situado bajo el telencéfalo formando parte del segmento más anterior del tubo neural.

El modelo prosomérico, es un modelo segmental basado en patrones de expresión genética (factores de transcripción y señales difusibles), información morfológica e información ontológica en general. El modelo establece que los segmentos (referidos como prosómeros, mesómeros o rombómeros, según la región del cerebro considerada) están codificados genéticamente. Este paradigma será nuestra principal herramienta teórica ya que ha resultado ser un marco de trabajo realmente útil a la hora de establecer comparaciones y ofrece una definición muy concreta del hipotálamo.

Para estudiar la evolución hipotálamo de vertebrados usamos un pequeño condríctio, la pintarroja *Scyliorhinus canicula* por diferentes razones. Por un lado, los gnatóstomos existentes pueden ser divididos en dos clases: condríctios –o peces cartilaginosos– y osteíctios o peces óseos. La última comprende a los peces de aletas rayadas y lobuladas incluyendo a la línea de los tetrápodos. Las comparaciones entre las líneas de condríctios y osteíctios nos permiten hacer comparaciones filogenéticas profundas sobre la naturaleza del antecesor común de los vertebrados mandibulados.

Finalmente, su pequeño tamaño relativo entre los tiburones, su fácil mantenimiento, su lento desarrollo (6-8 meses) que permite detalles del desarrollo imperceptibles en otros organismos, y una relación tamaño cerebral/tamaño corporal similar al de aves o mamíferos hacen de *S. canicula* un buen organismo modelo para su estudio en condiciones de laboratorio.

Hipotálamo de peces cartilaginosos.

Finalmente, para entender el significado de las diferencias que podamos observar en la evolución del hipotálamo de vertebrados tendremos que entender la organización estructural del hipotálamo de *S. canicula.* Clásicamente, el hipotálamo de condríctios ha sido subdividido en tres grandes regiones: a) región preóptica o anterior; b) región tuberal o medial; c) región mamilar o posterior.

a) Región preóptica o anterior.

La región preóptica alberga dos importantes agrupaciones celulares y dos órganos organizados en torno al receso preóptico. Una de estas agrupaciones celulares presenta células secretoras conservadas asociadas al sistema hipotálamo-hipofisario, el núcleo preóptico magnocelular. La otra es también una agrupación conservada rica en células catecolaminérgicas asociadas al quiasma óptico en cuanto a su posición. También pertenecen a esta región, estando íntimamente asociados al receso óptico, un órgano aminérgico caracterizado por células licor-contactantes y un órgano neurohemal.

b) Región tuberal o medial

La región tuberal o medial también presenta estructuras conservadas como el tracto hipotálamo-hipofisario, una eminencia media, o el lóbulo neurointermedio o neurohipófisis propiamente dicha. Otras estructuras están solo presentes en el hipotálamo tuberal de peces gnatóstomos, como los lóbulos inferiores hipotálámicos (formados por expansiones laterales de las paredes infundibulares) y el saco vasculoso. Los lóbulos inferiores del hipotálamo están asociados al control del comportamiento alimenticio mientras que el saco vasculoso es un órgano de función enigmática que se forma adyacentemente a la neurohipófisis. Éste último se forma a partir de la porción caudal de la evaginación de la neurohipófisis y, aunque anteriormente se pensaba que su función estaba relacionada con la percepción de la presión, ahora hay evidencias de su implicación en los ritmos circadianos.

c) Región mamilar o caudal

En la región caudal los derivados mamilares están fundamentalmente ocupados por dos estructuras funcionalmente integradas que forman dos órganos circunventriculares continuos: el órgano paraventricular (y su continuación caudomedial) y el órgano del receso posterior. Las paredes de ambos órganos están característicamente plegadas y forman un órgano denso en células licor-contactantes de naturaleza catecolaminérgica, serotoninérgica o peptidérgica.

Caudalmente al receso mamilar hay una estructura conocida como tubérculo posterior. Su identidad es controvertida ya que se ha adscrito tanto al hipotálamo como al diencéfalo según diferentes autores debido a sus conexiones funcionales con éste último. Además es una estructura bien conservada caracterizada por una distribución rica de células catecolaminérgicas.

**CAPÍTULO 1: Organización prosomérica del hipotálamo de un elasmobranquio, el melgacho *Scyliorhinus canicula*.**

Para entender cómo ha evolucionado el hipotálamo de vertebrados primeramente tendremos que esclarecer qué entendemos por hipotálamo y usar una definición del mismo que pueda ser trasladable o equiparable entre vertebrados. Dados nuestros objetivos, en este trabajo preliminar utilizaremos una aproximación *evo-devo* y el marco teórico del modelo prosomérico actualizado para definir qué es el hipotálamo en nuestro modelo de estudio, *Scyliorhinus canicula*, un representante de condríctios y gnatóstomos basales.

El modelo prosomérico en su versión más actualizada ha reconsiderado la situación del hipotálamo. Según este paradigma, el hipotálamo estaría situado bajo el telencéfalo constituyendo en conjunto el prosencéfalo secundario. Esta unidad a su vez da lugar a los segmentos más anteriores del cerebro: El segmento o prosómero más rostral sería el hp2 –o terminal- y el más caudal sería el segmento hp1 o peduncular. Este último a su vez estaría caudalmente en contacto con el segmento más anterior del diencéfalo, el segmento p3 o prosómero 3. La última versión del modelo prosomérico considera que cada uno de estos segmentos del prosencéfalo, al igual que segmentos de posiciones más caudales, constarían de placas del techo, alar, basal y suelo. También estarían separados uno del otro por la barrera intrahipotalámica (IHB) la cual se extendería desde la placa del suelo hasta la placa del techo. El segmento hp2 contiene una región denominada región acroterminal que se correspondería con el punto más rostral del cerebro, extendiéndose desde la placa del techo a la del suelo. Al ser el punto más rostral del cerebro, cualquier otro punto diferente a este debe considerarse como caudal.

En lo que se refiere al hipotálamo en sí, éste estaría dorsalmente separado del telencéfalo por la barrera hipotálamo-telencefálica (HTB). Por tanto el hipotálamo constaría de placa alar, basal y del suelo pero no placa del techo. Caudalmente el hipotálamo estaría separado del diencéfalo por la barrera hipotálamo-diencefálica (HDB). En lo que se refiere a dominios histogenéticos, el hipotálamo se entendería como organizado en cinco dominios longitudinales dorso-ventrales con sus respectivas divisiones rostrales y caudales debido al curso de la IHB. De dorsal a ventral estos dominios, con sus respectivas regiones terminales y pedunculares (referidas con el prefijo "retro" en el hipotálamo basal), estos dominios son: área paraventricular terminal y peduncular (TPa/PPa); área subparaventricular terminal y peuncular (TSPa/PSPa); área tuberal y retrotuberal (Tu/RTu); área perimamilar y periretromamilar (PM/PRM); área mamilar y retromamilar (MM/RM).

El modelo prosomérico establece que tanto los límites del hipotálamo como sus unidades histogenéticas se pueden definir por la expresión combinada de marcadores como *Foxg1*, *Otp*, *Dlx*, *Shh*, *Nkx2.1* y *Tbr1*. El estudio de los respectivos ortólogos de estos marcadores en la pintarroja nos ha permitido identificar los límites del hipotálamo así como unidades histogenéticas homólogas (referidas como "like") a las definidas en mamíferos: TPa/PPa-like (*ScOtp*), TSPa/PSPa-like (*ScDlx2/5*), Tu/RTu-like

(*ScNkx2.1+ScDlx2/5+ScShh+ScOtp*), PM/PRM-like (*ScNkx2.1+ScOtp*) y MM/RM-like (*ScNkx2.1*/*ScShh*). Además, el estudio de estructuras inmunoractivas a 5-HT y GFAP nos ha permitido definir tentativamente subdivisiones rostro-caudales en el hipotálamo alar (TPa/PPa-like y TSPa/PSPa-like) y la identificación de una comisura probablemente homóloga a la comisura retromamilar de mamíferos que separa hp2/hp1. En el hipotálamo basal hemos encontrado evidencias indirectas de estas divisiones rostro-caudales como la expresión de *ScNkx2.1* y *ScShh* en los dominios MM-like y RM-like (respectivamente). Además el estudio de estructuras inmunoreactivas a TH nos ha permitido esclarecer que al menos la parte más rostral del tubérculo posterior pertenece al RM-like según el modelo prosomérico. Con todo, hemos observado un elevado grado de conservación entre el hipotálamo de pintarroja y el de mamíferos, siendo aparentemente más conservado el hipotálamo alar que el hipotálamo basal.

**CAPÍTULO 2: Hipotálamo alar del tiburón: subdivisiones moleculares prosoméricas y tendencias evolutivas.**

En el capítulo anterior esbozamos los límites y compartimentos histogenéticos homólogos a los propuestos por el modelo prosomérico actualizado. Sin embargo, no definimos más subdominios ni abordamos cuestiones evolutivas. Precisamente con esos objetivos, en este segundo capítulo revisamos la expresión de los marcadores estudiados anteriormente junto con la expresión de *ScLhx9*, *ScLhx5*, *ScNeurog2*, *ScNkx2.8* y estructuras inmunoreactivas a Pax6, 5-HT, GAD, SS, TH.

El Pa-like de pintarroja, además de expresar *ScOtp*, también expresa *ScNeurog2*, *ScLhx5* y es inmunopositivo para Pax6. Estos genes también son expresados en el Pa de mamíferos revelando un patrón conservado a este nivel. La expresión rostralmente restringida de *ScLhx5* junto con la distribución de tractos immunoreactivos a 5-HT nos ha permitido identificar diferencias y subdominios rostro-caudales a nivel molecular en el Pa-like tal como propone el modelo prosomérico. Por otro lado, la expression de *ScOtp*, *ScNeurog2*, *ScLhx5* y *ScTbr1* dentro de un dominio mayor caracterizado por immunopositividad a Pax6 sugiere una organización prosencefálica alternativa a la propuesta por el modelo prosomérico. Según esta organización el Pa-like sería un subdominio de un territorio mayor, más relacionado con el palio y el p3 alar que con el resto del hipotálamo alar. A mayores, la identificación de células *ScOtp*-positivas posiblemente migradas desde el Pa-like a diferentes regiones del telencéfalo sugiere que la existencia de estructuras relacionadas con la amígdala y que ya estaban presentes en los gnatóstomos basales.

En el SPa-like, observamos la existencia de subdominios rostro-caudales y dorso-ventrales. La co-distribución de *ScDlx2/5* con immunopositividad a Pax6 de baja intensidad en el SPa-like nos ha permitido identificar un subdominio dorsal (SPaD). Este subdomnio también se caracteriza por distribución de células ScOtp-positivas en la parte marginal del mismo. El SPaD se diferenciaría de un subdominio ventral (SPaV) por la falta de estos marcadores y la co-distribución con la expresión alar de *ScNkx2.8*. La distribución de tractos

inmunoreactivos a 5-HT y células immunoreactivas a Pax6 en la región peduncular (caudal) del SPa también nos permitió diferenciar un subdomnio rostral o terminal (TSPa) de uno caudal o peduncular (PSPa). Estas subdivisiones en conjunto nos permitieron diferenciar cuatro subdominios en el SPa tal como sugiere el modelo prosomérico (TSPaD, PSPaD, TSPaV, PSPaV). Sin embargo, la identidad de estos subdominios parece no estar conservada entre mamíferos y condríctios.

El estudio del hipotálamo alar tangencialmente nos llevó al análisis y revisión de la barrera alar-basal (ABB). A nuestro modo de ver, este límite está caracterizado de forma confusa en la literatura. En este trabajo proponemos que el límite se puede caracterizar por la expresión alar y basal de *ScNkx2.8* o por el espacio definido entre el borde ventral de Pax6 en el hipotálamo alar y el borde dorsal de Shh en el hipotálamo basal. Además acuñamos el concepto novedoso de borde alar-basal (ABBr) para referirnos a la línea virtual (esta no sería ni alar ni basal) definida por el borde ventral de expresión de *ScDlx2/5* en el hipotálamo alar o el borde dorsal de expresión de *ScNkx2.1* en el hipotálamo basal.

En cuanto al análisis evolutivo nuestros datos reflejan que al menos la expresión de *Otp*, *Neurog2*, *Lhx5* y *Pax6* ya estaban presentes en el Pa-like de gnatóstomos basales. Una revisión detallada de la literatura sugiere que estos marcadores podrían incluso estar presentes antes de la transición entre agnatos y gnatóstomos, al contrario de lo propuesto por estudios recientes que señalan esta adquisición durante la transición anamnio-amniota. En cuanto al SPa-like, también parece haber una tendencia en la conservación de los genes *Dlx* y *Nkx2.8*/*Nkx2.2*. Sin embargo, estudios previos señalan una tendencia en la que *Nkx2.1* y *Shh* se expresarían en el SPa con una reducción paulatina desde lampreas a mamíferos. Curiosamente, los datos de pintarroja parecen contradecir esta tendencia y recuerdan a la situación en mamíferos. Esto puede deberse a una mayor expresión de Pax6 en pintarroja ya que hay estudios que sugieren que balance entre *Pax6/Nkx2.1* controla el desarrollo del palio y del hipotálamo alar sobre el hipotálamo basal, lo que también explicaría el gran desarrollo del palio en condríctios.

**CAPÍTULO 3: Hipotálamo basal del tiburón: subdivisiones moleculares prosoméricas y tendencias evolutivas.**

En el capítulo anterior profundizamos en la genoarquitectura y subdivisiones del hipotálamo alar abordando también el significado evolutivo de los datos obtenidos. En el presente capítulo procederemos de forma similar revisando la expresión de marcadores estudiados anteriormente junto con la expresión basal de *ScLhx5*, *ScEmx2*, *ScLmx1b*, *ScPitx2*, *ScPitx3a*, *ScNeurog2*, *ScFoxa1*, *ScFoxa2* y estructuras inmunoreactivas a PCNA, GAD, 5-HT, TH, CB, SS, y GFAP.

Los patrones de expresión aquí considerados han revelado la existencia de multitud de subdominios en los dominios histogenéticos previamente definidos en el hipotálamo basal según el modelo prosomérico. Una comparación preliminar entre dichos subdominios y los propios de mamíferos sugiere que aunque las homologías se cumplen a un nivel de análisis

simple no se cumplen a niveles más detallados, emergiendo importantes diferencias a pesar de expresarse los mismos genes de forma similar.

Por otro lado, la lógica de los patrones de expresión aquí considerados revelan que se puede interpretar que el hipotálamo basal de la pintarroja está dividido en tres dominios en función de la expresión –o no– de *ScEmx2* (*ScEmx2*-negativo: Tu/RTu-like; *ScEmx2*-positivo: parte del Tu-like junto con PM/PRM-like y MM-like; y *ScEmx2*-negativo: RM-like). Sin embargo, estos tres dominios histogenéticos no coincidirían con los dominios propuestos por el modelo prosomérico. Sorprendentemente, una comparación entre los datos observados en pintarroja y en mutantes deficientes para la señalización de Shh en el hipotálamo ventral y caudal revelan rasgos comunes como la sobreexpresión de *Emx2*, la infraexpresión de *Pitx2* y la hipoplasia del hipotálamo ventral y caudal. Esto sugiere que, al menos en esta región, los mecanismos que gobiernan la compartimentación son básicamente los mismos entre vertebrados, y que importantes diferencias pueden emerger debido a una señalización diferencial.

El estudio comparado del hipotálamo basal, sugiere una expresión altamente conservada de de los genes considerados en este estudio ya que muchos de ellos fueron adquiridos antes de la transición entre agnatos y gnatóstomos. Además, las diferencias observadas entre los patrones de expresión de estos genes remarcan la idea de que a pesar de expresarse genes similares, la existencia de subdominios homólogos es poco probable. Por otro lado, la organización propuesta en pintarroja en tres dominios histogenéticos diferentes a los prosoméricos parece probable al menos en vertebrados basales.

Finalmente, la expresión continua en el RM-like y la placa basal del diencéfalo de genes como *ScShh*, *ScLmx1b*, *ScPitx2*, *ScPitx3a*, *ScNeurog2*, *ScFoxa1*, *ScFoxa2*, que a su vez es complementaria a la expresión de genes como *ScNkx2.1*, *ScOtp*, *ScLhx5* y *ScEmx2* en el resto del hipotálamo basal sugiere que RM-like pertenece al diencéfalo. Estos datos también sugieren una interpretación alternativa de la HDB y del prosencéfalo secundario propuestos en el modelo prosómerico en la que el RM-like pertenecería al diencéfalo y la parte alar del segmento p3 diencefálico pertenecería al prosencéfalo secundario. Diferentes líneas de evidencia como son la immunonegatividad de PCNA en los límites en pintarroja, el estudio comparado de los patrones de expresión considerados, la expresión de *Wnt8a* en diferentes vertebrados, el curso de tractos mamilo-talámicos y propuestas segmentales precedentes alternativas al modelo prosomérico apoyan esta visión alternativa de la HDB y el prosencéfalo secundario.

USC
UNIVERSIDADE
DE SANTIAGO
DE COMPOSTELA

# CONCLUSIONS

USC
UNIVERSIDADE
DE SANTIAGO
DE COMPOSTELA

# CONCLUSIONS

1. The expression of *ScOtp*, *ScDlx2/5*, *ScNkx2.1* and *ScShh* led us to identify five longitudinal histogenetic domains in the shark, from dorsal to ventral: Pa-like (*ScOtp*), SPa-like (*ScDlx2/5*), Tu/RTu-like (*ScNkx2.1+ScDlx2/5+ScShh+ScOtp*), PM/PRM-like (*ScNkx2.1+ScOtp*) and MM/RM-like (*ScNkx2.1+ScShh*). The analysis of main histogenetic domains (single level analysis), revealed a strikingly degree of conservation among basal gnathostomes and mammals.

2. A deep analysis of the Pa-like domain revealed that besides *ScOtp*, this domain also showed *ScNeurog2*- and *ScLhx5*-expression and Pax6-immunoreactivity. This analysis also revealed a high degree of conservation in the Pa-like of shark and mammals even at more deep levels of analysis. Besides, the detection of 5-HT-immunoreactive tracts coursing through the medial forebrain bundle, joined to the abundant expression of *ScLhx5* led us to identify rostro-caudal subdivisions in the Pa-like, as predicted by the prosomeric model.

3. A deep analysis of the SPa-like domain revealed the existence of dorso-ventral and rostro-caudal subdomains as suggested by the prosomeric model. The dorsal one (SPaD-like) is characterized by the co-distribution of low-intense Pax6-immunoreactivity. The ventral subdomain is characterized by the alar co-expression of *ScNkx2.8*. The caudal subdomain (PSPa-like) differs from the rostral subdomain (TSPa-like) by the co-distribution of Pax6-immunoreactive cells in the marginal zone as well as for the presence of 5-HT-immunoreactive tracts of the medial forebrain bundle. The crossroad between dorso-ventral and rostro-caudal subdivisions leads to the identification of four subdivisions as proposed by the prosomeric model (TSPaD-, PSPaD-, TSPaV-, PSPaV-like). However, these domains present a similar but not the same genoarchitecture than those reported in mouse.

4. The identification of apparently migrated *ScOtp*-expressing cells in different domains of the telencephalon suggest the existence of subpalial (bed nucleus stria terminalis-like) and pallial (medial amygdala-like) amygdaloid structures. This work revealed that these amygdaloid derivatives would be already present in basal gnathostomes.

5. A detailed review of the literature suggests that the expression patterns of *Otp*, *Neurog2*, *Lhx5*, *Dlx2/5*, *Nkx2.8/Nkx2.2* and Pax6-immunoreactivity in the alar prosencephalon is conserved from early gnathostomes and could be even acquired before the agnathan-gnathostome transition.

6. Although we identified the hypothalamo-telencephalic border (HTB) by the expression of *ScFoxg1a* in the telencephalon and *ScOtp* in the Pa-like as proposed by the prosomeric model, we also noticed several expression patterns that suggest other interpretation. In fact, the expression of *ScOtp*, *ScNeurog2*, *ScTbr1*, *ScLhx5* and *ScLhx9* inside a broader domain of Pax6-immunoreactivity led us to suggest that an

alternative interpretation of the prosencephalic expression patterns and the hypothalamus could exist.

7. The alar-basal boundary (ABB) can be identified by the expression *of ScNkx2.8* or as the territory located between Pax6-immunoreativity in the alar plate and *ScShh*/Shh-immunoreactivity in the rostral basal plate. Of note, this boundary contains both alar and basal markers. We have thus defined the alar-basal border (ABBr) as the virtual point at which alar and basal plates abut. This ABBr can be defined in shark by the ventral border of *ScDlx2/5* in the alar plate or the dorsal border of *ScNkx2.1* in the basal plate.

8. A deep analysis of the basal hypothalamus by the additional study of *ScLhx5*, *ScEmx2*, *ScLmx1b*, *ScPitx2*, *ScPitx3a*, *ScNeurog2*, *ScFoxa1* and *ScFoxa2* expression revealed that the basal hypothalamus of the shark is better understood as being organized in three main domains characterized by the expression or lack of *ScEmx2* (*ScEmx2* negative: Tu/RTu-like; *ScEmx2* positive: part of the Tu-like+PM/PRM-like+MM-like; *ScEmx2* negative: RM-like). Of note this organization also involves an alternative view to that previously proposed by the prosomeric model.

9. The comparisons between the expression patterns obtained in the shark and those obtained in mutants defective for Shh signaling in the ventral and caudal hypothalamus reveal shared traits like *Emx2* upregulation and *Pitx2* downregulation besides hypoplasia compared to wild mice. This suggests that the patterning process among vertebrates are almost the same and differences can emerge by differences in signaling processes.

10. The expression patterns observed in the RM-like and basal plate of the diencephalon and other lines of evidence (PCNA-immunoreactivity, data from mutants, *Wnt8a* expression) suggests that the hypothalamo-diencephalic border (HDB) could have an alternative interpretation to that proposed by the prosomeric model, under which the RM-like is part of the diencephalon while the alar p3 (including the PThE) is part of the secondary prosencephalon. This interpretation is also supported by previous non-prosomeric segmental analysis.

# CONCLUSIONES

USC
UNIVERSIDADE
DE SANTIAGO
DE COMPOSTELA

# CONCLUSIONES

1. La expresión de *ScOtp*, *ScDlx2/5*, *ScNkx2.1* y *ScShh* nos ha permitido identificar cinco dominios histogenéticos longitudinales en el tiburón, que de dorsal a ventral son: Pa-like (*ScOtp*), SPa-like (*ScDlx2/5*), Tu/RTu-like (*ScNkx2.1+ScDlx2/5+ScShh+ScOtp*), PM/PRM-like (*ScNkx2.1+ScOtp*) and MM/RM-like (*ScNkx2.1+ScShh*). El análisis de los principales dominios histogenéticos (nivel de análisis simple), ha revelado un llamativo grado de conservación entre los gnatóstomos basales y mamíferos.

2. Un análisis más profundo del dominio Pa-like reveló que además de *ScOtp*, este dominio también muestra expresión de *ScNeurog2* y *ScLhx5* además de inmunoreactividad a Pax6. Este análisis también reveló un alto grado de conservación entre el Pa-like de tiburón y mamíferos incluso en niveles más profundos de análisis. Además, la detección de tractos inmunoreactivos a 5-HT cursando el fascículo prosencefálico medial junto con la abundante expresión rostral de *ScLhx5* nos ha permitido identificar subdivisiones rostro-caudales en el Pa-like, como predice el modelo prosomérico.

3. Un análisis más profundo del dominio SPa-like, reveló la existencia de subdominios dorso-ventrales y rostro-caudales como sugiere el modelo prosomérico. El subdominio dorsal (SPaD-like) está caracterizado por la co-distribución con inmunoreactividad a Pax6 de baja intensidad. El subdominio ventral está caracterizado por la co-expresión alar con *ScNkx2.8*. El dominio caudal (PSPa-like) difiere del subdominio rostral (TSPa-like) por la co-distribución con células Pax6 inmunoreactivas y tractos del fascículo prosencefálico medial. La intersección entre subdivisiones dorso-ventrales y rostro-caudales conlleva a la identificación de cuatro subdivisiones como propone el modelo prosomérico (TSPaD-, PSPaD-, TSPaV-, PSPaV-like). Sin embargo, estos dominios presentan una organización genoarquitectónica similar pero no la misma que aquella propuesta en ratón.

4. La identificación de células *ScOtp* positivas aparentemente migradas en diferentes dominios del telencéfalo sugiere la existencia de estructuras amigdaloides subpaliales (núcleo del lecho de la estría terminal-like) y paliales (amígdala media-like). Este trabajo reveló que estos derivados amigdaloides podrían estar ya presentes en gnatóstomos basales.

5. Una revisión detallada de la literatura sugiere que los patrones de expresión de *Otp*, *Neurog2*, *Lhx5*, *Dlx2/5*, *Nkx2.8/Nkx2.2* y la inmunoreactividad a Pax6 en el prosencéfalo alar está conservada desde los gnatóstomos basales y podría incluso haber sido adquirida durante la transición entre agnatos y gnatóstomos.

6. Aunque identificamos el borde hipotalámico-telencefálico (HTB) por la expresión de *ScFoxg1a* en el telencéfalo y *Otp* en el Pa-like como propone el modelo prosomérico, también nos percatamos varios patrones de expresión que sugieren otra interpretación. De hecho, la expresión de *ScOtp*, *ScNeurog2*, *ScTbr1*, *ScLhx5* y *ScLhx9* dentro de un dominio más extenso inmunoreactivo a Pax6 nos permite sugerir que una interpretación alternativa de los patrones de expresión prosencefálicos e hipotalámicos también podría existir.

7. La barrera alar-basal (ABB) puede ser identificada por la expresión de *ScNkx2.8* o como el territorio localizado entre la inmunoreactividad a Pax6 en la placa alar y la inmunopositividad a Shh/*ScSh*h en la placa basal rostral. Digno de mención, esta barrera también expresa otros marcadores alares y basales. De esta manera definimos el borde alar-basal (ABBr) como el punto virtual en el que limitan las placas alares y basales. Esta ABBr se puede definir en tiburón por el límite ventral de *ScDlx2/5* en la placa alar o por el límite dorsal de *ScNkx2.1* en la placa basal.

8. Un análisis más profundo del hipotálamo basal mediante el estudio adicional de los patrones de expresión de revelan que el hipotálamo basal de los tiburones se entiende mejor como organizado tres dominios principales caracterizados por la expresión de *ScEmx2* (*ScEmx2*-negativo: Tu/RTu-like; *ScEmx2*-positivo: parte del Tu-like+PM/PRM-like+MM-like); *ScEmx2*-negativo: RM-like). Esta organización también implica una visión alternativa a aquella propuesta por el modelo prosomérico.

9. Las comparaciones entre los patrones de expresión obtenidos en tiburón y aquellos obtenidos en mutantes defectivos para la señalización Shh en el hipotálamo ventral y caudal revelaron rasgos comunes como la regulación al alza de *Emx2* o regulación a la baja de *Pitx2* además de hipoplasia comparados con ratones salvajes. Esto sugiere que el proceso de formación del patrón entre vertebrados es prácticamente el mismo y que pueden surgir diferencias por divergencias en el proceso de señalización.

10. Los patrones de expresión observado en el RM-like y en la placa basal del diencéfalo y otras líneas de evidencia (inmunoreactividad a PCNA, datos de mutantes, expresión de *Wnt8a*) sugieren que el borde hipotalámico-diencefálico (HDB) podría tener una interpretación alternativa a aquella propuesta por el modelo prosomérico en la cual el RM-like es parte del diencéfalo mientras que el p3 alar (incluyendo la PThE) es parte del prosencéfalo secundario. Esta interpretación también está apoyada por análisis previos segmentales no-prosoméricos.

USC
UNIVERSIDADE
DE SANTIAGO
DE COMPOSTELA

## SUMMARY

The hypothalamus is a conserved integrative center with a complex organization result of a complex patterning processes. Here we make use of a *evo-devo* approach and the theoretical framework of the prosomeric model to understand the organization of the vertebrate hypothalamus. We studied the gene expression patterns of *ScFoxg1a*, *ScDlx2/5*, *ScOtp*, *ScShh*, *ScNkx2.1*, *ScTbr1*, *ScNeurog2*, *ScLhx5, ScLhx9*, *ScDlx2/5*, *ScNkx2.8, ScEmx2*, *ScLmx1b*, *ScPitx2, ScPitx3a*, *ScNeurog2*, *ScFoxa1* and *ScFoxa2* besides immunoreactivity to Pax6, PCNA and other immunomarkers in the embryonic hypothalamus and neighbour prosencephalic territories of a cartilaginous fish, the catshark, *Scyliorhinus canicula*. Our comparative analysis reveals the existence of conserved traits but also suggests an alternative organization for the vertebrate hypothalamus and even for the anterior prosencephalon of vertebrates to that proposed by the prosomeric model.

## KEYWORDS

hypothalamus, chondrichthyans, *evo-devo*, prosomeric model, prosencephalon

USC
UNIVERSIDADE
DE SANTIAGO
DE COMPOSTELA